



**This electronic thesis or dissertation has been
downloaded from Explore Bristol Research,
<http://research-information.bristol.ac.uk>**

Author:

Mega, Riccardo S

Title:

Decarboxylative Radical Additions to Vinyl Boronic Esters

General rights

Access to the thesis is subject to the Creative Commons Attribution - NonCommercial-No Derivatives 4.0 International Public License. A copy of this may be found at <https://creativecommons.org/licenses/by-nc-nd/4.0/legalcode>. This license sets out your rights and the restrictions that apply to your access to the thesis so it is important you read this before proceeding.

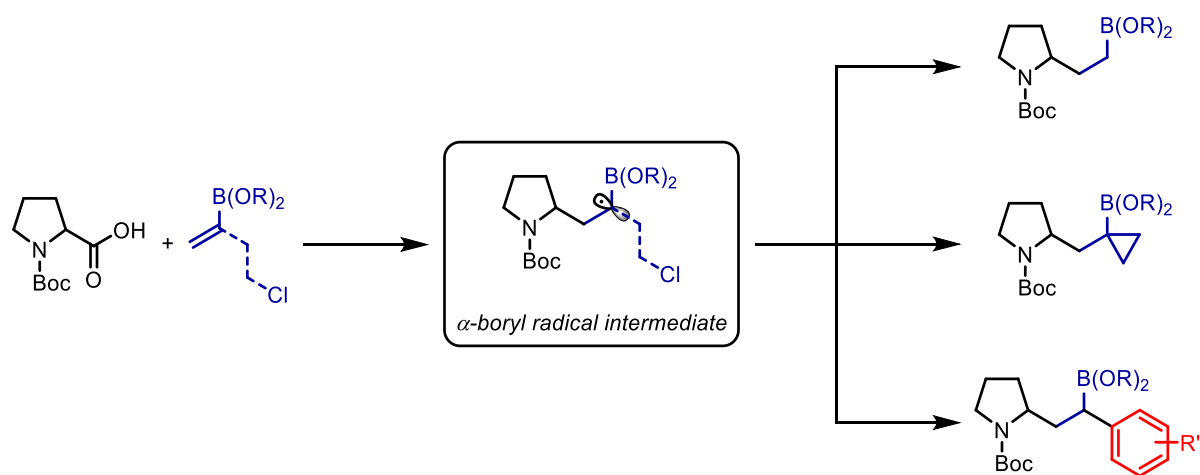
Take down policy

Some pages of this thesis may have been removed for copyright restrictions prior to having it been deposited in Explore Bristol Research. However, if you have discovered material within the thesis that you consider to be unlawful e.g. breaches of copyright (either yours or that of a third party) or any other law, including but not limited to those relating to patent, trademark, confidentiality, data protection, obscenity, defamation, libel, then please contact collections-metadata@bristol.ac.uk and include the following information in your message:

- Your contact details
- Bibliographic details for the item, including a URL
- An outline nature of the complaint

Your claim will be investigated and, where appropriate, the item in question will be removed from public view as soon as possible.

Decarboxylative Radical Additions to Vinyl Boronic Esters



Riccardo S. Mega

Supervisor: Professor Varinder K. Aggarwal

A dissertation submitted to the University of Bristol in accordance with the requirements for award of the degree of Doctor of Philosophy in the Faculty of Science, School of Chemistry, August 2020.

Word Count: 59741

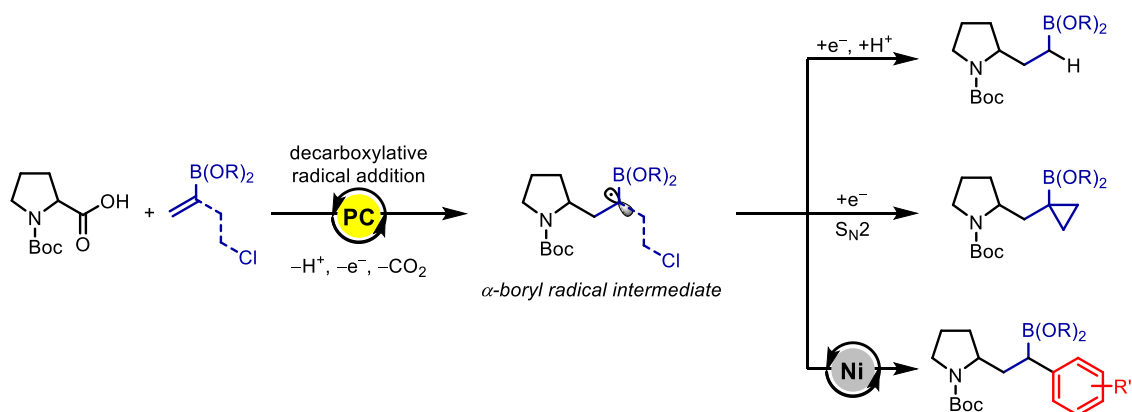
I. Abstract

This thesis details the development of novel decarboxylative radical addition reactions to vinyl boronic esters using photoredox catalysis, enabling the efficient and rapid access of functionalised alkyl boronic esters from abundant feedstock chemicals. Key to the success of these methodologies is the stabilised α -boryl radical intermediate generated upon radical addition to the vinyl boronic ester, which can undergo a range of terminating events to yield a diverse library of complex boronic ester products.

Firstly, the decarboxylative radical addition reaction of carboxylic acids to vinyl boronic esters was developed to directly access alkyl boronic esters using photoredox catalysis. The reaction was applied to a range of carboxylic acids, including α -amino, α -oxy and alkyl acids providing the corresponding boronic ester products in good to excellent yields. Moreover, the reaction could be applied to a range of substituted vinyl boronic esters. Mechanistic studies confirmed a radical-polar crossover mechanism, involving an unprecedented single-electron reduction of the α -boryl radical to the corresponding α -boryl anion, which is subsequently protonated.

Having set the stage for photoredox-mediated decarboxylative radical additions to vinyl boronic esters, we demonstrated that we could trap the α -boryl anion with an electrophile tethered to the vinyl boronic ester, enabling the synthesis of highly functionalised, polysubstituted cyclopropyl boronic esters. Mechanistic studies supported a radical-polar crossover mechanism involving an intramolecular S_N2 cyclisation to yield the cyclopropane.

Finally, to introduce further molecular complexity into these molecules, a decarboxylative conjunctive cross-coupling of vinyl boronic esters with carboxylic acids and aryl iodides using metallaphotoredox catalysis was developed. Trapping of the intermediate α -boryl radical with an aryl nickel complex enabled a cross-coupling event to yield complex benzylic boronic ester products. A range of α -amino acids, mainly secondary amino acids, and tertiary α -oxy acids with aryl iodides were successfully employed and the methodology was applied to the synthesis of four *sedum* alkaloid natural products.



II. Contents

I. Abstract	i
II. Contents	ii
III. Acknowledgements	v
IV. Author's Declaration	vi
V. Abbreviations and Acronyms	vii
1.0 Introduction	1
1.1 Boronic Acids and their Derivatives	1
1.1.1 Structure and Properties	1
1.1.2 Application in Organic Synthesis	1
1.1.3 Application in Medicinal Chemistry	4
1.2 α -Boryl Radicals in Organic Synthesis	6
1.2.1 Radical Additions to Vinyl Boronic Esters	8
1.2.2 Radical Additions to Vinyl Boronate Complexes	17
1.2.3 α -Halo Boronic Esters.....	23
1.2.4 Hydrogen Atom Transfer (HAT)	28
1.3 Photoredox Catalysis	31
1.3.1 Fundamentals	31
1.3.2 Photoredox-mediated Decarboxylations	34
1.3.3 Metallaphotoredox: Merging Nickel and Photoredox Catalysis	38
2.0 Synthesis of Alkyl Boronic Esters	44
2.1 Project Outline	44
2.2 Results and Discussion	47
2.2.1 Reaction Discovery	47
2.2.2 Optimisation.....	48
2.2.2.1 Cyclic Amino Acids.....	48
2.2.2.2 Monoprotected Acyclic Amino Acids	55
2.2.3 Substrate Scope.....	58

2.2.3.1 Unsuccessful Substrates	62
2.2.4 Mechanistic Studies	65
2.2.4.1 Deuteration Studies	65
2.2.4.2 Determination of α -Boryl Radical Reduction Potential	66
2.2.4.3 Final Proposed Mechanism	70
2.3 Conclusions	71
3.0 Synthesis of Cyclopropyl Boronic Esters	72
3.1 Project Outline	72
3.1.1 Concurrent Reports	74
3.2 Results and Discussion	75
3.2.1 Initial Result.....	75
3.2.2 Optimisation.....	76
3.2.2.1 Vicinally-substituted Cyclopropyl Boronic Esters.....	76
3.2.2.2 Geminally-substituted Cyclopropyl Boronic Esters.....	82
3.2.3 Substrate Scope.....	84
3.2.4 Mechanistic Studies	85
3.3 Conclusions.....	87
4.0 Conjunctive Cross-coupling of Vinyl Boronic Esters	88
4.1 Project Outline	88
4.1.1 Concurrent Reports	90
4.2 Results and Discussion	95
4.2.1 Initial Result.....	95
4.2.2 Optimisation.....	97
4.2.2.1 Phase I: Cyclic Amino Acids	97
4.2.2.3 Phase II: Monoprotected Acyclic Amino Acids and Cross-coupling Selectivity	110
4.2.3 Substrate Scope.....	112
4.2.3.1 Application to <i>Sedum</i> Alkaloids.....	115
4.2.3.2 Unsuccessful Substrates	116

4.2.3.2.1 Alkyl Carboxylic Acids	116
4.2.3.2.2 Acrylate Radical Acceptor	118
4.2.3.2.3 Electron-deficient Aryl Iodides.....	119
4.2.3.2.4 Other Unsuccessful Substrates	120
4.2.4 Proposed Mechanism	122
4.2.5 Conclusions and Outlook.....	124
5.0 Overall Summary.....	126
6.0 Supplementary Materials.....	128
6.1 General Information.....	128
6.2 Synthesis of Alkyl Boronic Esters	130
6.2.1 General Procedures and Reaction Set-up.....	130
6.2.2 Product Characterisation	132
6.2.3 Cyclic Voltammetry Studies	140
6.2.4 Additional Optimisation Tables	142
6.3 Synthesis of Cyclopropyl Boronic Esters	145
6.3.1 Synthesis of Homoallylic Chloride Vinyl Boronic Ester 202.....	145
6.3.2 General Procedures and Reaction Set-up.....	147
6.3.3 Product Characterisation	149
6.3.4 Quantum Yield Measurement	159
6.3.5 Additional Optimisation Tables	163
6.4 Conjunctive Cross-coupling of Vinyl Boronic Esters.....	164
6.4.1 General Procedures and Reaction Set-up.....	164
6.4.2 Product Characterisation	166
6.4.2.1 Application to <i>Sedum</i> Alkaloids.....	187
6.4.2.2 Unsuccessful Substrates	191
6.4.3 Additional Optimisation Tables	195
7.0 References.....	201

III. Acknowledgements

Firstly, I would like to thank Professor Varinder Aggarwal for the wealth of knowledge, guidance, and advice he has given me throughout my PhD. It has been a privilege to work in his group and research such an excited area of chemistry.

Secondly, I would like to thank Adam Noble, who introduced me to the world of photoredox catalysis and with whom I began my PhD project. Adam has been a mentor to me and has made an enormous impact on my development as a scientist. I am indebted to his support and invaluable advice throughout the years. It has been a pleasure to work with you, as well as to partake in multiple Tough Mudder's and the Bristol triathlon.

I would like to give a special thanks to the past and present members of N214 with whom I have had the pleasure of working alongside throughout my PhD. There have been many, but to mention a few: Changcheng, Chao, Björn, Elliot, Vinny, Chary, Valerio, Petr, Dan (with the beard), Hugo, Matt, David and Branca. I have also been lucky to work closely on projects with Daniel Pflästerer, Eddie, Chao, Björn and Vinny, and I am extremely grateful for all their help and support.

Thanks to the Aggarwal group as a whole for making my PhD as enjoyable and rewarding as it has been. In particular: Steve, Rory, Sheenagh, Charlotte, Jingjing, Durga, Kay, Adam Elmehriki, Ana, Joe Bateman, Johan, Alex Fawcett, Raffael Schrof, Dan Kaiser and Alex Zhurakovskiy. It has been an honour to work with you in this stimulating environment. I am also deeply grateful to all those who helped proofread my thesis: Adam Noble, Branca, Kay, Durga and Adam Elmehriki.

Finally, a special thank you to Branca who has always been there for me and managed to put up with me during the stressful periods of the PhD, and my friends and family for their continued support and love.

IV. Author's Declaration

I declare that the work in this dissertation was carried out in accordance with the Regulations of the University of Bristol. The work is original, except where indicated by special reference in the text, and no part of the dissertation has been submitted for any other academic award. Any views expressed in the dissertation are those of the author.

SIGNED:

DATE:

V. Abbreviations and Acronyms

acac	Acetylacetone
AIBN	Azobisisobutyronitrile
Ar	General aromatic group
ATRA	Atom Transfer Radical Addition
bpy	2,2'-Bipyridine
BRSM	Based on Recovered Starting Material
cat	Catecholato
CFL	Compact Fluorescent Light
COD	1,5-Cyclooctadiene
CV	Cyclic Voltammetry
d.r.	Diastereomeric Ratio
DABCO	1,4-Diazabicyclo[2.2.2]octane
dan	1,8-Diaminonaphthalenyl
DBN	1,5-Diazabicyclo[4.3.0]non-5-ene
DBU	1,8-Diazabicyclo[5.4.0]undec-7-ene
DCE	1,2-Dichloroethane
DCM	Dichloromethane
DFT	Density Functional Theory
DIPEA	Diisopropylethylamine
DLP	Dilauroyl Peroxide
DMA	Dimethylacetamide
DMAP	4-Dimethylaminopyridine
DME	Dimethoxyethane
dMeObpy	4,4'-Dimethoxy-2,2'-bipyridine
DMF	Dimethylformamide
dmgH	Dimethylglyoxime
DMI	1,3-Dimethyl-2-imidazolidinone
DMPU	<i>N,N'</i> -Dimethylpropyleneurea
DMSO	Dimethyl sulfoxide
dtbbpy	4,4'-Di- <i>tert</i> -butyl-2,2'-bipyridine
DTBHN	Di- <i>tert</i> -butyl hyponitrite

E ⁺	General electrophile
EDG	Electron-Donating Group
ee	Enantiomeric Excess
EPR	Electron Paramagnetic Resonance
equiv	Equivalents
er	Enantiomeric Ratio
es	Enantiospecificity
ET	Energy Transfer
EWG	Electron-Withdrawing Group
Fc	Ferrocene
FDA	Food and Drug Administration
FG	Functional Group
GABA	<i>gamma</i> -Amino Butyric Acid
GC	Gas Chromatography
glyme	Dimethoxyethane
HAT	Hydrogen Atom Transfer
HE	Hantzsch Ester
HOMO	Highest Occupied Molecular Orbital
HRMS	High-Resolution Mass Spectrometry
IC	Internal Conversion
IP	Ionisation Potential
IR	Infrared
ISC	Inter-System Crossing
LED	Light Emitting Diode
LG	Leaving Group
LUMO	Lowest Unoccupied Molecular Orbital
MIDA	<i>N</i> -Methyliminodiacetic acid
MLCT	Metal-to-Ligand Charge Transfer
Mpt	Melting point
NCS	<i>N</i> -Chlorosuccinimide
NMP	<i>N</i> -Methyl-2-pyrrolidone
NMR	Nuclear Magnetic Resonance
PC	Photocatalyst
phen	Phenanthroline

Phth	Phthalimide
pin	Pinacolato
ppy	2-Phenylpyridine
rr	Regiomer Ratio
r.t.	Room Temperature
R _f	Retention factor
RSE	Radical Stabilisation Energy
RSM	Recovered Starting Material
salen	<i>N,N'</i> -Ethylenebis(salicylimine)
SCE	Saturated Calomel Electrode
SET	Single Electron Transfer
SOMO	Singly Occupied Molecular Orbital
TBAB	<i>tert</i> -Butylammonium bromide
TBAI	<i>tert</i> -Butylammonium iodide
TBME	<i>tert</i> -Butyl methyl ether
TBS	<i>tert</i> -Butyldimethylsilyl
TDAE	Tetrakis(dimethylamino)ethylene
TEMPO	2,2,6,6-Tetramethylpiperidine 1-oxyl
TLC	Thin-Layer Chromatography
TM	Transition Metal
TMEDA	Tetramethylethylenediamine
TMU	Tetramethylurea
UHP	Urea Hydrogen Peroxide
μW	Microwave

1.0 Introduction

1.1 Boronic Acids and their Derivatives

1.1.1 Structure and Properties

Boronic acids and their derivatives belong to the family of oxygen-containing organoboron compounds stemming from boranes (Figure 1). These compounds possess a trivalent structure whereby the boron atom is bound to three other substituents. In the case of boronic acids the boron atom is bound to one carbon-based substituent and two hydroxy groups. Changing the hydroxy groups for alkyl/aryl-oxy groups, it becomes a boronic ester. The result of this trivalent structure is a sp^2 -hybridised boron atom with six valence electrons and a vacant p-orbital, which sits perpendicular to the plane of the molecule and is what gives boronic acid derivatives their Lewis acidic properties.^[1] Nucleophiles and bases are able to interact reversibly with this empty p-orbital to give tetrahedral boronate complexes.

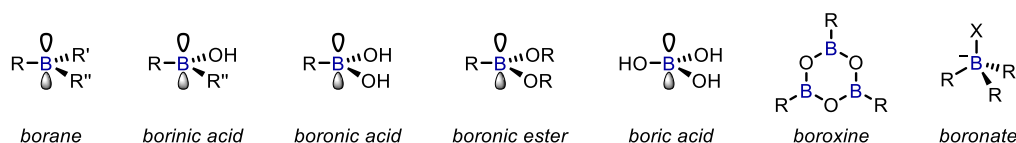


Figure 1. Oxygen-containing organoboron compounds, including borane and boronate. X = nucleophile or base.

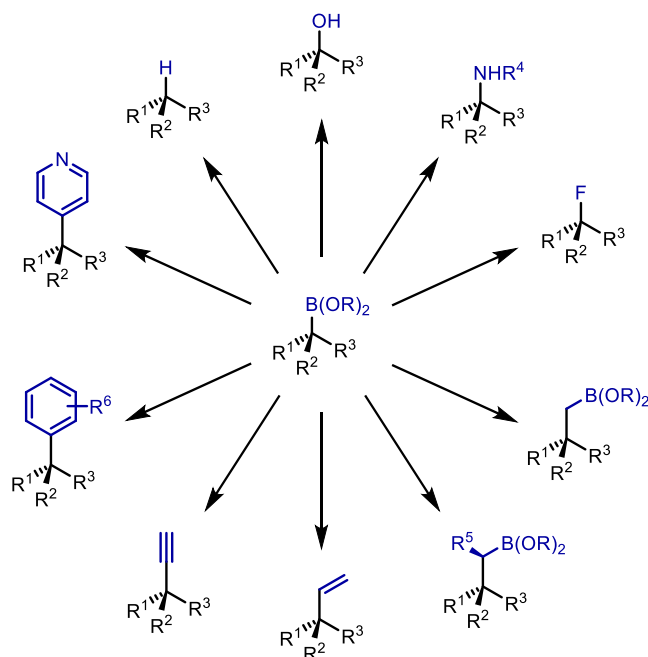
The reactivity and properties of boronic acid derivatives is mainly dependent on the substituents bound to the boron centre. However, in general, boronic acid derivatives are both highly bench- and chemically stable entities despite their wide reactivity profiles. Moreover, they are also considered green compounds due to their low toxicity profiles and environmentally benign degradation products, boric acids.^[2] These properties, and their ability to coordinate and change geometry through p-orbital interactions, is what enables boronic acid derivatives to be effective substrates in both synthetic organic chemistry and medicinal chemistry.

1.1.2 Application in Organic Synthesis

By far the most versatile and synthetically useful of the boronic acid derivatives are the boronic esters. They are less Lewis acidic than the corresponding boronic acids and thus less reactive, due to lone pair

donation from the alkyl/aryl-oxy groups into the empty p-orbital on the boron as a result of the σ -donating ability of the carbon atoms (over the hydrogen atoms). This also makes boronic esters less polar, and therefore easier to handle and purify while still maintaining their high stability and low toxicity.^[3]

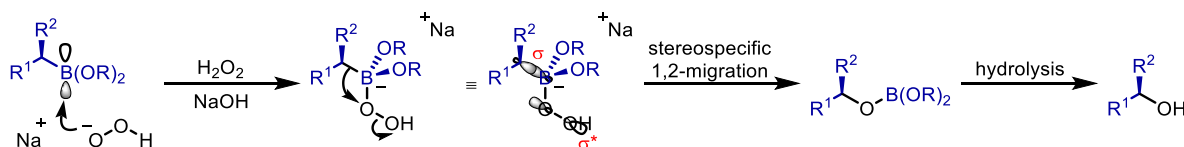
The versatility of boronic esters as synthetically useful building blocks in organic synthesis is exemplified by their ability to be readily transformed into a range of functional groups, forming new carbon-carbon and carbon-heteroatom bonds, often with complete stereocontrol.^[4] Typical transformations of boronic esters are shown in Scheme 1, and include oxidations, aminations, boron homologations, olefinations, alkylations, cross-couplings and protodeboronation. This accessibility to a vast array of functional groups and chemical space with stereocontrol makes boronic esters one of the most valuable functional groups in asymmetric synthesis, by behaving as a key intermediate in the two-step synthesis of almost any functional group. This is exemplified by the sheer number of total syntheses that utilise boronic esters to accomplish the final 3-D structure.^[5]



Scheme 1. Summary of typical transformations of boronic esters.

The oxidation of boronic esters to the corresponding alcohol is one of the more prevalent boronic ester transformations used in synthesis. First reported by Brown and co-workers in 1961 for the oxidation of organoboranes with basic hydrogen peroxide,^[6] boronic esters undergo stereospecific oxidation to the corresponding alcohol with ease and in excellent yields (normally quantitative). This opens up avenues for further functionality, such as ketones, esters, and ethers. The reaction proceeds through the nucleophilic attack of the peroxide anion to the empty p-orbital on boron, to form an intermediate

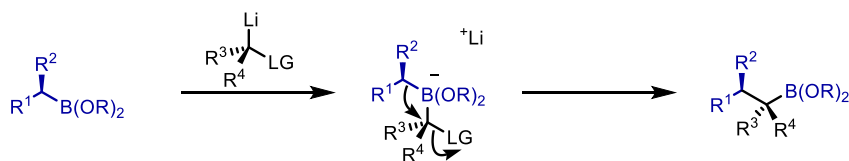
tetrahedral boronate complex. At this point the C-B σ -bond undergoes stereospecific 1,2-migration to the adjacent oxygen, expelling hydroxide (Scheme 2). Hydrolysis of the B-O bond reveals the alcohol product. The migration can only occur if the σ -orbital of the migrating C-B bond is aligned with the σ^* -orbital of the leaving group (hydroxide in this case), thus the migrating group must align anti-periplanar to the leaving group. This leads to retention of stereoconfiguration of the migrating group, but also inversion of the centre which is accepting the migrating group.



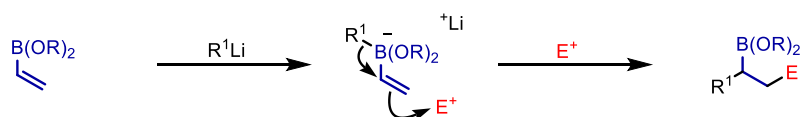
Scheme 2. Oxidation mechanism of boronic esters under basic hydrogen peroxide conditions.

The mechanism of oxidation highlights one of the characteristic polar reactivity pathways of boronate complexes, formed upon addition of a nucleophile to the boronic ester. In the case of a leaving group on the carbon adjacent to the boron atom, stereospecific 1,2-migration takes place (Scheme 3A). The enantioselectivity can either be substrate- (enantioenriched boronic ester) or reagent controlled (enantioenriched nucleophile).^[5] Alternatively, an electrophile-induced 1,2-migration can take place in the case of vinyl boronates (Scheme 3B).^[7] Boronate complexes can also be trapped with a range of electrophiles, with inversion of stereochemistry, by activation with organolithiums which generate (chiral) organometallic-type reagents (Scheme 3C).^[5] Finally, radical 1,2-migrations are also possible through the oxidation of an α -boryl radical (Scheme 3D); these are discussed in detail in section 1.2.2 and 1.2.4.^[8]

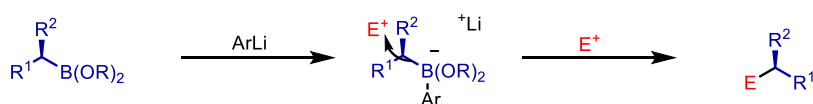
A: stereospecific 1,2-migration



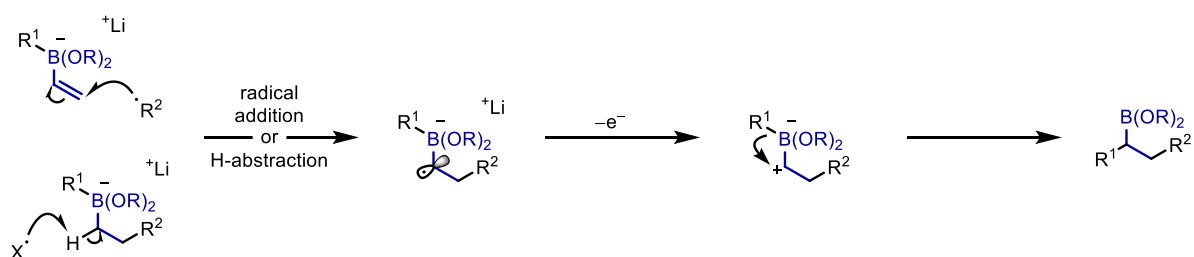
B: electrophile-induced 1,2-migration



C: electrophilic trapping of boronate complex



D: radical-induced 1,2-migration



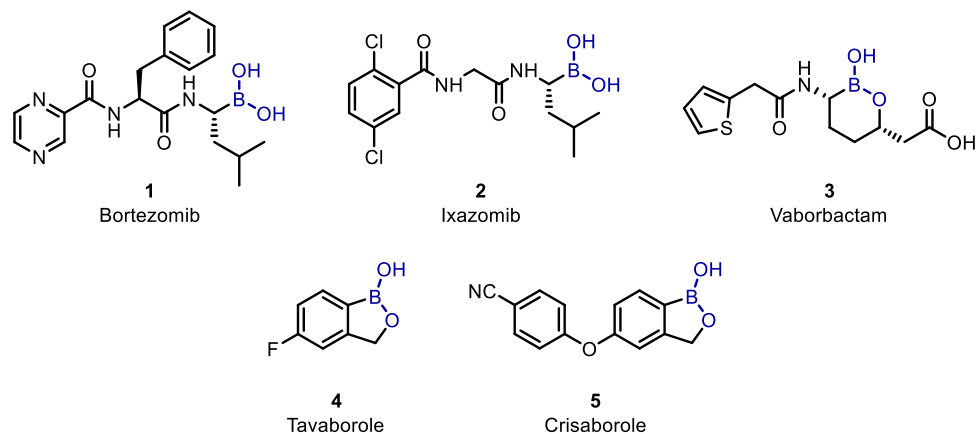
Scheme 3. Summary of reactivity pathways for boronate complexes.

1.1.3 Application in Medicinal Chemistry

In addition to their profound application in organic synthesis, boronic acids and their derivatives occupy a privileged position in medicinal chemistry.^[9] This is due to their ideal coordinate profiles, favourable physicochemical properties under physiological conditions, and low toxicity (boric acid, the degradation product of boronic acids, has a lethal dose similar to table salt).^[10,11] Moreover, occupying the same period as carbon, boronic acids are considered bioisosteres of carboxylic acids.^[12]

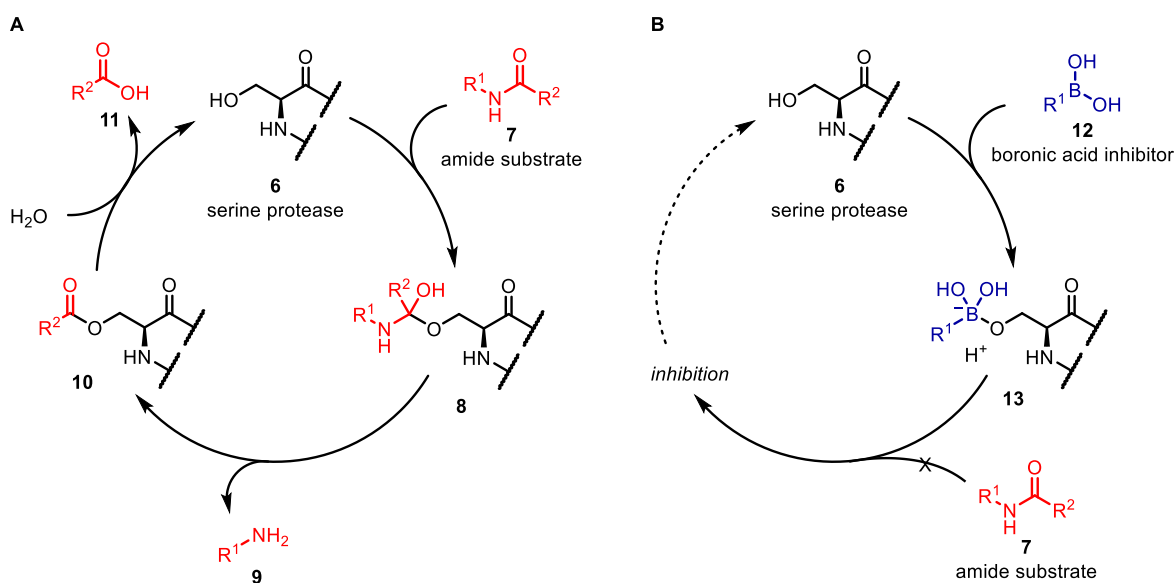
Boronic acids have been known since the 1970's to inhibit enzymatic processes, specifically (serine) proteases, which catalyse the breakdown of proteins and peptides via hydrolysis of the amide bond.^[13,14] From this, extensive research has gone into the application of boronic acids as inhibitors for different proteases with increased selectivity and potency,^[11] such as peptidic boronic acids.^[15] These studies led to the discovery of the two FDA-approved proteasome inhibitors, Bortezomib (**1**)^[16] and Ixazomib (**2**)^[17] for the treatment of multiple myeloma. Cancer treatments are not the only areas where boronic acids and their derivatives have seen application. Vaborbactam (**3**), the β -lactamase inhibitor, is used for the treatment of urinary tract infections in combination with antibiotics. Tavaborole (**4**), is an antifungal

agent used in the treatment of onychomycosis, and its analogue Crisaborole (**5**), is used to treat eczema (Scheme 4).^[10,18]



Scheme 4. Clinically approved boron-containing drugs.

Key to the success of boronic acids and their derivatives as protease inhibitors is their mild Lewis acidity. Boronic acids remain uncharged under physiological conditions and can reversibly interact with nucleophilic residues (oxygen and nitrogen) located in the target enzymes' active site. This Lewis acid-base interaction results in the formation of a boronate complex, which is equivalent to that of a sp^3 -hybridised carbon.^[10,12] For example, the inhibition mechanism of serine protease involves the formation of a boronate complex **13** through the coordination of the hydroxyl group of a serine residue **6**. It is this boronate complex which mimics the tetrahedral carbon intermediates **8** formed during amide bond hydrolysis and therefore blocks binding of the amide substrate **7** to the serine protease **6** (Scheme 5).^[1]

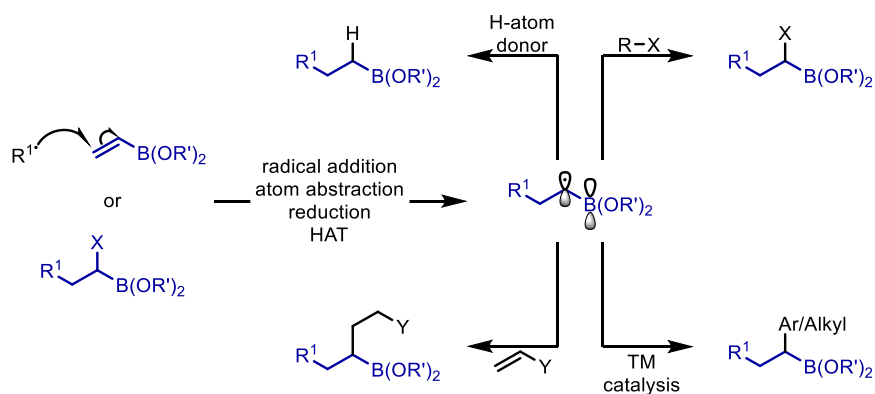


Scheme 5. A) Simplified mechanism of serine protease, with the histidine and aspartate residues removed for clarity.^[19] B) Inhibition pathway of serine protease by a boronic acid.

1.2 α -Boryl Radicals in Organic Synthesis

With the vast applications boronic acids and their derivatives have in synthetic organic chemistry and medicinal chemistry, it is no surprise that extensive research has been conducted into ways to incorporate boronic acid derivatives into both synthetically useful and biologically active molecules. For organic synthesis, boronic acid derivatives, specifically boronic esters, can be easily accessed through catalytic methods, such as hydroboration^[20] and C-H activation,^[21] or stoichiometric methods such as lithiation-borylation^[22] and more recently, mild radical borylations.^[23] These methods enable the rapid incorporation of boronic esters into organic molecules, even in an asymmetric fashion.^[24]

The use of α -boryl radicals in organic synthesis has seen a recent surge in research interest as a way to both introduce a boronic ester group into a molecule, but also functionalise boronic esters at the adjacent carbon, leaving the boronic ester group intact for further manipulation.^[25] α -Boryl radicals have the potential to open up new avenues of reactivity through novel disconnections, which would otherwise be inaccessible via their polar counterpart, whilst also demonstrating superior functional group tolerance. They can be accessed through three different modes: radical additions to unsaturated boronic esters, atom abstraction or reduction of α -halo boronic esters, or through hydrogen atom transfer (HAT). From the intermediate α -boryl radical, a range of different functionalisations can take place, including atom abstractions, further radical addition reactions, or transition metal cross-couplings (Scheme 6).

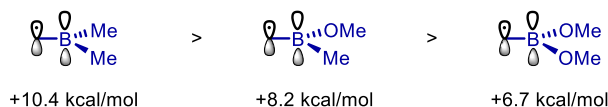


Scheme 6. The formation and functionalisation of α -boryl radicals in organic synthesis.

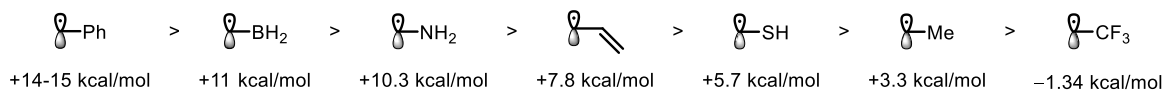
The characteristic feature of α -boryl radicals, and what enables them to be such effective intermediates in organic synthesis, is the ability of the empty p-orbital on boron to stabilise the adjacent carbon-centred radical. This was first recognised by Matteson in 1959 when he observed experimentally that the first radical transfer constant for atom transfer radical addition (ATRA) of CCl_4 to a vinyl boronic ester was similar to that of styrene (*vide infra*), providing evidence for stabilisation of the α -boryl radical intermediate by carbon-boron π -bond overlap.^[26,27] This α -boryl radical stabilisation by carbon-boron π -bond overlap was further confirmed by Walton and Carboni, using low temperature EPR spectroscopy. They found that the barrier for internal rotation about the $^{\bullet}\text{C}$ -B bond of the α -boryl radical was 3 ± 1 kcal/mol (a typical hydrocarbon radical such as $\text{H}_2\text{C}^{\bullet}\text{-C}_5\text{H}_9$ has a measured barrier for rotation of 0.5 kcal/mol).^[28] Walton and Carboni also computed the radical stabilisation energies (RSE) of various organoborons (Scheme 7A).^[28] RSEs are used to quantify the stabilities of radical species and as there is no way to define the absolute stability of a radical, these are relative quantities.^[29] It is defined by the energy difference of a group adjacent to a carbon-centred radical to stabilise or destabilise the radical relative to a hydrogen atom.^[30,31] A positive RSE implies net stabilisation of a radical compared to a methyl radical, whereas a negative value implies net destabilisation compared to a methyl radical. Walton and Carboni found the stability of an α -borane radical to be +10.4 kcal/mol, and increasing the number of oxygen substituents on boron resulted in decreased RSE, with a borinic ester giving an RSE of +8.2 kcal/mol and a boronic ester +6.7 kcal/mol. These results are consistent with one-electron stabilisation arising from p-orbital overlap of the carbon-centred radical with boron. The decrease in RSE, following the order borane > borinic ester > boronic ester, is a result of increased donation of electron density from the lone pair on the oxygen substituents into the vacant p-orbital, reducing its ability to interact with the adjacent radical. These RSEs can be compared to a range of other functional groups adjacent to a carbon-centred radical, such as trifluoromethyl (which is destabilising), methyl, vinyl, amino and phenyl. In these cases a different level of theory was used to compute the RSEs, with methyl borane giving a RSE of +11 kcal/mol, which can be used as a reference point (Scheme 7B).^[30] It is this radical stability which enables α -boryl radicals to be effective intermediates in organic

synthesis and participate in an array of different radical reactions, giving access to complex boron containing compounds. These different modes of reactivity are highlighted in the subsequent sections.

A: RSEs of organoborons



B: RSE scale



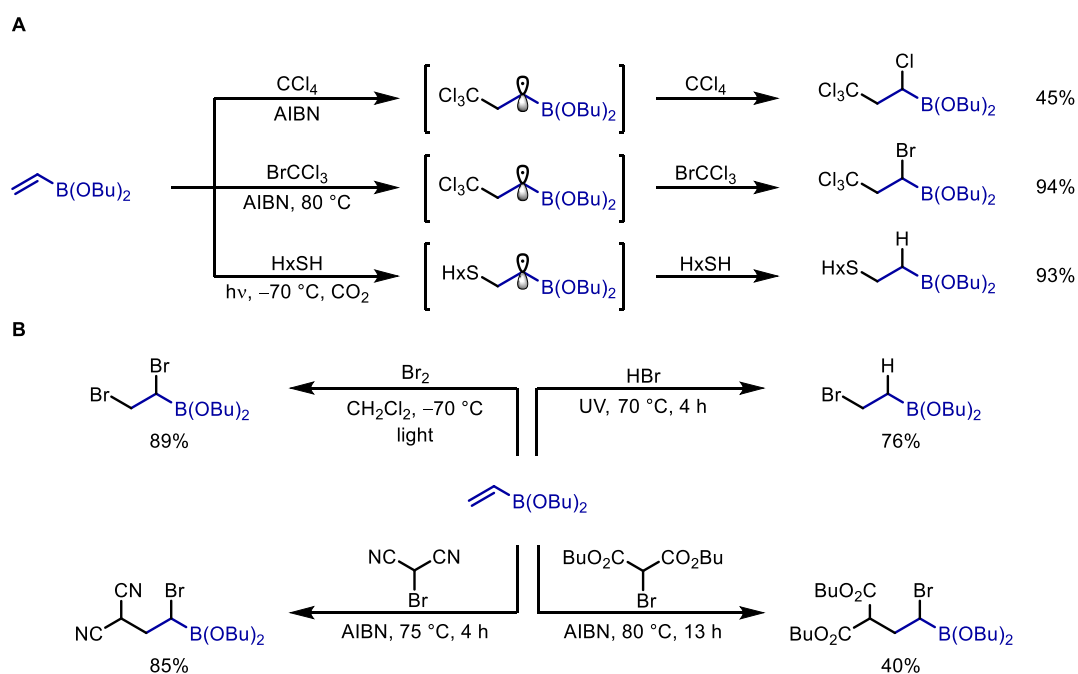
Scheme 7. A) RSEs of organoborons.^[28] B) RSEs of a range of functional groups adjacent to a carbon-centred radical.^[30]

1.2.1 Radical Additions to Vinyl Boronic Esters

Radical addition reactions to electron-deficient alkenes have received a lot of attention due to the synthetic utility of generating carbon-carbon bonds with excellent site-selectivity and functional group tolerance.^[32] There has also been a recent surge in using vinyl boronic esters as Michael acceptors, as an efficient way to access alkyl boronic esters.^[33] Electron-rich (nucleophilic) radicals, those with high energy singly occupied molecular orbitals (SOMO), readily undergo radical addition (conjugate addition) reactions to vinyl boronic esters to yield stabilised α -boryl radical intermediates. The mildly electron-deficient boronic ester group lowers the energy of the lowest unoccupied molecular orbital (LUMO), allowing greater overlap of the SOMO and LUMO. From this α -boryl radical intermediate, three different α -boryl functionalisations can take place: atom abstraction (from ATRA), trapping with a transition metal catalyst (additional discussion in section 4.1) or single-electron transfer (not discussed, see section 2.0 and 3.0).

Matteson reported the first ATRA reaction to vinyl boronic esters in 1959 (Scheme 8A).^[26] Using the radical initiator AIBN, the radical precursors, CCl_4 , BrCCl_3 and HxSH underwent atom abstraction to generate the corresponding carbon- or sulfur-centred radical. This could then undergo radical addition to the vinyl boronic ester to give the α -boryl radical intermediate. Propagation of the radical chain occurred with further atom abstraction, which in turn gives the alkyl boronic ester products in modest to excellent yields. Matteson later expanded this ATRA to include α - and β -substituted vinyl boronic esters, whereby only the more reactive BrCCl_3 could undergo ATRA to β -methyl vinyl boronic ester. Further calculations were also carried out for the first transfer constant for the radical addition, providing more evidence that the intermediate α -boryl radical is stabilised by carbon-boron π -bonding.^[27]

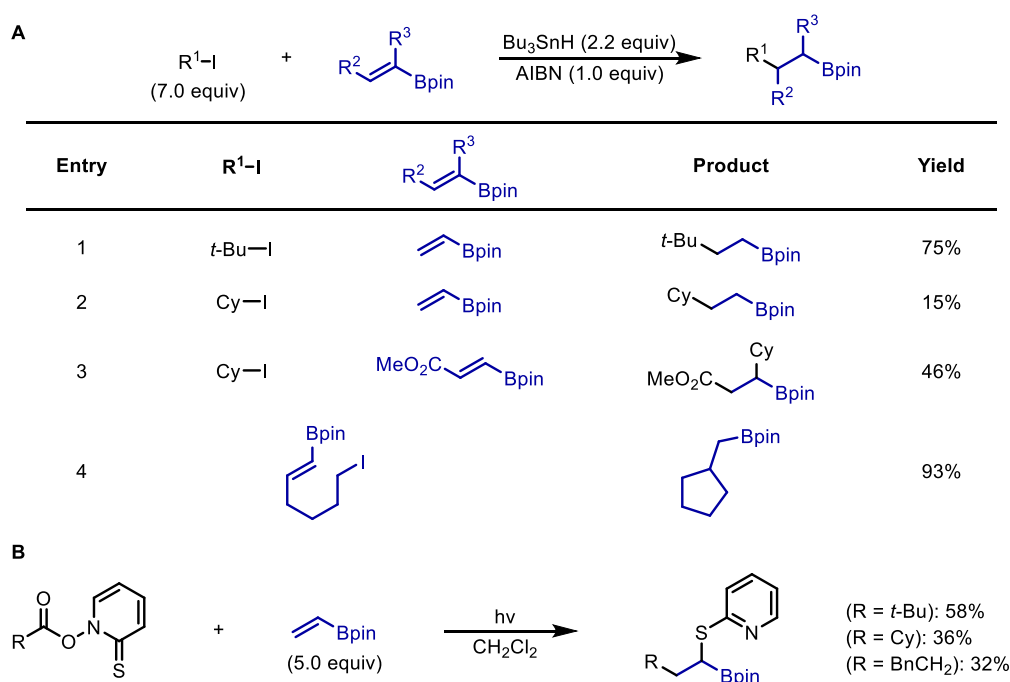
In the early to mid-1960's, Matteson expanded the scope of ATRA's to vinyl boronic esters by the dibromination and hydrobromination of vinyl boronic esters in excellent yields (Scheme 8B, top).^[34,35] Moreover, Matteson showed that even electron-deficient (electrophilic) radicals, such as those derived from bromomalononitrile and dibutyl bromomalonate, could undergo ATRA to vinyl boronic esters in modest to good yields (Scheme 8B, bottom).^[36] These examples highlight the ambiphilic nature of vinyl boronic esters, due to the mild electron-withdrawing nature of the boronic ester group. Interestingly, attempts to add bromomalononitrile to other olefins such as vinyl acetates, octene, acrylonitrile and ethyl acrylate resulted in polymeric mixtures. This suggests the α -boryl radical is significantly persistent, and is therefore able to abstract another bromine atom from bromomalononitrile to propagate the radical chain rather than undergoing radical addition to another molecule of vinyl boronic ester leading to detrimental polymerisation.



Scheme 8. ATRA reactions of vinyl boronic esters reported by Matteson.

Around twenty years later, Carboni and co-workers reported the inter- and intra-molecular radical additions of carbon-centred radicals to vinyl boronic esters from the corresponding alkyl iodides (Scheme 9A).^[37] Treatment of these alkyl iodides with AIBN and Bu_3SnH resulted in iodide abstraction, generating the corresponding alkyl radical, which underwent radical addition to the vinyl boronic ester. Hydrogen atom abstraction from the Bu_3SnH gave the alkyl boronic ester products. The effect of the radical nucleophilicity is exemplified in these cases, whereby the more nucleophilic *tert*-butyl radical gave a better yield overall (entry 1 vs 2). Unsurprisingly, in the case of the β -ester vinyl boronic ester, regioselectivity was reversed due to the greater electron-withdrawing nature of the ester group versus the boronic ester (entry 3). Intramolecular radical addition from the primary radical generated from the

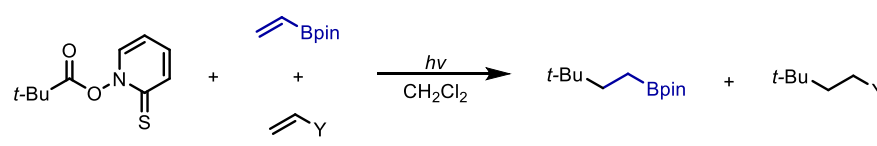
corresponding alkyl iodide proceeded to give the 5-*exo*-trig cyclisation product in excellent yield (93%, entry 4). Lee and co-workers also showed that these intramolecular radical additions to vinyl boronic esters were feasible using alkyl bromides and aldehydes (via α -oxy radical) under similar conditions.^[38] These types of radical addition reactions to electron-deficient alkenes, using Bu_3SnH , were termed the Giese reaction after the German chemist Bernd Giese.^[39] Carboni showed that Barton esters were also suitable radical precursors to carbon-centred radicals and showed that these could give the ATRA products in modest yields (Scheme 9B).



Scheme 9. Radical addition reactions to vinyl boronic esters reported by Carboni, showing selected examples. A) inter- and intramolecular addition using alkyl iodides as the radical precursor. B) Barton esters as radical precursors.

In the same report by Carboni and co-workers,^[37] the authors conducted competition experiments comparing the selectivity of a *tert*-butyl radical (generated from the corresponding Barton ester) to a series of different electron-deficient alkenes in comparison to vinyl-Bpin (Table 1). The Barton ester was irradiated in the presence of a 1:1 mixture of vinyl-Bpin and another electron-deficient alkene, and the product ratios were compared. The results showed that both the acrylate and the vinyl amide were more reactive towards the *tert*-butyl radical, signifying that they are better radical traps than vinyl-Bpin (entries 1 and 2). This was previously observed when the β -ester vinyl boronic ester was used as a radical trap, showing a switch in site-selectivity for the radical addition (Scheme 9A, entry 3). Incorporating electron-withdrawing groups on the boronic ester backbone also increased its reactivity towards the nucleophilic radical (entry 3). The only example where vinyl-Bpin was a better radical trap

was when styrene was employed, which gave exclusively the boronic ester product (entry 4). This was also observed by Pasto, where hydrobromination of ethylene β -styreneboronic ester gave site-selectivity consistent with the observations made by Carboni.^[40] Pasto proposed that the strong interaction between the vinyl group and the empty p-orbital on boron may provide greater stabilisation for the α -boryl radical intermediate along the reaction coordinate than is afforded by the aromatic system. These competition experiments give a good indication of where vinyl boronic esters lie on the reactivity scale with regards to other Michael acceptors.



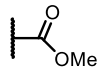
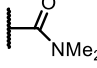
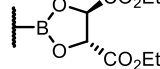
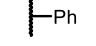
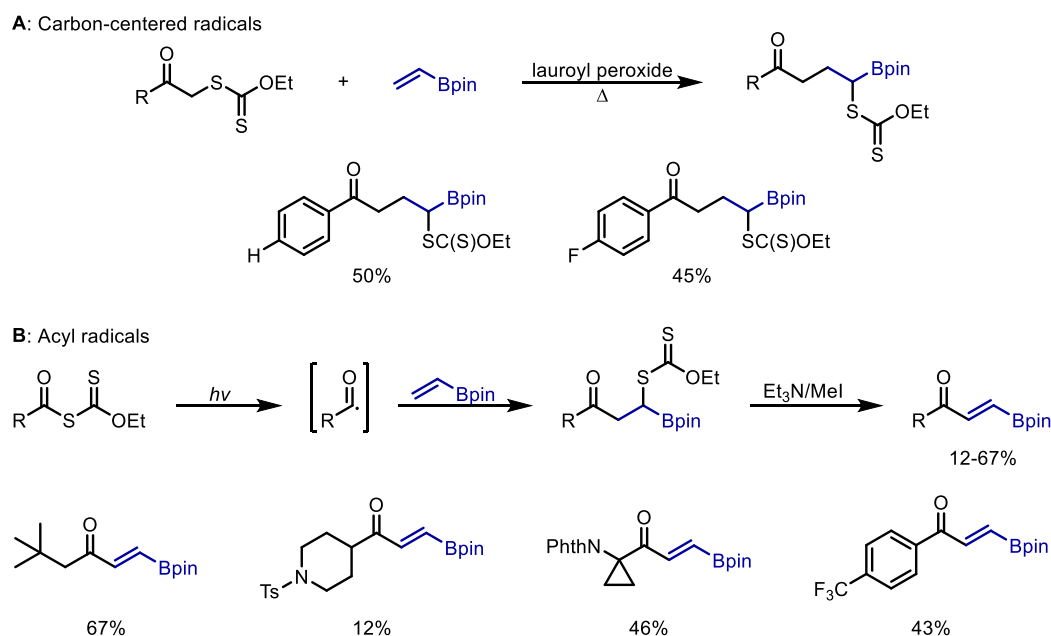
Entry	Y	Ratio	
		t-Bu-CH ₂ -CH ₂ -Bpin	t-Bu-CH ₂ -CH ₂ -Y
1		4	96
2		20	80
3		28	72
4		100	0

Table 1. Competition experiments comparing the radical additions of *tert*-butyl radicals to 1:1 vinyl-Bpin: electron-deficient alkenes.

In the early 2000's, Zard reported the use of xanthates as radical precursors, which could be used in ATRA with vinyl boronic esters (Scheme 10). In the first report, α -carbonyl xanthates were used in the presence of the radical initiator lauroyl peroxide to give an α -carbonyl radical, the radical equivalent of an enolate.^[41] Initially, these radicals were trapped with allyl boronic esters, but two examples with vinyl boronic esters were given and provided the α -xanthate boronic ester products in modest yields (Scheme 10A). As with the previous ATRA examples, this reaction proceeded under a radical chain mechanism. This method was later expanded to access γ -carbonyl vinyl boronic esters (Scheme 10B).^[42] By irradiating an acyl xanthate with a tungsten-halogen lamp, the resulting acyl radical can undergo radical addition to the vinyl boronic ester, with the α -boryl radical intermediate trapping out another xanthate group to propagate the chain mechanism. Competing premature decarboxylation was found to be problematic and depended on the stability of the resulting decarbonylated radical. Finally, treatment of the α -xanthate boronic ester products with triethylamine and methyl iodide resulted in the elimination of the xanthate group to afford the γ -carbonyl vinyl boronic ester products in satisfactory yields. This

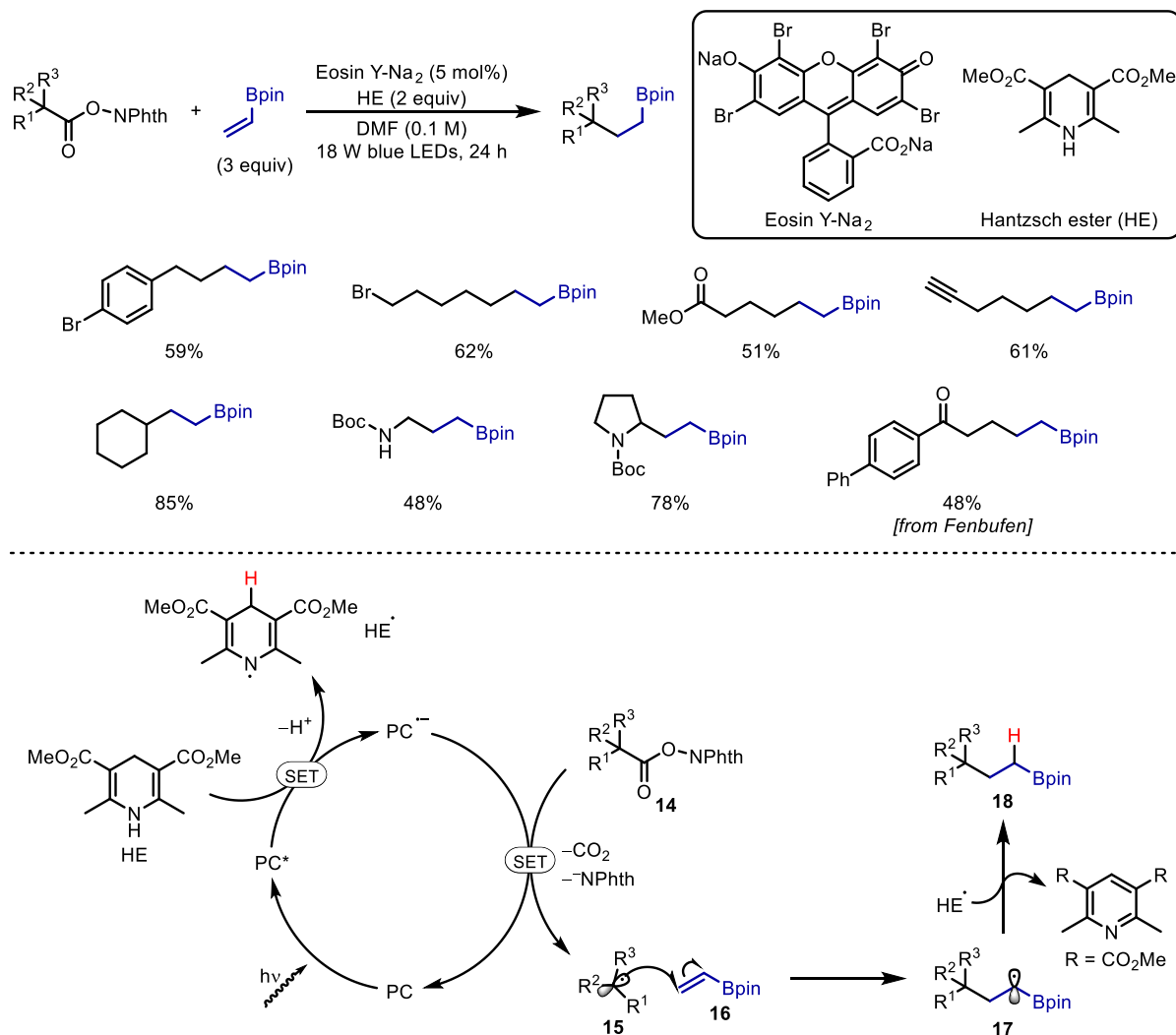
was a resourceful way to utilise the xanthate as both a radical and ionic leaving group, the former to generate the radical and the latter to allow the elimination to occur.



Scheme 10. Zard's ATRA reactions to vinyl boronic esters using xanthates as radical precursors. A) Addition of carbon-centred radicals to vinyl-Bpin. B) Addition of acyl radicals to vinyl-Bpin with selected examples.

Much more recently, Liao and co-workers reported a decarboxylative radical addition reaction to vinyl boronic esters using photoredox catalysis, with redox-active esters as the radical precursors (Scheme 11).^[43] This comes two years after the decarboxylative radical addition reaction to vinyl boronic esters reported by Aggarwal and co-workers, which uses abundant carboxylic acids as radical precursors (the work presented in this report, see section 2.0).^[44] The work focuses mainly on the use of primary, secondary and tertiary alkyl carboxylic acids (as the redox-active esters), which after the generation of the carbon-centred radical can undergo radical addition to vinyl-Bpin in good yields. The reaction is not only limited to alkyl carboxylic acids, but amino acids can also be utilised, in addition to natural products and drugs, such as fenbufen. The reaction is proposed to proceed via a photoredox cycle (see section 1.3); initial photoexcitation of the organic photocatalyst Eosin Y- Na_2 (PC) gives an oxidising species (PC*), which can be reductively quenched by the Hantzsch ester (HE) via single-electron transfer to give a highly reducing reduced state photocatalyst (PC⁻) and [•]HE radical (after deprotonation). Single-electron reduction from PC⁻ to the redox-active ester **14** results in extrusion of the phthalimide anion and CO_2 , giving the alkyl radical **15**. Radical addition to the vinyl boronic ester **16** affords the stabilised α -boryl radical intermediate **17**, which then subsequently abstracts a hydrogen atom from [•]HE to yield the alkyl boronic ester product **18** and the pyridine derivative by-product.

Radical trap experiments with TEMPO revealed that the redox-active ester produces the corresponding alkyl radical, and deuterium labelling studies confirmed that HE was the source of hydrogen atoms.

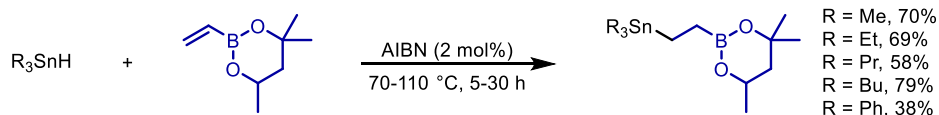


Scheme 11. Liao's photoredox-catalysed decarboxylative radical addition reaction to vinyl boronic esters using redox-active esters as the source of alkyl radical. Showing selected examples and the proposed mechanism.

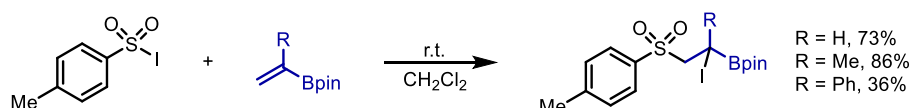
ATRA reactions to vinyl boronic esters are not only limited to carbon-centred radicals, heteroatom-centred radicals have also been used. In addition to the examples previously seen by Matteson (hydro-sulfonation, dibromination and hydrobromination (*vide supra*)), hydrostannation and halosulfonylation have also been reported, building upon the chemistry already developed for the addition of carbon-centred radicals. Fish showed that vinyl boronic esters could readily undergo hydrostannation (Scheme 12A).^[45] Five different organotin hydrides were added across the vinyl boronic ester in moderate to good yields, by heating the organotin hydride in the presence of the AIBN initiator. The reaction could also be conducted in the absence of AIBN, albeit at a significantly slower rate.

Besides Carboni's work on the addition of carbon-centred radicals to vinyl boronic esters, Carboni also reported the free-radical halosulfonylation of vinyl boronic esters (Scheme 12B).^[46] Various vinyl boronic esters were treated with *para*-toluenesulfonyl iodide at room temperature, to yield the α -iodo- β -sulfonyl boronic ester products in good yields.

A: Hydrostannation

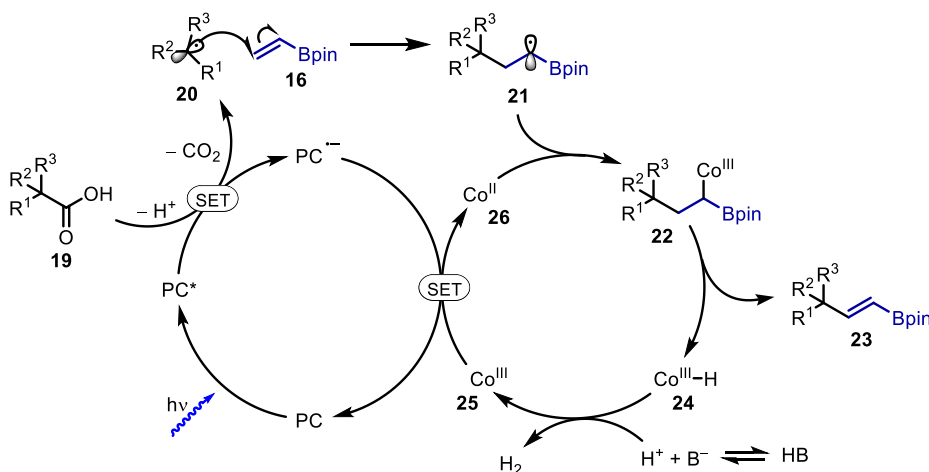
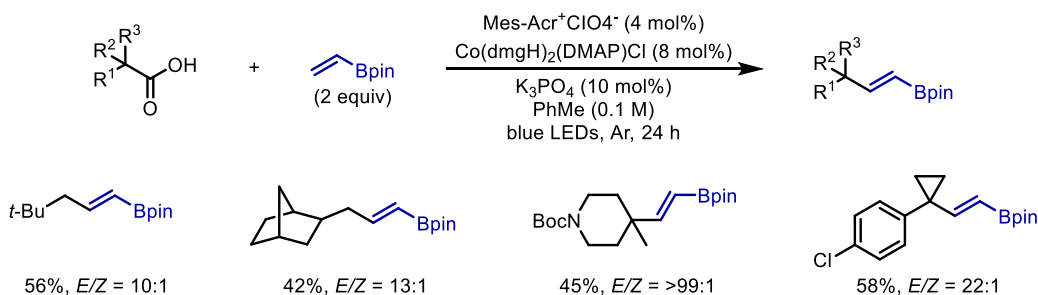


B: Halosulfonylation



Scheme 12. Addition of non-carbon-centred radicals to vinyl boronic ester via ATRA.

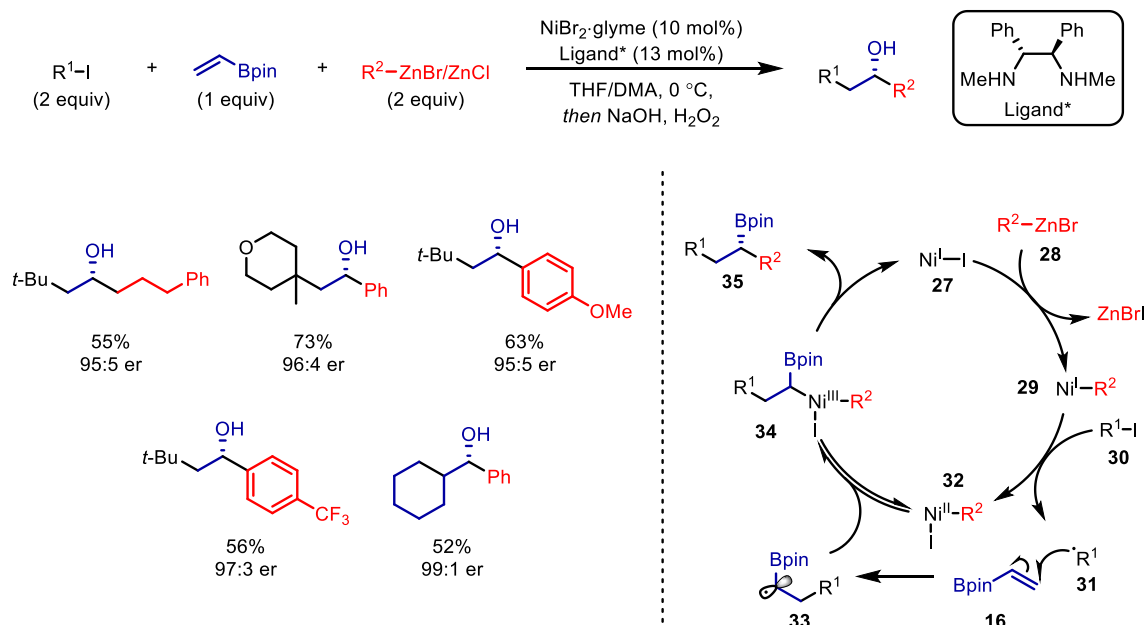
As well as ATRA reactions with vinyl boronic esters, radical addition reactions and subsequent trapping of the intermediate α -boryl radicals with transition metals to carry out further functionalisation have also been reported (see section 4.1.1 for further examples). Wu and co-workers reported a decarboxylative Heck-type coupling of alkyl carboxylic acids with a variety of olefins.^[47] Included in the scope were a number of examples which utilised vinyl boronic esters as the radical trap (Scheme 13). The reaction was achieved through the combination of an organo-photocatalyst and a cobalt catalyst. The corresponding substituted vinyl boronic acid products could be achieved in good yields with high selectivity for the *E*-isomer. Only sterically hindered carboxylic acids were used, presumably due to their slow rate of reactivity which favoured addition to the vinyl boronic ester over direct addition to the cobalt catalyst. The authors propose a dual catalytic mechanism, which involves initial photoexcitation of the Mes-Acr⁺ClO₄⁻ photocatalyst (PC) to generate a highly oxidising species (PC*). Single-electron transfer between PC* and the carboxylate of acid **19**, followed by loss of CO₂, yields the alkyl radical **20** and PC⁻. Radical addition to the vinyl boronic ester **16** yields the stabilised α -boryl radical intermediate **21**, which is subsequently trapped by Co(II) catalyst **26** to give the cobalt species **22**. β -Hydride elimination then affords the vinyl boronic ester product **23** and Co(III) hydride **24**. This hydride species can then react with either a proton or another molecule of **24** to release H₂ and generate Co(III) (**25**). Final single-electron transfer between **25** and PC⁻ completes the catalytic cycle. Radical clock and trapping experiments, Stern-Volmer fluorescence quenching studies and DFT calculations support this proposed mechanism.



Scheme 13. Wu's decarboxylative Heck-type coupling of carboxylic acids and olefins, showing selected vinyl boronic ester examples and the proposed mechanism.

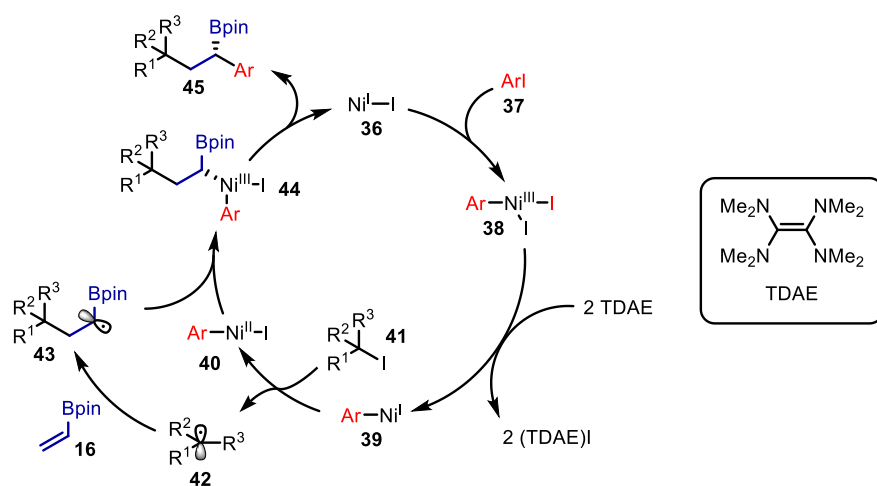
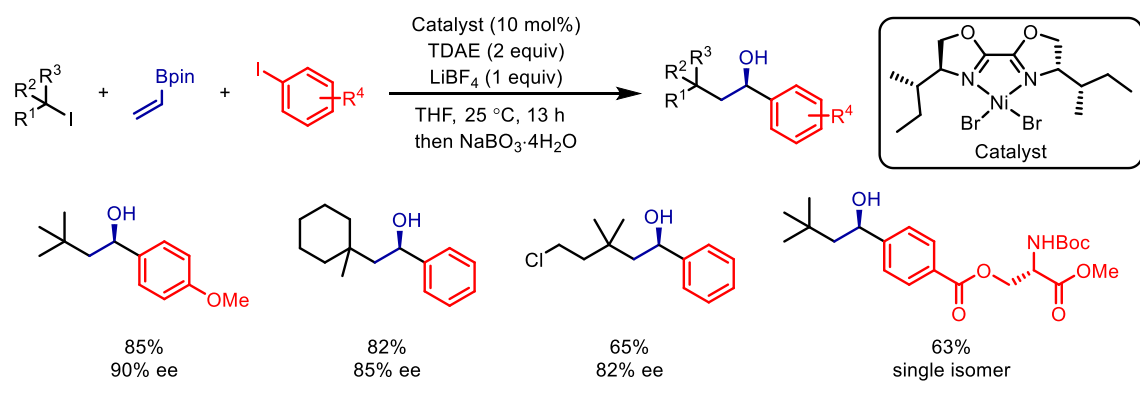
In 2019, Morcken and co-workers reported an enantioselective nickel-catalysed conjunctive cross-coupling of vinyl boronic esters with alkyl iodides and organozinc reagents to yield functionalised boronic ester products in high enantioselectivities using a chiral diamine ligand (Scheme 14).^[48] The reaction could be conducted both intermolecularly with tertiary alkyl iodides or intramolecularly with primary iodides tethered to the vinyl boronic ester, with a range of primary or aromatic organozinc reagents, providing the conjunctive cross-coupled products in useful yields and good enantiomeric ratios (er). Generally, enantioselectivities were better in the intramolecular variant and the reaction was unproductive with secondary, benzylic, allylic, and α -heteroatom iodides, presumably due to competing direct two-component coupling between the alkyl iodide and the organozinc reagent. Mechanistic studies are in favour of the proposed catalytic cycle depicted in Scheme 14. An *in situ* generated Ni(I) complex **27** initially undergoes transmetalation with the organozinc reagent **28** to give Ni(I) species **29**. **29** can then abstract the iodide from the alkyl iodide radical precursor to give the corresponding alkyl radical **31** and Ni(II) species **32**. Radical addition of **31** to the vinyl boronic ester **16** gives the intermediate α -boryl radical **33**, which is subsequently trapped by **32** to give the Ni(III) complex **34**. This trapping furnishes two equilibrating diastereomeric Ni(III) complexes **34**, one of which reductively

eliminates at a faster rate leading to the major enantiomer of the conjunctive cross-coupled product **35**,^[49] and regenerates the active Ni(I) catalyst **27**.



Scheme 14. Morcken's enantioselective nickel-catalysed conjunctive cross-coupling of vinyl boronic esters with alkyl iodides and organozinc reagents, showing selected examples and the proposed catalytic cycle.

More recently, Nevado and co-workers reported an asymmetric nickel-catalysed reductive conjunctive cross-coupling of alkenes with alkyl iodides and aryl iodides (Scheme 15).^[50] In this cross-electrophilic coupling, vinyl-Bpin was a competent olefin acceptor in combination with tertiary alkyl iodides and electron-rich aryl iodides. Using TDAE as the organic reductant and a chiral (bis)oxazoline ligand, the enantioenriched benzylic boronic ester products could be obtained in good yields and high ee. The reaction proceeds via a reductive nickel catalytic cycle, previously reported by the group.^[51,52] Initial oxidative addition of the aryl iodide **37** to Ni(I) **36** gives a Ni(III) intermediate **38**, which is reduced by TDAE to give the aryl Ni(I) species **39**. This can then activate alkyl iodide **41** to give the corresponding radical **42** and Ni(II) (**40**). The radical adds to the vinyl boronic ester and is subsequently trapped by **40** to give the alkyl Ni(III) complex **44**. Reductive elimination yields the enantioenriched boronic ester product **45**, completing the catalytic cycle. DFT calculations showed that the Ni(III) intermediate **44** is stabilised by coordinating sites on the olefin (the diol of the boronic ester), which contributes to the stereochemical outcome in the reductive elimination step.



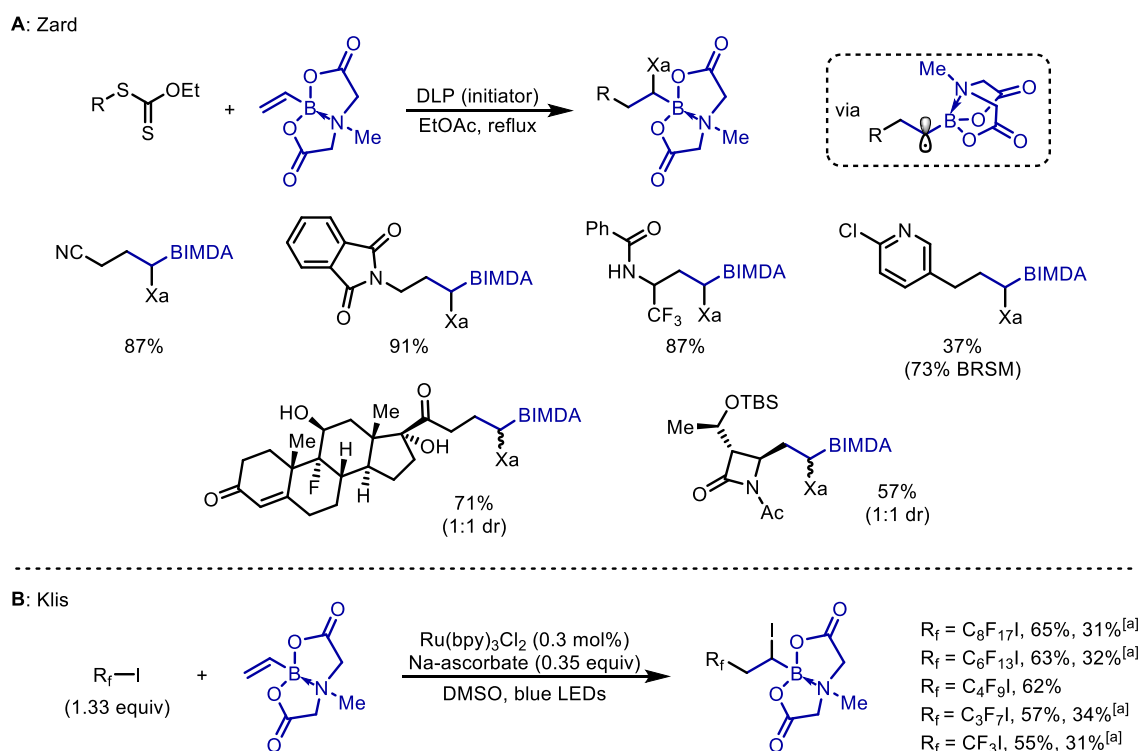
Scheme 15. Nevado's asymmetric nickel-catalysed reductive conjunctive cross-coupling of alkenes, showing selected examples with vinyl-Bpin.

1.2.2 Radical Additions to Vinyl Boronate Complexes

Although still in its infancy, radical additions to vinyl boronate complexes to generate unstabilised α -boryl radicals have also been reported. In contrast to vinyl boronic esters, vinyl boronate complexes bear an electron-rich alkene, and so show high reactivity towards electron-deficient (electrophilic) radicals, this time with optimal SOMO-HOMO interactions. From the α -boryl radical intermediate generated, two further transformations are possible: atom abstraction (ATRA) or radical-induced 1,2-migration.^[8]

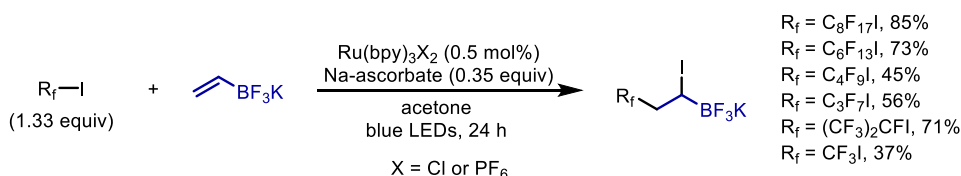
Zard was the first to report ATRA to vinyl boronate complexes, specifically vinyl-BMIDA, in which a dative bond between the nitrogen and the empty p-orbital on boron closes off any stabilisation of the adjacent α -boryl radical.^[53] Using xanthates as radical precursors, Zard showed that they could undergo ATRA smoothly with vinyl-BMIDA in good yields with both electrophilic and also mildly nucleophilic radicals (Scheme 16A). In a related report by Kliš and co-workers, the authors also reported an ATRA reaction of perfluoroalkyl iodides to vinyl-BMIDA boronate complexes, achieving the corresponding

α -iodo BMIDA boronate products in modest yields (Scheme 16B).^[54] Both these processes proceed under radical chain mechanisms and in the former dilauroyl peroxide (DLP) is used as the radical initiator, in the latter case the photocatalyst is only required as the initiator. The fact that the photocatalyst is required is most likely due to an inefficient radical chain process, which aids in the reduction of the perfluoroalkyl iodides to the corresponding electrophilic radical, with Na-ascorbate behaving as a sacrificial reductant. Attempts to utilise diethyl bromomalonate as the radical precursor to the electrophilic malonate radical proved unsuccessful. Kliš also used this methodology on ethynyl-BMIDA boronate complexes to yield to the α -iodo vinyl-BMIDA perfluoroalkyl products (not shown).



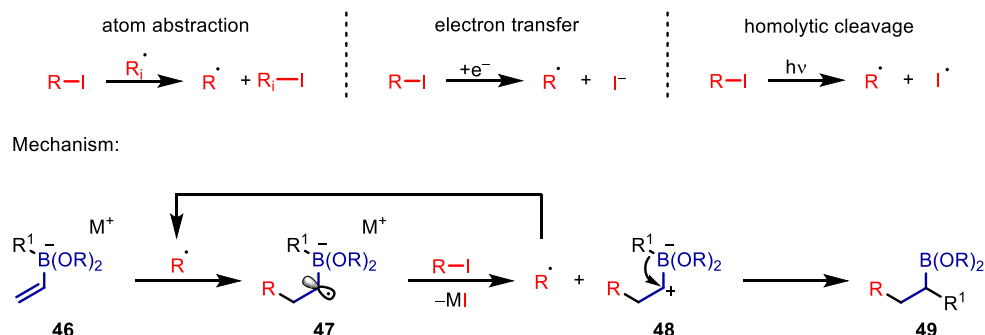
Scheme 16. ATRA reactions to vinyl-BMIDA. [a] No Na-ascorbate, LiBr (1.0 equiv).

Later, Kliš and co-workers also reported the photoredox-catalysed ATRA of perfluoroalkyl iodides with vinyl-BF₃K under similar reaction conditions (Scheme 17).^[55] These reactions gave improved yields over the analogous ATRA of perfluoroalkyl iodides with vinyl-BMIDA boronate complexes. This is in line with the recent observations made by Ueda and co-workers, who compared the atom abstraction ability of three different α -boryl radicals – α -Bpin, α -BMIDA and α -BF₃K – by carrying out the ATRA of alkyl bromides to the corresponding vinyl-organoborons.^[56] They found that higher reactivity was observed in the case of the α -BF₃K radical and could be attributed to the formation of a pseudo-radical anion due to the electron donation from the BF₃K group, making it more nucleophilic.



Scheme 17. Kliś ATRA to vinyl-BF₃K.

Vinyl boronate complexes formed by the addition of an organolithium or Grignard reagent to a vinyl boronic ester are also highly reactive towards electrophilic radicals. In these cases, functionalisation of the α -boryl radical occurs via a radical-induced 1,2-migration.^[8] Studer,^[57] Renaud,^[58] Aggarwal^[59] and Shi^[60] each independently reported radical-induced 1,2-migrations of vinyl boronate complexes, which proceed via the general radical chain mechanism depicted in Scheme 18. Initiation of the electrophilic radical from the corresponding alkyl halide can either occur through atom abstraction, electron transfer or homolytic cleavage. Then, radical addition of these electrophilic radicals to the vinyl boronate complex **46** gives α -boryl radical intermediate **47**. Rapid single-electron transfer between **47** and another molecule of alkyl halide results in the oxidation of α -boryl radical **47** to the corresponding carbocation **48**, which induces rapid 1,2-migration of the former organolithium/Grignard reagent to give boronic ester **49**. This SET propagates the radical chain process. An alternative mechanism involving the abstraction of the halide from the α -boryl radical intermediate to give an α -halo boronate complex, which can also promote 1,2-migration, has been ruled out by mechanistic studies in each case.



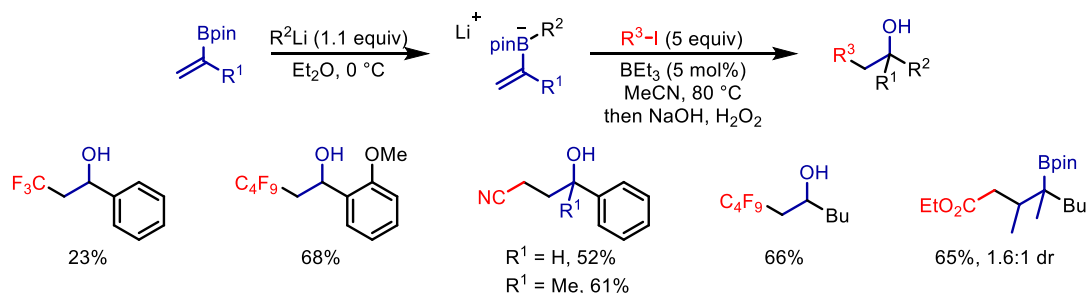
Scheme 18. General mechanism for the radical-induced 1,2-migration of vinyl boronate complexes proceeding via a radical chain process.

Studer and co-workers reported in 2017 the first radical-induced 1,2-migration between vinyl boronate complexes and electrophilic radical precursors, including perfluoroalkyl iodides, iodoacetonitrile and α -iodoesters, using BEt₃ as the radical initiator (Scheme 19A).^[57] Treatment of a vinyl boronic ester with a primary or secondary alkyl- or aryl-lithium generated the vinyl boronate complex *in situ*. Solvent switch to MeCN enabled the radical addition to yield the α -boryl radical intermediate, which upon oxidation promoted 1,2-migration. A range of highly functionalised boronic ester products could be

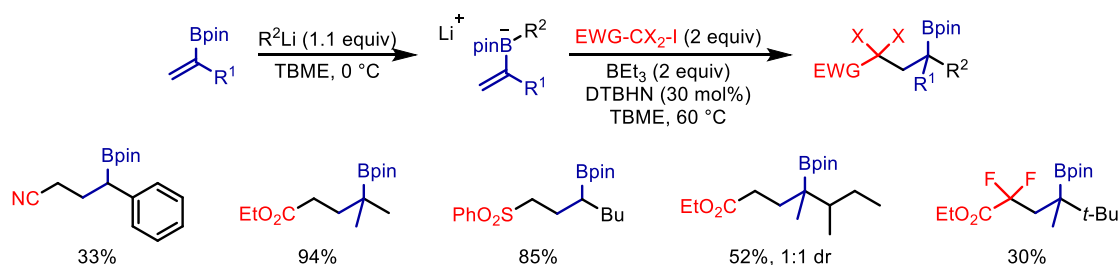
obtained in good yields (the boronic esters were oxidised for convenience in the substrate scope). Studer extended this methodology by adding vinyl organolithiums to chiral boronic esters to in order to eventually synthesise α -chiral ketones and chiral alkanes (not shown).^[61] In 2018, Renaud and co-workers reported a similar radical-induced 1,2-migration protocol (Scheme 19B).^[58] In this case, a solvent switch was not required and TBME was optimal for both the formation of the boronate complex and the radical-induced 1,2-migration. Moreover, the reaction could additionally utilise a range of electrophilic radical precursors including α -iodosulfonates and trichloriodomethane, substituted vinyl boronic esters, and tertiary organolithiums. However, two equivalents of BEt_3 and the initiator di-*tert*-butyl hyponitrite (DTBHN) were required to increase the yield and the reproducibility of the reaction.

Concurrently with Studer's initial report, Aggarwal and co-workers reported the reaction between vinyl boronates, formed *in situ* by addition of an organolithium, and alkyl iodides under visible-light conditions (Scheme 19C).^[59] Homolytic cleavage under the visible-light conditions yielded the electrophilic radical and initiated the radical chain mechanism. Even alkyl bromides could be employed in the presence of the photocatalyst $\text{Ru}(\text{bpy})_3\text{Cl}_2 \cdot 6\text{H}_2\text{O}$, which aids in radical initiation by single-electron reduction. A broad scope of radical precursors and organolithiums including tertiary organolithiums were presented, yielding the boronic ester products in high yields. More recently, Shi and co-workers have used similar visible light conditions to undergo a radical addition reaction of alkyl bromides to alkenyl diboronate complexes, generated *in situ* through the reaction of a vinyl Grignard reagent and B_2pin_2 (Scheme 19D).^[60] The migrating group in this case was -Bpin, giving a range of functionalised *gem*-bis(boryl)alkanes. The methodology showed a broad scope of alkenyl Grignard reagents as well as electron-deficient alkyl bromides. The use of NaI was required for the *in situ* conversion of the alkyl bromides to the corresponding iodides, in turn improving yields. Although a photocatalyst was used, a quantum yield of $\Phi = 49.8$ was measured, confirming a radical chain process and that the photocatalyst was used as an initiator (*tert*-butylammonium bromide (TBAB) is a sacrificial reductant that turns over the photocatalytic cycle).

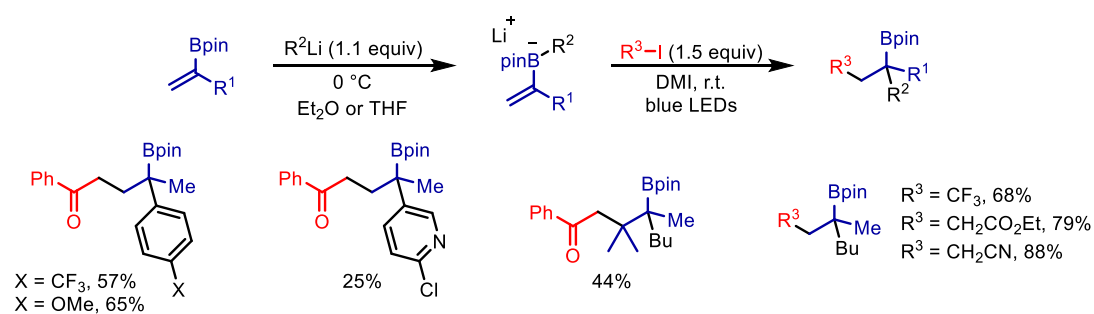
A: Studer (2017)



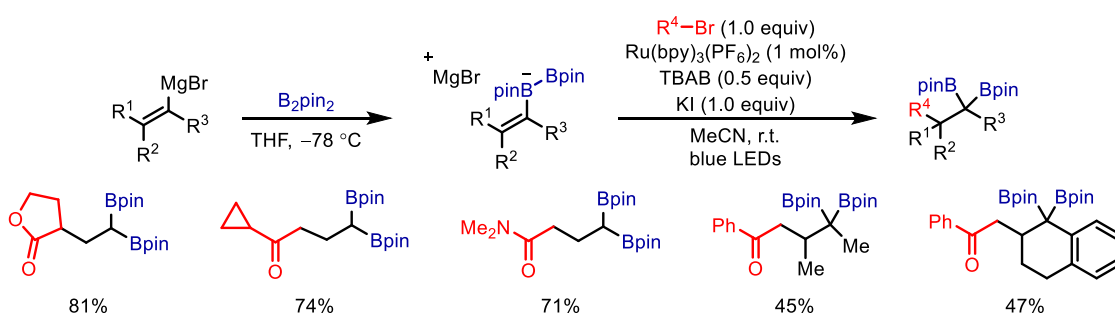
B: Renaud (2018)



C: Aggarwal (2017)



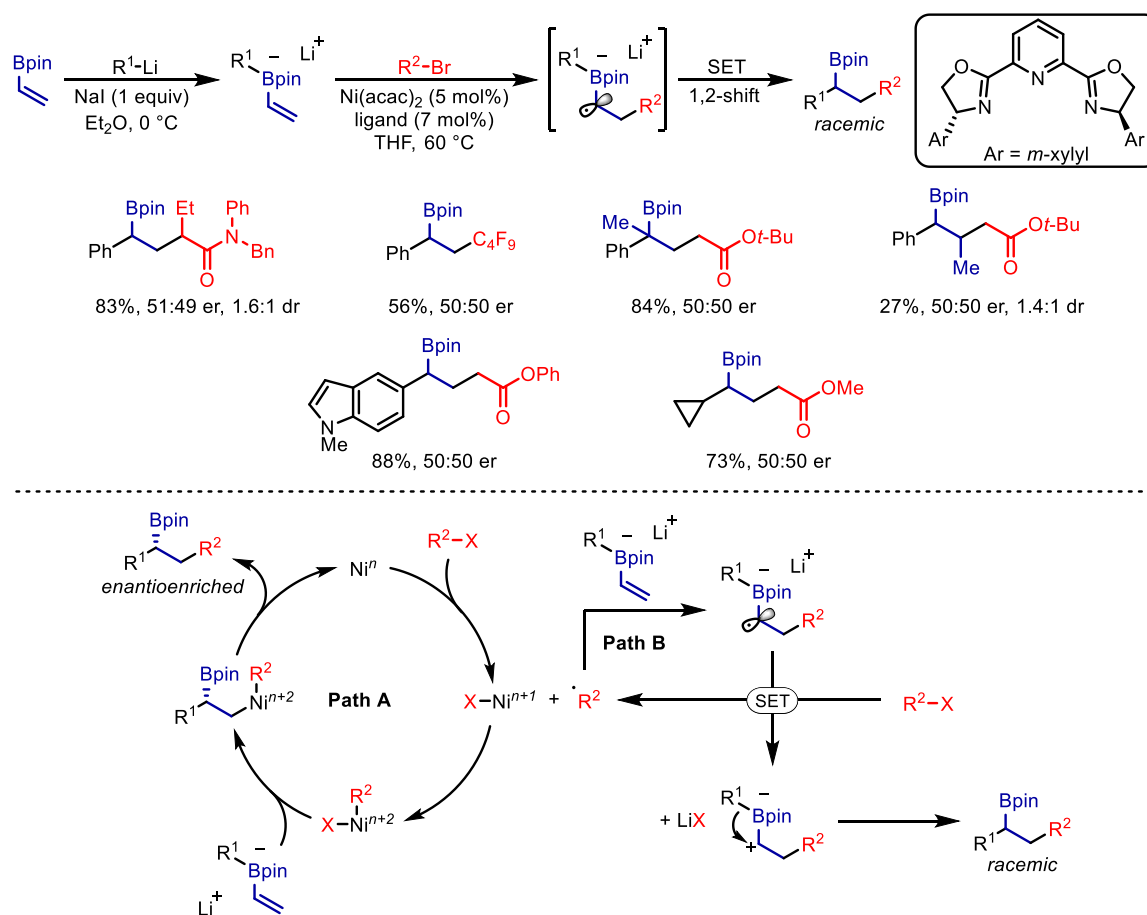
D: Shi (2019)



Scheme 19. Radical-induced 1,2-migration of vinyl boronate complexes, showing selected examples.

The same year, Morken and co-workers reported a similar nickel-catalysed enantioselective conjunctive coupling of vinyl boronic esters with alkyl halides and organolithiums (Scheme 20).^[62] Interestingly, they found that non-activated alkyl halides gave high levels of enantioselectivity, whereas for activated (electron-deficient) alkyl halides, such as those typically used as electrophilic radical precursors, racemic boronic ester products were yielded. Through mechanistic experimentation it was uncovered

that in the former case, non-activated alkyl halides undergo oxidative addition to the nickel catalyst, which then induces an enantioselective 1,2 boron shift of the preformed vinyl boronate complex. Reductive elimination yields the enantioenriched boronic ester products (Path A). In the latter case, electron-deficient alkyl halides are readily reduced, and thus the resulting electrophilic radical readily interacts with the electron-rich vinyl boronate complex to give the intermediate α -boryl radical, as in the case of Studer,^[57] Renaud,^[58] Aggarwal^[59] and Shi.^[60] This α -boryl radical intermediate can reduce another electron-deficient alkyl halide, in turn undergoing oxidation and inducing 1,2-migration, which results in racemic boronic ester products (Path B). In the case of the racemic products, which proceeded via an α -boryl radical, the scope of the electrophiles was broad, utilising a range of α -bromo-esters, -amides and -ketones, and perfluoroalkyl bromides. The scope of the organolithiums was limited to aryl and cyclopropyl organolithiums as attempts to utilise alkyl migrating groups such as methyl or benzyl were unsuccessful.



Scheme 20. Morcken's nickel-catalysed conjunctive coupling of vinyl boronic esters with alkyl halides and organolithiums. Selected examples for the racemic products given which proceed via the generation of an α -boryl radical.

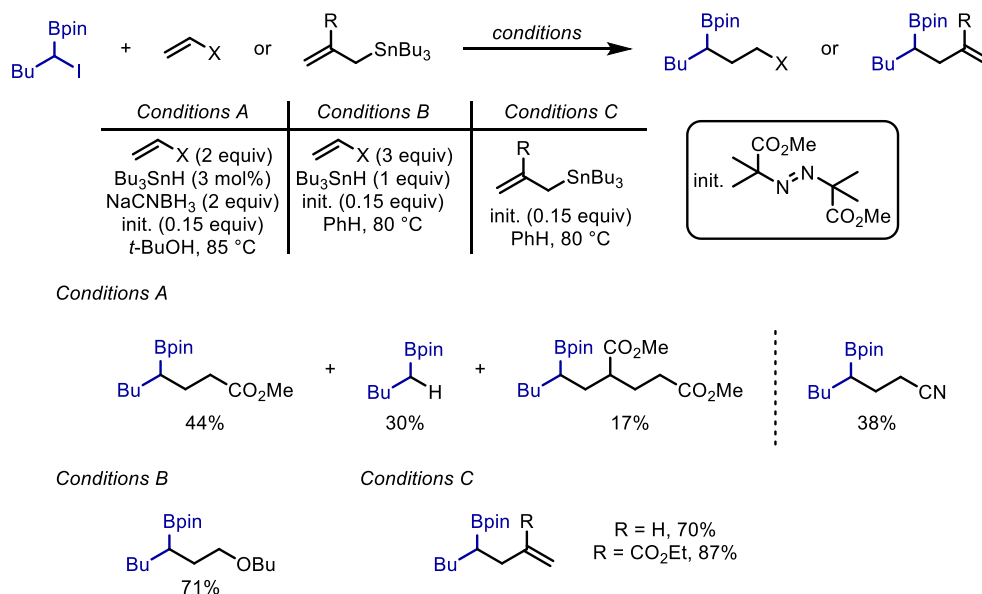
1.2.3 α -Halo Boronic Esters

α -Halo boronic esters offer an alternative and more direct way of accessing α -boryl radicals. These radical precursors can generate the corresponding α -boryl radicals through atom abstraction or reduction. These can then add to alkenes or be trapped with nickel catalysts to undergo (stereoselective) cross-couplings.

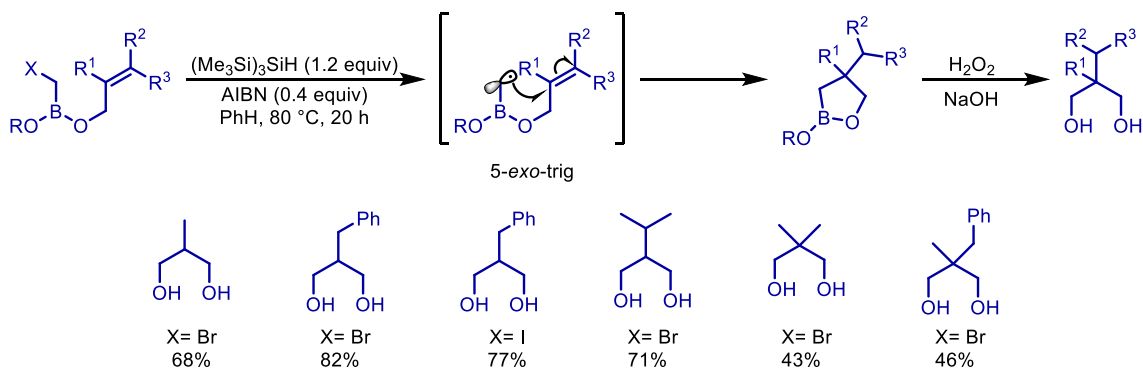
Batey and co-workers were the first to utilise α -iodo boronic esters in intermolecular Giese additions reactions to alkenes (Scheme 21A).^[63] Using dimethyl 2,2'-azobisisobutyrate (init.) as the radical initiator in combination with Bu_3SnH , and NaCNBH_3 as the co-reductant, the α -boryl radical formed through iodine-atom abstraction could undergo Giese addition to methyl acrylate and acrylonitrile in moderate yields. The role of NaCNBH_3 was to maintain a low concentration of the H-atom donor. Unfortunately, competing H-atom abstraction of the α -boryl radical and over-addition were also found in 30% and 17%, respectively, in the case of methyl acrylate. They also applied an electron-rich vinyl ether and found that the Giese addition occurred in 71%, because the electron-rich α -oxy radical generated is unreactive towards over-addition to another electron-rich alkene. These results highlight the ambiphilic nature of α -boryl radicals as they can add to both electron-deficient and electron-rich alkenes. However, a competition experiment was conducted with 1:1 methyl acrylate and vinyl ether, and it was seen that the α -boryl radical added exclusively to the methyl acrylate, emphasising its higher reactivity towards electron-deficient alkenes. The use of allyl stannanes as radical traps were also successful, yielding the homoallylic boronic ester products in high yields.

Batey and co-workers extended this methodology to the intramolecular Giese-type addition of α -halo boronic esters to alkenes tethered to the boronic ester diol backbone, to yield after oxidation 1,3-diols in good yields (Scheme 21B).^[64] In this case Bu_3SnH gave no reactivity and it was found that $(\text{Me}_3\text{Si})_3\text{SiH}$ was optimal. The exclusive 5-*exo*-trig cyclisation observed was a result of the short C-B bond.

A: Intermolecular radical additions of α -boryl radicals

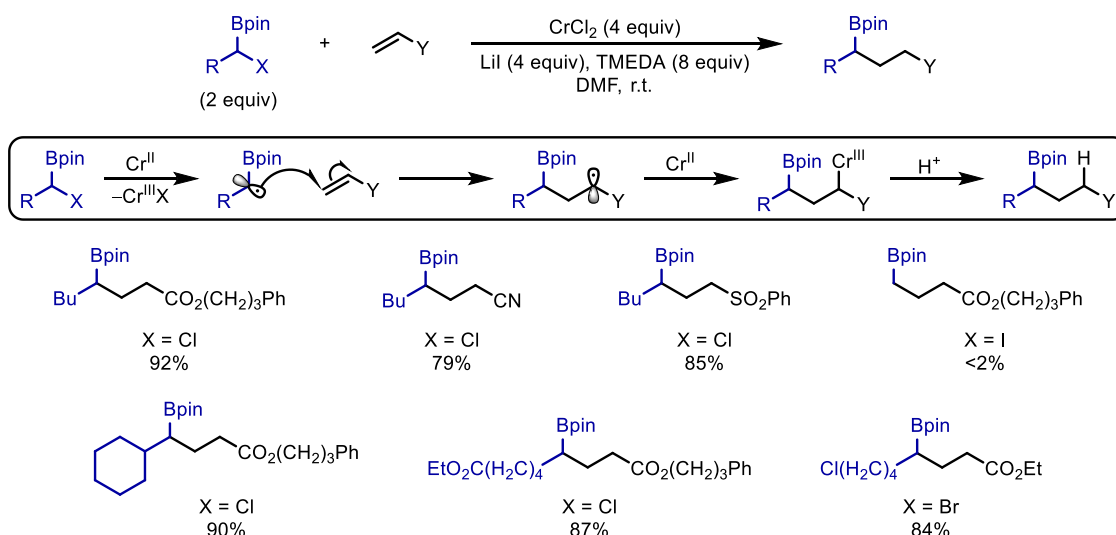


B: Intramolecular radical additions of α -boryl radicals



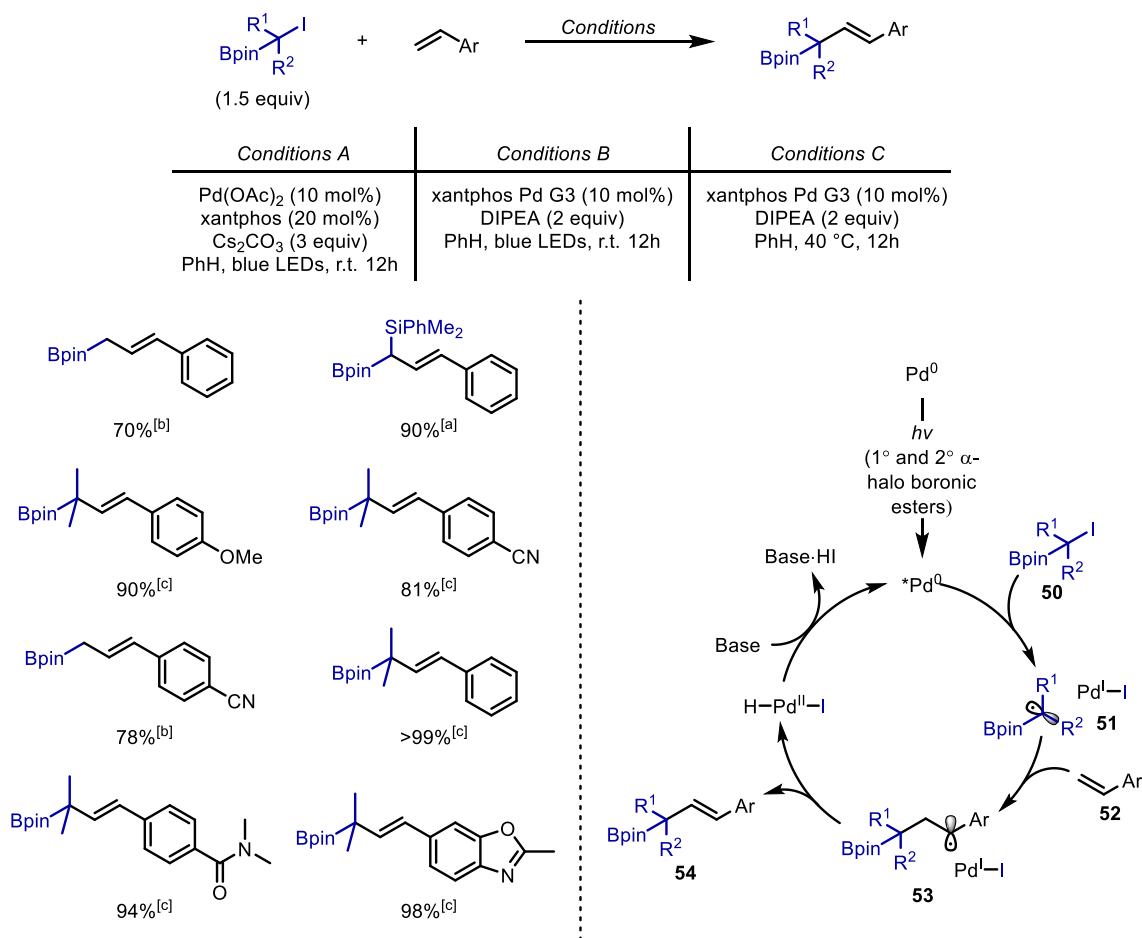
Scheme 21. Batey's inter- and intra-molecular radical additions of α -boryl radicals, using α -halo boronic esters as the radical precursor.

Takai and co-workers have reported the reduction of α -halo boronic esters to the corresponding α -boryl radicals using CrCl_2 as the stoichiometric reductant, which underwent smooth radical addition to a range of electron-deficient alkenes in excellent yields (Scheme 22).^[64] The addition of LiI generates the more easily reduced α -iodo boronic ester *in situ* and TMEDA enhances the reducing ability of the CrCl_2 . The authors propose a mechanism involving two single-electron reductions. The α -halo boronic ester is initially reduced to the α -boryl radical, which can then add to an electron-deficient alkene. Further reduction of this resulting radical by Cr(II) yields the Cr(III) complex, which upon protonation gives the alkyl boronic ester products. Unfortunately, use of iodomethyl boronic ester was unsuccessful and the use of electron-rich alkenes led to complex reaction mixtures.



Scheme 22. Takai's intermolecular radical additions of α -boryl radicals to electron-deficient alkenes, under reductive conditions, using α -halo boronic esters as radical precursors.

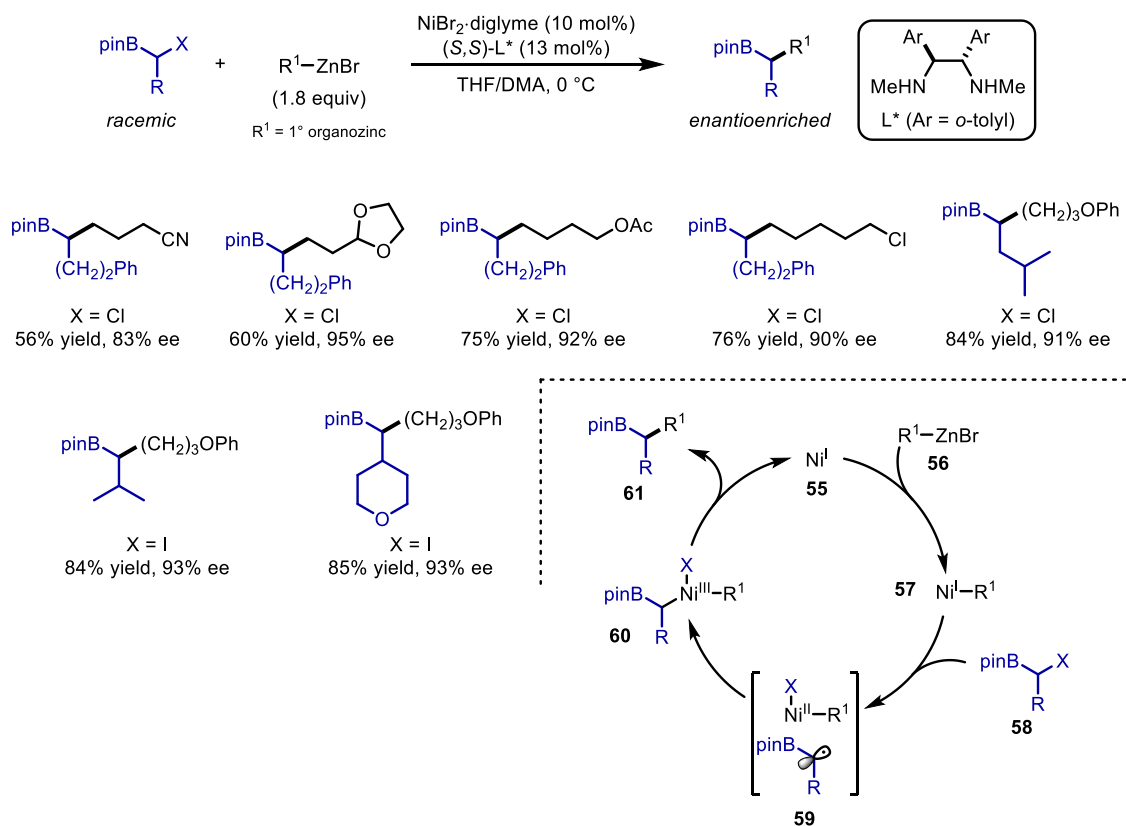
Heck reactions of alkyl halides with vinyl arenes/heteroarenes under (visible-light-mediated) palladium catalysis have been reported by Gevorgyan and co-workers (Scheme 23). The authors showed that primary and secondary α -iodo boronic esters could engage in radical Heck reaction with vinyl arenes under visible-light conditions,^[65] while in the case of tertiary α -iodo boronic esters the reaction proceeded thermally.^[66] In general, the reaction proceeded with excellent efficiency and in the case of tertiary α -iodo boronic esters a range of electron-rich and electron-deficient vinyl arenes/heteroarenes could be used. In both cases, mechanistic studies, including radical clock experiments, radical trapping and Stern-Volmer quenching studies, indicated a radical based mechanism involving initial single-electron reduction of the α -iodo boronic ester **50** to the corresponding α -boryl radical **51** by the Pd^0 catalyst. In the case of primary and secondary α -iodo boronic esters, the palladium catalysts had to undergo visible-light excitation to produce the active $^*\text{Pd}^0$ complex. Trapping of the α -boryl radical intermediate **51** with vinyl arene **52** yielded the alkyl radical intermediate **53**, which upon β -hydride elimination yielded the allylic boronic ester product **54**. Deprotonation completes the catalytic cycle.



Scheme 23. Gevorgyan's (visible-light-mediated) Heck reactions of alkyl halides with vinyl arenes/heteroarenes using palladium catalysis. [a] Using Conditions A. [b] Using Conditions B. [c] Using Conditions C.

In 2016, Fu and co-workers developed an asymmetric nickel-catalysed cross-coupling of α -halo boronic esters with organozinc reagents to yield enantioenriched boronic ester products in excellent yields and high ee (Scheme 24).^[67] The reaction proceeds under mild nickel catalysis conditions using a chiral diamine ligand which dictates the stereochemistry of the products. Good functional group tolerance was shown, including a robustness assay – addition of additives with a range of functional groups to see whether they withstand the reaction conditions. The reaction, however, was limited to primary organozinc reagents, secondary organozinc reagents gave low yields and moderated ee. Although not reported, the mechanism is thought to proceed in a similar fashion to related reactions developed by Fu.^[68] Transmetalation of the organozinc reagent **56** with an *in situ* generated Ni(I) complex **55** gives complex **57**. Inner-sphere single-electron reduction of the α -halo boronic ester **58** generates the α -boryl radical intermediate (**59**), which recombines with Ni(II) to give Ni(III) complex **60**. Reductive elimination yields the boronic ester product **61**, completing the catalytic cycle. The reductive elimination step has been computed in similar cross-couplings to be the enantio-determining step.^[49] This report has opened up a new avenue in radical chemistry by taking racemic radical precursors,

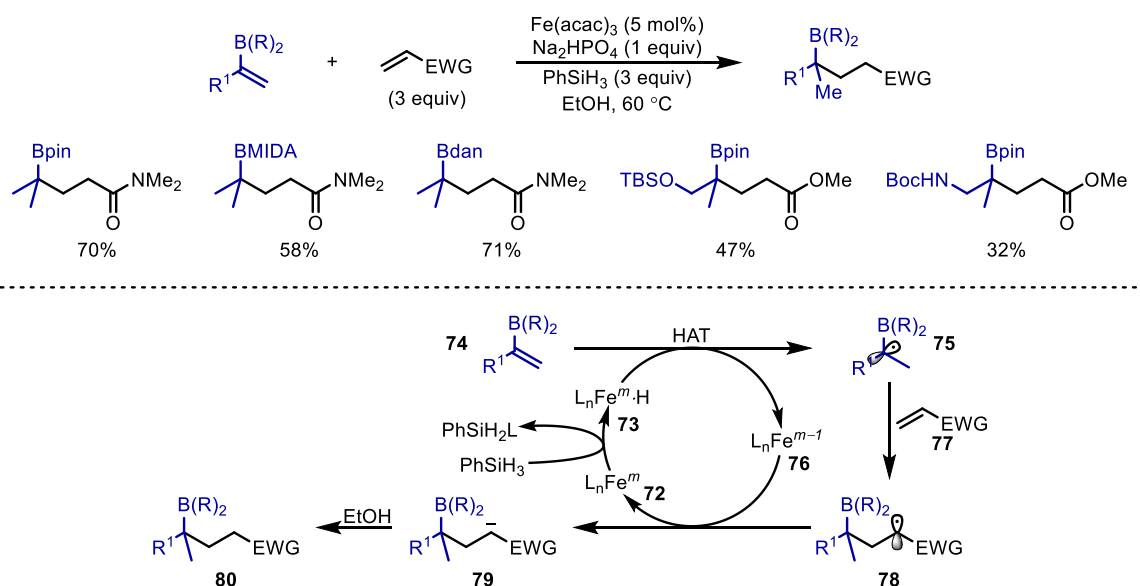
accessing the corresponding radical, and subjecting it to asymmetric catalysis to provide access to a range of valuable, enantioenriched targets.



Scheme 24. Fu's asymmetric synthesis of alkyl boronic esters via chiral nickel catalysis.

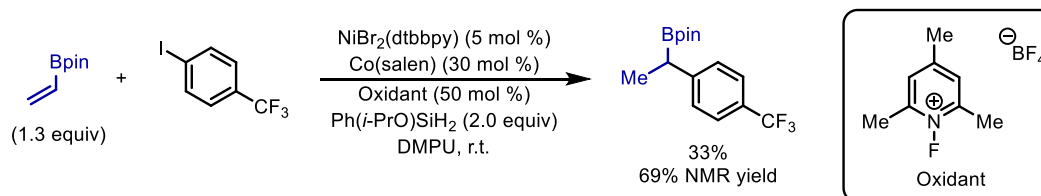
Martin and co-workers reported a similar transformation involving the cross-electrophilic coupling of α -halo boronic esters with aryl halides (Scheme 25).^[69] Under reductive conditions, a range of α -bromo boronic esters could be arylated with both electron-rich and electron-deficient aryl halides in good yields with excellent chemoselectivity and functional group tolerance. Mechanistic studies provide indirect evidence for a radical based mechanism involving initial oxidative addition of aryl halide **63** to Ni(0) to yield the Ni(II) species **64**. In low concentrations of α -boryl radical **65**, halogen transfer between the Ni(II) species **64** and the α -halo boronic ester gives the corresponding radical **65** and Ni(III) intermediate **66** – this has been termed self-initiation (reductive elimination from intermediate **66** generates Ni(I) complex **69**).^[70] Recombination of α -boryl radical with the Ni(II) species **64** gives the Ni(III) complex **67**. Reductive elimination furnishes the arylated boronic ester product **68**. The resulting Ni(I) complex **69** can then proceed to reduce another molecule of α -halo boronic ester **70**, propagating the catalytic cycle. Reduction of the Ni(II) **71** species with Zn completes the catalytic cycle.

which upon single-electron reduction from the iron complex **76** and protonation yields the boronic ester product **80**. This single-electron reduction completes the catalytic cycle.



Scheme 26. Baran's Fe-catalysed HAT vinyl boronic ester cross-coupling.

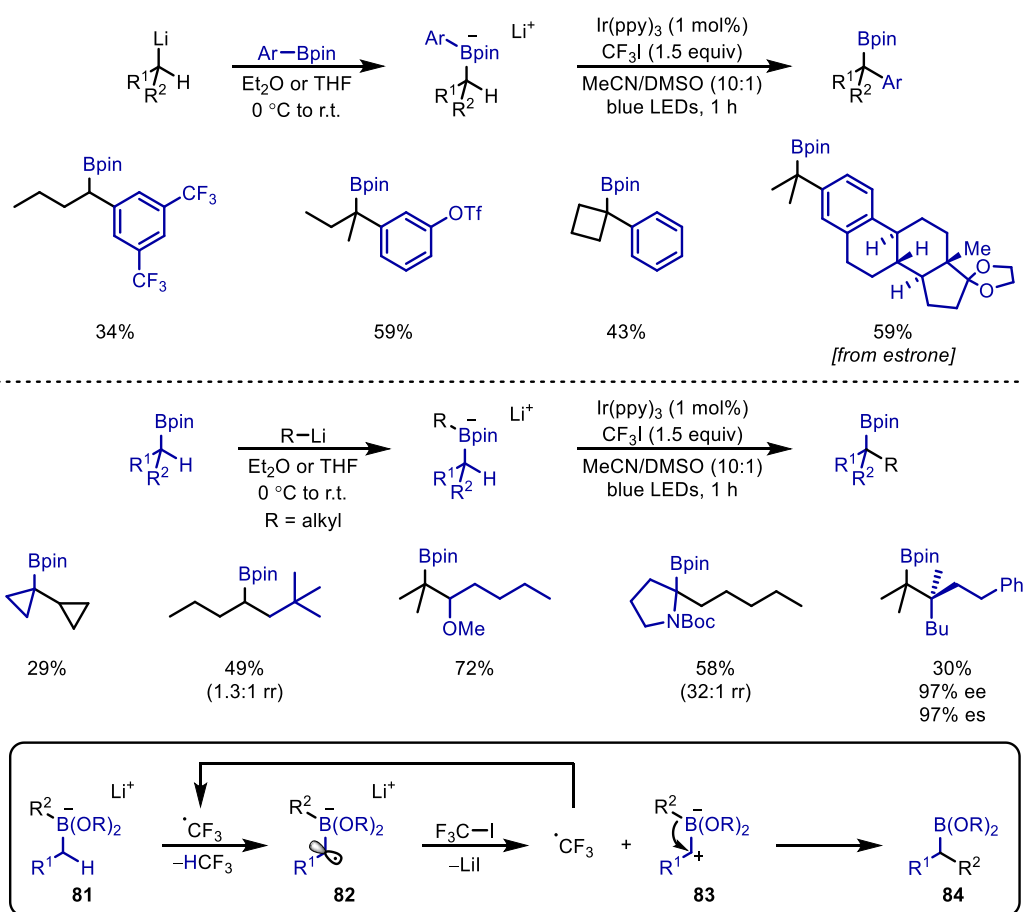
Shenvi and co-workers used a similar HAT approach to generate radicals from terminal olefins using a dual cobalt and nickel catalytic system to enable hydroarylation of olefins.^[73] This methodology was applied to a single example using vinyl-Bpin to access the α -boryl radical intermediate which was cross-coupled with 1-iodo-4-(trifluoromethyl)benzene in 33% yield (Scheme 27). The low yield was a result of instability on silica during chromatographic purification as a 69% NMR yield was recorded prior to purification. More recently, Shenvi has used iron^[74] and manganese^[75] in place of cobalt to carry out similar hydroarylations and hydroalkylations, respectively. In both cases, vinyl boronic esters were used and involved HAT to generate the α -boryl radical which is readily trapped with nickel to enable a cross-coupling event.



Scheme 27. Shenvi's dual cobalt/nickel HAT cross-coupling, single example with vinyl-Bpin.

The radical-induced 1,2-migration of boronate complexes enabled by selective HAT of α -boryl C-H's to reactive CF_3 radicals has recently been reported by Studer and co-workers (Scheme 28).^[76] This reaction is analogous to the Matterson homologation,^[77] and Fu^[67] and Martin's^[69] cross-coupling of α -

halo boronic esters. The reaction proceeds under visible-light conditions using CF_3I as the source of CF_3 radical. The reaction involves the initial formation of a boronate complex **81** by addition of an organolithium to the boronic ester. Selective α -boryl C-H abstraction from a CF_3 radical generates α -boryl radical intermediate **82**, which has already been shown to be a reductant and thus can reduce another molecule of CF_3I , propagating the radical chain process ($\Phi = 8.8$), and in turn be oxidised to the zwitterionic species **83** inducing 1,2-migration to give boronic ester **84**. Despite being a radical-chain process, $\text{Ir}(\text{ppy})_3$ was used as an initiator. $\text{Ir}(\text{ppy})_3$ in its excited state can reduce CF_3I to the corresponding CF_3 radical. The reaction was applied to α -arylation and α -alkylation reactions, including stereospecific couplings, and proceeded in moderate yields as a result of competing oxidation of the boronate complexes to the corresponding alkyl radicals.^[78] The HAT followed a general trend of activating weaker, less sterically hindered C-H bonds. Studer and co-workers extended this methodology to enable 1,*n*-boron migrations but using B_2pin_2 and Grignard reagents, in a similar way to that done by Shi and co-workers (*vide supra*),^[60] to synthesise 1,*n*-bisborylalkanes (not shown).^[79]



Scheme 28. Studer's radical-induced 1,2-migration via HAT of alkyl boronate complexes.

1.3 Photoredox Catalysis

1.3.1 Fundamentals

Since the seminal works of Yoon,^[80] MacMillan,^[81] and Stephenson,^[82] photoredox catalysis has emerged as a powerful tool for novel bond forming reactions in organic synthesis. Originally finding application in water splitting,^[83] solar cells^[84] and organic-light emitting diodes,^[85] recent developments in the field of organic chemistry have unveiled a range of innovative synthetic methodologies that allow molecules to participate in unique reaction pathways, which were previously inaccessible with the use of more traditional reaction methods or thermal control.^[86] These approaches utilise readily available metal polypyridyl complexes or organic dyes, which upon photoexcitation can engage in single-electron transfer with organic molecules to facilitate radical reaction pathways under mild conditions. This diverse reactivity displayed by photoredox catalysis has made the field highly desirable for synthetic organic chemists as it has the potential to unlock many more unprecedented methodologies to forge challenging carbon-carbon/heteroatom bonds.

The key property exhibited by photoredox catalysts, is their ability to convert visible light energy into chemical energy under mild conditions. The photophysical changes that take place can be summarized by the Jablonski diagram (Figure 2).^[87,88] Upon visible-light irradiation, photocatalysts (**PC**) absorb a photon, exciting an electron from the singlet ground state (S_0) to a higher energy singlet excited state (S_1^n), which typically relax down by internal conversion (k_{IC}) to the lowest spin-allowed singlet excited state (S_1^0). At this stage, the electron can either decay to the ground state (S_0) via radiative (emission of a photon) fluorescence (k_f) or internal conversion (k_{IC}). Alternatively, the electron can undergo rapid intersystem crossing (k_{ISC}) to the excited triplet state (T_1^n), followed by internal conversion to generate a long-lived triplet excited state (T_1^0). This triplet state is long-lived due to the spin-forbidden relaxation to the singlet ground state. At this stage two productive quenching processes can occur and is what gives photocatalysts their unique reactivity: they can either engage in intermolecular redox processes via single-electron transfer (SET), or undergo triplet-triplet energy transfer (ET). In the latter scenario, the decay of the T_1^0 to S_0 excites another molecule (**Q**) from its ground state **Q**(S_0) to its lowest energy triplet state **Q**(T_1^0). Slow deactivation (due to spin-forbidden relaxation) of the T_1^0 can also occur through radiative phosphorescence (k_p) or non-radiative internal conversion (k_{IC}).

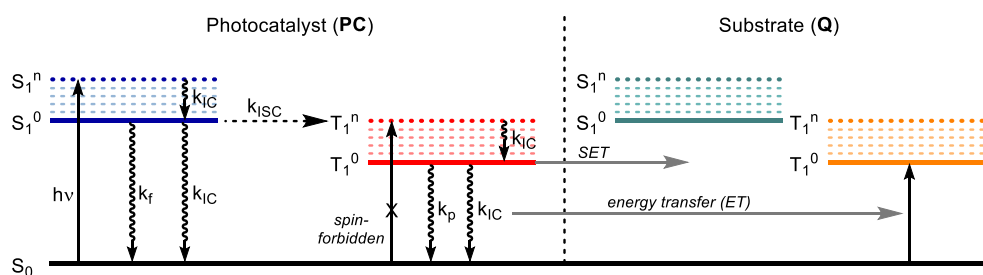


Figure 2. Generalised Jablonski diagram for photocatalysts.

A typical example of a commercially available and widely used photocatalyst is $\text{Ir}[\text{dF}(\text{CF}_3)\text{ppy}]_2(\text{dtbbpy})\text{PF}_6$ (Figure 3). This photocatalyst can absorb visible-light energy at a maximum absorption of 380 nm, which is highly beneficial as it allows the maximum energy gain for the photocatalyst without undesirable direct excitation of organic substrate molecules. An electron is excited from the metals t_{2g} orbital to the pyridyls π^* orbital, known as metal-to-ligand charge transfer (MLCT). This singlet excited state then undergoes rapid intersystem crossing (ISC) to the long-lived excited triplet state, which has a lifetime of 2300 ns. Focusing on redox processes, the long-lived excited triplet states allow photocatalysts to behave as both oxidants and reductants upon excitation. The excited state can either accept an electron into the lower energy t_{2g} orbital, acting as an oxidant, or the photocatalyst can donate the higher energy electron from the π^* orbital, acting as a reductant.^[86] In order to compute this unique redox character, standard reduction potentials ($E_{1/2}^{\text{red}}$) are used as a measure of how strongly oxidising or reducing the excited state (or ground state) species is, these describe the potential associated with the electrochemical half-reaction going from the oxidised to the reduced species. These values can be measured experimentally using cycling voltammetry. The more positive the value is, the more oxidising it is; the more negative the value is, the more reducing it is. In order for an electron transfer to be thermodynamically feasible, the redox potentials of the oxidant or reductant must be more positive, or more negative than the substrate, respectively.^[89] In the case of $\text{Ir}[\text{dF}(\text{CF}_3)\text{ppy}]_2(\text{dtbbpy})\text{PF}_6$, the half-reaction ${}^*\text{Ir}(\text{III}) + e^- \rightarrow \text{Ir}(\text{II}) = E_{1/2}^{\text{red}} [{}^*\text{Ir}(\text{III})/\text{Ir}(\text{II})] = +1.21 \text{ V}$ vs saturated calomel electrode (SCE) in MeCN, which means the excited state ${}^*\text{Ir}(\text{III})$ is a strong oxidant. Moreover, for the half reaction $\text{Ir}(\text{IV}) + e^- \rightarrow {}^*\text{Ir}(\text{III}) = E_{1/2}^{\text{red}} [\text{Ir}(\text{IV})/{}^*\text{Ir}(\text{III})] = -0.89 \text{ V}$ vs SCE in MeCN, which also makes it a strong reductant.^[90]

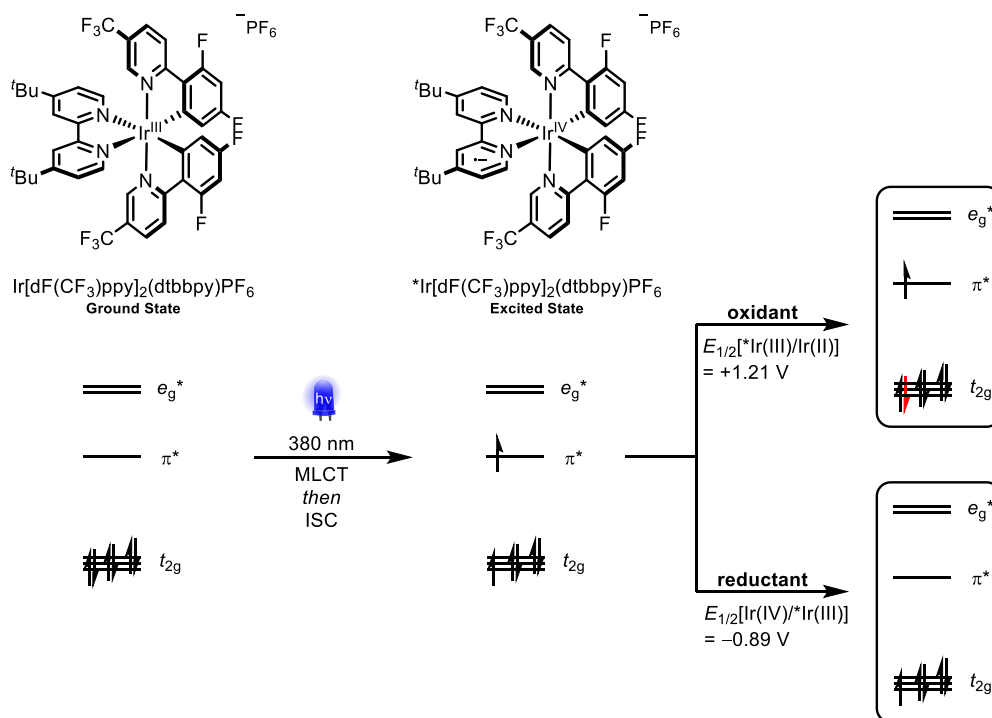
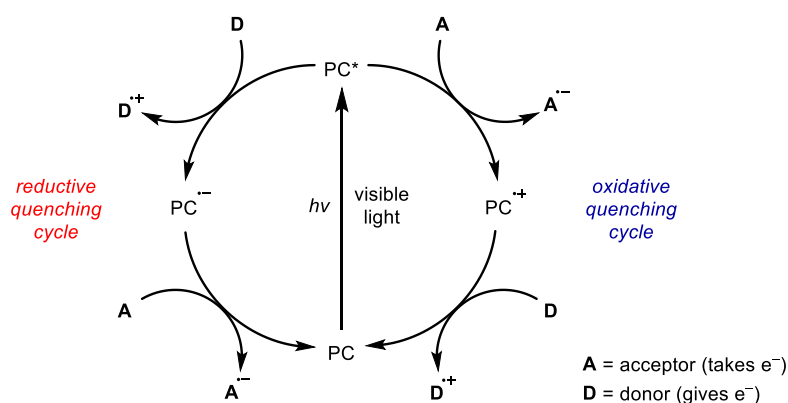


Figure 3. Key molecular orbitals involved in the photochemistry of $\text{Ir}[\text{dF}(\text{CF}_3)\text{ppy}]_2(\text{dtbbpy})\text{PF}_6$.

The unique dual redox ability results in the photoredox cycle proceeding via two different quenching mechanisms (Scheme 29). Under reductive quenching, the excited state photocatalyst behaves as an oxidant, oxidising a donor species (**D**), and in turn forming the reduced state photocatalyst (PC^-). Alternatively, the cycle may proceed via an oxidative quenching mechanism whereby the photocatalyst acts as a reductant, donating an electron to an acceptor species **A** and in turn forming the oxidised state of the photocatalyst (PC^+).^[91] Whether a process proceeds through a reductive or oxidative quenching cycle depends on the standard reduction potentials of the photocatalyst and the substrate (**D** or **A**) undergoing the SET. Fortunately, the reduction potentials of the photocatalyst can be easily tuned by modifying the ligand: the greater the electron donation from the ligand, the more reducing the photocatalyst will be, on the other hand, the more electron-withdrawing the ligand, the more oxidising the photocatalyst will be.^[87] As these are redox-neutral processes, the photocatalyst's ground state is regenerated by a second SET event.



Scheme 29. The reductive and oxidative quenching cycle of photocatalysts.

This thesis will focus on the reductive quenching of the photocatalyst and so a number of commonly used photocatalysts with selected redox potentials are given in Figure 4.^[90,92]

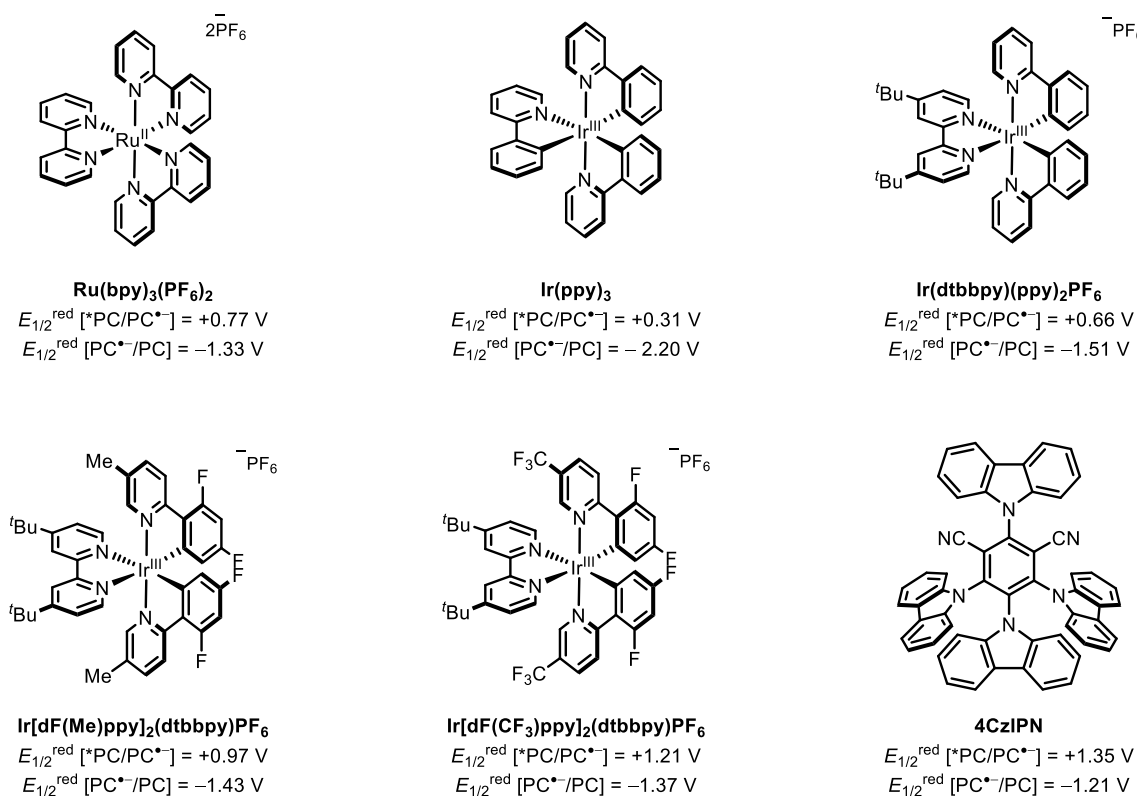


Figure 4. Commonly employed photocatalysts and their corresponding reduction potentials proceeding via a reductive quenching cycle.

1.3.2 Photoredox-mediated Decarboxylations

Radical precursors are employed in order to generate reactive organic radicals using photoredox catalysis. These can readily undergo redox processes with the different states of the photocatalyst

behaving as either an electron donor (**D**) or acceptor (**A**). Oxidisable radical precursors are employed to generate reactive radicals in a reductive quenching scenario or upon oxidation for regenerating the ground state photocatalysts; upon single-electron oxidation they fragment to yield the radical. These are typically easily accessible and bench stable, and include carboxylic acids, oxalates, amines, boronates and silicates (Figure 5).^[86]

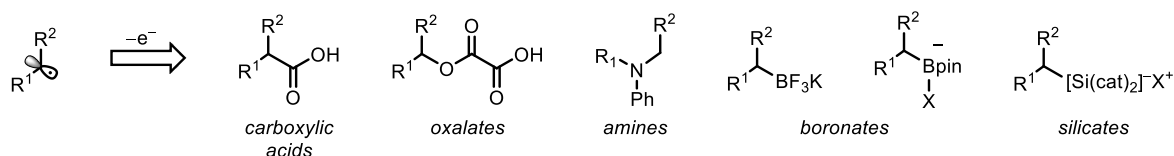
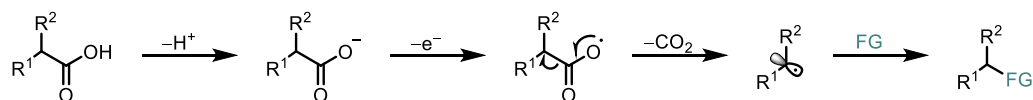


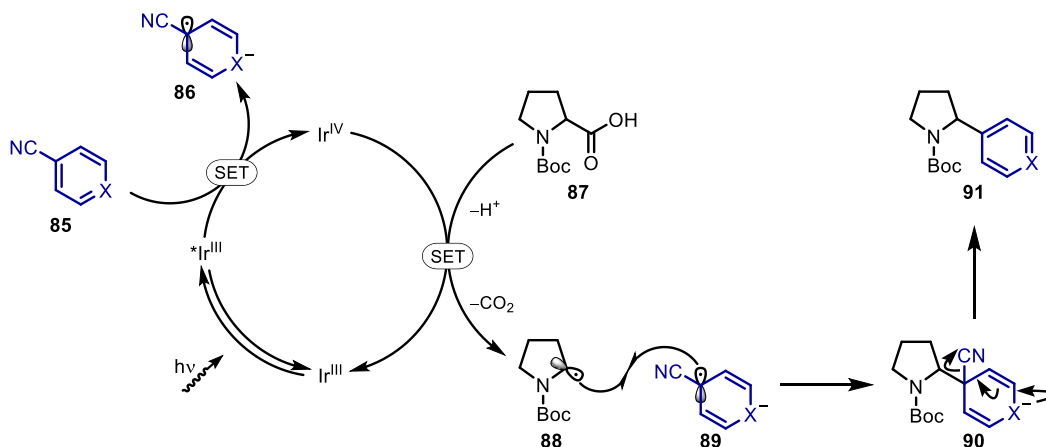
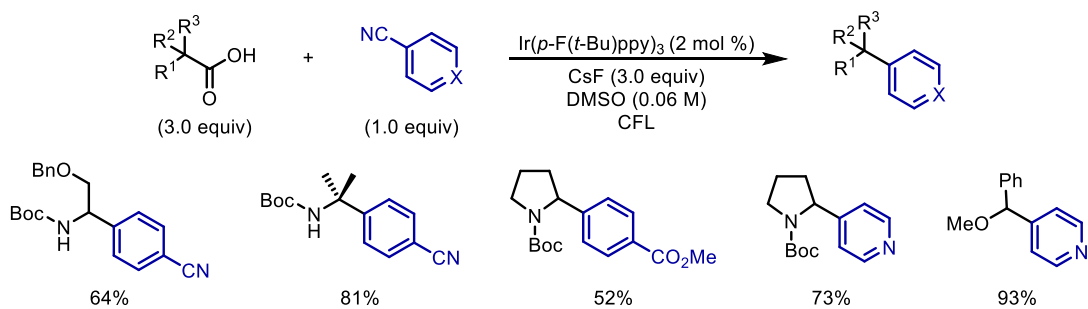
Figure 5. Oxidisable radical precursors.

Carboxylic acids occupy a privileged position amongst the oxidisable radical precursors as they are readily available biomass feedstocks, which are prevalent in natural products and drug molecules. Taking these abundant starting materials, such as α -amino acids and alkyl acids, the generation of the corresponding radical species can be directly achieved through initial oxidation of the carboxylate and subsequent decarboxylation expelling CO_2 (Scheme 30). The carboxylate group can be thought of as a traceless activating group. This mechanism of decarboxylation enables the direct conversion of inexpensive carboxylic acids to other functional groups (FG) through radical couplings, in turn, rapidly building up molecular complexity.^[93,94]



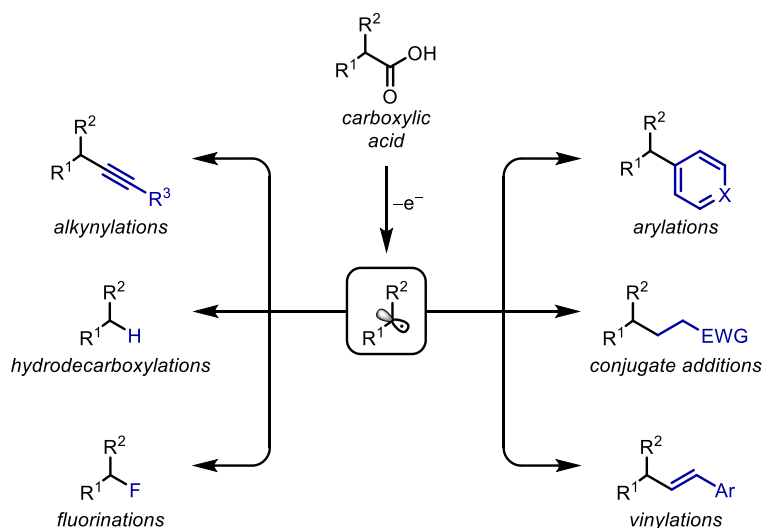
Scheme 30. Mechanism of oxidation via single-electron oxidation.

MacMillan and co-workers were the first to carry out a general photoredox-mediated decarboxylative transformation in 2014, involving the direct decarboxylative arylation of α -amino and α -oxy acids with cyanoarenes to furnish high-value benzylic amine or ether products (Scheme 31).^[95] A broad scope of substrates were amenable to the reaction conditions and gave the corresponding products in good yields, displaying excellent functional group tolerance. The authors propose that upon photoexcitation, the photocatalyst ($^*\text{Ir(III)}$) can undergo oxidative quenching to Ir(IV) , reducing cyanoarene **85** to the corresponding radical anion **86**. Regeneration of the ground state photocatalyst Ir(III) occurs through oxidation of the carboxylate of amino acid **87** to give α -amino radical **88**. Radical-radical coupling of **88** and **89** and subsequent cyanide elimination from intermediate **90** gives the benzylic amine products (**91**).



Scheme 31. MacMillan's decarboxylative arylation of α -amino and α -oxy acids using photoredox catalysis.

Since this report MacMillan, and others, have expanded the field of these photoredox-mediated decarboxylations to carry out conjugate additions,^[96] vinylations,^[97] alkynylations,^[98] hydrodecarboxylations,^[99,100] and fluorinations,^[101–103] all under mild photocatalytic conditions. These transformations highlight the ability to convert carboxylic acids directly into a range of different functional groups and emphasises the diversity and applicability of these photoredox-mediated decarboxylations (Scheme 32).

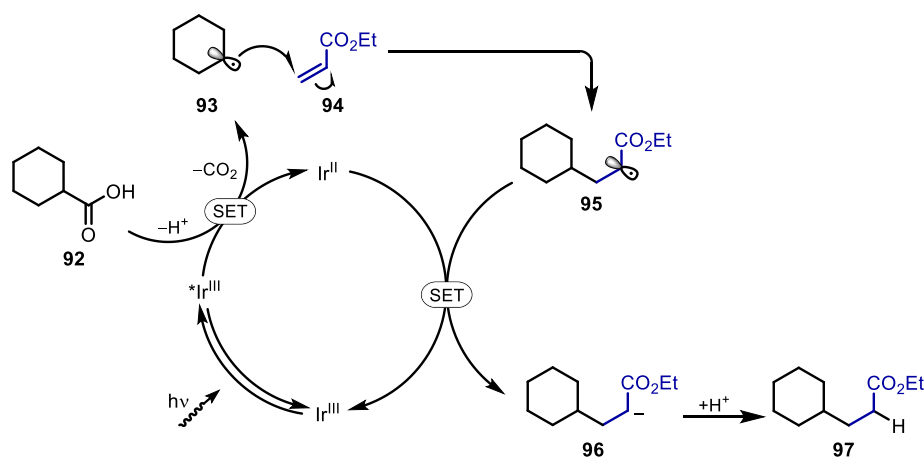
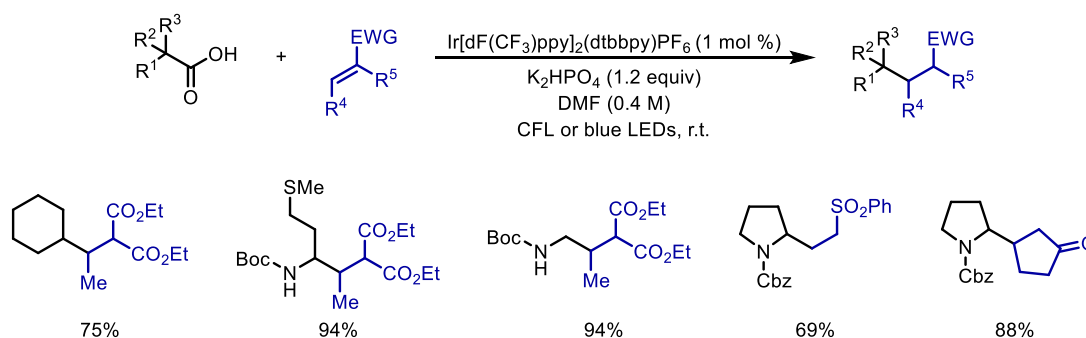


Scheme 32. Photoredox-mediated decarboxylative functionalisations.

One highly practical and efficient process developed by MacMillan and co-workers is the radical conjugate addition of carboxylic acids to electron-deficient alkenes.^[96] These are key sp^3 - sp^3 carbon-carbon bond forming reactions in organic synthesis.^[104] Typically, other traceless activating groups have been used as Michael donors for conjugate addition reactions, such as halides, cuprates, boronic esters and Grignard reagents.^[105] However, the use of carboxylic acids under photoredox catalysis provides a greater advantage as they do not need pre-activation and are widely available, expanding the scope of the reaction. Moreover, by generating the radical under mild photoredox conditions, greater functional group tolerance is observed, along with a reduced cost of performing the reaction, and CO_2 being the by-product which does not interfere with purification.

MacMillan demonstrated that a range of carboxylic acids, including alkyl, α -amino and α -oxy acids, could be used in conjunction with an array of Michael acceptors under these photoredox conditions. Excellent product yields were attained, displaying good functional group tolerance. The reaction was also applied to the synthesis of the anticonvulsant drug pregabalin (commercialised by Pfizer under the name Lyrica) (Scheme 33). The authors propose a closed photoredox mechanism. Initial excitation of the Ir(III) photocatalyst gives the highly oxidising $^*Ir(III)$ state ($E_{1/2}^{red} [^*Ir(III)/Ir(II)] = +1.21$ V vs SCE in MeCN). This can oxidise the carboxylate of acid **92** (hexanoate, $E_{1/2}^{red} = +1.16$ V vs SCE), generating the carboxyl radical which readily decarboxylates to deliver the nucleophilic radical **93**, which in turn forms the reduced state Ir(II) species. Radical **93** can then add to the electron-deficient alkene **94**, forming a new carbon-carbon bond and an α -carbonyl radical **95**. This α -carbonyl radical **95** ($E_{1/2}^{red} = -0.60$ V vs SCE) is rapidly reduced by the Ir(II) complex ($E_{1/2}^{red} [Ir(III)/Ir(II)] = -1.37$ V vs SCE), completing the catalytic cycle and forming enolate **96** which upon protonation yields the product **97**. MacMillan has recently expanded the scope of this methodology to linear peptides ranging from 3-15

amino acids, using a water soluble photocatalysts.^[106] These reactions are examples of a radical-polar crossover, in which reactivity initially occurs via the radical pathway and then upon reduction engages in polar reactivity (in this case protonation of the enolate).^[107]



Scheme 33. MacMillan's decarboxylative radical addition reaction to electron-deficient alkenes using photoredox catalysis.

1.3.3 Metallaphotoredox: Merging Nickel and Photoredox Catalysis

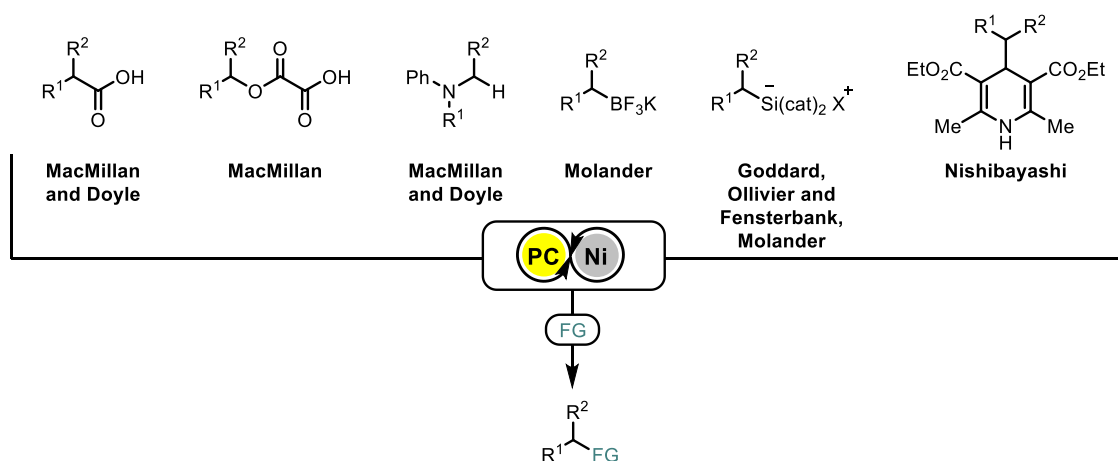
Since the early work of Sanford and co-workers in 2011 on the synergistic photoredox/palladium-catalysed C-H arylation,^[108] a variety of different transition metals, including nickel, gold, copper, and cobalt have been used in conjunction with photoredox catalysis. This fusion of photoredox and transition metal catalysis is termed metallaphotoredox catalysis.^[86,109] These powerful reaction manifolds have the ability to utilise the unique reactivity of photoredox catalysis in combination with transition metal cross-couplings, which have become indispensable tools for synthetic organic chemists.

The reactivity of transition metals stems from their ability to access different oxidation states through two-electron redox events, such as oxidative addition or reductive elimination. This ability to cycle through different oxidations states is what enables transition metals to achieve cross-couplings. If

combined with a photocatalyst, single-electron redox alterations can be achieved, providing access to high-valent metal species, which can enhance the rate of certain mechanistic steps, such as reductive elimination, or facilitate catalyst turnover by regenerating the active catalyst. The photocatalysts can alter the oxidation state of transition metals via a number of different modes: i) SET between the two catalysts, ii) SET between radical precursors which subsequently interact with the transition metal or iii) SET between a radical species which can undergo SET with the metal catalyst.^[86] These interactions enable access to unique reactivity pathways and in turn novel cross-coupling reactions.

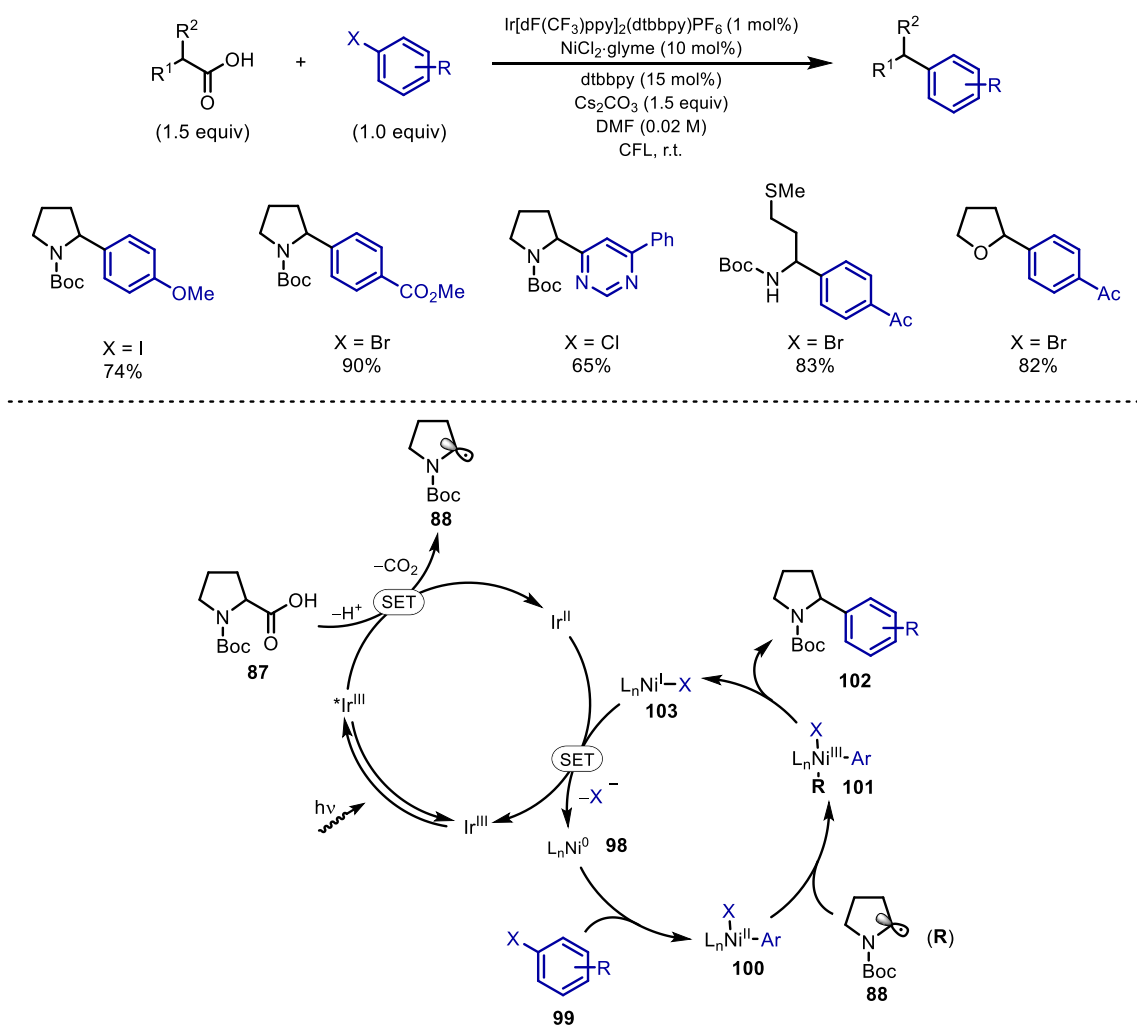
Of all the metals which can participate in metallaphotoredox catalysis, nickel has been at the forefront due to its unique ability to undergo single-electron oxidation changes through either SET processes or engaging radical intermediates.^[110] In addition to this, nickel is a relative electropositive transition metal and so, oxidative addition, which leads to loss of electron density around the metal centre, occurs readily and allows for the use of less reactive electrophiles such as alkyl halides. Moreover, β -hydride elimination is slower for nickel (compared to palladium), due to the higher energy barrier for Ni-C bond rotation prior to β -hydride elimination, this means unlike palladium, when alkyl-nickel complexes are formed detrimental β -hydride elimination does not dominate.^[111,112]

The groups of MacMillan,^[113,114] Doyle,^[113,115] Molander,^[116] Goddard, Ollivier and Fensterbank,^[117] and Nishibayashi^[118] have all made significant contributions to this nickel/photoredox subfield, applying a range of oxidisable radical precursors as coupling partners to achieve novel redox-neutral cross-coupling reactions under metallaphotoredox conditions (Scheme 34).^[109,110] Of all these radical precursors, carboxylic acids are by far the most easily obtainable and versatile, and have been shown to undergo a range of functionalisations enabled by metallaphotoredox catalysis.^[119]



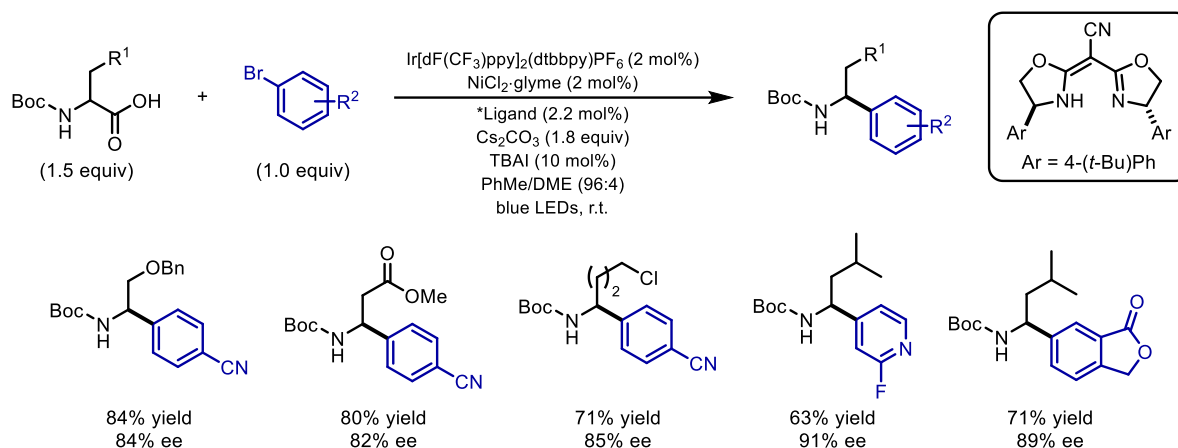
Scheme 34. Oxidisable radical precursors used as coupling partners in metallaphotoredox-catalysed transformations.

Building upon previous work in the field of photoredox-mediated decarboxylations, MacMillan, Doyle and co-workers reported a method for the sp^3 - sp^2 cross-coupling of carboxylic acids with aryl halides under metallaphotoredox conditions (Scheme 35).^[113] Utilising $\text{Ir}[\text{dF}(\text{CF}_3)\text{ppy}]_2(\text{dtbbpy})\text{PF}_6$ and $\text{NiCl}_2 \cdot \text{glyme}$ under basic conditions, α -amino and α -oxy acids were cross-coupled with aryl halides in good to excellent yields. The mechanism was proposed to proceed via a dual catalytic cycle. Initial photoexcitation of the Ir(III) photocatalyst gives the excited state $^*\text{Ir}(\text{III})$. Upon deprotonation, the carboxylate of **87** can be oxidised by the $^*\text{Ir}(\text{III})$, resulting in extrusion of CO_2 to deliver the α -amino radical **88** and Ir(II) species. Concurrently, the aryl halide coupling partner **99** undergoes oxidative addition to the Ni(0) complex **98**, giving the Ni(II) intermediate **100**. This Ni(II) intermediate can trap the α -amino radical **88** to give the alkyl Ni(III) species **101**, which can reductively eliminate to give the direct (two-component) cross-coupled product **102** and Ni(I) halide **103**. Finally, SET between the reduced state of the photocatalyst Ir(II) and Ni(I) halide **103** completes the catalytic cycles. This process is thermodynamically feasible given the redox potentials of the two species: $E_{1/2}^{\text{red}} [\text{Ir}(\text{III})/\text{Ir}(\text{II})] = -1.37$ V vs SCE and $E_{1/2}^{\text{red}} [\text{Ni}(\text{II})/\text{Ni}(\text{I})] = -1.20$ V vs SCE. This reaction demonstrates that carboxylic acids can be used as unconventional alternatives to traditional nucleophilic coupling partners in cross-coupling reactions.



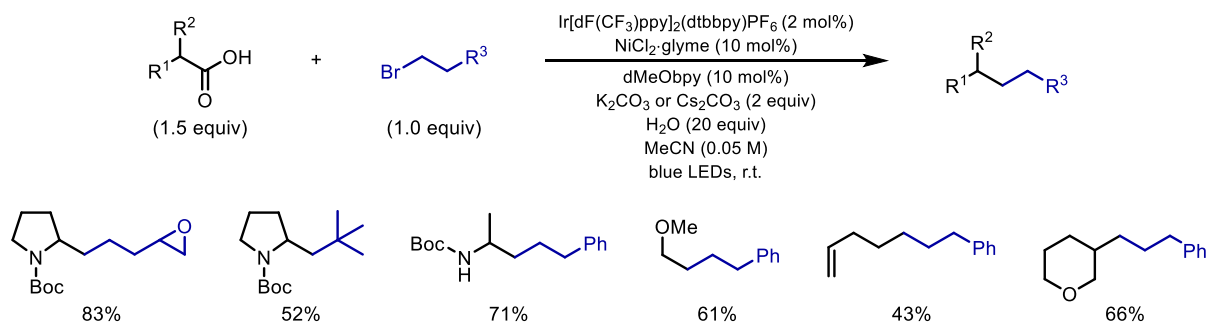
Scheme 35. MacMillan and Doyle's decarboxylative arylation enabled by metallaphotoredox catalysis.

Furthermore, in collaboration with Fu, MacMillan and co-workers developed the asymmetric variant of the metallaphotoredox-catalysed decarboxylative arylation (Scheme 36).^[120] By modifying the reaction conditions slightly and using a readily available chiral bis(oxazoline) ligand, the arylated products were obtained in good ee and excellent yields. This is yet another advantage of using the combination of photoredox catalysis with transition metal catalysis: photoredox allows the generation of reactive radical intermediates under benign conditions, and transition metals, combined with chiral ligands, enable stereinduction.



Scheme 36. MacMillan and Fu's asymmetric arylation of α -amino acids using metallaphotoredox catalysis.

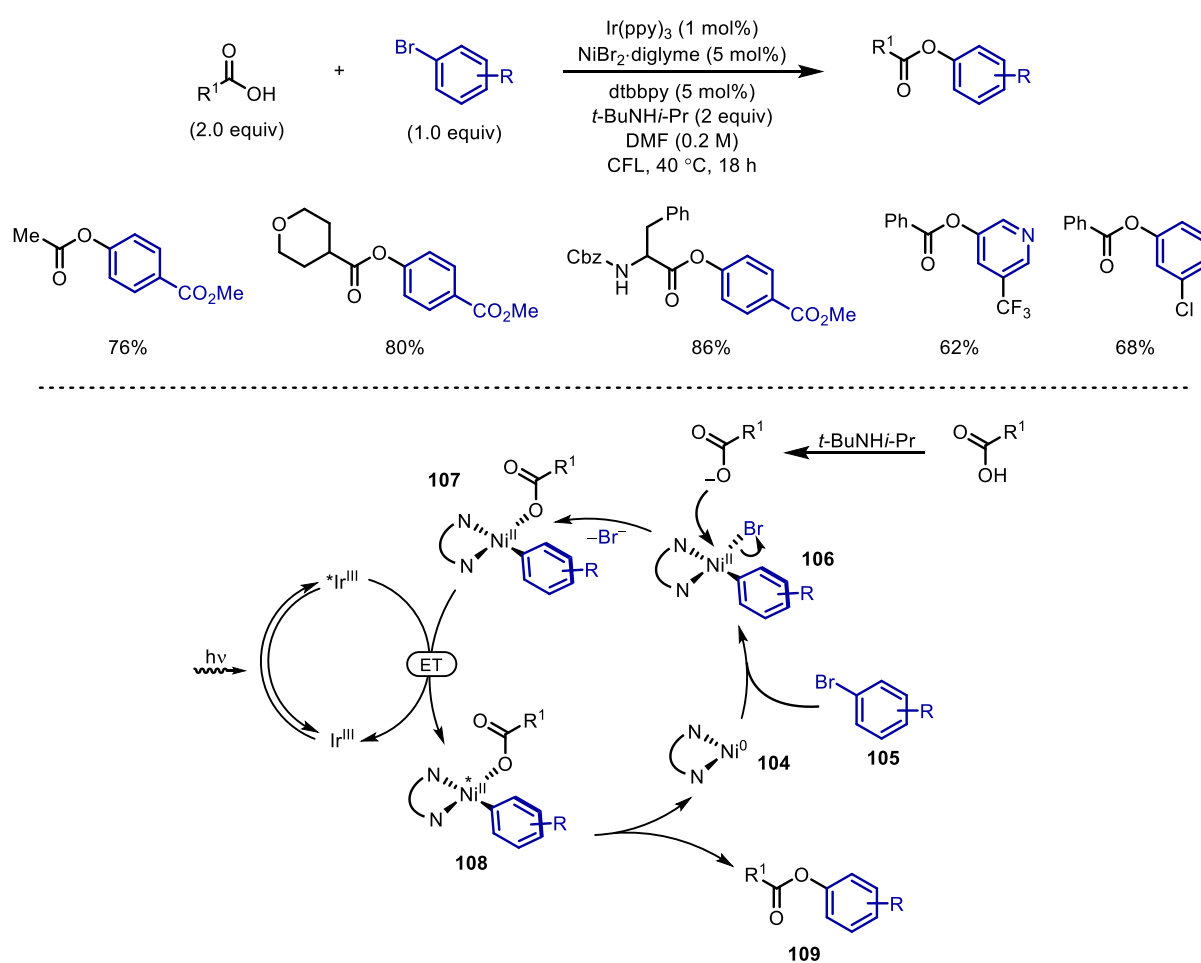
Going one step further, MacMillan and co-workers later reported the decarboxylative $\text{sp}^3\text{-sp}^3$ cross-coupling of carboxylic acids with alkyl halides using metallaphotoredox catalysis (Scheme 37).^[121] Proceeding via the same mechanistic pathway, the authors showed that a range of primary and secondary carboxylic acids (alkyl, α -amino, α -oxy) could undergo the cross-coupling with primary and secondary alkyl bromides in excellent yields. The advantageous characteristics of nickel were important in this case, as β -hydride elimination normally plagues $\text{sp}^2/\text{sp}^3\text{-sp}^3$ cross-couplings.^[111,112] Vinylation of carboxylic acids have also been conducted under similar metallaphotoredox conditions.^[122]



Scheme 37. MacMillan's metallaphotoredox-catalysed alkylation of α -amino and α -oxy acids.

Metallaphotoredox is not only limited to SET processes. In 2017, MacMillan and co-workers developed an esterification reaction of carboxylic acids with electron-deficient aryl bromides using a combination of an iridium photocatalyst and nickel, proceeding via a triplet-triplet energy transfer process (Scheme 38).^[123] A range of carboxylic acids proceeded to give the ester products in good yields with no decarboxylation observed under these conditions. This is unsurprising considering the weakly oxidising Ir(ppy)_3 photocatalyst used ($E_{1/2}^{\text{red}}[\text{*Ir(III)/Ir(II)}] = +0.31\text{ V vs SCE}$). Carrying out significant mechanistic studies, the authors proposed an energy transfer mechanism. The Ni(0) catalyst (**104**)

undergoes oxidative addition to aryl bromide **105**, to yield a Ni(II) intermediate **106**. Displacement of the bromide ligand by the carboxylate yields the Ni(II) species **107**. Concurrently, the photocatalyst Ir(III) is photoexcited to give $^*Ir(III)$. At this point energy transfer between the triplet excited state of the photocatalyst and the Ni(II) species **107** generates an electronically excited Ni(II) species **108** and the ground state photocatalyst (Ir(III)). Reductive elimination from the photoexcited nickel **108** yields the ester product **109**, regenerating the active Ni(0) catalyst **104**. The authors found that the minimum triplet excited energy required to generate the excited state Ni(II) species was ~ 40 kcal/mol. This could be tuned by changing the ligand backbone of the iridium: the more electron-rich the ligand, the greater the triplet energy.



Scheme 38. MacMillan's esterification of carboxylic acids with electron-deficient aryl bromides using metallaphotoredox energy transfer catalysis.

These examples of the synergistic merger of nickel and photoredox catalysis illustrate the power of metallaphotoredox in the field of organic chemistry. It can therefore be expected that a wealth of exciting novel methodologies will be reported in this area in the near future.

2.0 Synthesis of Alkyl Boronic Esters

The data presented in this chapter has been partially published in:

A. Noble, R. S. Mega, D. Pflästerer, E. L. Myers, V. K. Aggarwal, *Angew. Chem. Int. Ed.* **2018**, *57*, 2155–2159.^[44]

This project was carried out in collaboration with Dr Adam Noble, Dr Daniel Pflästerer and Dr Eddie Myers, their contributions to the project are highlighted (†) and are included to provide a complete picture of the work.

2.1 Project Outline

Boronic acids and their derivatives occupy a privileged position in the chemical sciences. In addition to their application in synthetic organic chemistry as function handles and medicinal chemistry as carboxylic acid bioisosteres (see section 1.1), they have also been used widely in polymer chemistry^[124] and biochemistry.^[125] It is therefore no surprise that extensive research into new methods that incorporate boron into synthetically and medicinally relevant compounds has been conducted.

Radical borylation reactions have seen a recent surge in interest in the past few years due to their high functional group tolerance, mild reaction conditions and ability to convert feedstock materials such as carboxylic acids, amines and alcohols into the corresponding boronic esters.^[23] These reactions proceed via the borylation of a carbon-centred radical generated from the corresponding radical precursor. We wondered whether we could incorporate boron into synthetically and medicinally relevant compounds via an alternative radical pathway, utilising readily available feedstock materials as both the radical precursor and acceptor.

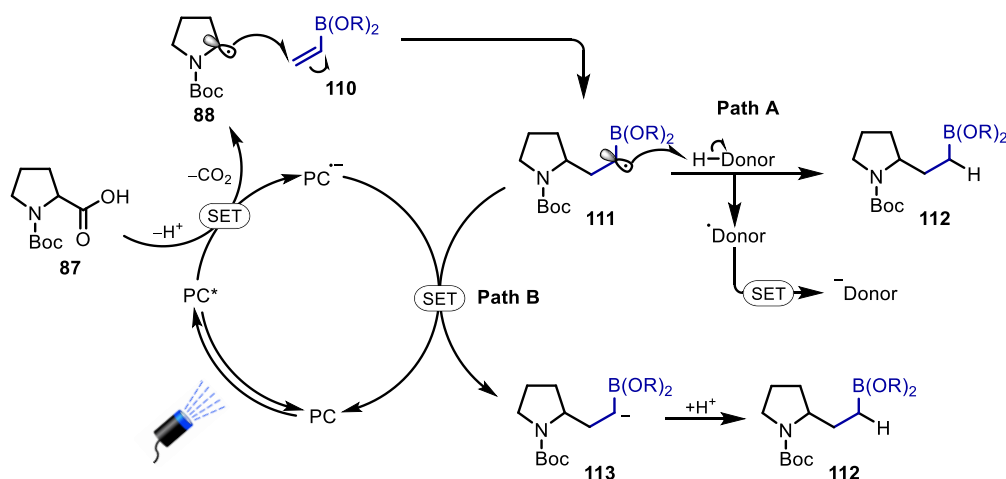
Radical addition reactions to vinyl boronic esters have proved to be efficient for rapidly accessing alkyl boronic esters (see section 1.2.1). These current methods, however, are limited to the use of pre-synthesised radical precursors such as Barton esters, iodides, or xanthates, and also require radical initiators or UV light in order to proceed. Therefore, the full potential of these methods to access more complex and synthetically useful boronic esters is still to be exploited. One way this could be achieved is with the application of photoredox catalysis. This would enable the generation of reactive radical intermediates under mild reaction conditions, extending the reactivity profile of vinyl boronic esters to a wider range of radical precursors. We envisioned that we could utilise carboxylic acids as radical precursors, because they are known to undergo decarboxylation to give nucleophilic radicals under

photoredox catalysis.^[93] These radicals can then readily combine with vinyl boronic esters to give the alkyl boronic ester products. The combination of substrates and reaction conditions would enable the rapid synthesis of complex alkyl boronic esters from readily available, abundant starting materials (Scheme 39).



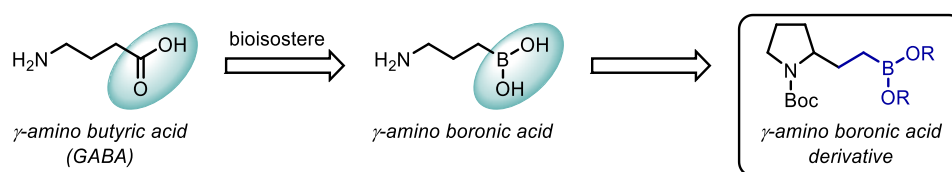
Scheme 39. Project outline; decarboxylative radical additions to vinyl boronic esters using photoredox catalysis.

The proposed photocatalytic mechanism of this transformation is depicted in Scheme 40, using Boc-Pro-OH (**87**) as the example carboxylic acid. Under visible-light irradiation, the photocatalyst (PC) is excited to give a highly oxidising species (PC^{*}), which can undergo single-electron transfer with the carboxylate of Boc-Pro-OH (**87**) to give a carboxyl radical and a reduced state photocatalyst (PC^{•-}). After decarboxylation of the carboxyl radical, the resulting nucleophilic α -amino radical **88** undergoes radical addition to vinyl boronic ester **110** to give a stabilized α -boryl radical intermediate (**111**). At this stage there are two pathways this α -boryl radical intermediate can take in order to complete the catalytic cycle. Path A involves hydrogen atom abstraction from a donor species (H-Donor) to give the alkyl boronic ester product **112**. Single-electron reduction of this donor by the reduced state of the photocatalyst completes the cycle. Work from Matteson,^[26] Carboni^[37] and others have shown this hydrogen atom abstraction is feasible (see section 1.2.1). Moreover, single-electron reduction of a donor species (\cdot Donor) using photocatalysis has also been reported.^[126] Alternatively, in Path B, the α -boryl radical intermediate **111** can undergo direct single-electron reduction to the corresponding α -boryl anion **113**, followed by protonation to give the final product **112**. Single-electron reduction of an α -boryl radical to the corresponding anion is unknown, however, this process maybe thermodynamically feasible due to the stabilising effect the empty p-orbital on boron has on the adjacent carbanion.^[127]



Scheme 40. Proposed mechanism for the decarboxylative radical addition reaction to vinyl boronic esters.

Should this protocol be successful, the *gamma*-amino alkyl boronic ester products **112** exhibit an interesting motif similar to that of *gamma*-amino butyric acid (GABA), the main inhibitory neurotransmitter in the central nervous system. GABA relaxes the activity of neurons by inhibiting nerve transmissions, calming a person, serving as a method to treat stress and anxiety.^[128] As boronic acids are effective carboxylic acid bioisosteres, this methodology would enable the rapid synthesis of a range of *gamma*-amino boronic acid derivatives. These GABA bioisosteres, which are unknown – maybe due to the lack of efficient processes to synthesise them – could have potential biological activity.^[129] Moreover, this reaction manifold could also be applied to a range of other carboxylic acids, including α -oxy and alkyl, as well as other alkenyl boronic esters, enabling rapid access to synthetically useful alkyl boronic esters from readily available starting materials.

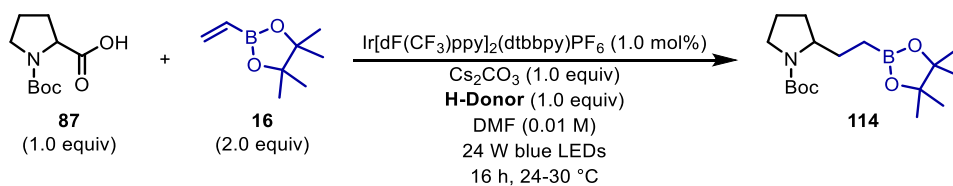


Scheme 41. γ -Amino boronic acid derivatives as bioisosteres of GABA.

2.2 Results and Discussion

2.2.1 Reaction Discovery

In order to explore the proposed reaction manifold, test reactions were conducted using Boc-Pro-OH **87** and vinyl-Bpin **16** as the model substrates (Table 2). Knowing that the commercially available Ir[dF(CF₃)ppy]₂(dtbbpy)PF₆ photocatalyst ($E_{1/2}^{\text{red}} [\text{Ir(III)/Ir(II)}] = +1.21 \text{ V vs SCE in MeCN}$) is oxidising enough to oxidise the cesium salt of **87**, Boc-Pro-OCs ($E_{1/2}^{\text{red}} = +0.95 \text{ V vs SCE in MeCN}$),^[113] it was chosen as the starting photocatalyst in combination with Cs₂CO₃ as the base in DMF under 24 W blue LED light irradiation. We initially screened a range of hydrogen atom donors (H-Donors) in order to obtain the desired alkyl boronic ester product **114** (Path A, Scheme 40). Unfortunately, only trace product was observed in the presence of commonly employed hydrogen atom donors (entries 1-6). On the other hand, in the absence of a hydrogen atom donor, we observed 23% yield of the desired product (entry 7). This suggests that the reaction may be proceeding via single-electron reduction of the intermediate α -boryl radical (Path B, Scheme 40). The low yields obtained in the cases where hydrogen atom donors were used are likely due to other non-productive pathways, such as polymerisation,^[130] as large amounts of vinyl-Bpin **16** had been consumed. Unfortunately, the polymerisation product and Boc-Pro-OH starting materials could not be observed, or quantified, by GC or other spectroscopic methods. Moreover, in retrospect, the chosen hydrogen atom donors (entries 1-6) were polarity mismatched with the α -boryl radical, therefore hydrogen atom abstraction would be unlikely, which could then lead to other non-productive pathways.



Entry	H-Donor	GC Yield (%)	
		114	Vinyl-Bpin (16)
1		9	82
2		0	83
3		0	83
4		0	48
5		13	47
6		14	17
7	None	33	77

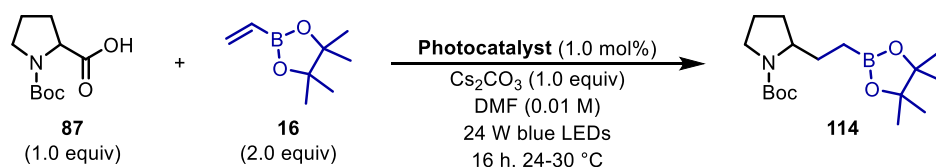
Table 2. Initial test reactions with hydrogen atom donors for the decarboxylative radical addition reaction to vinyl boronic esters. Yields were determined by GC with 1,2,4-trimethoxybenzene as the internal standard.

2.2.2 Optimisation

2.2.2.1 Cyclic Amino Acids

With this initial reaction discovery and the starting conditions in hand, we conducted an optimisation for this novel decarboxylative radical addition reaction to vinyl boronic esters. We commenced our optimisation with the screening of a range of photocatalysts, each with different redox potentials (Table 3). Changing to Ir[dF(CF₃)ppy]₂(bpy)PF₆, where the *tert*-butyl groups have been removed from the bipyridine ligands, resulted in a drop in yield from 33% to 21% (entries 1-2). This is because the photocatalyst is less reducing than Ir[dF(CF₃)ppy]₂(dtbbpy)PF₆ and so does not turn over the catalytic cycle as efficiently. Most interestingly, the Ir(dtbbpy)(ppy)₂PF₆ photocatalyst proved to be optimal,

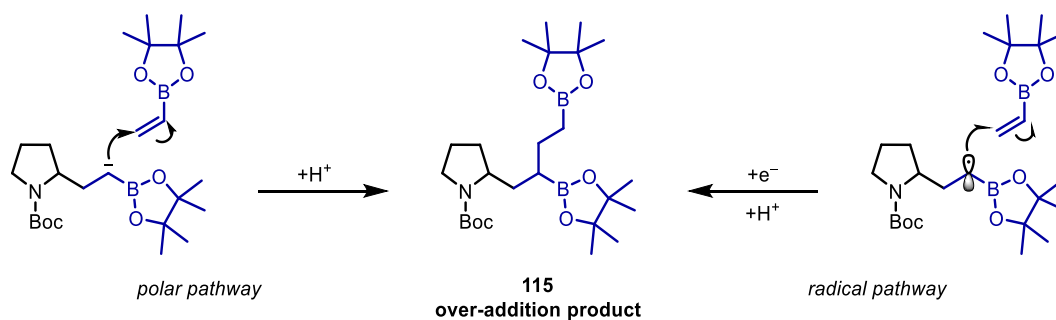
giving an excellent yield of 84% (entry 3). This was surprising as the catalyst in its excited state is much less oxidising than the cesium salt of **87** ($E_{1/2}^{\text{red}} [^* \text{Ir(III)/Ir(II)}] = +0.66 \text{ V vs SCE}$ in MeCN and Boc-Pro-OCs, $E_{1/2}^{\text{red}} = +0.95 \text{ V vs SCE}$ in MeCN)^[90,95] and so, in theory, electron transfer would be thermodynamically unfavourable. This result suggests that although the electron transfer is not spontaneous, it still occurs under these conditions to give the carboxyl radical, which after decarboxylation gives the stabilised α -amino radical. In retrospect, Stern-Volmer quenching studies^[131] would have confirmed whether the excited state photocatalyst was being quenched by the carboxylate of **87**, and if not, this would have suggested an alternative mechanism was operative. As anticipated, the remaining iridium and ruthenium photocatalysts gave no desired product, due to their low oxidation potentials in their excited state (Ir(ppy)_3 $E_{1/2}^{\text{red}} [^* \text{Ir(III)/Ir(II)}] = +0.31 \text{ V vs SCE}$ and $\text{Ru(bpy)}_3\text{Cl}_2$ $E_{1/2}^{\text{red}} [^* \text{Ru(II)/Ru(I)}] = +0.77 \text{ V vs SCE}$)^[90] (entries 4-5). We also trailed the organic photocatalyst, 4CzIPN, now commonly used in the place of iridium photocatalysts due to its similar redox potentials,^[92] but this disappointingly gave a low yield of 18% (entry 6).



Entry	Photocatalyst	GC Yield (%)	
		Product 114	Vinyl-Bpin (16)
1	$\text{Ir}[\text{dF}(\text{CF}_3)\text{ppy}]_2(\text{dtbbpy})\text{PF}_6$	33	77
2	$\text{Ir}[\text{dF}(\text{CF}_3)\text{ppy}]_2(\text{bpy})\text{PF}_6$	21	58
3	$\text{Ir}(\text{dtbbpy})(\text{ppy})_2\text{PF}_6$	84	7
4	$\text{Ir}(\text{ppy})_3$	0	116
5	$\text{Ru}(\text{bpy})_3\text{Cl}_2 \cdot 6\text{H}_2\text{O}$	0	116
6 [†]	4CzIPN [*]	18	30

Table 3. Photocatalyst screen. ^{*}1.5 equivalents of vinyl-Bpin **16** used. Yields were determined by GC with 1,2,4-trimethoxybenzene as the internal standard.

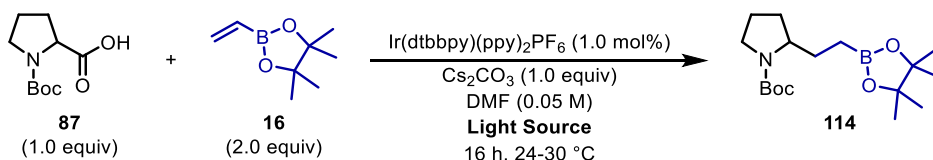
As observed previously in the reaction discovery, large amounts of vinyl-Bpin starting material had been consumed in all cases (Table 3, entries 1-6). In addition to the suspected radical polymerisation the vinyl-Bpin could be undergoing,^[130] the over-addition product **115** was also observed and confirmed by ¹H NMR (Scheme 42). We suspect that the formation of **115** could occur through a polar or a radical pathway. Either pathway may be plausible as α -boryl anions have been shown to be nucleophilic and undergo intermolecular alkylation,^[127] and the radical pathway is the same mechanism as the radical polymerisation of vinyl boronic esters.^[130] Fortunately, this side-product was only observed in small amounts, likely due to the slow rate of the α -boryl anion or radical adding to the vinyl boronic ester.



Scheme 42. Possible polar or radical pathways for the formation of over-addition product **115**.

Moving forward, we screened a variety of inorganic and organic bases (see supplementary materials, section 6.2.4, Table S 1). As expected, the base was required for the transformation to proceed, no reactivity was observed without base. This is because a carboxylate is required to undergo single-electron oxidation. Although all the carbonate bases worked to varying degrees, Cs₂CO₃ was far superior. This may be due to the increased solubility of cesium salts in DMF, DMF solvates the cesium cation well, which effectively leaves the carboxylate as a ‘naked anion’, this is known as the ‘cesium effect’.^[132] Other bases, including KOH, K₃PO₄ and the organic base DBU, were also compatible but gave modest yields.

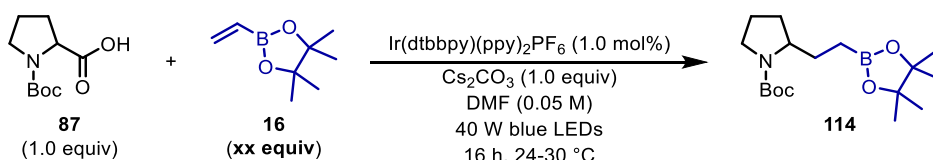
With the knowledge that Cs₂CO₃ was the optimal base we next turned our attention to different light sources (Table 4). Typically, these reactions were not homogenous, despite the improved solubility of cesium salts in DMF, and over the course of the reaction they became milky white fine suspensions. We wondered whether using more powerful 40 W blue LEDs (Kessil™ lamps) would allow greater light penetration into the reaction system, as so far 24 W blue LED strips had been used. It turned out that the power of the lamp did not have any significant impact on the reaction as both 24 W and 2 × 40 W blue LEDs gave excellent yields of >80% (entries 1-2). In addition to the blue LEDs, we also tested a 20 W CFL as the light source, which has a much broader spectrum of light wavelengths, however, this gave a very low yield of 8% (entry 3). From these results we opted to continue optimisation using the 40 W blue LEDs, this was because the power output of the 24 W blue LED strips were known to diminish steadily over time and prolonged use (the power output of these LEDs were measured periodically on a Coherent LabMax-TOP laser power meter equipped with a Coherent Power/Max PS10 sensor) and therefore could not be standardised, thus we opted for the more powerful and reliable 40 W blue LEDs. At this stage of the optimisation we also decided to work at higher reaction concentrations (0.05 M compared to 0.01 M) as these would be more practical at later stages of the project when we would increase the scale of the reaction. From the results in the light source screening, no difference in reaction outcome was observed at the higher concentration.



Entry	Light Source	GC Yield (%)	
		114	Vinyl-Bpin (16)
1	24 W blue LEDs	84	21
2	2 × 40 W blue LEDs	86	16
3	20 W CFL	8	73

Table 4. Screening different light sources. All reactions were fan cooled to maintain a temperature of 24-30 °C. Yields were determined by GC with 1,2,4-trimethoxybenzene as the internal standard.

The equivalents of vinyl-Bpin **16** were next evaluated (Table 5). We found that by lowering the loading of vinyl-Bpin from 2.0 (86%, entry 3) to 1.5 equivalents gave an improved yield of 91% (entry 2), with no **16** remaining at the end of the reaction despite the 0.5 equivalent excess. Lowering the equivalents further to 1.0 resulted in a much lower yield of 67% (entry 1). Increasing the equivalents to 2.5 unfortunately did not give any improvements in yield (78%, entry 4). These results indicate that >1.5 equivalents are needed due to the competing side-reactions of the vinyl-Bpin, whereas higher equivalents favour over-addition, thus reducing the yield.



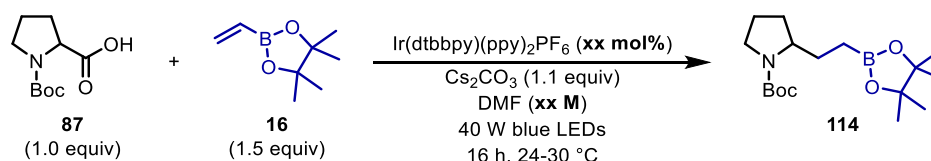
Entry	Equivalents of Vinyl-Bpin (16)	GC Yield (%)	
		114	Vinyl-Bpin (16)
1	1.0	67	0
2	1.5	91	0
3	2.0	86	19
4	2.5	78	45

Table 5. Varying equivalents of vinyl-Bpin **16**. Yields were determined by GC with 1,2,4-trimethoxybenzene as the internal standard.

To ensure that all reaction parameters had been assessed, we conducted a solvent screen and varied the equivalents of Cs_2CO_3 (see supplementary materials, section 6.2.4, Table S 2 and Table S 3

respectively). Despite a range of solvents affording good yields (including DMA, DMI and DMSO), DMF still proved to be optimal. Moreover, the use of standard reagent grade ('wet') DMF proved to be more beneficial than the corresponding anhydrous DMF. Presumably this is due to the increased water content which aids in the final protonation step of the α -boryl anion (see proposed mechanism, Scheme 40, Path B). In the case of Cs_2CO_3 equivalents, we found that a slight excess of Cs_2CO_3 (1.1 equivalents) was ideal; ensuring that all the Boc-Pro-OH **87** starting material was in the carboxylate form.

Finally, with these promising results in hand, we wanted to compare the effects of photocatalyst loading in combination with concentration: 1 and 2 mol% $\text{Ir}(\text{dtbbpy})(\text{ppy})_2\text{PF}_6$ at both 0.05 M and 0.1 M (Table 6). Doubling the concentration to 0.1 M (entry 2) from the standard conditions (entry 1), the yield improved from 87% to 92%. Moving to 2 mol% loading of photocatalyst, we observed an excellent yield of 96% (entry 3), however upon increasing the concentration to 0.1 M the yield dropped significantly to 39%. In the latter experiment, we observed a very dark, cloudy reaction mixture, which may suggest a significant lack of light penetration into the system and thus result in a lower yield. With two promising reaction conditions (entries 2 and 3), we opted for the lower photocatalyst loading of 1 mol% and higher reaction concentration (0.1 M). This would be more economical due to the cost of the iridium photocatalyst and also more practical by working at higher concentration on a larger scale.

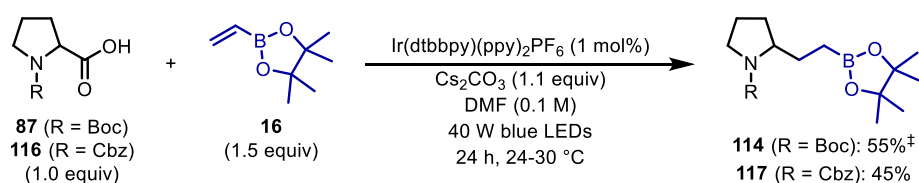


Entry	Photocatalyst loading / mol%	Concentration / M	GC Yield (%)	
			114	Vinyl-Bpin (16)
1	1.0	0.05	87	n.d.
2	1.0	0.10	92	n.d.
3	2.0	0.05	96	n.d.
4	2.0	0.10	36	n.d.

Table 6. Screening of photocatalyst loading and concentration. Yields were determined by GC with 1,2,4-trimethoxybenzene as the internal standard.

With the final optimal conditions in hand, we moved onto scale up and isolation of the boronic ester products (Scheme 43). First, we scaled up our model reaction to 0.3 mmol – typically optimisation was conducted at 0.05 mmol scale – and were disappointed to find we could only isolate 55% of the desired product **114** after leaving the reaction for 24 hours.[†] The product (**114**) showed instability on silica gel during chromatography and we initially thought this was the cause of the low isolated yield. To solve this, it was key that the crude product had minimal contact with silica gel throughout purification by

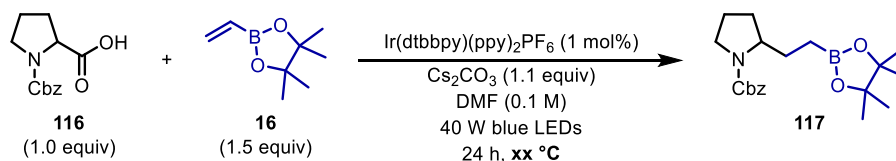
carrying out rapid column chromatography. However, applying these rapid chromatography conditions to Cbz-protected proline **116** still gave a lower than expected isolated yield of 45% (**117**). By acidifying the aqueous phase and carrying out an extraction, we were able to recover 28% of the Cbz-protected proline starting material **116**, which gives 73% yield of **117** based on recovered starting material (BRSM). At this stage, we decided to look more closely at our reaction set-up, specifically light penetration, and reaction temperature.



Scheme 43. Scale up and isolation with the optimised reaction conditions using two proline derivatives **87** and **116**.

Using Cbz-protected proline **116** as the model substrate on a 0.3 mmol scale, we conducted multiple experiments using different photochemistry set-ups to determine whether the yield could be improved on this scale (Table 7). Our standard reaction set-up, which had been used in the optimisation, consisted of shining a 40 W blue LED lamp into a polished dewar (to aid reflection) containing the reaction vial (distance from lamp to vial was 7 cm), with fan assisted cooling (entry 1). As seen previously, this set-up gave a low yield of 39% with large amounts of recovered starting material (RSM).[‡] Surprisingly, removing the dewar and repositioning the lamp improved the yield to 51%, still with a considerable amount of **116** remaining (entry 2).[‡] This improvement in yield may be due to the lights now shining directly at the reaction mixture as opposed to at an angle into the dewar. This meant that more light was available to the reaction mixture, emphasising the importance of light penetration. To increase the amount of light getting into the reaction mixture, we positioned the vial above a mirror that was at a 45° angle (not shown in schematic diagrams), so light would be reflected up into the vial, which increased the yield to 59% (entry 3).[‡] In addition to the light set-up, we also looked at reaction temperature. We first removed the fan and allowed the LEDs to heat up the reaction to 30 °C, which gave a yield of 58% (entry 4).[‡] Moving the lamp closer to the reaction (5 cm away) gave a similar yield of 59%, with a higher reaction temperature of 38 °C (entry 5). Using two blue LED lamps to try and maximise light penetration gave an improved yield of 64% with still 27% **116** remaining (entry 6). By replacing the second lamp with a mirror and placing the lamp 5 cm away from the reaction vial, we were able to get a comparable yield of 64% with similar amounts of recovered starting material (entry 7), suggesting that by only using a mirror behind the reaction vial, it would be the equivalent of using a second lamp. This is likely due to the mirror being beneath the vial, which allows light to penetrate from the bottom of the reaction, unlike when using a second lamp. These set-up techniques demonstrated the importance of light and temperature on our reaction, especially when conducting the

reaction on a larger scale. It was this final set-up (entry 7) that we opted to use for the substrate scope (see section 6.2.1 for photochemical equipment and set-up).

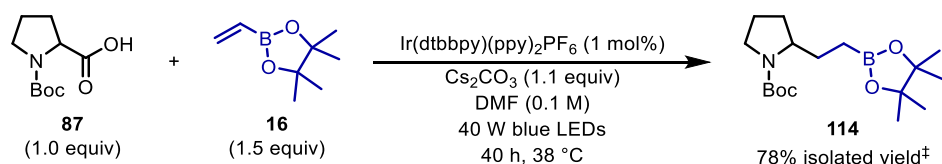


Entry	Set-up	Reaction	Isolated	Recovered
		Temperature / °C	Yield of 117 (%)	Starting Material 116 (%)
1 [‡]		24	39	55
2 [‡]		24	51	41
3 [‡]		24	59	33
4 [‡]		30	58	33
5		38	59	37
6		38	64	27
7		38	64	28

= 40 W blue LEDs, = reaction vial, = dewar, = fan, = mirror.

Table 7. Different set-up techniques shown by the schematic diagrams.

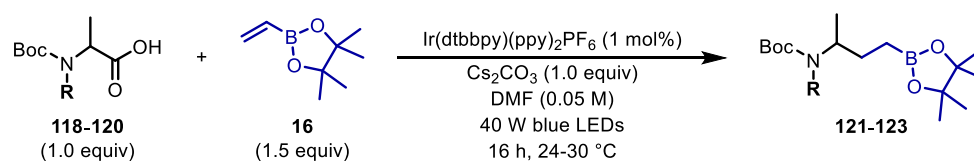
With the reaction conditions, purification and set-up optimised, we repeated our model reaction with Boc-Pro-OH on a 0.3 mmol scale (Scheme 44). Taking into consideration the amount of starting material remaining in the screening of different set-ups (Table 7), we extended the reaction time to 40 hours and were delighted to successfully isolate the desired alkyl boronic ester product **114** in 78% yield.[‡] This increase in yield proved the importance of light, temperature and reaction time.



Scheme 44. Scale-up of model substrate using the optimised reaction and set-up conditions.

2.2.2.2 Monoprotected Acyclic Amino Acids

During our optimisation studies for cyclic amino acids, monoprotected acyclic amino acids (possessing a free NH group) were also investigated to ensure generality of the reaction conditions. Unexpectedly, when Boc-protected alanine (Boc-Ala-OH, **118**) was tested under the optimised conditions, product **121** was formed in a very poor yield of 4% (Table 8, entry 1). However, changing to Boc-*N*-Me-Ala-OH (**119**) showed a drastic increase in yield to 65% (entry 2), then moving to Boc-*N*-Bn-Ala-OH (**120**) the yield improved further to 79% (entry 3). These vast differences in yield between monoprotected and bis-protected alanine highlighted the significant effect a free NH group had on the reaction outcome, almost shutting it down entirely, and by simply masking it with a protecting group, the yield could be enhanced to what was expected. From these results, it was clear further optimisation was required. Enabling the reaction to proceed in the presence of the free NH group would be key to enhancing the scope of the protocol, as we could take advantage of the widespread availability of monoprotected amino acids and also avoid the need to mask the NH with a protecting group.

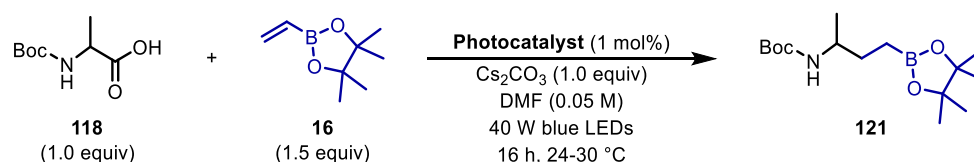


Entry	R	NMR Yield of 121-123 (%)
1 [‡]	H (118)	4 (121)
2 [‡]	Me (119)	65 (122)
3 [‡]	Bn (120)	79 (123)

Table 8. Screening of Boc-Ala-OH derivatives. Yields were determined by ¹H NMR with 1,2,4-trimethoxybenzene as the internal standard.

We pondered whether the presence of the free NH group had an impact on the redox potential of the amino acid, in other words, alter its ability to undergo oxidation. MacMillan and co-workers have shown that acyclic monoprotected amino acids bearing a free NH group could undergo decarboxylative radical

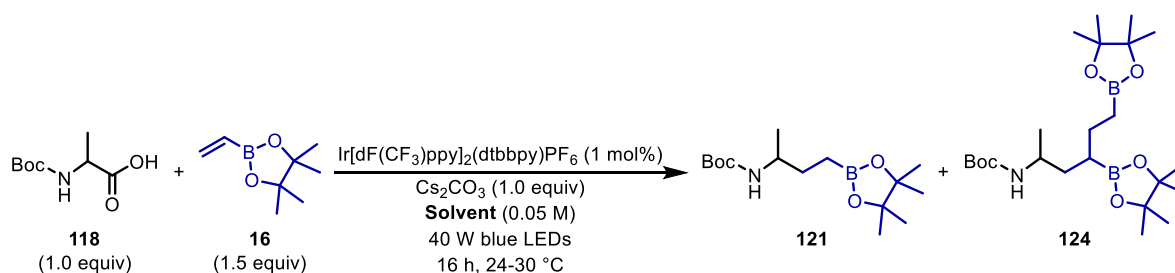
additions to activated Michael acceptors in excellent yields using the fluorinated iridium photocatalyst, Ir[dF(CF₃)ppy]₂(dtbbpy)PF₆.^[133] In its photoexcited state, Ir[dF(CF₃)ppy]₂(dtbbpy)PF₆ ($E_{1/2}^{\text{red}}$ [*Ir(III)/Ir(II)] = +1.21 V vs SCE in MeCN)^[90] is much more oxidising than Ir(dtbbpy)(ppy)₂PF₆ ($E_{1/2}^{\text{red}}$ [*Ir(III)/Ir(II)] = +0.66 V vs SCE in MeCN).^[90] With this in mind, we performed the reactions of Boc-Ala-OH **118** with two commercially available fluorinated iridium photocatalysts, both being more oxidising than Ir(dtbbpy)(ppy)₂PF₆ (Table 9). As expected, Ir(dtbbpy)(ppy)₂PF₆ gave a low yield of 8% (entry 1). However, the yields improved to 31% and 39% with Ir[dF(Me)ppy]₂(dtbbpy)PF₆ ($E_{1/2}^{\text{red}}$ [*Ir(III)/Ir(II)] = +0.97 V vs SCE in MeCN)^[90] and Ir[dF(CF₃)ppy]₂(dtbbpy)PF₆, respectively (entries 2 and 3). These results proved highly promising, suggesting that the free NH does impact the redox potential of the acid and may be a result of intramolecular hydrogen-bonding between the free NH and the carboxylate anion. This, however, was not further investigated.



Entry	Photocatalyst	NMR Yield of 121 (%)
1	Ir(dtbbpy)(ppy) ₂ PF ₆	8
2	Ir[dF(Me)ppy] ₂ (dtbbpy)PF ₆	31
3	Ir[dF(CF ₃)ppy] ₂ (dtbbpy)PF ₆	39

Table 9. Screen of photocatalysts with Boc-Ala-OH **118**. Yields were determined by ¹H NMR with 1,2,4-trimethoxybenzene as the internal standard.

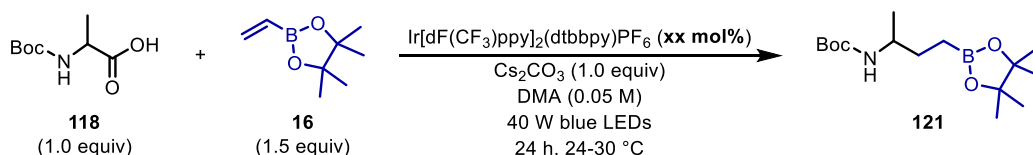
In addition to the desired product, the over-addition product **124** was also observed in a ratio of 7:3 (**121:124**) when the fluorinated iridium catalysts were employed. In the case of the cyclic amino acids, this competing pathway was suppressed by changing to the less oxidising Ir(dtbbpy)(ppy)₂PF₆ photocatalyst. As this was not an option with monoprotected amino acids, we decided to re-investigate solvents to try and eliminate the unwanted over-addition (Table 10). We initially focused on amide-based solvents, with DMF providing a low yield of 29% with 13% over-addition product (entry 1). We saw a similar trend with DMI, with a 6:4 **121:124** ratio (entry 2). No over-addition was observed with the use of DMPU, but product **121** was only observed in 12% yield (entry 3). The breakthrough came when we switched to DMA, giving a major improvement in yield to 58% and completely suppressing over addition (entry 4). DMSO also suppressed over-addition but gave a lower yield of **121** (38%, entry 5). Interestingly, over-addition was observed exclusively in 48% when CHCl₃ was used, showing a complete switch in selectivity. A range of other solvents were also examined; however, no further improvements were made (see supplementary materials, section 6.2.4, Table S 4).



Entry	Solvent	NMR Yield (%)	
		121	124
1	DMF (anhydrous)	29	13
2	DMI (anhydrous)	26	15
3	DMPU (anhydrous)	12	0
4	DMA (anhydrous)	58	0
5	DMSO (anhydrous)	38	0
6	CHCl ₃ (anhydrous)	0	48

Table 10. Solvent screen (partial) for monoprotected acyclic amino acid Boc-Ala-OH **118**. Yields were determined by ¹H NMR with 1,2,4-trimethoxybenzene as the internal standard.

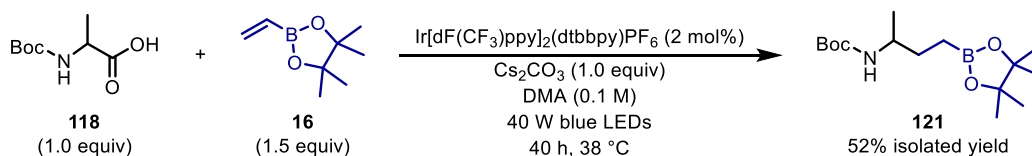
With the optimal solvent in hand, we finally investigated the loading of photocatalyst to determine whether this could improve the reaction outcome (Table 11). For practicality, we conducted this screen on an increased scale (0.1 mmol) and for a longer period of time to account for scalability. When a lower loading of 0.5 mol% was used, the yield dropped to 30% (entry 1). However, increasing the loading to 2 mol% showed an excellent yield of 71% (entry 3). Increasing it further resulted in a significant drop in yield (8%, entry 4), which is likely a result of poor light penetration due to the reaction mixture becoming much cloudier and darker. From these results, it was clear that 2 mol% photocatalyst loading was the ‘sweet spot’ for this protocol, so we concluded our optimisation campaign for the decarboxylative radical addition reaction to vinyl boronic esters.



Entry	Photocatalyst loading / mol%	NMR Yield of 121 (%)
1	0.5	30
2	1.0	58
3	2.0	71
4	5.0	8

Table 11. Photocatalyst loading screen for monoprotected acyclic amino acid Boc-Ala-OH **118**. Yields were determined by ¹H NMR with 1,2,4-trimethoxybenzene as the internal standard.

As with the cyclic amino acid Boc-Pro-OH (**87**) we scaled up the reaction of Boc-Ala-OH (**118**) under the new optimal reaction reactions (Scheme 45). Considering the increased scale, we increased the reaction concentration (to the optimal 0.1 M) and conducted the reaction for a prolonged period of time under the ideal light set-up conditions. Pleasingly, we were able to successfully isolate the desired boronic ester product **121** in 52% yield. We suspect that the lower than expected yield was due to the presence of the free NH negatively impacting the stability of the boronic ester, especially on silica gel. Nevertheless, this was an excellent result and the optimisation gave a vast improvement from the cyclic amino acid conditions, enabling incorporation of a much wider range of amino acid substrates.



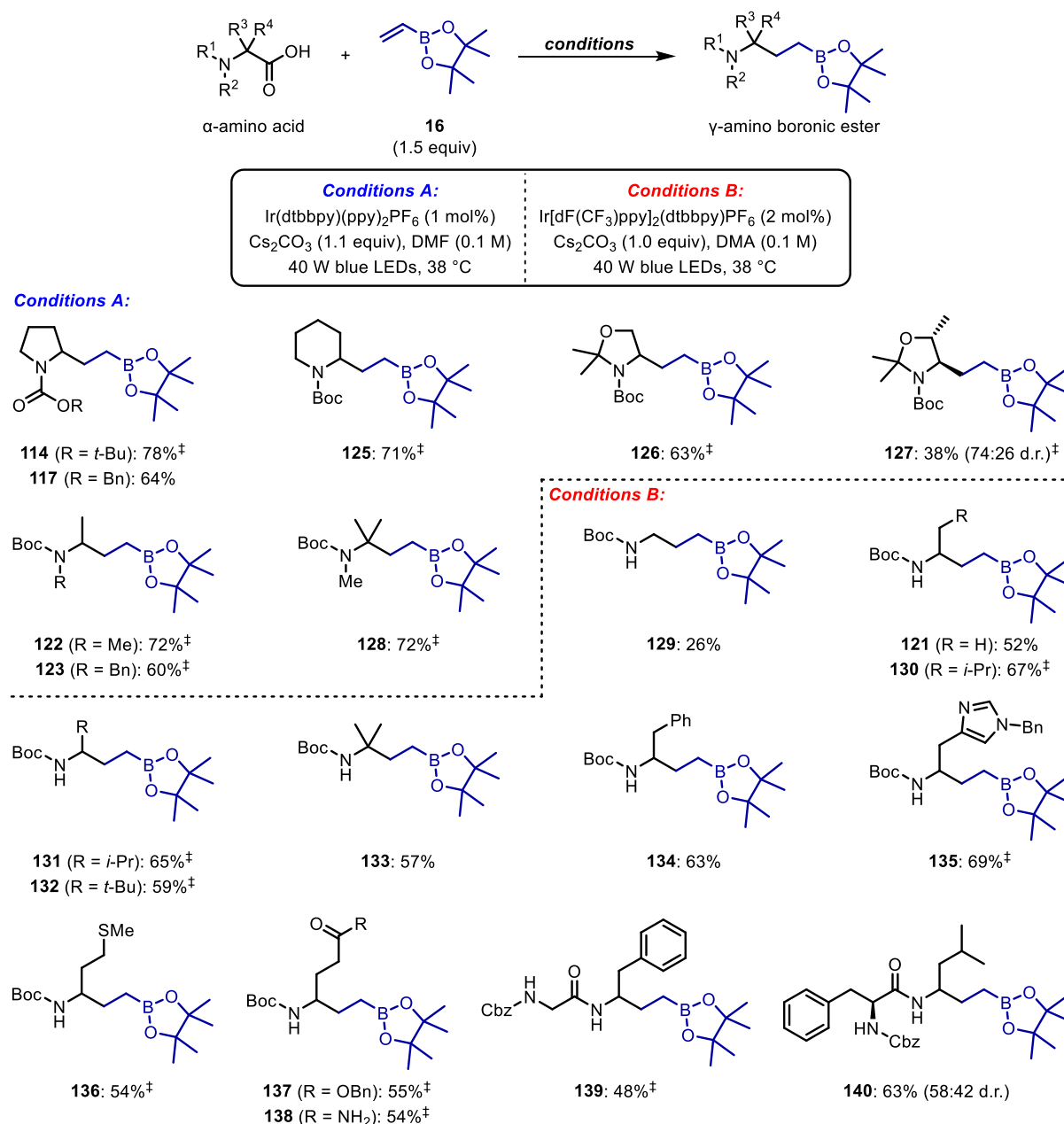
Scheme 45. Scale-up of Boc-Ala-OH **118** under the optimised reaction and set-up conditions.

2.2.3 Substrate Scope

With the optimal reaction conditions in hand for both cyclic and acyclic amino acids, we next looked to exploring the scope of the reaction. We began by investigating the generality of α -amino acids as these are abundant, readily available starting materials (Scheme 46). A range of cyclic amino acids were first tested under the optimal cyclic amino acid conditions (conditions A), which gave the boronic ester products in modest to good yield (**114**, **117**, **125-127**, 38-78%). The reaction was tolerable of different carbamoyl protecting groups (**114**[†] and **117**), increased ring sizes (**125**[†]) and heterocyclic amino acids

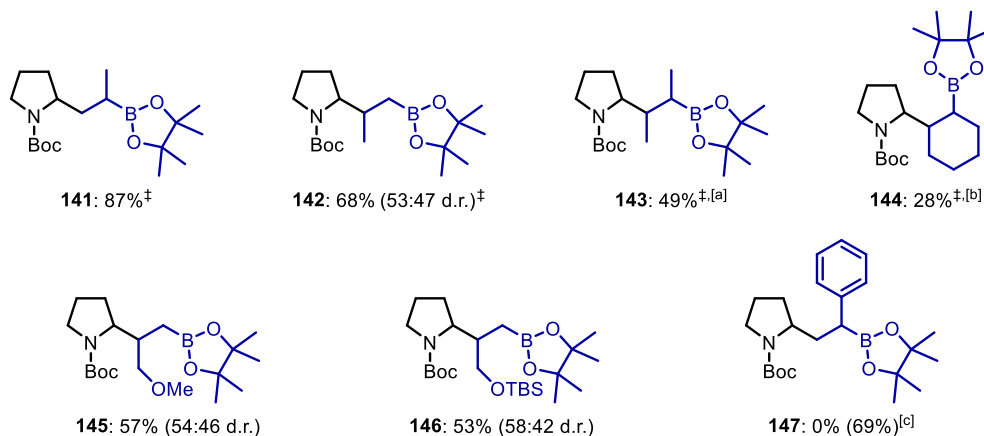
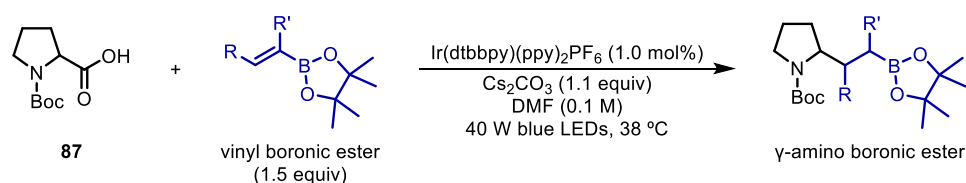
derived from serine and threonine (**126**[‡] and **127**[‡], respectively). Under the same reaction conditions, bisprotected acyclic amino acids were also compatible. Methylated and benzylated Boc-Ala-OH gave the corresponding boronic esters products in good yields (**122**[‡], 72% and **123**[‡], 60% respectively) and the sterically hindered tertiary amino acid Boc-*N*-Me-Aib-OH also proceeded with high efficiency to give the product in 72% yield (**128**[‡]).

Moving to monoprotected amino acids (those bearing a free NH group), under our second set of reaction conditions (conditions B), the primary amino acid Boc-Gly-OH reacted with low efficiency (**129**, 26%). However, changing to the secondary amino acids Boc-Ala-OH and Boc-Leu-OH the yield more than doubled (**121**, 53% and **130**[‡], 67%, respectively). The drop in yield of 20% between mono and bisprotected Boc-Ala-OH substrates (**121** vs **122**[‡], respectively) highlights the difference in reaction outcome by having a free NH group present, even after further optimisation. Moving to more hindered substrates – with an *i*-propyl and *t*-butyl group adjacent to the α -amino radical centre – the reactions proceeded in good yields (**131**[‡], 65% and **132**[‡], 59% respectively). The hindered tertiary amino acid Boc-Aib-OH also gave the boronic ester product (**133**) in a similar yield of 57%, observing a similar drop in yield of 15% from its corresponding bisprotected derivative **128**[‡]. As well as simple hydrocarbon sidechains, a range of other functional groups, including aromatics (**134**), heteroaromatics (**135**[‡]), thioethers (**136**[‡]), esters (**137**[‡]) and primary amides (**138**[‡]) were tolerated under these mild reaction conditions. In addition to amino acids, the dipeptides Z-Gly-Phe-OH and Z-Phe-Leu-OH could also be applied, giving the complex boronic ester products **139**[‡] and **140** in good yields (48% and 63%, respectively). These dipeptides demonstrate that the reaction is not only limited to simple amino acids, but has the potential to be applied to more complex, biologically relevant peptides or even proteins as exemplified by MacMillan and co-workers in their work on decarboxylative alkylations of native proteins.^[106]



Scheme 46. α -Amino acid scope for the synthesis of γ -amino boronic esters. See supplementary materials for exact experiment procedures. Yields are of isolated products after chromatographic purification.

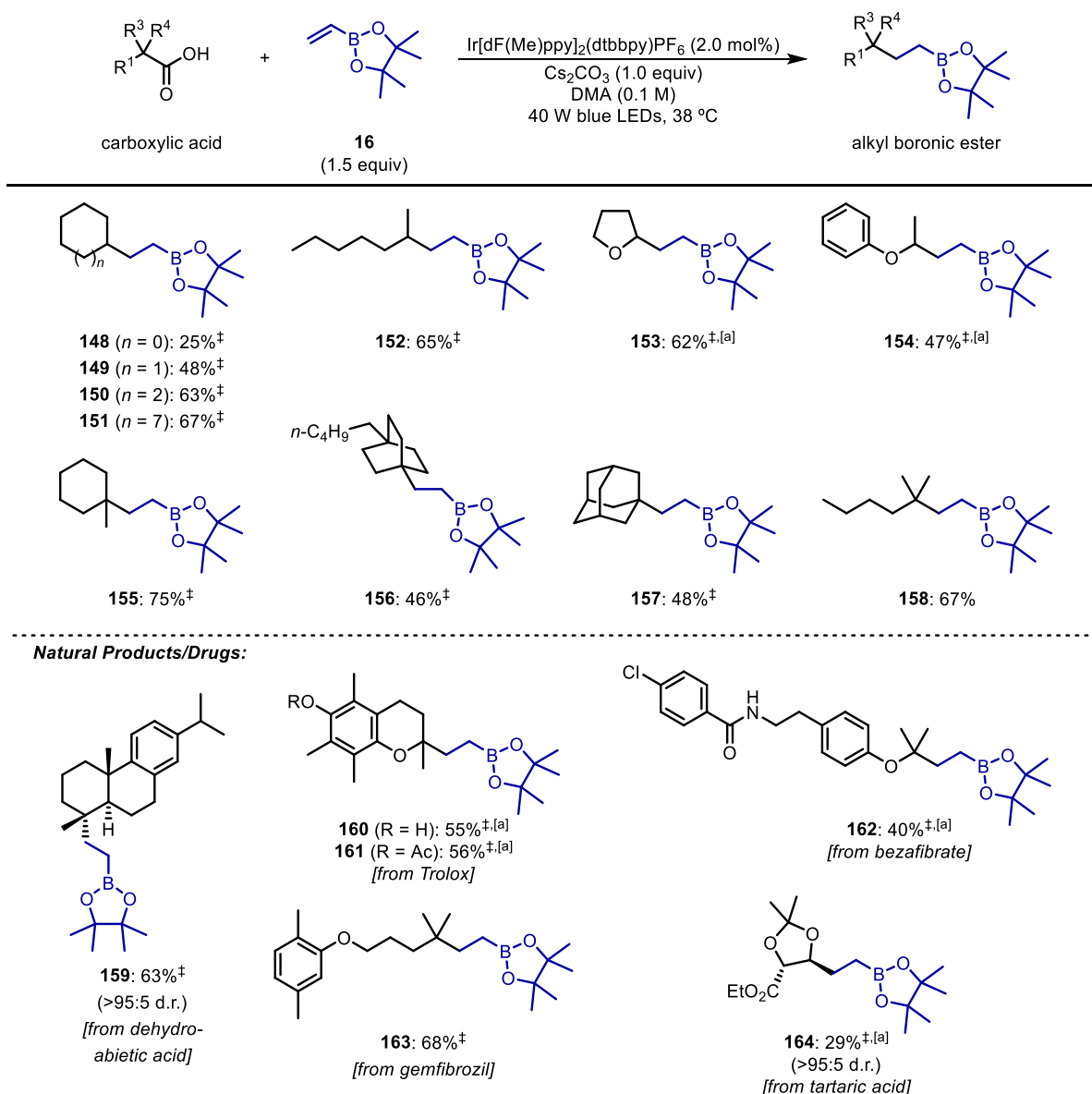
We next explored the scope of alkenyl boronic esters with Boc-Pro-OH **87** (Scheme 47). We found that both 1- and 2-propenyl boronic esters underwent successful radical addition to yield the boronic ester products (**141**[‡], 87% and **142**[‡], 68% respectively). However, α,β -disubstituted alkenyl boronic esters resulted in lower yield, presumably due to the increased steric hinderance of these substrates (**143**[‡], 49% and **144**[‡], 28%). Protected alcohols on the alkenyl boronic esters were also found to be tolerated under the reaction conditions (**145**, 57% and **146**, 53%). Unexpectedly, when an α -styrenyl boronic ester was used, no desired product **147** was observed, but instead the corresponding protodeboronated product was isolated in 69% yield (*vide infra*).



Scheme 47. Alkenyl boronic ester scope for the synthesis of γ -amino boronic esters. See supplementary materials for exact experiment procedures. Yields are of isolated products after chromatographic purification. [a] d.r. could not be determined. [b] 44:33:19:4 d.r. [c] Yield of protodeboronation product (**147'**) given in parentheses.

To further expand the scope of this decarboxylative radical addition reaction, we wanted to utilise simple alkyl carboxylic acids (Scheme 48). Although initial studies showed that Ir[dF(CF₃)ppy]₂(dtbbpy)PF₆ was capable of delivering the desired alkyl boronic ester products, it was found that the more reducing Ir[dF(Me)ppy]₂(dtbbpy)PF₆ photocatalyst gave, in general, better yields for the alkyl carboxylic acid substrates. We were pleased to see a range of simple secondary alkyl carboxylic acids of varying ring size, proceeding to give the corresponding 6- (**148'**), 7- (**149'**), 8- (**150'**) and 12-membered ring (**151'**) boronic ester products in moderate to good yields. Acyclic secondary alkyl carboxylic acids were also compatible (**152'**). Secondary α -oxy carboxylic acids also reacted in good efficiency (**153'**, 62% and **154'**, 47%). Moreover, simple cyclic tertiary alkyl carboxylic acids delivered the boronic ester products in good yields (**155'**-**157'**, 46-75%), as well as linear tertiary carboxylic acids (**158**, 67%).

Finally, to highlight the utility of this methodology, we subjected a range of carboxylic acid natural products and drugs to the reaction conditions to incorporate the dimethylene boronic ester moiety (**159'**-**164'**). These biologically relevant molecules included the diterpenoid, dehydroabiatic acid (**159'**, 63%, >95:5 d.r.), the vitamin E analogue Trolox (**160'**, 55%) and its acetate derivative (**161'**, 56%), the fibrate drugs bezafibrate (**162'**, 40%) and gemfibrozil (**163'**, 68%), and tartaric acid (**164'**, 29%, >95:5 d.r.). These examples demonstrate the utility of this methodology in late stage functionalisation of complex, biologically relevant molecules containing a range of different functional groups including phenols, esters, aromatic ethers, chlorides and amides.



Scheme 48. Alkyl carboxylic acid scope, including natural products and drugs for the synthesis of alkyl boronic esters. See supplementary materials for exact experiment procedures. Yields are of isolated products after chromatographic purification. [a] Ir[dF(CF₃)ppy]₂(dtbbpy)PF₆ (2.0 mol%) used.

2.2.3.1 Unsuccessful Substrates

Unfortunately, despite the excellent functional group tolerance displayed, not all substrates proved successful in the decarboxylative radical addition reaction to vinyl boronic esters. A summary of these substrates is shown in Figure 6. Not all unsuccessful substrates were studied in detail, however three key observations were made depending on the substrates employed: no reactivity resulting in recovered starting material (RSM) (**165**[‡]-**169**[‡]), protodecarboxylation of benzylic carboxylic acids (**170**[‡]) and protodeboronation of α -styrenyl boronic esters (**171**).

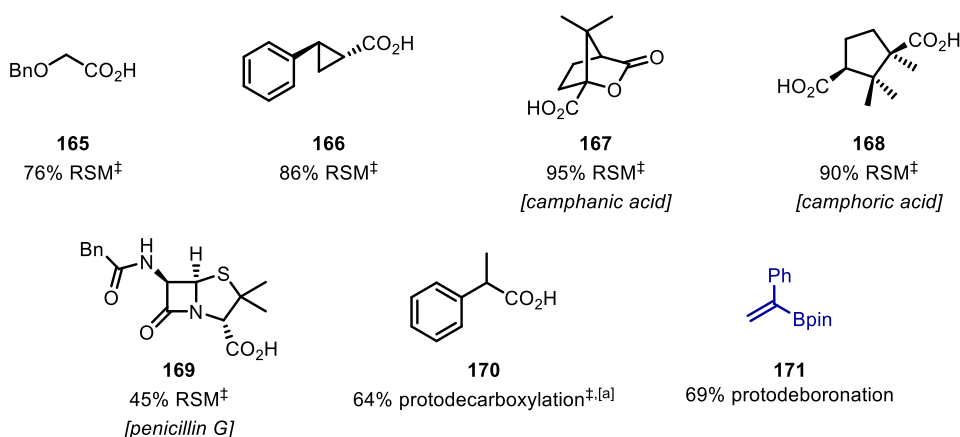
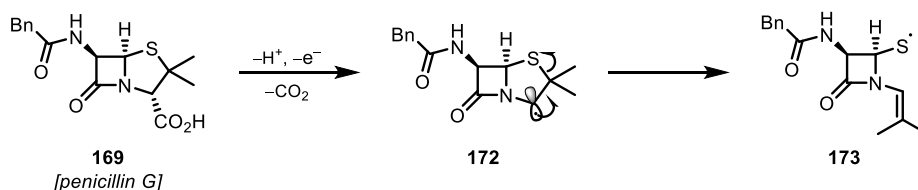


Figure 6. Unsuccessful carboxylic acid and alkenyl boronic ester substrates for the decarboxylative radical addition reaction to vinyl boronic esters. [a] ¹H NMR yield.

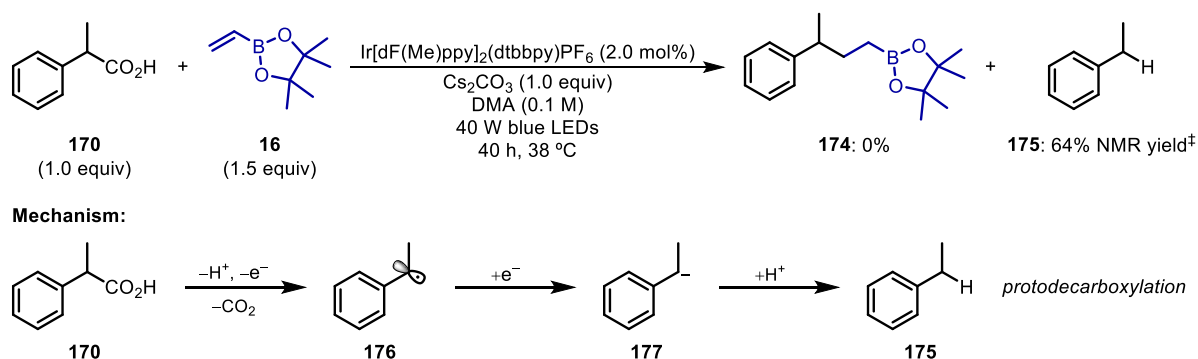
In the majority of unsuccessful cases we were able to recover >75% of the acid starting materials (**165**[‡]-**169**[‡]; complete starting material recovery was not achieved most likely due to loss during the work-up). This suggests that the acids were unable to undergo single-electron oxidation to the corresponding carboxyl radical and thus not decarboxylate. Although not definitive, this may be due to the difficulty in accessing the corresponding alkyl radical as a result of a higher oxidation potential outside the range of the photocatalysts used. The oxidation potentials of these acids have not been reported in the literature and due to time constraints were not determined using cyclic voltammetry. In the case of penicillin G **169**, although 45% of the starting acid was recovered, degradation of the starting material through a competing ring opening of the 5-membered ring after decarboxylation (**172**) to give the sulfur-centred radical **173** (Scheme 49) may also be operating; a similar bond cleavage was observed by Stoodley and co-workers.^[134] However, no products resulting from this ring-opened radical intermediate were observed.



Scheme 49. Potential ring-opening of penicillin G **169** after decarboxylation.

In the case of the benzylic carboxylic acid **170**, no desired product was observed, instead, a 64% NMR yield of ethyl benzene **175** was found (Scheme 50).[‡] This suggests that single-electron oxidation and decarboxylation of the carboxylate of **170** takes place. However, the resulting benzylic radical **176** ($E_{1/2}^{\text{red}} = -1.43$ V vs SCE in MeCN)^[135] is then be readily reduced by the reduced state of the photocatalyst Ir[dF(Me)ppy]₂(dtbbpy)PF₆ ($E_{1/2}^{\text{red}}$ [Ir(III)/Ir(II)] = -1.43 V vs SCE in MeCN)^[90] to give

the corresponding benzylic anion **177**, which upon protonation yields ethyl benzene **175**. This has been observed before by Sawaki and co-workers,^[136] and König and co-workers have used this photocatalytic approach to access benzylic anions, which were subsequently trapped with aldehydes to yield alcohol products.^[137] Under our reaction conditions, the rate of single-electron reduction (to the anion) is faster than radical addition to the vinyl boronic ester, hence no product was observed.



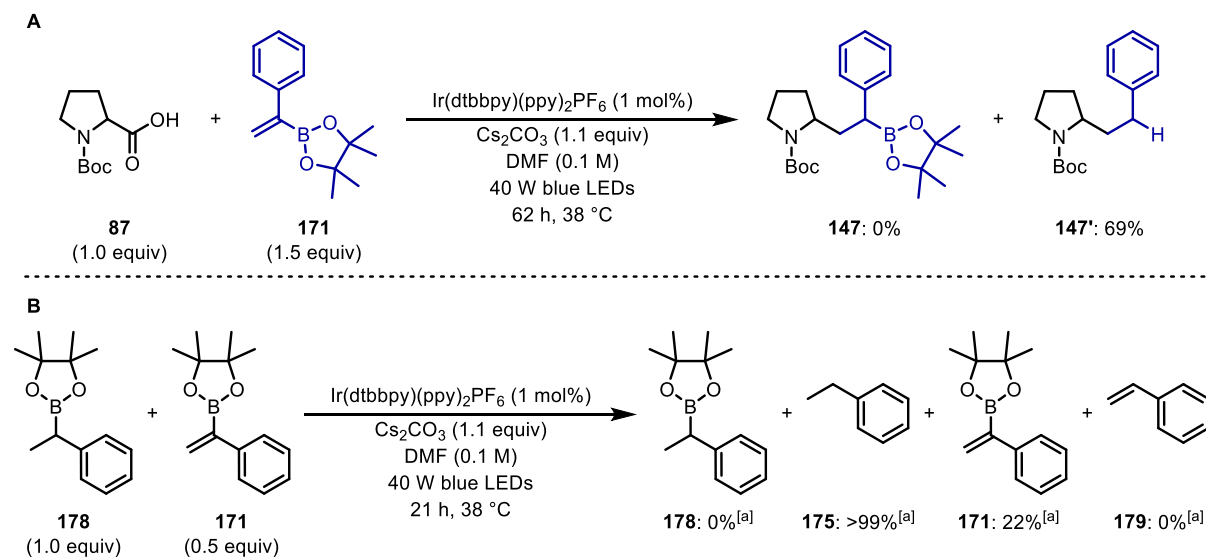
Scheme 50. Protodecarboxylation observed in the case of benzylic carboxylic acid **170** and its mechanism of formation.

Interestingly, no desired product was observed in the reaction between Boc-Pro-OH **87** and α -styrenyl boronic ester **171**, instead the protodeboronated product **147'** was isolated in 69% yield (Scheme 51A). This was a surprising result as we expected the α -styrenyl boronic ester to be a very good radical trap given the success of styrenes in decarboxylative radical addition reactions.^[138] This would have been an efficient way to access functionalised benzylic boronic esters.

To determine the origin of this protodeboronation, we subjected benzylic boronic ester **178** to the reaction conditions without amino acid **87** and 0.5 equivalents of α -styrenyl boronic ester **171** to mimic complete conversion (Scheme 51B). We found that by irradiating the reaction for 21 hours, no benzylic boronic ester **178** remained, but instead >99% yield of ethyl benzene **175** was formed, in addition to 22% recovered α -styrenyl boronic ester **171**. This result suggests the desired benzylic boronic ester does initially form (exemplified by **178** at the start of the reaction) and is then subsequently protodeboronated under the reaction conditions. Recovery of the α -styrenyl boronic ester **171**, and no styrene **179** observed, disfavours the possibility of **171** undergoing protodeboronation followed by radical addition to styrene.

Based on these findings we believe the protodeboronation to be proceeding via a radical mechanism. Ley and co-workers have shown that benzylic boronate complexes, formed by the complexation of a benzylic boronic ester and Lewis base, can undergo single-electron oxidation under photoredox conditions to cleave the C-B bond and give the corresponding benzylic radicals, which were then trapped with various acceptors.^[139–141] Under our photoredox conditions, transient boronate complexes

could form from the reaction of benzylic boronic ester **147** with Cs₂CO₃ or DMF. The resulting boronate complex can then undergo single-electron oxidation from the photoexcited photocatalyst to yield the corresponding benzylic radical. Subsequent single-electron reduction by the reduced state photocatalyst gives the benzylic anion, which can then be protonated to give the protodeboronated product.



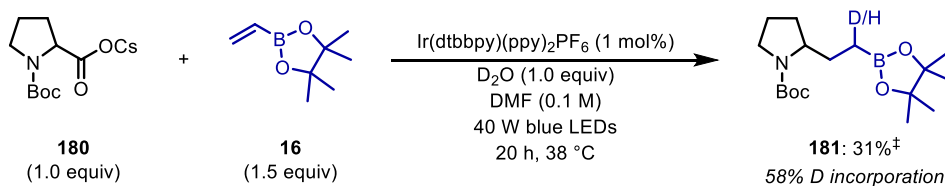
Scheme 51. Protodeboronation of benzylic boronic esters and the studies to determine its origin. [a] GC yield.

2.2.4 Mechanistic Studies

2.2.4.1 Deuteration Studies

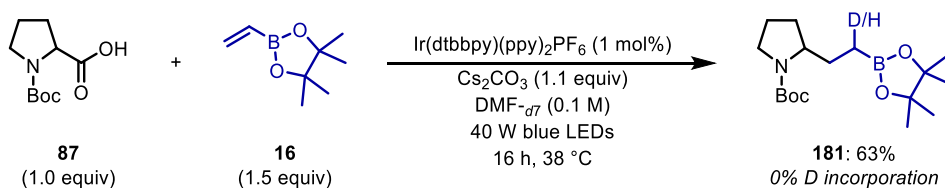
In order to probe the mechanism of the reaction – confirming whether single-electron reduction of the α -boryl radical is taking place or hydrogen atom abstraction – we conducted deuteration studies to identify the origin of the hydrogen atom adjacent to boron in the alkyl boronic ester products.

We began by conducting the reaction between the preformed cesium salt of Boc-Pro-OH **180** and freshly distilled vinyl-Bpin **16** in the presence of 1.0 equivalent of D₂O in anhydrous DMF (Scheme 52). If the α -boryl radical were undergoing reduction to the corresponding α -boryl anion, deuteration by D₂O would be observed at this site. The use of anhydrous DMF and the preformed cesium salt of Boc-Pro-OH removed any other proton sources in the reaction mixture. After irradiating the reaction for 20 hours, we were able to isolate the boronic ester product **181** in 31% yield and observed 58% α -boryl D-incorporation, as determined by ¹H NMR.[†] This experiment confirms the formation of an α -boryl anion and confirms reduction of the α -boryl radical is occurring.



Scheme 52. Deuteration study with D_2O .

Although the deuteration study with D_2O confirms that reduction of the α -boryl radical to the corresponding anion occurs, it does not rule out hydrogen atom abstraction entirely, despite a range of hydrogen atom donors proving ineffective in this reaction (Table 2). DMF has been shown to be a suitable hydrogen atom donor in photoredox processes,^[142] a process that could also be occurring under our reaction conditions and contributing to the lack of complete deuterium incorporation in the D_2O experiment. In order to investigate this further, we conducted the reaction between Boc-Pro-OH **87** and vinyl-Bpin **16** in $\text{DMF-}d_7$ (Scheme 53). If DMF were the source of hydrogen atoms, we would observe α -boryl deuteration in this case. Interestingly, no deuterium incorporation was observed under these conditions, with the boronic ester product being isolated in 63%.



Scheme 53. Deuteration study with $\text{DMF-}d_7$.

The result from these two deuteration studies confirm the formation of an α -boryl anion under these reaction conditions through the reduction of the α -boryl radical by the reduced state photocatalyst rather than the alternative hydrogen atom abstraction pathway. It is likely that the incomplete deuterium incorporation observed in the D_2O study is a result of H_2O contamination in the reaction, either from the DMF, D_2O or the hygroscopic cesium salt.

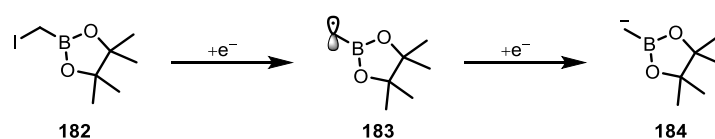
2.2.4.2 Determination of α -Boryl Radical Reduction Potential

With strong evidence supporting reduction of the α -boryl radical intermediate to the corresponding anion, we sought to determine its unknown reduction potential. This would not only confirm whether

the reduced state of the photocatalyst could reduce the radical to the anion, but also be of synthetic value for future work in the field of α -boryl radicals.

Cyclic voltammetry is the typical method employed to measure the standard reduction potential of substrates.^[143] For an electrochemically reversible process, a reliable method of calculating the standard reduction potential is to average the forward and reverse peak potentials. Organic compounds tend to undergo chemically irreversible electron transfers due to the high reactivity of the resulting oxidised/reduced species, which undergo rapid degradation. Therefore, to estimate the standard reduction potentials, the potential at half the maximum current in the cyclic voltammogram (CV), termed the half-peak potential ($E_{p/2}$), is used.^[89,144]

To measure the reduction potential of the α -boryl radical we used iodomethylboronic acid pinacol ester **182** as a model, as this could undergo two single-electron reductions to form anion **184** via the intermediate α -boryl radical **183** (Scheme 54). It was envisioned that two peaks would be observed in the CV corresponding to each electron transfer event. From this we would be able to determine the reduction potential of the α -boryl radical **183** to the corresponding anion **184**. Unfortunately, only one irreversible reduction peak was observed in the CV, corresponding to the two single-electron reductions (Figure 7). Only one irreversible peak was observed since the second reduction (**183** to **184**) is more thermodynamically favourable than the first reduction (**182** to **183**); the second reduction occurs at a potential equal to or greater (less negative) than the first. Taking an average value from three different scan rates (50, 100 and 200 mV/s), the half peak potential, which corresponds to the reduction potential, was determined to be $E_{p/2} = -2.38$ V vs Fc/Fc⁺ in MeCN. This can be converted to a value of $E_{p/2} = -2.00$ V vs SCE (see supplementary materials for full experimental details, section 6.2.3). Although this value does not provide a definitive reduction potential for the α -boryl radical, we know that it would be equal to or greater than (more positive value) -2.00 V.



Scheme 54. Proposed two single-electron reductions of iodomethylboronic acid pinacol ester **182** to determine the reduction potential of the α -boryl radical intermediate using cyclic voltammetry.

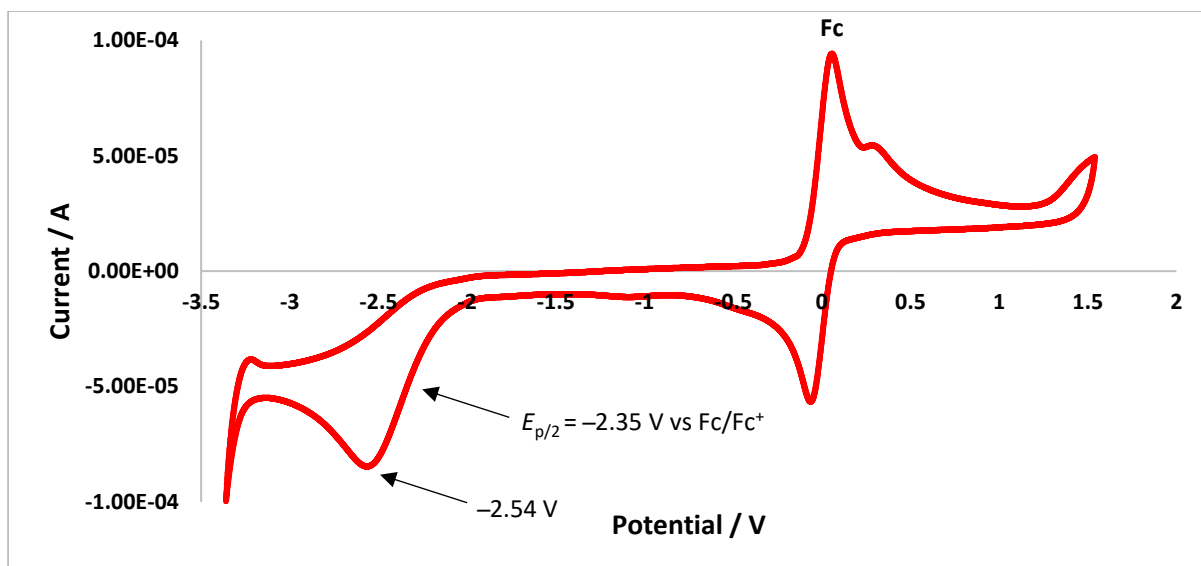
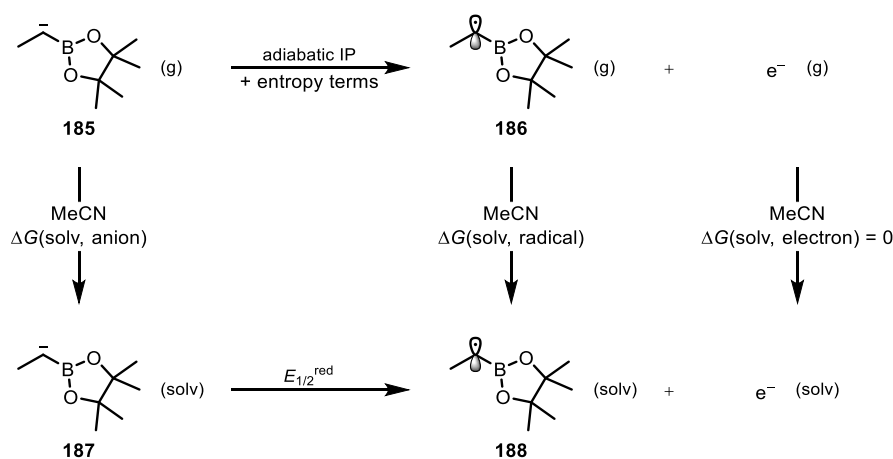


Figure 7. Cyclic voltammogram of iodomethylboronic acid pinacol ester **182** at a scan rate of 100 mV/s, referencing to ferrocene (Fc).

As we were unable to determine the reduction potential experimentally using CV, we decided to use computation to estimate the reduction potential using the methods described by Liu, Guo and co-workers.^[145] Using density functional theory (DFT), we were able to compute the energies associated with the free energy cycle depicted in Scheme 55, specifically, the enthalpy (H) and Gibbs free-energy (G) of the ethyl Bpin anion and radical in the gas phase (**185** and **186**, respectively), as well as the corresponding potential energies (E) in the solvated phase (in MeCN, a commonly used solvent for calculating redox potentials). A summary of the computed energies is given in Table 12.[‡]



Scheme 55. Free-energy cycle for the calculation of the reduction potential of the α -boryl radical intermediate.

Parameter (phase)	Computed Energies	
	Ethyl Bpin anion	Ethyl Bpin radical
H [kcal/mol] (gas)	-307362.4358	-307249.4480
G [kcal/mol] (gas)	-307300.9863	-307281.2206
E [Hartree] (gas)	-490.0574316	-490.0260448
E [Hartree] (solv)	-490.1371310	-490.0295160

Table 12. Computed energies of the given parameter. Values were computed using the B3LYP functionals and 6-311++G(2df,2p) basis set using Gaussian 09.[‡]

From the free energy cycle (Scheme 55), the relationship between reduction potential, gas-phase adiabatic ionisation potential and solvation Gibbs free-energy is given by equation (1).^[145] Where $E_{1/2}^{red}$ is the reduction potential (unit: V), IP is gas-phase adiabatic ionisation potential (unit: eV), $-T\Delta S$ is the gas-phase entropy term (unit: kcal/mol), $\Delta G(\text{solv, radical})$ and $\Delta G(\text{solv, anion})$ are the solvation free energies (unit: kcal/mol), F is the Faraday constant (23.06 kcal/mol·V) and the last term -4.43 is the free-energy change associated with the saturated calomel electrode (SCE) in MeCN (unit: eV), as reported by Isse and Genarro.^[146] $\Delta G(\text{solv})$ of the electron is ignored in this calculation because it equals zero. This equation is derived from the relationship between the standard redox potential and the free-energy change of the system (equation (2)).

$$E_{1/2}^{red} = \text{IP} + \frac{-T\Delta S + \Delta G(\text{solv, radical}) - \Delta G(\text{solv, anion})}{F} - 4.43 \quad (1)$$

$$E^\circ = \Delta G^\circ / F \quad (2)$$

The ionisation potential (IP) can be calculated using equation (3) to give a value of 5.18 eV after adding a correction factor of 0.28 eV.^[145]

$$\text{IP} = H(\text{radical}) - H(\text{anion}) \quad (3)$$

$$= -307249.4480 + 307362.4358$$

$$= 112.9878 \text{ kcal/mol}$$

$$= 4.90 \text{ eV}$$

$$\text{IP (corrected)} = 4.90 \text{ eV} + 0.28 \text{ eV} = 5.18 \text{ eV}$$

The change in Gibbs free energy (ΔG) is related to the change in enthalpy (ΔH) and entropy (ΔS) at constant temperature and pressure by equation (4). Rearranging this equation gives the gas-phase entropy term $T\Delta S$, equation (5), which was calculated to be 94.04 kcal/mol after correcting for the entropic contribution from electron spin degeneracy (+0.82 kcal/mol).^[145]

$$\Delta G = \Delta H - T\Delta S \quad (4)$$

$$T\Delta S = \Delta H - \Delta G \quad (5)$$

$$\begin{aligned} &= (H(\text{radical}) - H(\text{anion})) - (G(\text{radical}) - G(\text{anion})) \\ &= (-307249.4480 + 307362.4358) - (-307281.2206 + 307300.9863) \\ &= 93.22 \text{ kcal/mol} \end{aligned}$$

$$T\Delta S (\text{corrected}) = 93.22 + 0.82 = 94.04 \text{ kcal/mol}$$

The $\Delta G(\text{solv})$ for the anion and radical were calculated from the corresponding potential energies (E) in the gas and solvated phase using equation (6). To give a value of $\Delta G(\text{solv, anion}) = -50.012 \text{ kcal/mol}$ and $\Delta G(\text{solv, radical}) = -2.178 \text{ kcal/mol}$.

$$\Delta G(\text{solv}) = E(\text{solv}) - E(\text{gas}) \quad (6)$$

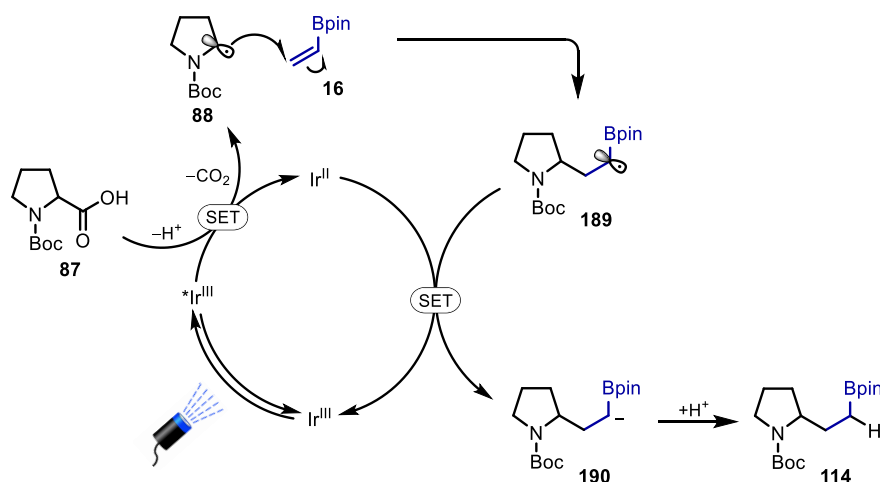
$$\begin{aligned} \Delta G(\text{solv, anion}) &= -490.1371310 + 490.0574316 = -0.0796994 \text{ Hartree} \\ &= -50.012 \text{ kcal/mol} \end{aligned}$$

$$\begin{aligned} \Delta G(\text{solv, radical}) &= -490.0295160 + 490.0260448 = -0.0034712 \text{ Hartree} \\ &= -2.178 \text{ kcal/mol} \end{aligned}$$

Inputting these values into equation (1) gives a computed reduction potential of $E_{1/2}^{\text{red}} = -1.25 \text{ V}$ vs SCE for the α -boryl radical. Comparison to the reduction potential of the reduced state photocatalysts^[90] Ir(dtbbpy)(ppy)₂PF₆ ($E_{1/2}^{\text{red}}$ [Ir(III)/Ir(II)] = -1.51 V vs SCE in MeCN) Ir[dF(CF₃)ppy]₂(dtbbpy)PF₆ ($E_{1/2}^{\text{red}}$ [Ir(III)/Ir(II)] = -1.37 V vs SCE in MeCN) and Ir[dF(Me)ppy]₂(dtbbpy)PF₆ ($E_{1/2}^{\text{red}}$ [Ir(III)/Ir(II)] = -1.43 V vs SCE in MeCN) confirms electron transfer would be thermodynamically favourable based on this value of $E_{1/2}^{\text{red}} = -1.25 \text{ V}$ vs SCE, which is the case as productive catalysis is seen.

2.2.4.3 Final Proposed Mechanism

Taking into consideration our experimental observations (no reactivity with hydrogen atom donors) and mechanistic studies, including deuteration studies and reduction potential calculations, there is strong evidence to suggest a radical-polar crossover mechanism involving the single-electron reduction of an α -boryl radical to the corresponding anion (Scheme 56). Initial oxidation of the cesium salt of Boc-Pro-OH **87** by the highly oxidising photoexcited iridium photocatalyst (*Ir(III)) gives a carboxyl radical which decarboxylates to the corresponding alkyl radical **88**. This nucleophilic radical then undergoes radical addition to vinyl-Bpin **16** yielding the stable α -boryl radical intermediate **189**. Finally, single-electron transfer between the reduced state of the photocatalyst (Ir(II)) and the α -boryl radical gives the corresponding anion **190**, which then yields the alkyl boronic ester product **114** upon protonation.



Scheme 56. Final proposed mechanism for the decarboxylative radical addition reaction to vinyl boronic esters.

A radical chain mechanism, whereby the photocatalyst behaves as an initiator and SET between **189** and the carboxylate of **87** propagates the chain, cannot be ruled out at this time, as Stern-Volmer quenching studies and quantum yield measurements were not conducted.

2.3 Conclusions

In conclusion, the first visible-light mediated decarboxylative radical addition reaction to vinyl boronic esters was developed to rapidly synthesise alkyl boronic esters from readily available carboxylic acids and vinyl boronic esters. The reaction displayed excellent functional group tolerance and was amenable to a range of carboxylic acids, including α -amino, α -oxy, and alkyl carboxylic acids. In addition, the reaction supported a range of substituted vinyl boronic esters, leading to highly functionalised alkyl boronic ester products. The products are not only synthetically valuable due to the incorporation of the boronic ester group, but may have medicinal applications as boron analogues of GABA.

A radical-polar crossover mechanism involving an unprecedented single-electron reduction of the α -boryl radical to the corresponding anion was supported by deuterium labelling studies. Although cyclic voltammetry proved unsuccessful in determining the unknown reduction potential of the α -boryl radical, computational methods calculated the value to be $E_{1/2}^{\text{red}} = -1.25$ V vs SCE. This not only supports the proposed mechanism but provides key mechanistic insight for future work in the field of α -boryl radical chemistry.

3.0 Synthesis of Cyclopropyl Boronic Esters

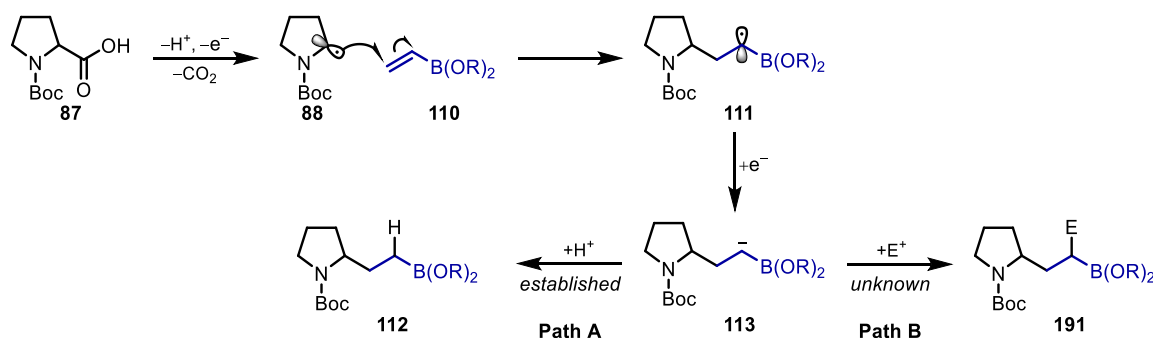
The data presented in this chapter has been partially published in:

C. Shu, R. S. Mega, B. J. Andreassen, A. Noble, V. K. Aggarwal, *Angew. Chem. Int. Ed.* **2018**, *57*, 15430–15434.^[147]

This project was carried out in collaboration with Dr Chao Shu and Björn Andreassen, their contributions to the project are highlighted (†) and are included to provide a complete picture of the work.

3.1 Project Outline

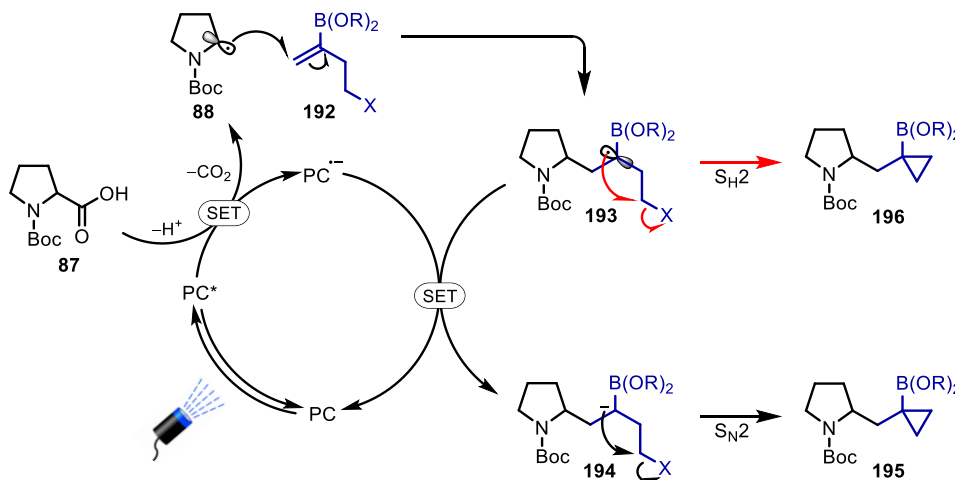
The photoredox-catalysed decarboxylative radical addition reaction to vinyl boronic esters proved to be an efficient method to access functionalised alkyl boronic esters (**112**) from readily available carboxylic acids **87** and vinyl boronic esters **110** (Scheme 57, Path A).^[44] Having proved that the reaction proceeds via a radical-polar crossover mechanism involving the single-electron reduction of an α -boryl radical (**111**) to the corresponding α -boryl anion (**113**), we wondered whether it would be possible to trap the intermediate anion **113** with a carbon-based electrophile. This would result in a dicarbofunctionalisation reaction yielding further functionalised alkyl boronic ester products **191** (Scheme 57, Path B).



Scheme 57. Decarboxylative radical addition to vinyl boronic esters with subsequent trapping of the α -boryl anion.

Targeting cyclopropanes, we envisioned if an electrophilic site, such as a halide, were tethered to the vinyl boronic ester (**192**), rapid intramolecular alkylation could occur. This would provide a decarboxylative radical addition-polar cyclisation cascade to synthesise cyclopropyl boronic esters (**196**), proceeding via the same redox-neutral photoredox cycle as previously developed (Scheme 58,

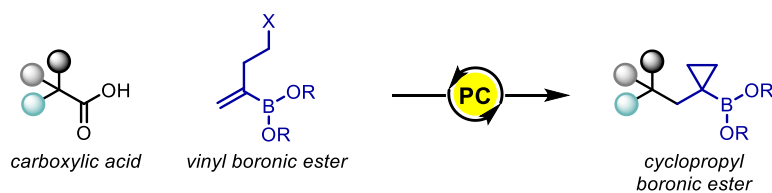
S_N2 pathway).^[144] Alternatively, the intermediate α -boryl radical could instead undergo radical S_H2 , 3-*exo-tet* cyclisation to yield the same cyclopropyl boronic ester product **196** (Scheme 58, S_H2 pathway). This S_H2 cyclopropanation mechanism has been previously reported by Suero^[148,149] and Charette^[150] when iodides were used as the leaving group.



Scheme 58. Proposed mechanism for the synthesis of cyclopropyl boronic esters using photoredox-catalysis.

We opted to target cyclopropanes, as the cyclopropyl fragment is a common component of many bioactive natural products and drug molecules and has been a longstanding carbocycle of interest due to its unique structural properties.^[151,152] The cyclopropyl group is known to increase receptor selectivity, improve metabolic stability and enhance potency as a result of the coplanarity of the three carbon atoms, shorter C-C bonds, and shorter and stronger C-H bonds compared to alkanes.^[151] It is also known to behave as a bioisostere for lipophilic alkyl groups.^[153] Due to these attractive properties, an abundance of methods to synthesise and incorporate the cyclopropyl ring have been developed.^[154–156] These generally employ reactive carbenoids such as in the Simmons-Smith reaction, metal-catalysed decomposition of electron-deficient diazo compounds, or Michael addition-ring closure reactions including the Corey-Chaykovsky reaction. Although these reactions have been well investigated, they do not always display broad functional group tolerance, mild reaction conditions or the ability to further decorate the cyclopropyl ring via the transformation of a functional handle.

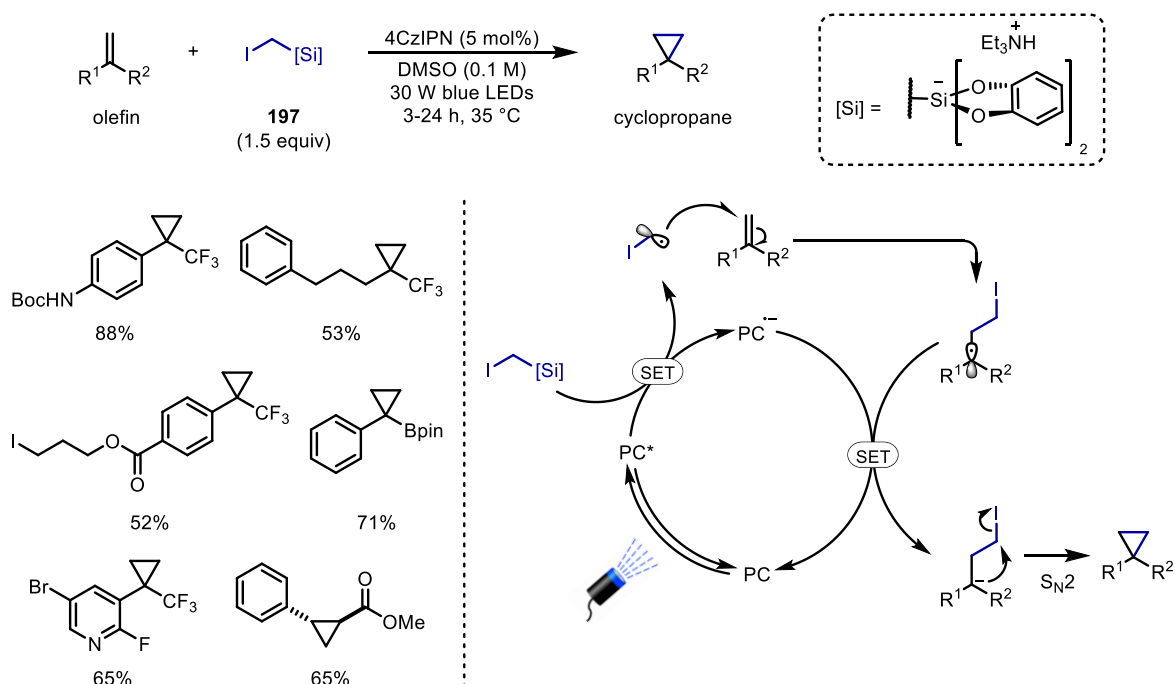
Should our proposed methodology succeed, it would allow the rapid synthesis of complex cyclopropyl boronic ester under mild reaction conditions. The methodology will allow the incorporation of the cyclopropyl unit into medicinally relevant compounds containing a carboxylic acid group. As with our previous methodology, these boronic ester products (when used with α -amino acids) are also bioisosteres of GABA, further illustrating their potential. Moreover, by having the boronic ester functional group in place, rapid structural diversification to synthesise a range of polysubstituted cyclopropanes can be carried out, which is usually required for biological studies (Scheme 59).



Scheme 59. Project outline: synthesis of cyclopropyl boronic esters via a radical addition-polar cyclisation cascade.

3.1.1 Concurrent Reports

During peer review of the manuscript describing the results of this project, Molander and co-workers published a redox-neutral photocatalytic cyclopropanation reaction of olefins (Scheme 60).^[157] They developed a bench stable iodomethyl silicate reagent (**197**), which produces a carbenoid-like radical to introduce a one-carbon unit in a formal [2+1] cycloaddition. In combination with 4CzIPN as the photocatalyst and visible-light, a range of olefins, including α -trifluoromethyl alkenes, styrene derivatives and Michael acceptors underwent the cyclopropanation reaction. Computational studies and mechanistic experiments revealed that the reaction proceeds via a radical-polar crossover reaction involving a polar S_N2 ring closure as opposed to a radical S_H2 ring closure. This is due to a fast, barrierless SET between the reduced state of the photocatalyst and the intermediate radical generated after radical addition.



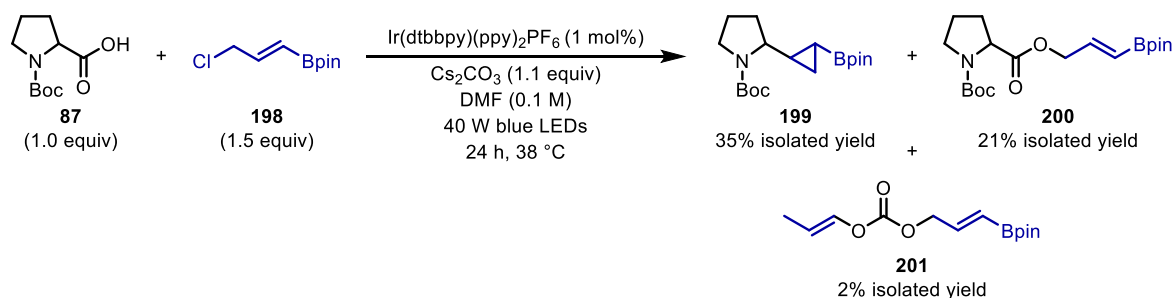
Scheme 60. Molander's redox-neutral photocatalytic cyclopropanation of olefins, showing selected examples and the proposed mechanism.

Since the report by Molander^[157] and ours,^[147] a range of other similar radical-polar crossover cyclopropanation reactions of olefins have been reported^[158] including the use of different leaving groups on the homoallylic radical acceptor^[159–161] and halomethyl silicates as the one-carbon cyclopropanating reagent.^[162–164] From these reports it is clear that these cyclopropanation reactions are highly sought after in the chemical industry as they enable the synthesis of structurally diverse cyclopropanes under mild reaction conditions, avoiding the use of highly reactive or toxic reagents.

3.2 Results and Discussion

3.2.1 Initial Result

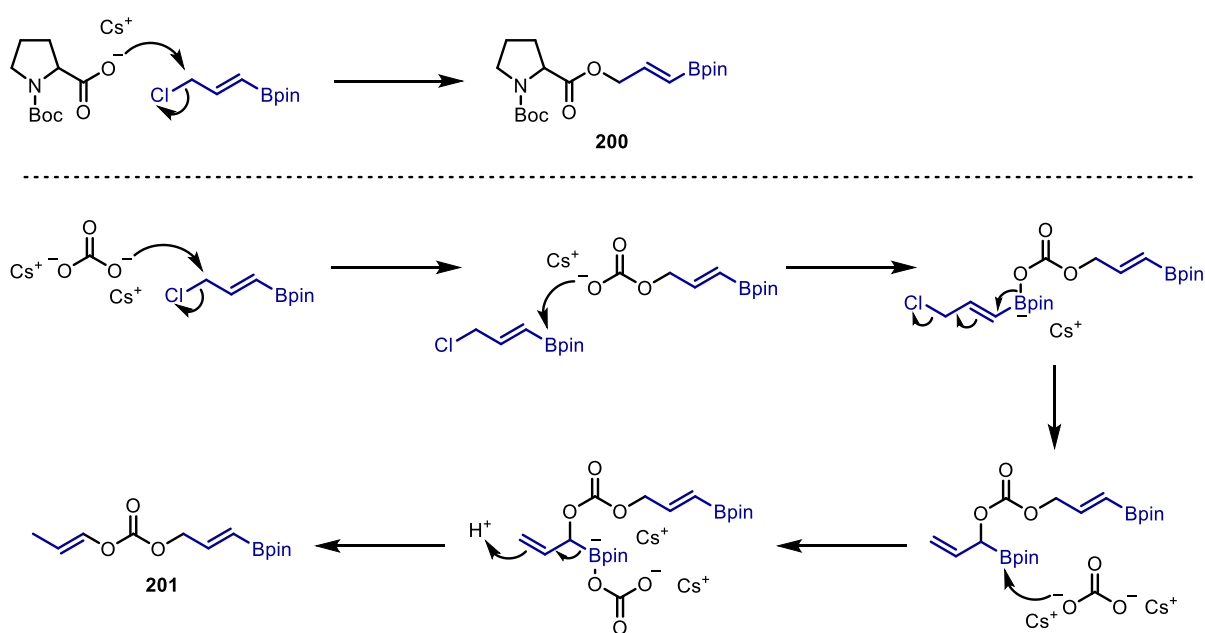
To check the viability of this proposed intramolecular trapping of the α -boryl anion intermediate, we decided to use the commercially available 2-chloromethyl vinyl boronic ester **198** as the radical acceptor. Intramolecular alkylation from the pendant alkyl chloride would yield a vicinally-substituted cyclopropyl boronic ester product. Utilising the optimal reaction conditions previously developed for the decarboxylative radical addition reaction to vinyl boronic esters,^[44] Boc-Pro-OH **87** and 2-chloromethyl vinyl boronic ester **198** were irradiated for 24 h in the presence of Ir(dtbbpy)(ppy)₂PF₆ and Cs₂CO₃ in DMF (Scheme 61). Pleasingly, the reaction successfully yielded the desired cyclopropyl boronic ester product **199** in 35% isolated yield. In addition to this, ester **200**, resulting from the direct alkylation of Boc-Pro-OH **87**, and **201**, resulting from the double alkylation of Cs₂CO₃, were isolated in 21% and 2% yield, respectively. No intermediate hydroalkylation, derived from the protonation of the α -boryl anion, was observed.



Scheme 61. Initial test reaction for the synthesis of vicinally-substituted cyclopropyl boronic ester **199**.

This initial result proved promising, demonstrating that the intramolecular cyclisation was feasible and outcompetes potential protonation of the intermediate anion. However, in order to achieve optimal yields of the cyclopropyl boronic ester product, the other competing alkylation pathways had to be

suppressed (Scheme 62). These challenges arise from the high reactivity of the allylic chloride **198**, an activated electrophile, with the carboxylate of Boc-Pro-OH and the carbonate base. In the case of **201**, we suspect the dialkylation arises from initial alkylation of Cs_2CO_3 , followed by a series of rearrangements, to give the dialkylated product. Similar reactivity of allylboronate complexes with electrophiles has been reported by Aggarwal and co-workers.^[165] From this mechanism, it is also plausible that a range of other alkylated products could arise, even though they were not observed.



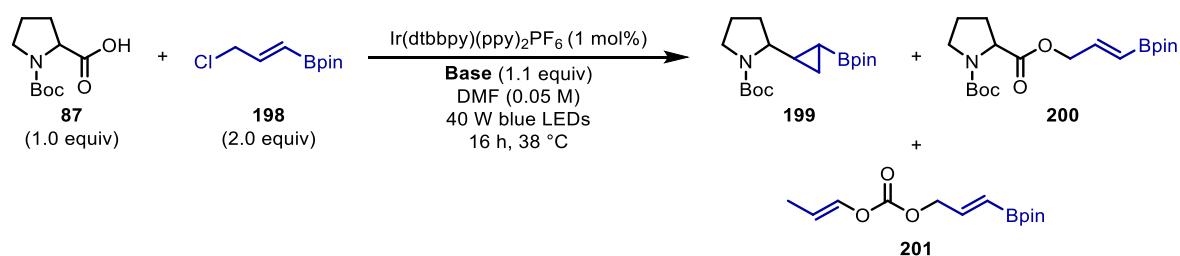
Scheme 62. Mechanisms of the alkylation side reactions.

3.2.2 Optimisation

3.2.2.1 Vicinally-substituted Cyclopropyl Boronic Esters

We began optimisation by screening a variety of bases for the cyclopropanation reaction at more dilute reaction conditions with two equivalents of 2-chloromethyl vinyl boronic ester **198** (Table 13). We previously demonstrated that Cs_2CO_3 was the ideal base for the decarboxylative radical addition reactions to vinyl boronic esters, most likely due to its improved solubility in DMF as a result of the ‘cesium effect’.^[132] This, however, also increases the reactivity of the ‘naked anion’ in nucleophilic substitution reactions, compared to their potassium and sodium counterparts, and in turn aids the alkylation of Boc-Pro-OH to give ester **200** as well as **201**. Therefore, we wondered whether changing to an alternative counter-ion or base would reduce the reactivity of the carboxylate and thus reduce the amount of unwanted alkylation.

We found that Cs₂CO₃ (entry 1) and K₂CO₃ (entry 2) gave comparable yields of desired product **199** (47% and 48%, respectively) with also similar yields of alkylation side-products **200** and **201**, showing a slight reduction when K₂CO₃ was used. Changing to Na₂CO₃ (entry 3), although lower yielding (37%), suppressed the amount of unwanted alkylation of **87** to 4%, but in turn gave increased carbonate alkylation (**201**, 16%). This increase in **201** would not be an issue as it could be countered by increasing the equivalents of base and 2-chloromethyl vinyl boronic ester **198**. In addition to carbonate bases, other inorganic and organic bases were screened (entries 4-7), but were found to be inferior to the carbonate bases. In all cases the 2-chloromethyl vinyl boronic ester **198** was still present at the end of the reaction as expected (being in excess), but also proved stable under these photocatalytic conditions. Unfortunately, the Boc-Pro-OH **87** starting material was not recovered to check whether the reaction had gone to completion. This was due to the difficulty in obtaining reliable recovered starting material yields on small scale (0.05 mmol), either through isolation or using other analytical methods.

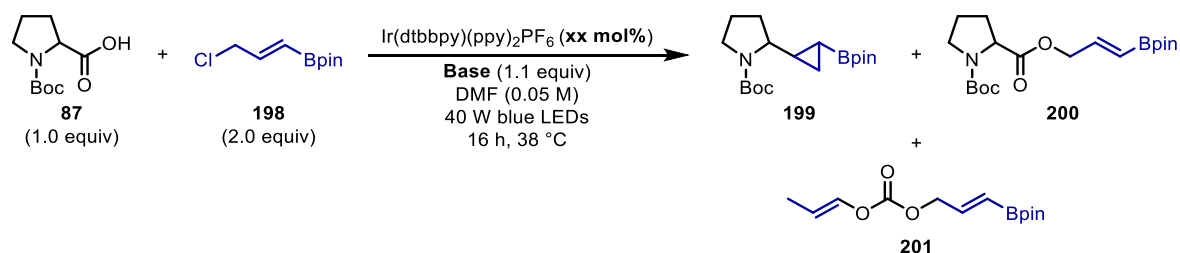


Entry	Base	NMR Yield (%)			
		199	200	201	198
1	Cs ₂ CO ₃	47	20	5	62
2	K ₂ CO ₃	48	17	3	58
3	Na ₂ CO ₃	37	4	16	48
4	KOH	35	16	-	73
5	KOAc	30	19	-	41
6	K ₃ PO ₄	23	7	-	83
7	DBU	35	20	-	60

Table 13. Screening of bases for the synthesis of vicinally-substituted cyclopropyl boronic esters. Yields were determined by ¹H NMR with 1,2,4-trimethoxybenzene as the internal standard.

With the carbonate bases proving to be optimal for this cyclopropanation reaction, we decided to increase the photocatalyst loading for each of the carbonate bases to see whether the yield could be improved (Table 14). Increasing the photocatalyst loading to 2 mol% showed an improvement in yield across all three bases (entries 2-4). We were delighted to see that in the case of Cs₂CO₃ (entry 2) and K₂CO₃ (entry 3) the yields were improved to 53% and 55%, respectively, with a drop in unwanted

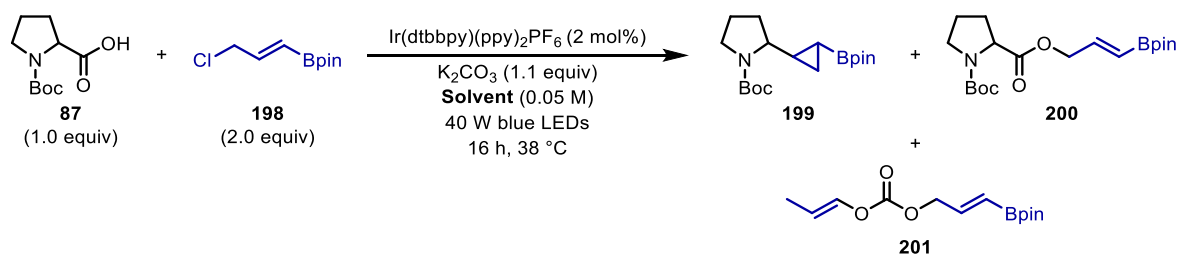
alkylation side-product **200**. Due to the high cost of Ir(dtbbpy)(ppy)₂PF₆ we did not wish to further increase the photocatalyst loading. With these results we selected K₂CO₃ as the optimal base.



Entry	Base	Photocatalyst Loading	NMR Yield (%)			
			199	200	201	198
1	Cs ₂ CO ₃	1 mol%	46	22	3	55
2	Cs ₂ CO ₃	2 mol%	53	11	4	56
3	K ₂ CO ₃	2 mol%	55	8	9	54
4	Na ₂ CO ₃	2 mol%	46	5	0	56

Table 14. Photocatalyst loading screen with the carbonate bases. Yields were determined by ¹H NMR with 1,2,4-trimethoxybenzene as the internal standard.

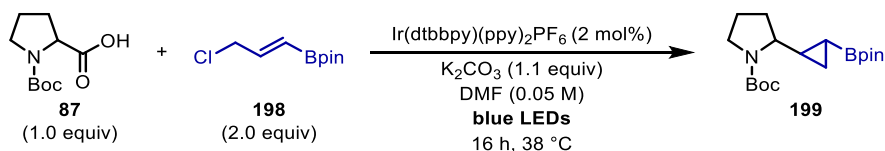
Solvents were next explored (Table 15). Anhydrous DMF had been used throughout the optimisation to avoid any water protonating the intermediate α -boryl anion. Comparing anhydrous DMF (55%, entry 1) to reagent grade ('wet') DMF (44%, entry 2), we saw a drop in yield of 11%, confirming it was necessary to keep the solvent anhydrous, although no protonated intermediate with the pendent chloride was observed by ¹H NMR. As a result of this observation, the remaining solvents screened were anhydrous. DMA had previously been shown to promote the decarboxylative radical additions to vinyl boronic esters in good yield, which was also the case with the formation of **199**, giving a yield of 51% with similar levels of alkylation side products **200** and **201** to DMF (entry 3). The cyclic urea solvents DMI (37%, entry 4) and DMPU (44%, entry 5) initially looked promising with no competing alkylation taking place, however, complete consumption of the 2-chloromethyl vinyl boronic ester **198**, despite being in excess, suggested an increased rate of other competing reaction pathways. Changing to MeCN resulted in a lower yield of 18% with trace amounts of alkylation side-product **200** (entry 6). Switching to DCM (entry 7) and DCE (entry 8), which were optimal in the case of alternative radical acceptors (work carried out by Dr Chao Shu, not included in this report),^[147] also gave low yields of 21% and 24%, respectively. No product was observed when CHCl₃ was employed (entry 9). These results concluded that anhydrous DMF was still the optimal solvent for this reaction.



Entry	Solvent	NMR Yield (%)			
		199	200	201	198
1	DMF (anhydrous)	55	14	4	56
2	DMF	44	14	3	69
3	DMA (anhydrous)	51	11	5	53
4	DMI (anhydrous)	37	0	0	0
5	DMPU (anhydrous)	44	0	0	0
6	MeCN (anhydrous)	18	3	0	69
7*	DCM (anhydrous)	21	0	0	190
8*	DCE (anhydrous)	24	0	0	194
9*	CHCl ₃ (anhydrous)	0	0	0	171

Table 15. Solvent screen for the synthesis of vicinally-substituted cyclopropyl boronic esters. Yields were determined by ¹H NMR with 1,2,4-trimethoxybenzene as the internal standard. *Yields were determined by GC with 1,2,4-trimethoxybenzene as the internal standard.

With the yields plateauing at 55%, we next considered whether enhancing light penetration could improve the reaction outcome. Throughout the course of the reaction we observed a heterogeneous mixture, which hinders light penetration and could lead to inefficient catalysis. The Penn OC photoreactor m1 was developed by Merck in collaboration with the MacMillan group, and has been shown to reduce reaction times and improve the yield of many established photoredox reactions due to the claimed ten-fold increase in power over standard blue LED set-ups.^[166] To probe this, we carried out two scale-up reactions (0.3 mmol) with the latest reaction conditions: one with the standard 40 W blue LED set-up and the other with the Penn OC photoreactor (Table 16). To our surprise, we were able to isolate the desired vicinally-substituted cyclopropyl boronic ester product **199** in very similar yields: 44% with 40 W blue LEDs (entry 1) and 42% with the photoreactor (entry 2). These results suggested that light penetration was not a limiting factor and that both set-ups worked to the same degree. We also took the opportunity to recover the Boc-Pro-OH starting material (**87**), which we were not able to isolate on small scale or track by analytical methods, and found that <5% Boc-Pro-OH **87** was remaining in both cases, showing that these reactions had essentially gone to completion.



Entry	Blue LEDs	Isolated Yield (%)	Recovered 87 (%)
1	40 W blue LED Lamp	44	4
2	Penn OC Photoreactor m1	42	5

Table 16. Scale-up reactions with different blue LED set-ups.

With trace amounts of Boc-Pro-OH **87** starting material remaining after 16 hours, and the total mass balance not being accounted for between the desired cyclopropyl boronic ester product **199** and the side-product ester **200**, it was clear other reaction pathways were consuming the starting material. Looking more closely at the side-products **200** and **201**, formed during the course of the reaction, these could also function as radical traps for the intermediate α -amino radical (Figure 8). Moreover, if the rate of nucleophilic substitution between the carboxylate and 2-chloromethyl vinyl boronic ester **198** to generate **200** (or **201**) was fast, there could be a large concentration of **200** (or **201**) present throughout the course of the reaction. This would mean that there would be a greater probability of the α -amino radical attacking these radical traps (**200** or **201**) than the starting vinyl boronic ester **198**. Although, none of these products were observed, it is a plausible explanation for the low recovery of the starting acid **87**.

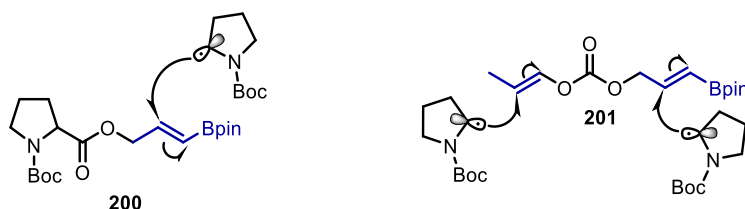


Figure 8. Side-products generated *in situ* behaving as radical traps; possible competing pathways for the α -amino radical.

We subsequently investigated the effect of the photocatalyst. We had previously shown that increased loadings of Ir(dtbbpy)(ppy)₂PF₆ were beneficial (Table 14), however, due to the expense of this photocatalyst we did not want to increase the loading beyond 2 mol%. Therefore, we investigated the use of the more economical organo-photocatalyst 4CzIPN, which can be readily synthesised on gram-scale. 4CzIPN is typically used as a replacement for iridium photocatalysts, not only due to cost, but also due to its redox potential window, which overlaps well with the commonly used Ir(dtbbpy)(ppy)₂PF₆ and Ir[dF(CF₃)ppy]₂(dtbbpy)PF₆ photocatalysts (Figure 9).^[92]

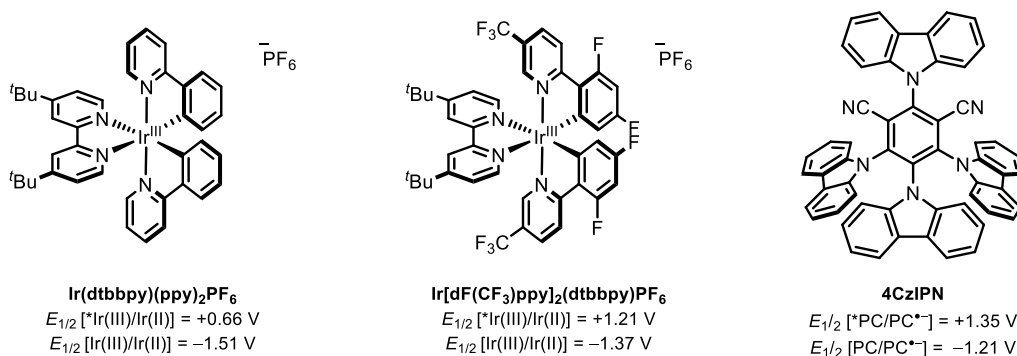
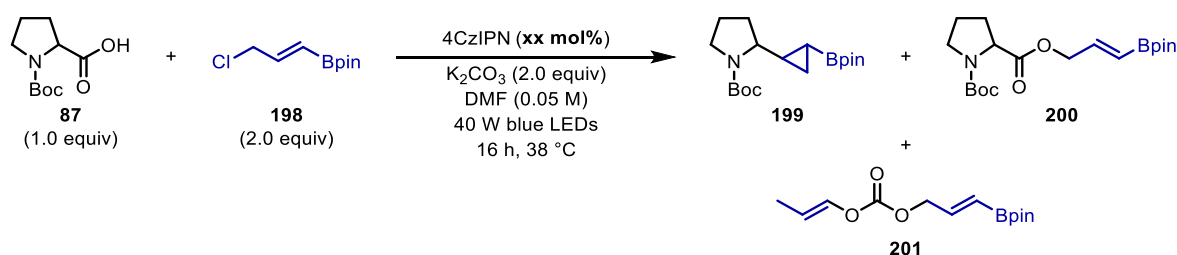


Figure 9. Commonly used iridium photocatalysts and 4CzIPN, comparing redox potentials.^[90,92]

To investigate the viability of 4CzIPN in our reaction, we conducted a screen of various photocatalyst loadings (1-10 mol%) (Table 17). We opted for two equivalents of base for this screen as it was shown that in parallel optimisation studies with alternative radical acceptors this was more beneficial.[‡] The yield steadily increased from 30% to 40% going from 1 mol% to 5 mol% loading (entries 1-4). Unfortunately, no improvement in yield was seen when increasing the photocatalyst loading further to 10 mol% (entry 7). The result of this screen confirmed that 4CzIPN was a viable alternative for this transformation.



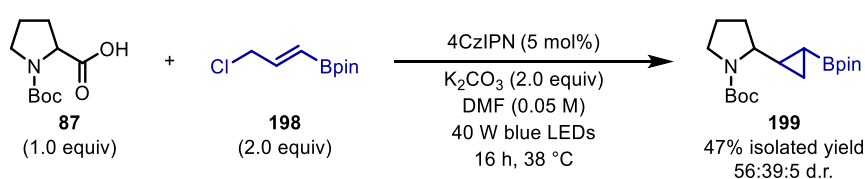
Entry	Photocatalyst Loading	GC Yield (%)			
		199	200	201	198
1	1 mol%	30	8	2	65
2	2 mol%	36	5	2	60
3	5 mol%	40	3	1	65
4	10 mol%	37	4	2	58

Table 17. 4CzIPN loading screen. Yields were determined by GC with 1,2,4-trimethoxybenzene as the internal standard.

After further unsuccessful screens, including equivalents of 2-chloromethyl vinyl boronic ester **198** with both Cs₂CO₃ and K₂CO₃, and additional solvent screening (see supplementary materials, section 6.3.5, Table S 6 and Table S 7, respectively), we decided to conclude the optimisation for this challenging vicinally-substituted cyclopropyl boronic ester and focus on geminally-substituted cyclopropyl boronic

esters. We propose that due to the high reactivity of the 2-chloromethyl vinyl boronic ester **198**, resulting in undesired alkylation reactions, the yield of the cyclopropyl boronic ester could not be further improved as the Boc-Pro-OH **87** starting material was either being consumed in alkylation reactions or other competing radical pathways. Moreover, although two sets of conditions were technically developed, one using the iridium photocatalyst Ir(dtbbpy)(ppy)₂PF₆ and the other with 4CzIPN, we opted to proceed with the 4CzIPN reaction conditions as it is more cost effective.

With these reaction conditions in hand, we scaled up the reaction to 0.3 mmol. Pleasingly, we were able to isolate the desired vicinally-substituted cyclopropyl boronic ester **199** in 47% yield, with no Boc-Pro-OH **87** starting material remaining (Scheme 63). The product **199** was isolated as an inseparable mixture of diastereomers with a d.r. of 56:39:5 (determined after purification by ¹H NMR).

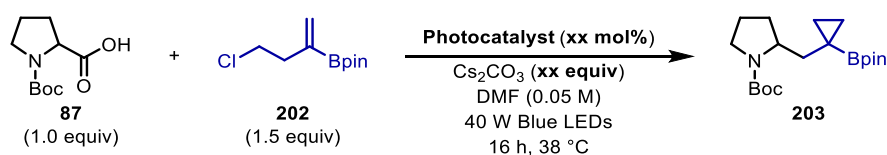


Scheme 63. Scale up reaction for the synthesis of vicinally-substituted cyclopropyl boronic esters.

3.2.2.2 Geminally-substituted Cyclopropyl Boronic Esters

In contrast to the vicinally-substituted cyclopropyl boronic esters, the optimisation for the synthesis of geminally-substituted cyclopropyl boronic esters was relatively straightforward (Table 18). We prepared the homoallylic chloride vinyl boronic ester **202** in one step from the corresponding commercially available homoallylic alcohol vinyl boronic ester (see supplementary materials for details, section 6.3.1), and investigated its reaction with Boc-Pro-OH **87**. Using the optimal conditions for the decarboxylative radical additions to vinyl boronic esters,^[44] we were very pleased to achieve a 76% yield of the desired geminally-substituted cyclopropyl boronic ester **203** (entry 1). This high yield was expected based on previous results obtained with decarboxylative radical additions to α -substituted vinyl boronic esters, such as **202**, which are very good radical traps due to the formation of a stabilised tertiary α -boryl radical intermediate. Moreover, as **202** is not an activated electrophile, no competing alkylation products were observed. By increasing the loading of Cs₂CO₃ to two equivalents, the yield was further improved to 90% (entry 2). As in the case of the vicinally-substituted cyclopropyl boronic ester, we wished to move to the cheaper 4CzIPN photocatalyst. With 5 mol% loading of 4CzIPN, we obtained cyclopropyl boronic ester **203** in quantitative yield (entry 3). This was the real breakthrough in this methodology as we could obtain a highly functionalised cyclopropane with a functionalisable boronic ester group in quantitative yield with only traceless CO₂ and CsCl as the by-products. In

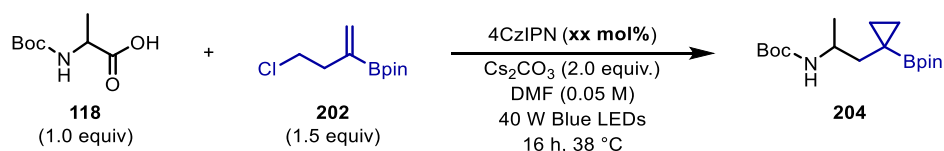
addition to this, by lowering the photocatalyst loading to just 1 mol% the same efficiency was observed (entry 4). Finally, control experiments without base (entry 5), photocatalyst (entry 6), or light (entry 7), demonstrated their essential role for productive catalysis.



Entry	Photocatalyst	Photocatalyst Loading	Equivalents of Cs ₂ CO ₃	GC Yield (%)
1	Ir(dtbbpy)(ppy) ₂ PF ₆	1 mol%	1.0	76
2 [‡]	Ir(dtbbpy)(ppy) ₂ PF ₆	1 mol%	2.0	90
3	4CzIPN	5 mol%	2.0	>99
4 [‡]	4CzIPN	1 mol%	2.0	>99
5 [‡]	4CzIPN	1 mol%	-	2
6 [‡]	none	-	2.0	3
7 ^{‡[a]}	4CzIPN	1 mol%	2.0	0

Table 18. Optimisation of the photoredox-catalysed synthesis of geminally-substituted cyclopropyl boronic esters. [a] Reaction conducted in the dark. Yields were determined by GC with 1,2,4-trimethoxybenzene as the internal standard.

Previously, in the optimisation for the decarboxylative radical additions to vinyl boronic esters, we observed that acyclic monoprotected amino acids bearing a free NH group gave lower than expected yields under the same reaction conditions that were successful for cyclic amino acids.^[44] However, we were pleased to find that simply increasing the loading of 4CzIPN from 1 mol% to 2 mol% provided cyclopropyl boronic ester **204** from Boc-Ala-OH **118** in quantitative yield (Table 19). This is because 4CzIPN is a strong oxidant in its photoexcited state ($E_{1/2}^{\text{red}} [^*PC/PC^{\bullet-}] = +1.35 \text{ V vs SCE in MeCN}$).^[92]



Entry	Photocatalyst Loading	NMR Yield (%)
1	1 mol%	60
2	2 mol%	>99
3	5 mol%	>99

Table 19. 4CzIPN loading screen for monoprotected acyclic amino acids. Yields were determined by ¹H NMR with 1,2,4-trimethoxybenzene as the internal standard.

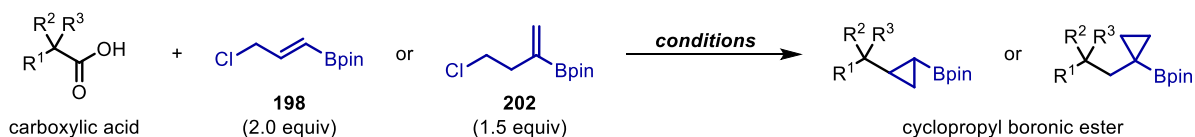
3.2.3 Substrate Scope

With three sets of reaction conditions in hand for the synthesis of cyclopropyl boronic esters we concluded our optimisation campaign, and turned our attention to scaling up and exploring the scope of the reaction (Scheme 64). As previously shown, we were able to isolate the vicinally-substituted cyclopropyl boronic ester **199** in 47% yield with 56:39:5 d.r. using conditions A. Moving to the synthesis of geminally-substituted cyclopropyl boronic esters, cyclic amino acids and bis-protected acyclic amino acids all gave the desired products in very high yields (**203**, **205-207**). The model substrate gave **203** in an excellent isolated yield of 99%, demonstrating the efficiency of the methodology even when scaled up. Using the Cbz-protecting group gave a good yield of 82% (**205**[†]). Changing to the six-membered ring, Boc-Pip-OH gave a high yield of 88% (**206**). And the reaction also proceeded smoothly with the use of bis-protected acyclic amino acids such as Boc-*N*-Me-Ala-OH (87%, **207**[†]).

For acyclic amino acids bearing a free NH group, the primary amino acid Boc-Gly-OH gave the corresponding cyclopropyl boronic ester **208** in 55% yield. We found that upon increasing the sterics around the carbon adjacent to the carbon-centred radical resulted in a gradual decrease in yield (**204**, **209-210**). The tertiary amino acid Boc-Aib-OH also performed well to yield **211**[†] in 58% despite the increased steric hindrance.

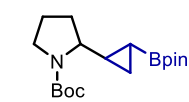
To highlight the robustness of this methodology, a range of amino acids possessing various functional groups were submitted to the reaction conditions. Highly functionalised cyclopropyl esters bearing a phenyl ring (**212**), heteroaromatic (**213**), sulfide (**214**), ester (**215**[†]) and primary amide (**216**) were synthesised in good to excellent yields. Even more structurally complex dipeptides could incorporate the cyclopropyl boronic ester in modest to good yields (**217**, 38% and **218**[†], 61%). We were surprised to observe a drop in yield for dipeptide **217** as the same reacting amino acid Boc-Phe-OH gave a superb yield of 91% (**212**). These examples not only emphasise the robustness of the chemistry, but also illustrate the densely functionalised cyclopropyl boronic esters that can be accessed through this methodology.

α -Oxy acids were also compatible, with tetrahydro-2-furoic acid yielding boronic ester **219** in 76% yield. Alkyl carboxylic acids, including natural products and drug molecules, also underwent the radical addition-polar cyclisation cascade in good yields (**220**[†]-**223**[†]) demonstrating the potential of this methodology in late-stage diversification of bioactive molecules.



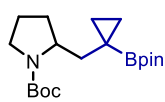
Conditions A:	Conditions B:	Conditions C:
4CzIPN (5 mol%) K ₂ CO ₃ (2.0 equiv), DMF (0.05 M) 40 W blue LEDs, 38 °C	4CzIPN (1 mol%) Cs ₂ CO ₃ (2.0 equiv), DMF (0.05 M) 40 W blue LEDs, 38 °C	4CzIPN (2 mol%) Cs ₂ CO ₃ (2.0 equiv), DMF (0.05 M) 40 W blue LEDs, 38 °C

Conditions A:

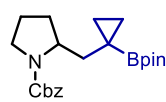


199: 47% (56:39:5 d.r.)

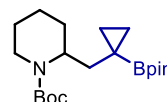
Conditions B:



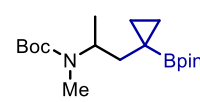
203: 99%



205: 82%[‡]

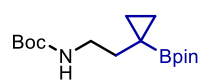


206: 88%

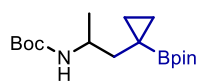


207: 87%[‡]

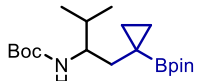
Conditions C:



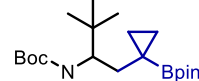
208: 55%[‡]



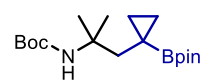
204: 87%



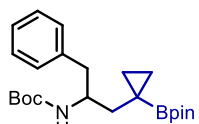
209: 61%



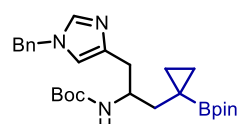
210: 53%



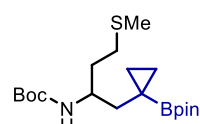
211: 58%[‡]



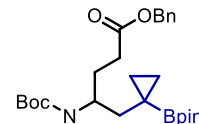
212: 91%



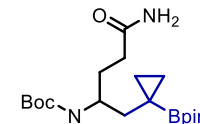
213: 90%[‡]



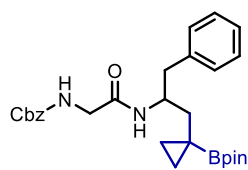
214: 79%



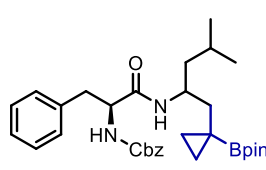
215: 55%[‡]



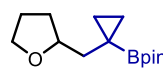
216: 82%



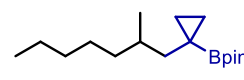
217: 38%



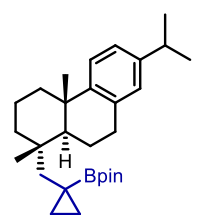
218: 61% (50:50 d.r.)[‡]



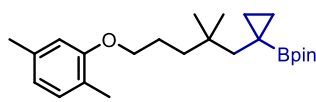
219: 76%



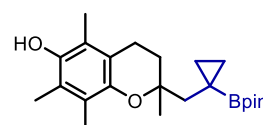
220: 62%[‡]



221: 73% (>95:5 d.r.)
[from dehydroabietic acid]



222: 60%[‡]
[from gemfibrozil]



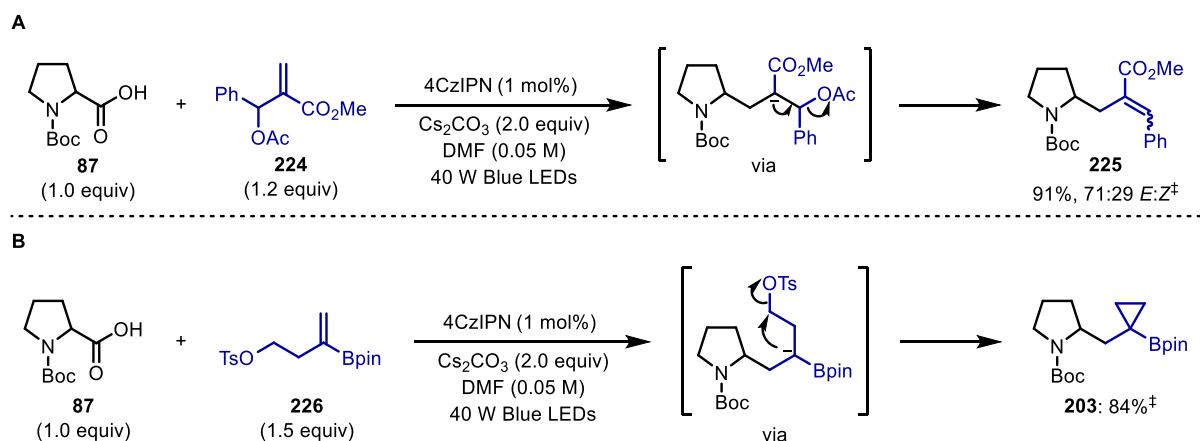
223: 60%[‡]
[from Trolox]

Scheme 64. Carboxylic acid scope for the synthesis of cyclopropyl boronic esters. See supplementary materials for exact experiment procedures. Yields are of isolated products after chromatographic purification.

3.2.4 Mechanistic Studies

In order to elucidate the mechanism of the reaction and confirm whether the intramolecular cyclisation occurs via a radical or polar pathway we conducted an experiment with Boc-Pro-OH **87** and allyl acetate **224** under slightly modified reaction conditions (Scheme 65A)[‡]. Although **224** was not a vinyl boronic

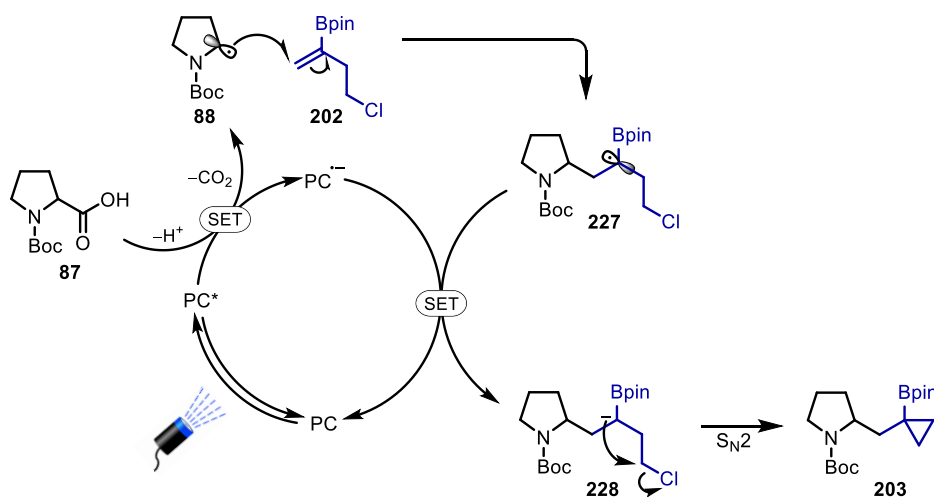
ester radical acceptor, it would still give us insight into whether carbanion intermediates were present. Alkene product **225** was formed in 91% yield (71:29 *E:Z*), via elimination of the acetate group. This elimination would only occur if reduction of the α -carbonyl radical to the corresponding carbanion took place. Moreover, using homoallylic tosylate **226** as the radical acceptor successfully yielded the desired cyclopropyl boronic ester **203** in a good yield of 84% (Scheme 65B)[‡]. Again, this cyclisation would only occur if the intermediate α -boryl radical was reduced to the corresponding anion. The results of these experiments strongly support a radical-polar crossover mechanism.



Scheme 65. Mechanistic studies to investigate the presence of carbanion intermediates.

Although these experiments do not completely rule out a radical S_H2 cyclisation, given the poor leaving group ability of a chlorine radical (compared to iodine as previously reported),^[167] it is unlikely that the cyclisation proceeds via an S_H2 mechanism. Moreover, the results of these experiment are in line with the computational studies carried out by Molander and co-workers on the cyclopropanation of olefins using iodomethyl silicates, whereby they compared the activation barriers of radical and polar cyclisations with various leaving groups and concluded the mechanism proceeds via a polar pathway.^[157]

Based on these mechanistic studies we propose a closed photoredox catalytic cycle involving a decarboxylative radical additional-polar cyclisation cascade as depicted in Scheme 66. Initial photoexcitation of 4CzIPN (PC) gives a highly oxidising species (PC*, $E_{1/2}^{\text{red}}$ [PC/PC*] = +1.35 V vs SCE in MeCN),^[92] which can readily oxidise the carboxylate of Boc-Pro-OH **87** ($E_{1/2}^{\text{red}}$ = +0.95 V vs SCE in MeCN),^[95] which after decarboxylation generates the electron-rich α -amino radical **88**. This radical then adds to the vinyl boronic ester **202**, forming the stabilised α -boryl radical intermediate **227**. Single-electron transfer between the reduced state of the 4CzIPN (PC⁻, $E_{1/2}^{\text{red}}$ [PC/PC⁻] = -1.21 V vs SCE in MeCN)^[92] and **227** ($E_{1/2}^{\text{red}}$ = -1.25 V vs SCE in MeCN)^[44] affords the corresponding α -boryl anion **228**, completing the photocatalytic cycle. Rapid intramolecular 3-*exo-tet* cyclisation yields the cyclopropyl boronic ester product **203**.



Scheme 66. Proposed photoredox-catalysed decarboxylative radical addition-polar cyclisation cascade mechanism.

A quantum yield of $\Phi = 0.65$ was measured for the model reaction between Boc-Pro-OH **87** and homoallylic chloride vinyl boronic ester **202**, which suggests that a radical chain mechanism cannot be entirely ruled out. It is possible the photocatalyst behaves as an initiator and SET between **227** and the carboxylate of **87** is the chain-propagating step. This, however, was not further investigated.

3.3 Conclusions

In summary, a novel photoredox-catalysed decarboxylative radical addition-polar cyclisation cascade reaction for the synthesis of highly functionalised, polysubstituted cyclopropyl boronic esters was developed. Three sets of reaction conditions were established depending on the choice of substrate employed, either (i) 2-chloromethyl vinyl boronic ester **198**, or in the case of homoallylic chloride vinyl boronic ester **202**, (ii) fully substituted amino acids or (iii) acyclic amino acids bearing a free NH group. Excellent functional group tolerance and chemoselectivity were observed, yielding the cyclopropyl boronic esters in good to excellent yields. The use of natural products and drug molecules exemplified the ability to use this methodology in late stage diversification of bioactive molecules, simultaneously installing the cyclopropyl fragment and a boronic ester functional handle.

Mechanistic studies confirmed that the reaction proceeds via a radical-polar crossover mechanism involving the polar cyclisation of the α -boryl anion with the tethered chloride. Although, the radical S_H2 cyclisation cannot be entirely ruled out, the poor leaving group ability of a chlorine radical^[167] in addition to the computational studies conducted by Molander and co-workers^[157] strongly suggests this mechanistic scenario is unlikely.

4.0 Conjunctive Cross-coupling of Vinyl Boronic Esters

The data presented in this chapter has been partially published in:

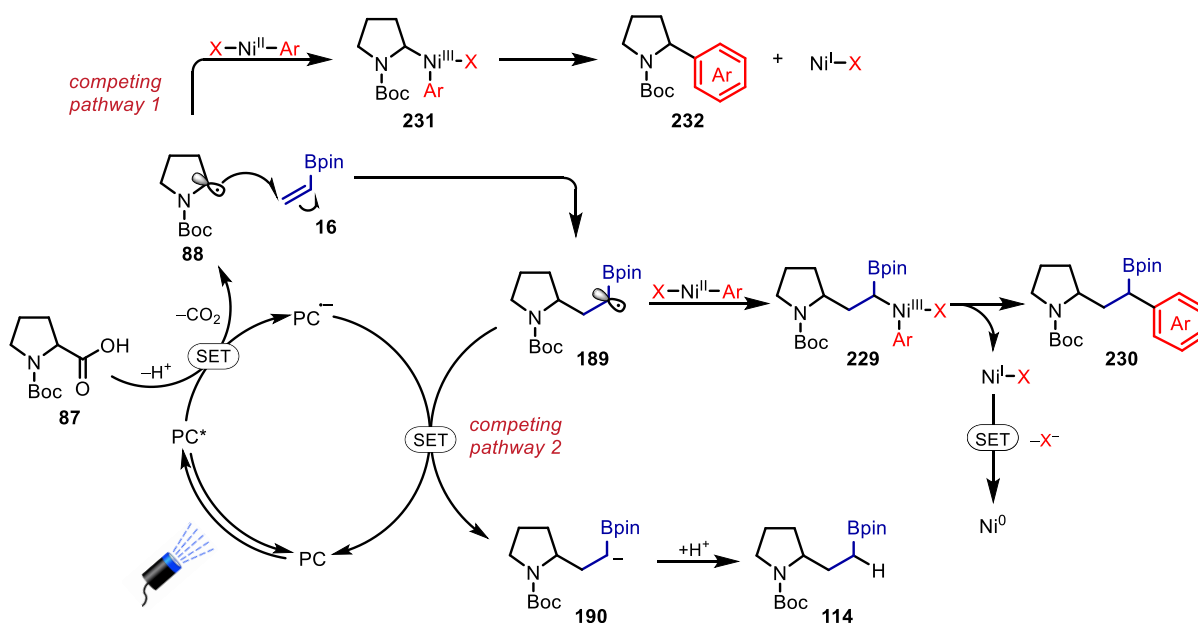
R. S. Mega, V. K. Duong, A. Noble, V. K. Aggarwal, *Angew. Chem. Int. Ed.* **2020**, *59*, 4375–4379.^[168]

This project was carried out in collaboration with Vincent K. Duong and Dr Adam Noble, their contributions to the project are highlighted (†) and are included to provide a complete picture of the work.

4.1 Project Outline

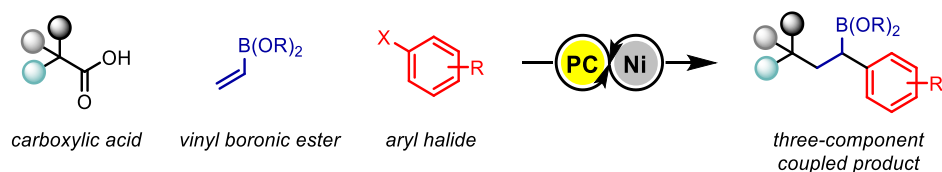
So far, we have shown that photoredox-catalysed decarboxylative radical addition reactions to vinyl boronic esters are a powerful way to rapidly access alkyl boronic esters. We have proved that these reactions proceed via a closed cycle, radical-polar crossover mechanism (Scheme 67). Under visible light irradiation, a photocatalyst can be excited to give a highly oxidising species capable of undergoing SET with the carboxylate of a carboxylic acid. Upon decarboxylation, the resulting electron-rich radical **88** can add to the vinyl boronic ester **16** to generate a stabilised α -boryl radical intermediate **189**. Single-electron reduction of this α -boryl radical to the corresponding anion **190** followed by protonation gives the hydroalkylation product **114**. If a chloride leaving group was tethered to the vinyl boronic ester, ring closure takes place to yield the corresponding cyclopropyl boronic ester.

Given the recent developments in metallaphotoredox catalysis, and the application of α -halo boronic esters in nickel-catalysed cross-couplings, we wondered if we could trap the intermediate α -boryl radical **189** with a Ni(II) complex, formed by the oxidative addition of an aryl halide to a Ni(0) catalyst, to give a Ni(III) species **229** (Scheme 67). Upon reductive elimination this would yield a highly functionalised benzylic boronic ester **230**. Then single-electron transfer between the reduced state of the photocatalyst (PC^{•-}) and the resulting Ni(I) complex would synchronise the two catalytic cycles.



Scheme 67. Decarboxylative radical additions to vinyl boronic esters. Proposed trapping of intermediate α -boryl radical with a Ni(II) complex and competing pathways.

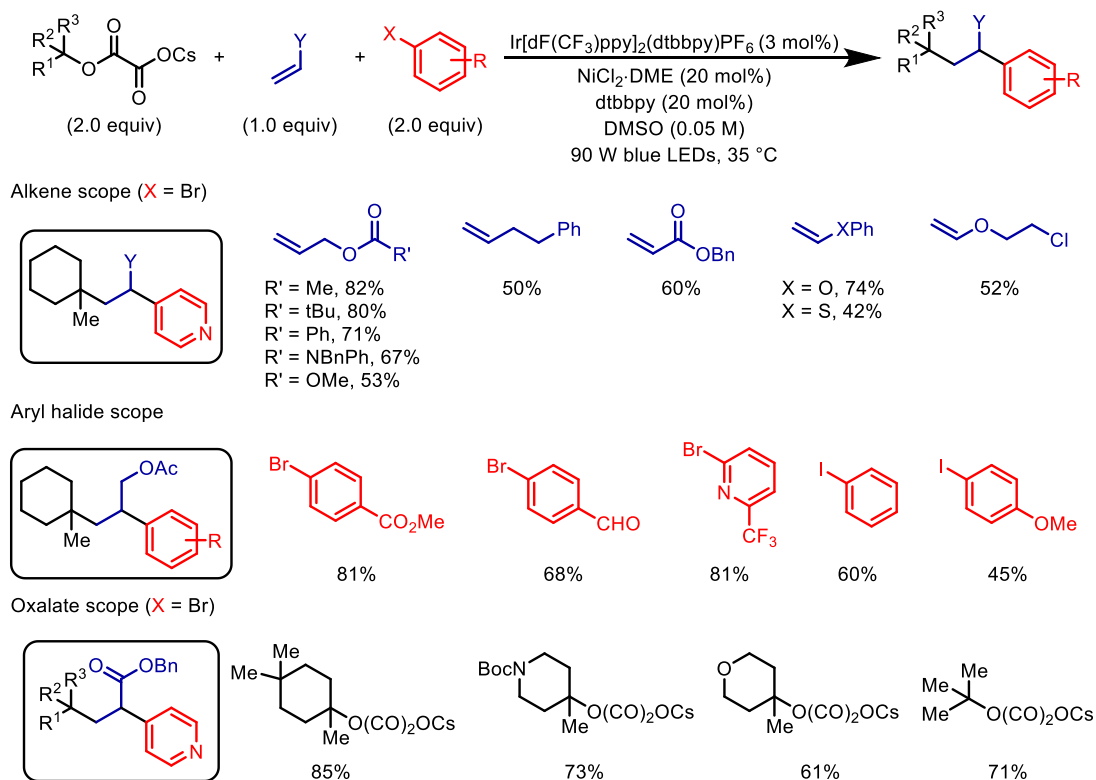
In order to effectively develop this conjunctive cross-coupling two key challenges, which are both established reaction pathways in (metalla)photoredox catalysis, must be addressed (Scheme 67, competing pathways). Firstly, the rate of addition of the electron-rich radical **88** to the vinyl boronic ester **16** must be faster than trapping with the Ni(II) complex as this would lead to unproductive two-component cross-coupled product **232** (competing pathway 1).^[113] Secondly, the rate of trapping of the α -boryl radical intermediate **189** with the Ni(II) complex must be faster than single-electron reduction of the α -boryl radical **189** to the corresponding anion **190** by the reduced state of the photocatalyst as this would lead to the formation of the hydroalkylation product **114** (competing pathway 2).^[44] Together with the challenge of getting two catalysts to work in harmony, if successful, this reaction would furnish an unprecedented three-component decarboxylative conjunctive cross-coupling of vinyl boronic esters with carboxylic acids and aryl halides (Scheme 68). It would allow the rapid, convergent build-up of molecular complexity by forging two carbon-carbon bonds in a single step using readily available feedstock starting materials. Not only this, the incorporation of the boronic ester functional handle would enable further diversification of the products, as well as the products themselves being GABA bisoesters when α -amino acid substrates are used.



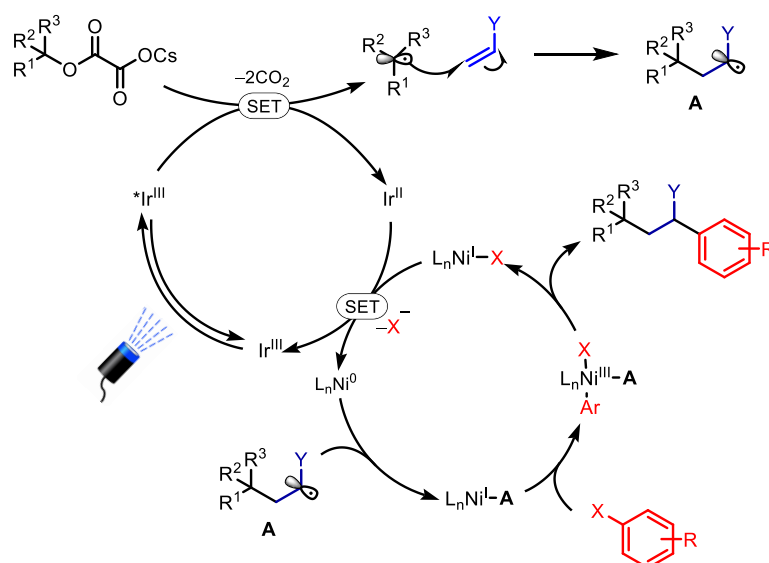
Scheme 68. Project outline: decarboxylative conjunctive cross-coupling of vinyl boronic esters with carboxylic acids and aryl halides.

4.1.1 Concurrent Reports

During the course of this project multiple related methodologies were published involving the conjunctive cross-coupling of alkenes with a range of radical precursors and aryl halides under metallaphotoredox catalysis. Chu and co-workers were the first to publish in this area, utilising tertiary alkyl oxalates (derived from alcohols) as radical precursors with a range of alkenes and aryl halides (Scheme 69).^[169] They demonstrated that unactivated alkenes as well as electron-rich and electron-deficient alkenes were compatible, and a broad scope of aryl halides were tolerated regardless of electronics; although, electron-neutral and electron-rich aryl iodides were not as efficient as electron-deficient aryl bromides. The scope with respect to the alkyl oxalates was limited to substrates derived from tertiary alcohols, as the increased sterics are required to suppresses undesired direct two-component coupling. Moreover, two equivalents of the oxalate are needed, and they require two-steps to synthesise from alcohols. The group carried out some mechanistic studies, using the radical trapping reagent TEMPO and a radical clock reaction, which were consistent with a radical process. Moreover, a stoichiometric experiment with a preformed Ni(II) complex gave no reaction, suggesting the reaction does not involve radical addition to a Ni(II) complex, but instead a radical addition to Ni(0) followed by oxidative addition of the aryl halide to a Ni(I) species. The proposed mechanism is depicted in Scheme 69.



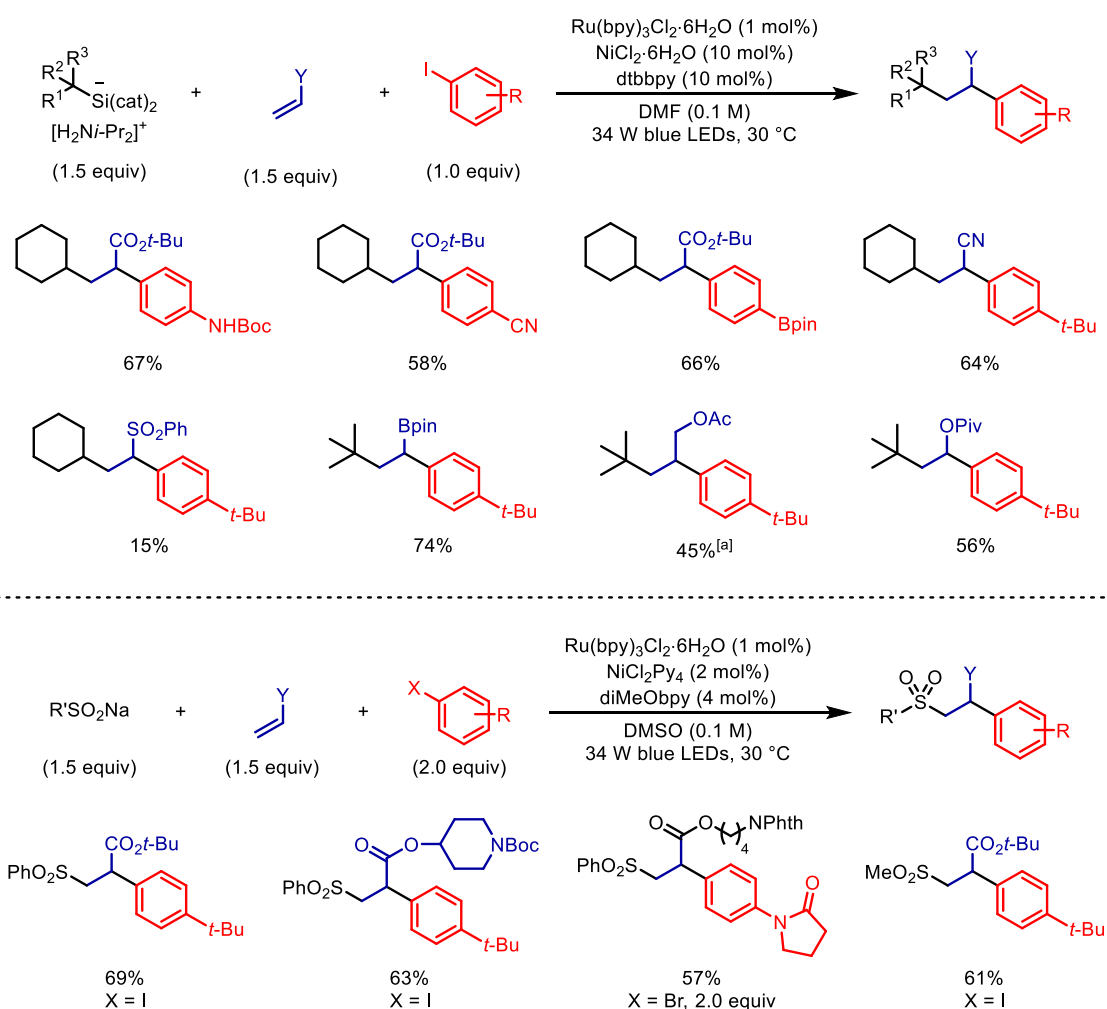
Proposed Mechanism:



Scheme 69. Chu's metallaphotoredox-catalysed conjunctive cross-coupling of alkenes with tertiary oxalates and aryl halides; selected examples and the proposed mechanism are shown.

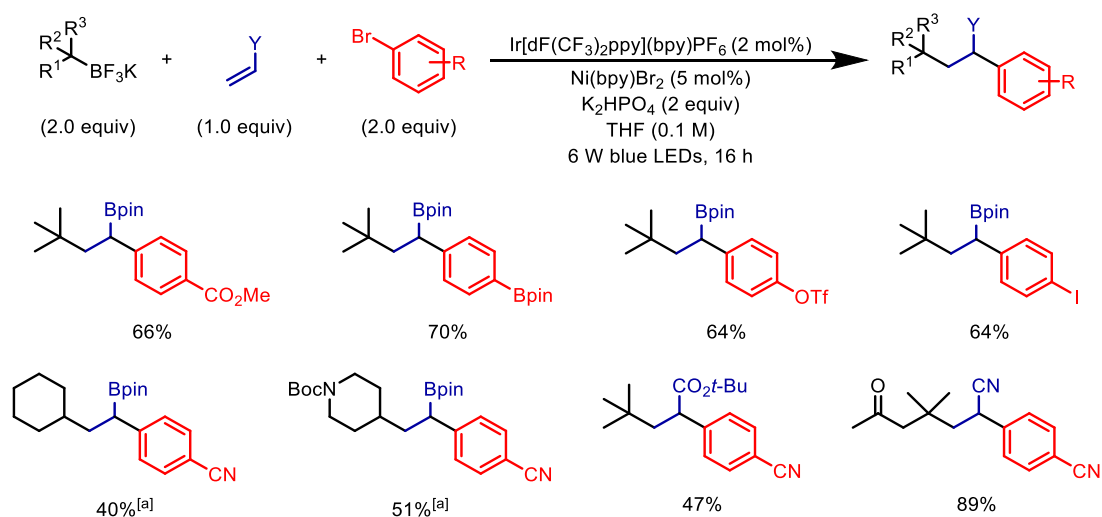
Later, Nevado and co-workers reported the use of readily oxidisable alkyl silicates as the radical precursor in combination with a range of alkenes and aryl halides under metallaphotoredox conditions (Scheme 70).^[170] Unfortunately, these alkyl silicates are not commercially available and so must be synthesised in three steps from the corresponding trichlorosilane, limiting the scope to simple alkyl

substrates. They showed that secondary alkyl silicates could undergo the conjunctive cross-coupling with electron-deficient alkenes and aryl iodides in good yields. They found that the stoichiometry of the three coupling partners was key to the formation of the conjunctive cross-coupling product: an excess of the silicate and alkene minimised undesired two-component (Hiyama-type) coupling. In order to utilise unactivated and electron-rich alkenes, such as vinyl boronic esters, allyl acetates and vinyl pivalates, they had to use tertiary alkyl silicates as otherwise two-component coupling would dominate due to the slow radical addition to the alkene. Under modified reaction conditions, they also reported the use of sulfinates as radical precursors in order to carry out a carbosulfonylation of electron-deficient alkenes with aryl halides. Mechanistic studies support the expected radical pathway and they report that the mechanism proceeds in a similar manner to that reported by Chu and co-workers with the nickel proceeding through the $\text{Ni}^{\text{I/III/I}}$ oxidation states,^[169] but do not rule out the alternative $\text{Ni}^{\text{II/III/I}}$ scenario.



Scheme 70. Nevado's metallaphotoredox-catalysed conjunctive cross-coupling of alkenes using either alkyl silicates or sulfinates with aryl halides, showing selected examples. [a] 5.5 equivalents of radical acceptor used.

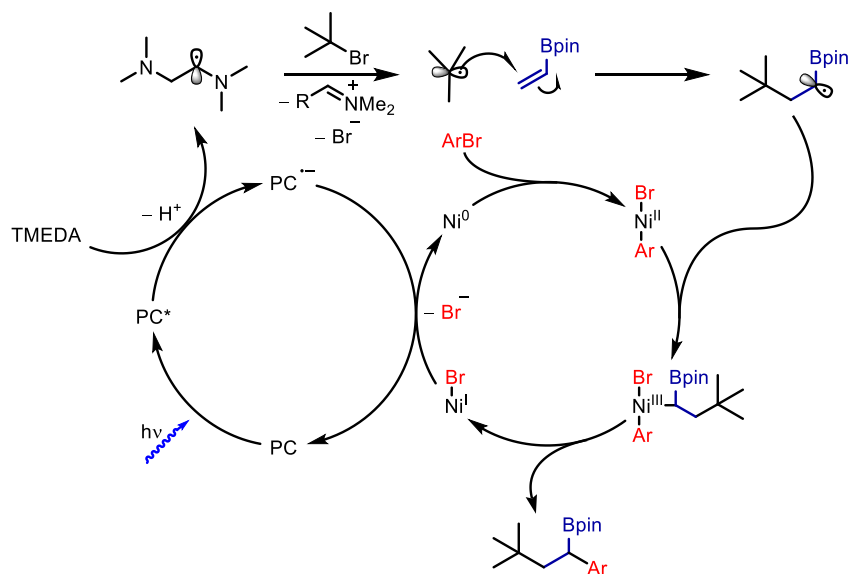
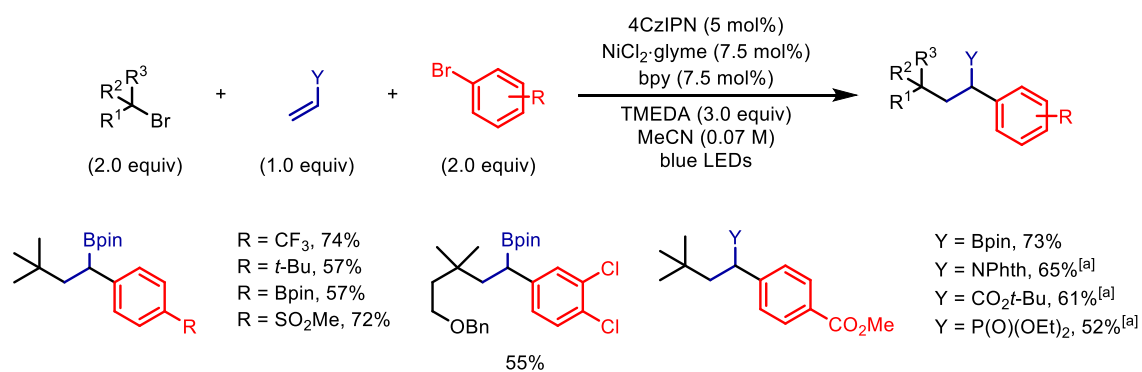
Following on from these works, Molander and co-workers reported the conjunctive cross-coupling of olefins (focusing on vinyl boronic esters) with alkyl trifluoroborate salts as the radical precursor and aryl bromides (Scheme 71).^[171] A very broad scope of coupling partners was reported displaying excellent functional group tolerance, including a robustness assay – addition of additives with a range of functional groups to see whether they withstand the reaction conditions. Although, optimal yields were achieved with tertiary trifluoroborates, secondary alkyl trifluoroborates were also compatible, albeit in lower yields due to the competing direct two-component coupling of the trifluoroborate with the aryl halide.^[172] Competition experiments between secondary and tertiary trifluoroborates revealed that the conjunctive cross-coupling reaction is 16× faster than the direct two-component cross-coupling with tertiary radicals, and 2.5× faster with secondary radicals. Attempts to utilise more complex alkyl trifluoroborates with more stabilised radicals such as benzyl, α -oxy and α -amino gave either no reactivity or exclusive direct two-component coupling. For the scope of olefins, vinyl-Bpin was the primary focus due the synthetic value of the functional handle in the products, however acrylates and acrylonitrile also performed well. The scope with respect to the aryl halides was broad and the reaction was impartial to electronics, except in the case of pyridine heterocycles, which yielded the corresponding protodeboronated products as a result of the electron-withdrawing nature of the α -pyridyl group.^[173] In addition to the wide substrate scope, derivatives of an intermediate to the preclinical candidate TK-666 (Gram-positive bacterial thymidylate kinase inhibitor) were synthesised. Although no mechanistic studies were reported, it is highly likely the reaction proceeds via the same mechanistic pathway as Chu's and Nevado's methodologies.



Scheme 71. Molander's metallaphotoredox-catalysed conjunctive cross-coupling of alkenes using alkyl trifluoroborates with aryl bromides, showing selected examples. [a] Ni(phen)Br₂ (5 mol%) used.

Upon publication of this project,^[168] Martin and co-workers reported the cross-electrophilic conjunctive cross-coupling of vinyl boronic esters using tertiary alkyl and aryl bromides under metallaphotoredox

catalysis using TMEDA as the sacrificial reductant and 4CzIPN as the organo-photocatalyst (Scheme 72).^[174] A range of aryl bromide coupling partners underwent the conjunctive cross-coupling in high yields regardless of the electronics of the aromatic ring, however no heterocycles such as pyridines were used, presumably due to competing protodeboronation. The reaction was limited to tertiary alkyl bromides due to the competing direct two-component coupling with secondary alkyl bromides; however, tertiary alkyl bromides proceeded efficiently to yield the difunctionalised vinyl boronic ester products in good yields. The reaction was not only limited to vinyl boronic esters as the olefin radical acceptors, but also vinyl phthalimides, acrylates, and vinyl phosphonates were compatible. Preliminary mechanistic studies confirm a radical pathway, with Stern-Volmer luminescence studies showing that the excited state of 4CzIPN is quenched by TMEDA, confirming its role as a sacrificial reductant. In its oxidised state TMEDA can behave as reductant^[175] and thus reduce the alkyl bromide to the corresponding radical. It is also possible that this TMEDA α -amino radical can abstract the bromine atom^[176] to give the same intermediate. Moreover, a stoichiometric experiment with a preformed Ni(II) complex was conducted and proceeded to yield the desired conjunctive cross-coupled product, suggesting the reaction proceeds via the Ni^{II/III} pathway, which is in contrast to that reported by Chu. Although not reported, the proposed mechanism is likely to proceed as depicted in Scheme 72 with the oxidised form of TMEDA reducing the tertiary alkyl bromide, or abstracting the bromine atom, to the corresponding radical. Alternatively, the reduced state of the photocatalyst (PC⁻) can reduce the tertiary alkyl bromide, and reduction of Ni(I) to Ni(0) is a result of SET from the oxidised form of TMEDA.



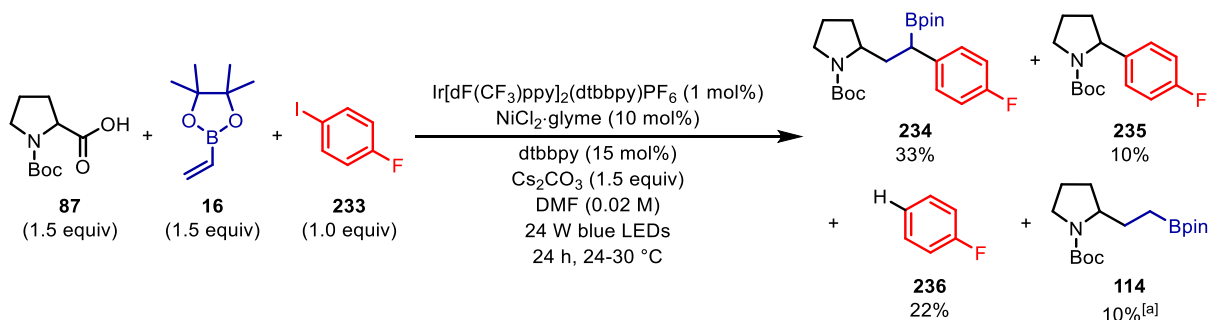
Scheme 72. Martin's cross-electrophile metallaphotoredox-catalysed conjunctive cross-coupling of alkenes with alkyl and aryl bromides, showing selected examples and the proposed mechanism. [a] *t*-BuBr (3.0 equiv), dtbbpy (7.5 mol%) used.

4.2 Results and Discussion

4.2.1 Initial Result

Investigations into the three-component conjunctive cross-coupling began by using similar conditions to those used by MacMillan and co-workers for the metallaphotoredox-catalysed two-component coupling of carboxylic acids and aryl halides.^[113] Boc-Pro-OH **87**, commercially available vinyl-Bpin **16** and 4-fluoroiodobenzene **233** were irradiated under blue LED light (24 W blue LED strips) for 24 hours in combination with Ir[dF(CF₃)ppy]₂(dtbbpy)PF₆, NiCl₂·glyme, dtbbpy and Cs₂CO₃ in DMF (Scheme 73). Fan cooling was used to maintain a reaction temperature between 24-30 °C. To our delight, we were successfully able to attain the desired conjunctive cross-coupled product **234** in 33%

¹⁹F NMR yield. In addition, side-products were identified as the direct two-component coupling product **235** in 10% yield, protodehalogenation product **236** in 22% yield and 10% of the Giese hydroalkylation product **114**. The remaining mass balance consisted of 17% of the aryl iodide starting material **233** and trace quantities of several other unidentifiable side-products.



Scheme 73. Initial reaction to test the viability of the metallaphotoredox-catalysed conjunctive cross-coupling of vinyl boronic esters. Yields were determined by ¹⁹F NMR with hexafluorobenzene as the internal standard. [a] GC yield.

This initial result proved highly promising, demonstrating that the desired transformation was indeed feasible, however it was clear the challenges we initially predicted were heavily competing with the desired transformation and had to be tackled in order to achieve the best possible selectivity for the conjunctive cross-coupling. It was clear how the direct two-component cross-coupling **235** and the Giese hydroalkylation product **114** were formed as they are both results of established (metalla)photoredox processes,^[44,113] however, the mechanism for protodehalogenation to form side-product **236** was not clear. We suspect it is a result of single-electron reduction of the aryl iodide from the reduced state of the photocatalyst, which should be possible, although this electron transfer may not be spontaneous due to the photocatalysts reduction potential being outside the range of the aryl iodide (Ir[dF(CF₃)ppy]₂(dtbbpy)PF₆, $E_{1/2}^{\text{red}}$ [Ir(III)/Ir(II)] = -1.37 V vs SCE in MeCN^[90] and the reduction potential of iodobenzene has been measured to be between -1.59 V and -2.24 V vs SCE^[177]). A control experiment without the nickel catalyst and ligand yielded almost exclusively the protodehalogenation product **236**, suggesting that the nickel/ligand are not involved and that the protodehalogenation is a photochemical transformation (*vide infra*). Upon reduction to the corresponding aryl radical, hydrogen atom abstraction is possible from the solvent DMF. The competing single-electron reduction would interfere with the turnover of the nickel catalyst and thus hinder the conjunctive cross-coupling. Careful tuning of the system would be required in order to favour SET between the reduced state of the photocatalyst and the Ni(I) complex generated after reductive elimination (see Scheme 67).

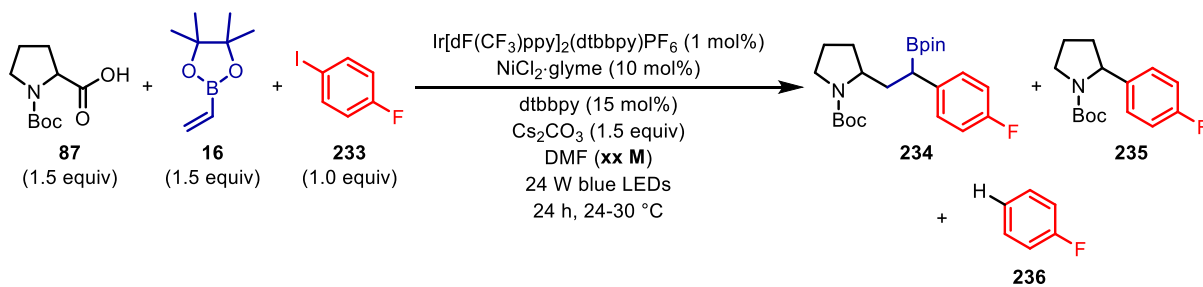
4.2.2 Optimisation

After successful realisation that the conjunctive cross-coupling was feasible, we began optimising this challenging transformation in order to minimise the competing side-reactions. An extensive optimisation campaign was conducted with each parameter investigated individually. The optimisation was divided into two phases: the first phase involved investigation of cyclic amino acids initially with an iridium photocatalyst and then completed with an organic photocatalyst, and the second phase looked at amino acids bearing a free NH group and the cross-coupling selectivity. Only the key parametric changes will be discussed in the following sections and additional optimisation tables have been added to the supplementary material for completeness. We conducted all screens using stock solutions to minimise error within a study, and repeated standard reactions to account for variability between different screens.

4.2.2.1 Phase I: Cyclic Amino Acids

We opted to utilise Boc-Pro-OH **87**, vinyl-Bpin **16** and 4-fluoroiodobenzene **233** as our model system (as in the initial test reaction), because the products of this reaction could be rapidly and easily monitored by ^{19}F NMR and would provide us with all the necessary information with respect to the aryl iodide limiting reagent. Moreover, as the other two components, **16** and **233**, were in excess we did not always monitor the formation of the Giese hydroalkylation product **114**.

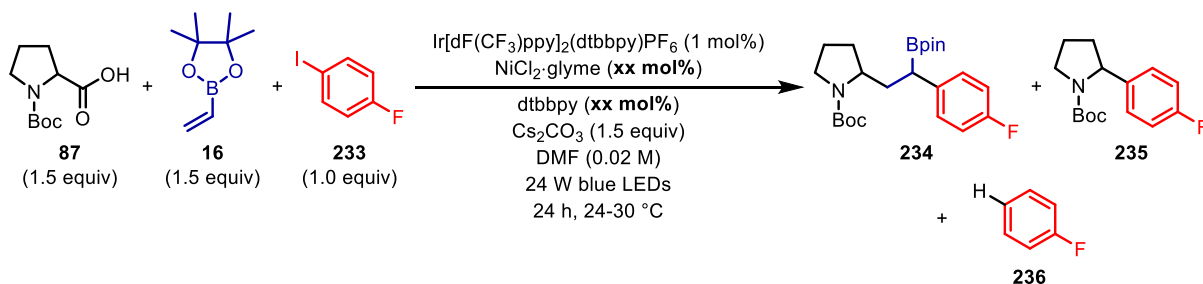
In line with our previous decarboxylative radical additions to vinyl boronic esters, initial investigations into base and solvent indicated that Cs_2CO_3 and DMF were optimal (see supplementary materials, section 6.4.3, Table S 8 and Table S 9, respectively). Concentration had a large impact on the yield of the reaction, with lower concentrations proving beneficial (Table 20). We found by diluting the reaction from the original 0.02 M (entry 2) to 0.01 M (entry 1) complete consumption of the aryl iodide starting material **233** was observed and the yield of **234** increased by 11% without further increasing the yield of undesired direct two-component-coupling. This suggests that the conjunctive cross-coupling is favoured at lower concentrations. Sadly, the amount of protodehalogenation **236** was not reduced at any concentration (entries 1-5). Moreover, it was evident that the rate of the reaction decreased as the reaction concentration increased, which can be seen in the steady increase in aryl iodide starting material **233** remaining as concentration was increased (entries 1-5). We decided to use 0.01 M for further studies and did not lower the concentration further as this would become impractical at larger scales.



Entry	Concentration / M	¹⁹ F NMR Yield (%)			
		234	235	236	233
1	0.01	43	12	19	0
2	0.02	32	10	26	4
3	0.05	22	4	18	27
4	0.10	19	4	21	36
5	0.20	17	2	17	50

Table 20. Reaction concentration screen. Yields were determined by ¹⁹F NMR with hexafluorobenzene as the internal standard.

In parallel to the reaction concentration screen, we also examined the effects of varying the loading of NiCl₂·glyme and the ligand dtbbpy (Table 21). By maintaining a ratio of 1:1.5 of NiCl₂·glyme:dtbbpy, we found that the loading had minimal effect on the yield of the conjunctive cross-coupling product **234** and the ratio of **234**:**235**. Even when dropping to very low loadings of 2.5 mol% NiCl₂·glyme and 3.75 mol% of dtbbpy productive catalysis was occurring (entry 1). The levels of protodehalogenation **236** were also consistent (~20%) at each loading (entries 1-5). With these results, we decided to proceed with the loading of 5 mol% NiCl₂·glyme and 7.5 mol% dtbbpy (entry 2) as this would be synthetically and economically more attractive.



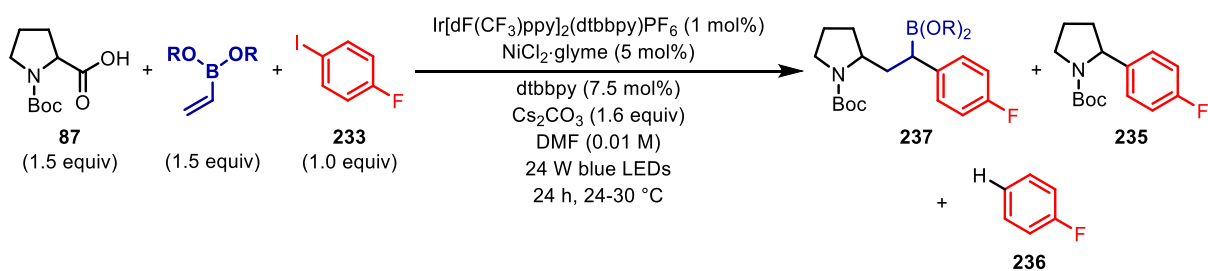
Entry	NiCl ₂ -glyme loading / mol%	dtbbpy loading / mol%	¹⁹ F NMR Yield (%)			
			234	235	236	233
1	2.5	3.75	35	12	19	17
2	5.0	7.50	40	11	21	11
3	10	15.0	38	13	20	7
4	15	22.5	43	14	22	4
5	20	30.0	41	13	20	3

Table 21. NiCl₂-glyme and dtbbpy loading screen, maintaining a ratio of 1:1.5. Yields were determined by ¹⁹F NMR with hexafluorobenzene as the internal standard.

Further optimisations of the base loading found 1.6 equivalents to be optimal as this ensured that all of the Boc-Pro-OH starting material **87** was in the cesium salt form, which would aid oxidation and decarboxylation (see supplementary materials, section 6.4.3, Table S 10). Temperature was also important, with optimal temperatures between 24-30 °C maintained by fan cooling. Lowering the temperature to 10 °C slowed down the rate of the reaction with large amounts of starting material remaining after 24 hours. On the other hand, removing fan assisted cooling and allowing the temperatures to reach 38+ °C caused a drop in yield of the desired product **234** by 10%. We also conducted a time study and found that the aryl halide starting material **233** was fully consumed after 12 hours. Furthermore, no reduction in yield was observed after prolonged periods of time, indicating that the benzylic boronic ester product is stable under the reaction conditions – this was not the case in the previous decarboxylative radical addition reaction to styrenyl boronic esters, which gave exclusive protodeboronation (*vide supra*).^[44]

Next, we investigated the effect of the diol ligand on the boronic ester (Table 22). In general, we saw that increasing the sterics on the diol backbone, particularly at the positions adjacent to the oxygens, gave slightly better yields for **237**. This was most evident with the 5-membered boronic esters (entry 1 vs 2). For the 6-membered boronic esters, a slight improvement in yield was observed upon adding substituents adjacent to the oxygens of the diol (entries 3-7), with the unsymmetrical diol 2-methylpentane-2,4-diol proving to be optimal (entry 7), with 51% yield of the conjunctive cross-coupled product **237** and improved **237:235** ratio over the standard vinyl-Bpin (entry 1). The conformation this

vinyl boronic ester must adopt with the unsymmetrical diol moiety must have an effect on either the radical addition step or the addition of the α -boryl radical to the Ni(II) complex, however, this effect is still unknown. Moreover, this unsymmetrical vinyl boronic ester is also commercially available making it more accessible. Interestingly, increasing the sterics further to have two gem-dimethyl groups adjacent to the oxygen resulted in a lower yield (entry 8). Unsurprisingly, the vinyl-BMIDA gave no desired product **237** and 46% direct two-component cross-coupling **235** (entry 9). This is due to the polarity mismatch during the radical addition step: an electron rich α -amino radical will not add to the electron rich vinyl-BMIDA, thus direct two-component coupling dominates.



Entry	Vinyl boronic ester	¹⁹ F NMR Yield (%)			
		237	235	236	233
1		47	18	19	0
2 [‡]		30	7	17	19
3		46	14	17	1
4		46	13	16	3
5		45	15	17	0
6		48	16	16	2
7		51	19	15	2
8 [‡]		43	23	19	7
9 [‡]		0	46	16	21

Table 22. Screening of vinyl boronic esters. Yields were determined by ¹⁹F NMR with hexafluorobenzene as the internal standard.

After finding the optimal vinyl boronic ester, we decided to increase the equivalents of this vinyl boronic ester from 1.5 to 2.0 equivalents as we found this to be beneficial. This would mean more vinyl boronic ester present in greater excess to improve the rate of radical addition over direct addition to the nickel complex. Moreover, there was also the possibility that radical polymerisation of the vinyl boronic ester

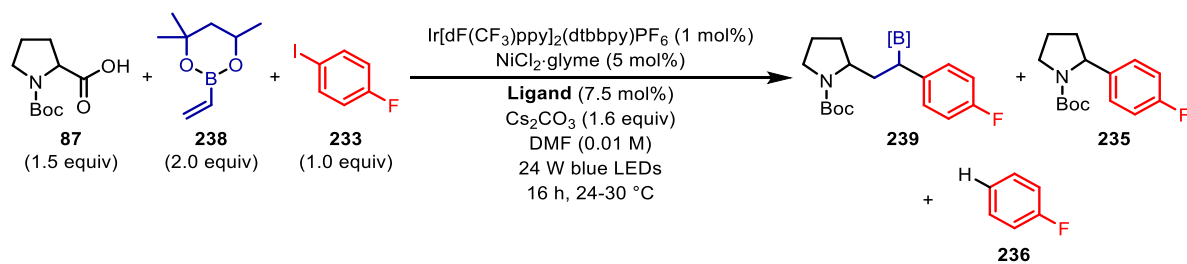
was taking place during the course of the reaction, thereby consuming the radical acceptor,^[130] so having more present would compensate for this.

Nickel catalysts were subsequently investigated (see supplementary materials, section 6.4.3, Table S 11). We first trailed a range of Ni(II) catalysts with dtbbpy as the ligand. Unsurprisingly, all the Ni(II) halides catalysts performed similarly with no difference between chloride or bromide nickel complexes. Ni(OTf)₂ was also tested, though was inferior to the dihalide complexes. At the same time, the aryl (pseudo)halide coupling partner was looked into (see supplementary materials, section 6.4.3, Table S 12). The more reactive aryl iodide used proved to still be the best coupling partner, with the corresponding aryl bromide showing very low reactivity. It was later confirmed that no productive nickel catalysis was taking place with the aryl bromide and instead the Giese hydroalkylation product was the major product. This was surprising considering MacMillan utilised aryl bromides for the direct two-component cross-coupling reaction and here only 5% of this was observed.^[113] The corresponding triflate was also tested, however this gave diminished yields with preference for direct two-component coupling.

Continuing with NiCl₂·glyme as the nickel catalyst of choice, we screened a wide range of ligands to see whether the electronic and/or steric effect of the ligand could influence our desired transformation (Table 23). Bipyridine (bpy) ligands were first trailed with different substituents on the backbone. In comparison to the standard dtbbpy ligand (entry 1), changing to the more electron-rich methoxy analogue resulted in a drop in yield of the conjunctive cross-coupled product **239** but with similar amounts of **235** and **236** (entry 2). A decrease in yield of **239** was also observed with bpy (entry 3). A large drop in yield was observed with dFbpy giving only 24% of **239** (entry 10), suggesting that electronics influence the reaction outcome, however a trend was not obvious. An improvement in yield was noted when the more powerful 40 W blue LEDs were used with dtbbpy (entry 9, 57% yield). Phenanthroline ligands were also suitable for the reaction, however gave lower yields in general (entries 5-7). In terms of sterics, we found that when *ortho*-substituted ligands were used (entries 4,7 and 8), no reactivity other than protodehalogenation was observed. This could be due to the *ortho*-substituents blocking the coordination sites on the nickel catalyst, hindering the oxidative addition of the aryl iodide and/or addition of the radical species. In general, the further away the substituent on the ligand was from the coordinating nitrogen, the better the yield, however no improvement in **239:235** ratio was observed.

Moving away from aromatic bipyridine and phenanthroline ligands, (bis)oxazoline ligands were also tested as they have been used extensively in asymmetric catalysis,^[178] including nickel^[179] and metallaphotoredox catalysis.^[120] Unfortunately, these resulted in no productive catalysis (entries 8 and 11). We initially thought this was because of the *ortho*-substituents on the (bis)oxazoline (entry 8), however removing these and using more powerful 40 W blue LEDs gave the same result (entry 11).

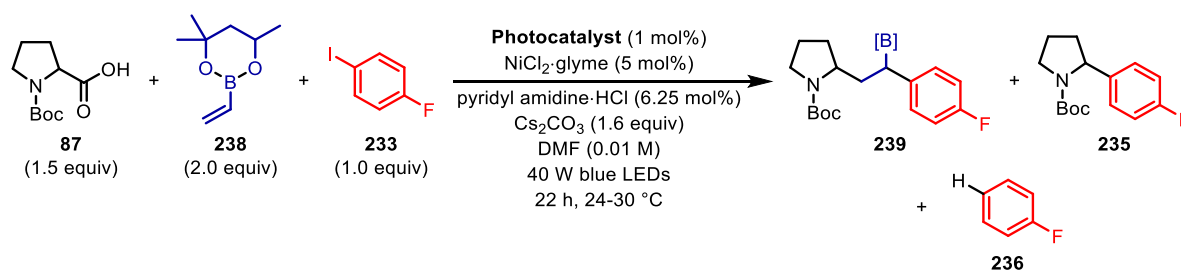
We did have a breakthrough when the pyridyl amidine ligand was employed under 40 W blue LEDs (entry 12). This ligand gave an improvement in yield of **239**, but more importantly was the first case where we had observed a significant reduction in protodehalogenation, from an average of 18% down to 7%. As the ligand influences the electronics of the nickel centre, it was apparent that the pyridyl amidine ligand facilitated favourable SET between the reduced state photocatalyst and Ni(I) over reduction of the aryl iodide to the protodehalogenation product **236**. Note, at the time of this screening, it appeared that 0.5 mol% of the photocatalyst worked to the same degree as 1 mol% (this was later disproved, *vide infra*). In addition to these ligands, more than ten mono- and bidentate phosphine ligands were also screened (not shown), but no productive catalysis was observed in all cases other than protodehalogenation. It appeared only aromatic based nitrogen ligands were compatible for the desired transformation.



Entry	Ligand	¹⁹ F NMR Yield (%)			
		239	235	236	233
1		53	14	19	0
2		45	11	23	4
3		48	16	26	0
4		0	0	20	69
5		38	16	38	2
6		36	10	29	18
7		0	0	36	59
8		0	0	15	80
9 ^[a]		57	17	16	0
10 ^[a]		24	7	32	9
11 ^[a]		0	0	17	77
12 ^[a]		59	24	7	0

Table 23. Nickel ligand screen. [a] Reactions irradiated with 40 W blue LEDs with Ir[dF(CF₃)ppy]₂(dtbbpy)PF₆ (0.5 mol%). Yields were determined by ¹⁹F NMR with hexafluorobenzene as the internal standard.

We next decided to investigate photocatalysts in combination with the more powerful 40 W blue LEDs (Table 24). Prior to this, the nickel and ligand loadings were further refined to NiCl₂·glyme 5 mol% and pyridyl amidine 6.25 mol%. Using 1 mol% photocatalyst loading, Ir[dF(CF₃)ppy]₂(dtbbpy)PF₆ gave the conjunctive cross-coupled product **239** in 64% yield, with the yield of protodehalogenation **236** remaining consistent at 7% (entry 1). Changing to the more reducing Ir[dF(Me)ppy]₂(dtbbpy)PF₆ photocatalyst gave comparable yields (entry 2). At this stage, we decided trial the cheaper organic photocatalyst 4CzIPN, as it had recently been shown to be compatible in metallaphotoredox cross-coupling reaction of carboxylic acids (and trifluoroborates) with aryl halides as an alternative to the iridium photocatalysts.^[92] Pleasingly, the reaction worked, yielding **239** in 42% yield, however the levels of protodehalogenation **236** had reset themselves to 14%, similar to what they were before changing to the pyridyl amidine ligand (entry 3). This was a promising result despite the lower yield and so we decided to proceed with 4CzIPN as the more economical photocatalyst.



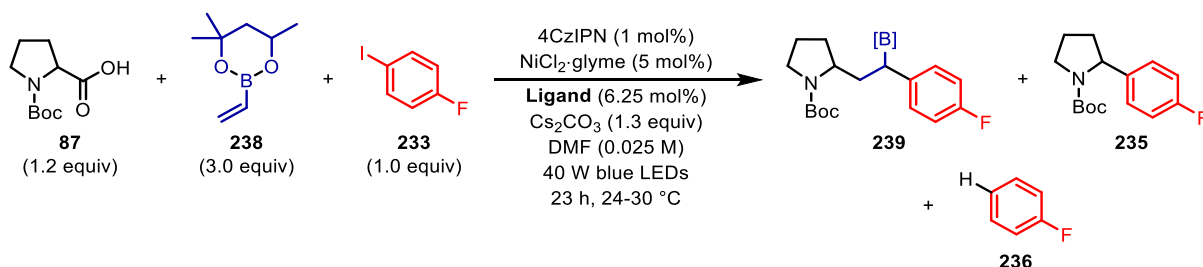
Entry	Photocatalyst	¹⁹ F NMR Yield (%)			
		239	235	236	233
1 [‡]	Ir[dF(CF ₃)ppy] ₂ (dtbbpy)PF ₆	64	18	7	0
2 [‡]	Ir[dF(Me)ppy] ₂ (dtbbpy)PF ₆	66	17	7	0
3	4CzIPN	42	11	14	9

Table 24. Photocatalyst screen with 40 W blue LEDs. Yields were determined by ¹⁹F NMR with hexafluorobenzene as the internal standard.

Further fine tuning of the reaction conditions (with Ir[dF(Me)ppy]₂(dtbbpy)PF₆) found that the concentration could be increased to 0.025 M with no change in yield; 3.0 equivalents of vinyl boronic ester **238** provided a small increase in yield by reducing the amount of direct two-component coupling **235**; and the loading of Boc-Pro-OH could be reduced to 1.2 equivalents without impacting the reaction outcome (see supplementary materials, section 6.4.3, Table S 13, Table S 14 and Table S 15, respectively).

Continuing with 4CzIPN, we previously showed that by changing ligand we were able to influence the amount of protodehalogenation taking place. With this in mind, we screened a small set of bipyridyl and phenanthroline ligands with 4CzIPN to see whether we could lower the amount of

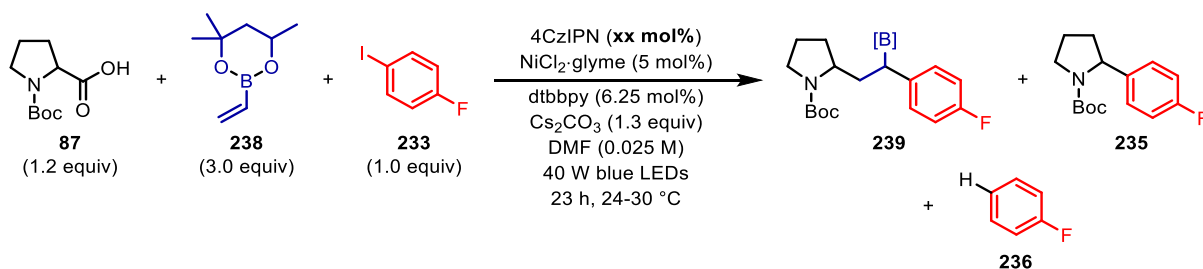
protodehalogenation and in turn improve the yield for the desired conjunctive cross-coupling (Table 25). The electron rich dMeObpy ligand gave a lower yield than the pyridyl amidine, displaying more protodehalogenation (entry 1 vs 2). However, upon changing to the less electron rich dtbbpy, a significant improvement in yield of **239** was observed (56%), with less unknown side-product peaks in the ^{19}F NMR (entry 3, unknown product peaks not shown). Unfortunately, dtbbpy did not reduce the amount of protodehalogenation. Using bpy as the ligand also gave an improvement in yield over the pyridyl amidine, however was inferior to dtbbpy (entry 4). Surprisingly, there was no trend with the electronics of the bipyridyl ligands on the reaction outcome. In general, all the phenanthroline ligands gave diminished yields for the conjunctive cross-coupling and increased amounts of protodehalogenation (entries 5-7). From this screen it was clear that we had to switch back to the dtbbpy ligand, despite not reducing the amount of protodehalogenation.



Entry	Ligand	^{19}F NMR Yield (%)			
		239	235	236	233
1		38	8	20	5
2		29	14	34	0
3		56	13	25	1
4		46	12	25	7
5		35	10	33	18
6		18	4	30	25
7		16	4	27	36

Table 25. Ligand screen with 4CzIPN. Yields were determined by ^{19}F NMR with hexafluorobenzene as the internal standard.

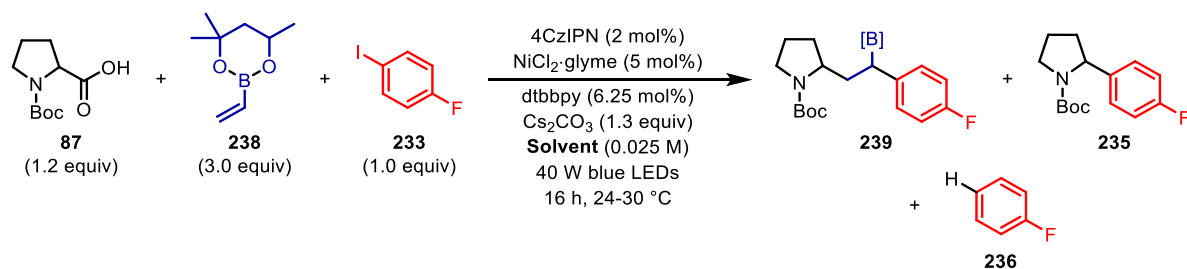
With the optimal ligand in hand, we next moved onto the effects of 4CzIPN loading. As this is a cheap and easily accessible catalyst, we decided to screen from 0.5 – 5.0 mol% loading (Table 26). Lowering the amount of 4CzIPN to 0.5 mol% caused a 10% drop in yield of **239** and a 7% increase in protodehalogenation **236** (entries 1 and 2). However, increasing the loading further to 2.0 and 5.0 mol% saw an increase in 5% and 6%, respectively, of **239** (over the standard reaction, entry 2), as well as slightly lowered protodehalogenation (entries 3 and 4, respectively). From these results (and repeat experiments) we decided to use 2 mol% loading going forwards.



Entry	4CzIPN loading / mol%	¹⁹ F NMR Yield (%)			
		239	235	236	233
1	0.5	48	13	27	1
2	1.0	58	11	20	0
3	2.0	63	11	17	1
4	5.0	64	12	19	5

Table 26. 4CzIPN loading screen. Yields were determined by ¹⁹F NMR with hexafluorobenzene as the internal standard.

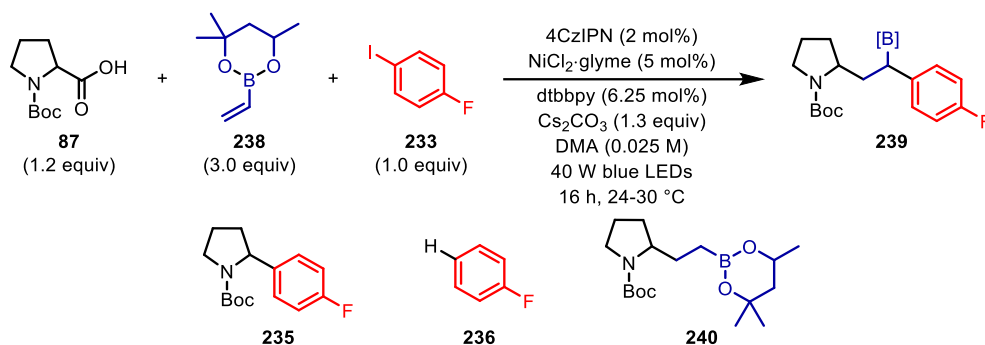
At this stage, we carried out further optimisation studies, including modifying the ratio of **87:233** in attempt to reduce protodehalogenation, the equivalents of vinyl boronic ester **238** together with concentration (see supplementary materials, section 6.4.3, Table S 16 and Table S 17, respectively), as well as a time study proving the reactions were complete after 12 hours. However, no significant improvements in yield, **239:235** ratio or reduction in protodehalogenation were observed. The breakthrough came when we re-investigated DMA as the solvent based on the results of Phase II of optimisation (*vide infra*). Using DMA as the reaction solvent showed an increase in yield of **239** to 78%, improved **239:235** ratio as well as a drop in protodehalogenation (Table 27, entry 2). DMA gave a visibly cleaner ¹⁹F NMR spectrum with fewer unknown side-products. Through this one change, we had found a solution to minimise protodehalogenation and in turn improve the yield of the desired conjunctive cross-coupling.



Entry	Solvent	¹⁹ F NMR Yield (%)			
		239	235	236	233
1	DMF (anhydrous)	65	12	16	7
2	DMA (anhydrous)	78	10	7	0

Table 27. Changing to DMA as solvent. Yields were determined by ¹⁹F NMR with hexafluorobenzene as the internal standard.

After an extensive optimisation campaign, we had reached the final optimal reaction conditions, using 4CzIPN as the photocatalyst. At this stage, before scaling up the reaction, we decided it was worth making minor modifications to the ‘standard conditions’ in order to ensure the robustness of our vast screenings, and to conduct control experiments in order to ensure the necessity of specific components (Table 28). To maintain standardisation of reagent quality, specifically the nickel catalyst, Cs₂CO₃ and the ligand, we opted to move reaction set-up to within a nitrogen filled glovebox. Under these new glovebox conditions, using ‘fresh reagents’, we saw a slight improvement in yield (entry 1). Changing the optimal vinyl boronic ester **238** for vinyl-Bpin **16** resulted in a 10% drop in yield for the conjunctive cross-coupled product with an increase in Giese hydroalkylation **240** and protodeboronation **236** (entry 2). Changing the aryl iodide for the corresponding bromide resulted in inefficient nickel catalysis and an increase in yield of the Giese hydroalkylation product **240** (entry 3). Lowering the equivalents of the vinyl boronic ester **238** to 1.5 equivalents resulted in a reduced yield for conjunctive cross-coupling due to competitive two-component cross-coupling, however it was good to see that selectivity was still good in this instance (comparing entries 1 and 4, 6:1 vs 3:1). Increasing the loading of the nickel catalyst and the dtbbpy resulted in no improvement in efficiency (entry 5). Changing to other solvents, DMF, DMSO and MeCN, also resulted in no improvement in reaction outcome, confirming that we had indeed found the optimal reaction conditions (entries 6-8). Control experiments confirmed the essential roles of the photocatalyst, nickel/ligand system, base, and light, with no reactivity taking place in their absence (entries 9-12). Interestingly, 59% protodehalogenation was observed in the absence of the nickel and ligand (entry 10) with only 11% Giese hydroalkylation. This suggests protodehalogenation is indeed a photochemical process, which can be inhibited to some extent with various nickel/ligand combinations.



Entry	Modification of ‘standard conditions’	¹⁹ F NMR Yield (%)				
		239	235	236	240 ^[a]	233
1	None	79	13	7	8	0
2	Vinyl-Bpin (16) instead of 238	69	7	17	17	0
3	ArBr instead of 233	5	2	11	52	58
4	1.5 equiv of 238	67	22	11	8	0
5	10 mol% [Ni], 15 mol% dtbbpy	75	13	12	8	0
6	DMF as solvent	70	13	16	11	0
7	DMSO as solvent	23	5	27	15	18
8	MeCN as solvent	38	12	20	17	19
9	No photocatalyst	0	0	7	0	69
10	No [Ni]/dtbbpy	0	0	58	11	0
11	No base	0	0	2	0	75
12	No light	0	0	0	0	89

Table 28.^[168] Final optimisation studies and control experiments. Yields were determined by ¹⁹F NMR with hexafluorobenzene as the internal standard. [a] GC yield.

We next looked to scaling up the reaction (Scheme 74). On a 0.3 mmol scale, we were successfully able to obtain the boronic ester **239** in 77% ¹⁹F NMR yield. Sadly, the benzylic boronic ester proved to be unstable on TLC and so we decided to oxidise the boronic ester to the corresponding alcohol by adding solid urea-H₂O₂ post-light irradiation and stirring for 1 hour, yielding the corresponding alcohol **239-OH** in an excellent 76% isolated yield as two separable diastereomers (48:52 d.r.). This reaction proved that we were able to scale up with no loss of efficiency, as well as oxidise the product in quantitative yield.

Despite the boronic ester product being unstable on TLC, we found that conducting the reaction on a smaller scale (0.1 mmol), in addition to rapid column chromatography, the boronic ester **239-[B]** could be isolated with minimal degradation, in a good 64% isolated yield as a mixture of diastereomers (d.r. and relative stereochemistry could not be assigned). Attempts to use deactivated silica gel with either

2% Et₃N or 35% wt. H₂O showed no improvements in minimising boronic ester degradation. Overall, this was still a fantastic result as it meant the resulting boronic esters could be isolated and thus be subjected to a range of further transformations in order to introduce even more complexity.^[4]

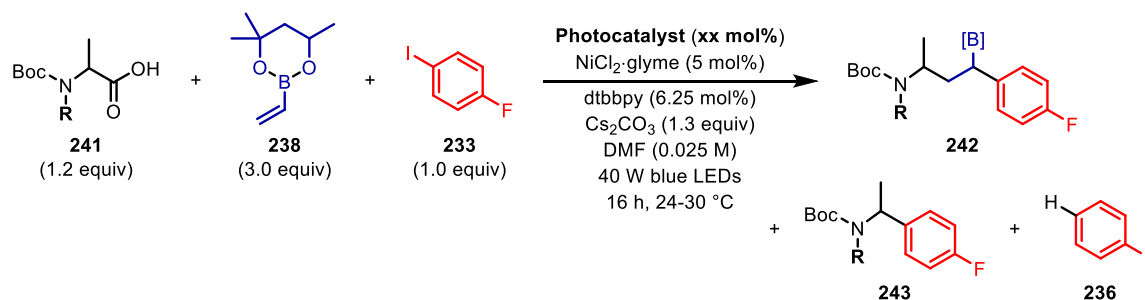


Scheme 74. Scale up of model reaction. [a] 0.3 mmol scale, isolated after oxidation with urea-H₂O₂ (3 equiv), 48:52 d.r. [b] 0.1 mmol scale, d.r. could not be assigned.

4.2.2.3 Phase II: Monoprotected Acyclic Amino Acids and Cross-coupling Selectivity

Phase II of optimisation began towards the end of Phase I and investigated the application of acyclic amino acids bearing a free NH group in the conjunctive cross-coupling. We encountered problems with acyclic amino acids bearing a free NH group during the decarboxylative radical addition reaction to vinyl boronic esters, and were overcome by changing to a more oxidising photocatalyst and using DMA as the reaction solvent.^[44] In the case of the cyclopropyl boronic esters,^[147] acyclic amino acids were not an issue as the vinyl boronic ester was a better radical acceptor (leading to a stabilised tertiary α -boryl radical) and the oxidation potential of 4CzIPN is in line with that of the fluorinated iridium photocatalyst used. A summary of the investigation, using Boc-Ala-OH as the model substrate, is given in Table 29.

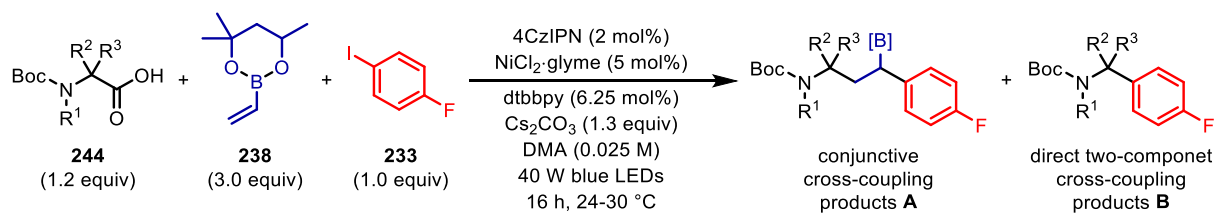
Using DMF as the solvent, a low yield of the conjunctive cross-coupled product **242** was obtained in 36% with 19% direct two-component coupling **243**. Comparing the effects of having a free NH group over a bis-protected amino acid, a major improvement in conversion was observed with Boc-*N*-Me-Ala-OH giving 59% conjunctive cross-coupling and a much better ratio of **242**:**243** (entry 3). However, changing to the removable bis-Boc-protected alanine, a drop in yield was seen with very high levels of protodehalogenation (entry 4). Here we suspect that the oxidation potential of the Boc₂-Ala-OH is outside the range of the photocatalyst and so the photochemical protodehalogenation process dominates. Changing to DMA as the solvent (the optimal reaction conditions from Phase I) saw a slight increase in yield to 39% **242**, but a much cleaner ¹⁹F NMR spectrum with fewer unknown side-product peaks (entry 5). Changing to DMSO as the solvent resulted in a drop in yield, with protodehalogenation dominating (entry 6). Sadly, increasing the loading of 4CzIPN in DMA only resulted in further increases in direct two-component coupling (entry 7).



Entry	R	Solvent	Photocatalyst (x mol%)	¹⁹ F NMR Yield (%)			
				242	243	236	233
1	H	DMF	4CzIPN (2 mol%)	36	19	15	14
2	Me	DMF	4CzIPN (2 mol%)	59	6	18	3
3	Boc	DMF	4CzIPN (2 mol%)	7	0	57	9
4	H	DMA	4CzIPN (2 mol%)	39	26	12	0
5	H	DMSO	4CzIPN (2 mol%)	13	7	50	0
6	H	DMA	4CzIPN (7 mol%)	41	36	11	0

Table 29. Summary of optimisation for acyclic amino acids using Boc-Ala-OH as the model substrate. Yields were determined by ¹⁹F NMR with hexafluorobenzene as the internal standard.

From the results varying the R substituent on Boc-Ala-OH, it was evident that the generation of the initial α -amino radical was not the issue (for R = H and R = Me), instead it appeared that direct two-component cross-coupling became more competitive when R = H. This led us to consider the effects of sterics on cross-coupling selectivity and find the limits of where selectivity switches from conjunctive cross-coupling to direct two-component cross-coupling; in previous reports there has been a reliance on the use of tertiary alkyl radical precursors in order to overcome this competition.^[169,174] To explore the effects of sterics we compared the ratios between the two cross-coupling products (**A** and **B**) using primary, secondary and tertiary α -amino acids (Table 30). Using the primary α -amino acid Boc-Gly-OH, none of the desired conjunctive cross-coupled product was formed, but instead exclusive direct two-component coupling was observed (entry 1). This is the least sterically demanding substrate and so rapid addition to nickel is favoured, despite the excess of vinyl boronic ester. By methylating the nitrogen atom to give Boc-N-Me-Gly-OH, selectivity for the conjunctive cross-coupling was increased to give a ratio of 24:76 **A**:**B** (entry 2). The switch in selectivity for the conjunctive cross-coupling was found upon changing to the secondary α -amino acid Boc-Ala-OH giving a ratio of 67:33 **A**:**B** (entry 3). This is due to the increased sterics around the intermediate α -amino carbon-centred radical. Further increasing the sterics by N-methylation resulted in selective conjunctive cross-coupling, with no direct two-component cross-coupling being isolated (>95:5 selectivity, entry 4). As we expected, the use of the tertiary α -amino acid Boc-Aib-OH gave exclusive selectivity for the conjunctive cross-coupling (entry 5).



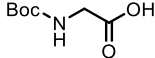
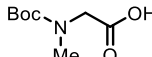
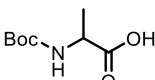
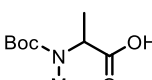
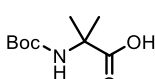
Entry	Substrate	Product ratios (A:B)
1	 Boc-Gly-OH	<5:95
2	 Boc-N-Me-Gly-OH	24:76
3	 Boc-Ala-OH	67:33
4	 Boc-N-Me-Ala-OH	>95:5
5	 Boc-Aib-OH	>95:5

Table 30.^[168] Effect of sterics on cross-coupling selectivity.

From these cross-coupling selectivity studies (Table 30) and the optimisation studies (Table 29), we concluded our optimisation of the decarboxylative conjunctive cross-coupling of vinyl boronic esters. In the case of acyclic amino acids, yields were good for the conjunctive cross-coupling, however increased sterics around the α -amino radical centre were required in order to improve selectivity; this is because acyclic amino acids bearing a free NH group are on the boundary of the selectivity switch between the conjunctive and direct two-component coupling reactions. In the case of cyclic amino acids this selectivity and yields are generally better overall.

4.2.3 Substrate Scope

We commenced exploring the scope of the decarboxylative conjunctive cross-coupling of vinyl boronic esters with respect to the carboxylic acids, using 4-fluoroiodobenzene (**233**) as the model aryl iodide (Scheme 75). Due to the partial instability of the benzylic boronic ester products, we decided to isolate the products as the corresponding alcohols after oxidation with urea-H₂O₂. In almost all cases, the two diastereomers of the alcohol products could be separated by column chromatography.

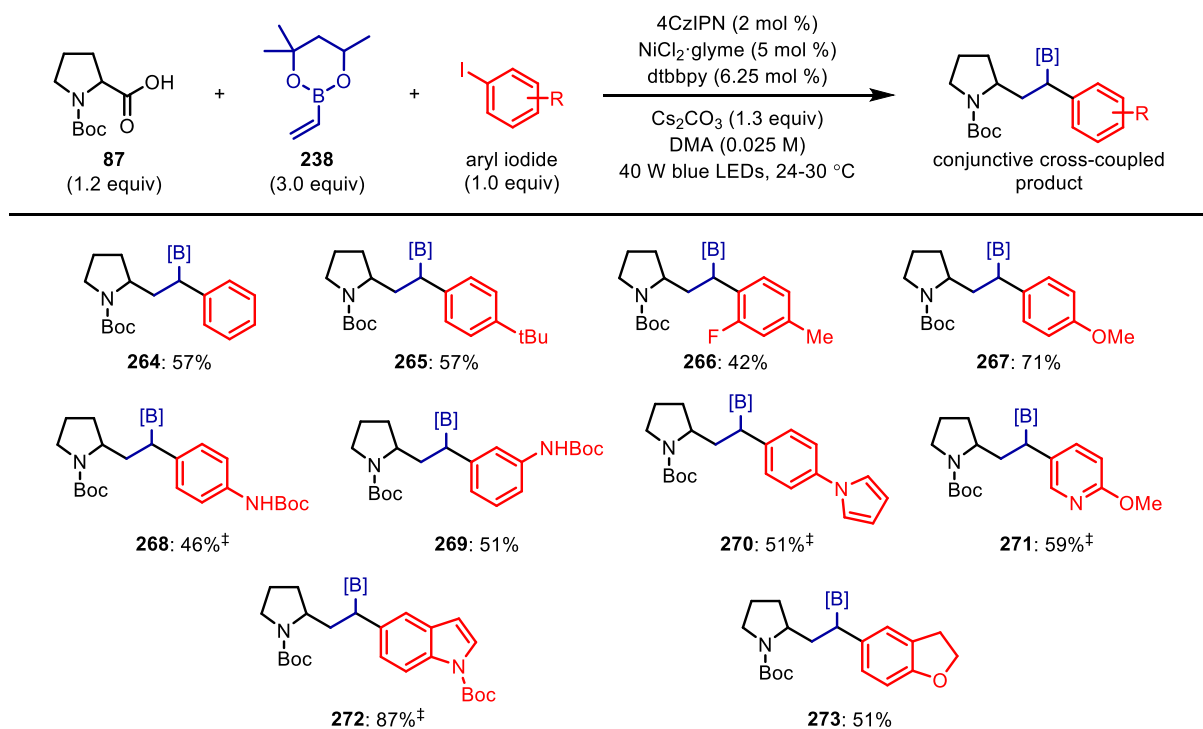
As previously shown, the model reaction using Boc-Pro-OH, **239**-[OH] could be isolated in 76% yield, and as the boronic ester product **239**-[B] in 64% yield, highlighting the drop in yield due to instability.

Changing to the alternative Cbz-carbamate protecting group, the conjunctive cross-coupling proceeded in a good yield of 61% (**245**). A range of other cyclic secondary amino acids reacted in moderate to high efficiency, including a four-membered ring (**246**[†], 34%), a six-membered ring (**247**[†], 78%), and the five-membered heterocycle derived from Boc-threonine (**248**[†], 61%). A cyclic tertiary amino acid also gave a good yield of the conjunctive cross-coupled product (**249**[†], 58%).

As well as cyclic amino acids, a range of acyclic amino acids were also compatible, exhibiting excellent functional group tolerance in the conjunctive cross-coupling (**251-260**). From the cross-coupling selectivity studies, we showed that primary, secondary and tertiary acyclic amino acids could all undergo the conjunctive cross-coupling with different levels of selectivity according to the sterics surrounding the α -amino radical. The primary amino acid Boc-Gly-OH failed to give any conjunctive cross-coupling product **250**, instead gave 31% direct two-component coupling product **250'**. N-methylation to give Boc-Sar-OH resulted in some conjunctive cross-coupling (**251**, 11%), but direct two-component coupling was the major product (**251'**, 35%). Changing to the secondary amino acid Boc-Ala-OH gave 44% conjunctive cross-coupling product **252**, with 22% direct two-component coupling product **252'**. The selectivity switched completely upon methylation of Boc-Ala-OH, giving **253** in 54% yield as the only isolated product. As expected, the tertiary acyclic amino acid Boc-Aib-OH gave exclusive conjunctive cross-coupling (**254**, 34%), with an improvement in yield observed upon removing the free NH group by N-methylation (**255**[†], 54%). As an alternative to N-methylation of the Boc-protected amino acid, a phthalimide protecting group could also be used, providing the conjunctive cross-coupled product **256** in 43% yield. Increasing the sterics adjacent to the α -amino radical did not impact the yield, giving **257** in 50% yield. A range of functional groups were also shown to be compatible with this system, including a phenyl ring (**258**, 33%), a sulfide (**259**, 32%) and an ester (**260**, 23%). **259** highlights the power of this methodology, building up molecular complexity in a single step by introducing five different heteroatoms (O, N, S, B and F) into a molecule (prior to oxidation), with the opportunity to further functionalise the boronic ester functional handle.

The reaction was not only limited to amino acids as α -oxy acids, including the vitamin E analogue Trolox (**261**[†], 77%), the fibrate drug bezafibrate (**262**[†], 27%) and the herbicide clofibric acid (**263**, 23%), could also be employed. The improved yields of cyclic acids over acyclic acids is highlighted here. In the case of the acyclic acids bezafibrate and clofibric acid, no other side-products were isolated, and even after prolonged reaction times the yields could not be improved. The successful application of these molecules shows the potential to rapidly access molecular complexity during late stage functionalisation of biologically important compounds.

respectively. A range of heterocycles could also be incorporated, including pyrrole (**270**[‡], 51%), pyridine (**271**[‡], 59%), indole (**272**[‡], 87%) and benzodihydrofuran (**273**, 51%), demonstrating the utility of this chemistry with complex, medically relevant coupling partners.

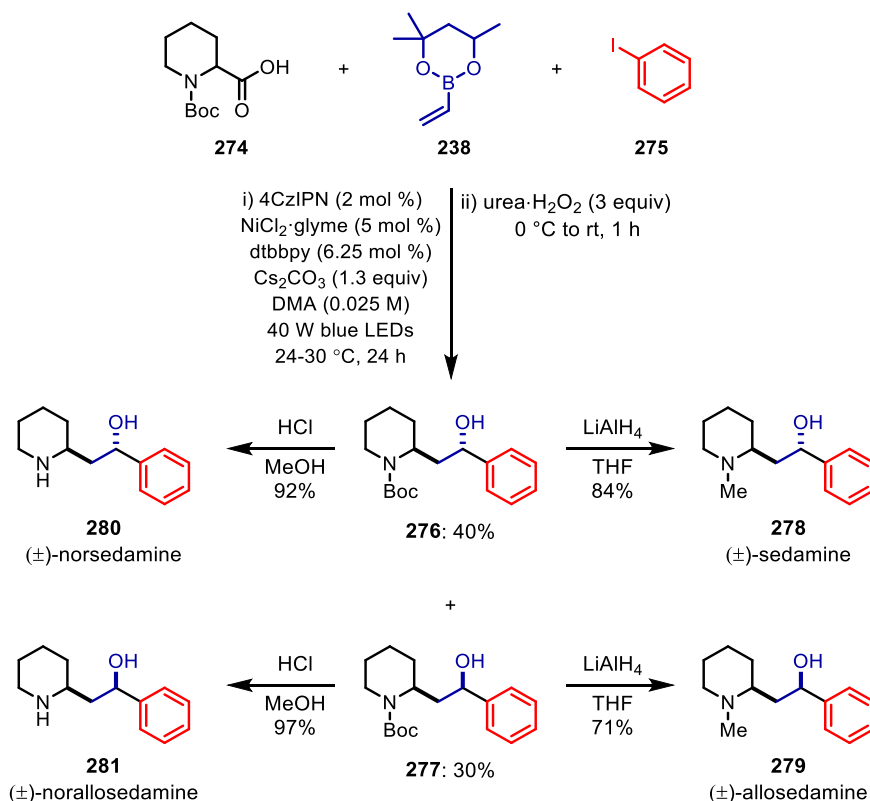


Scheme 76. Aryl iodide scope for the decarboxylative conjunctive cross-coupling of vinyl boronic esters. Yields are of isolated products after oxidation with urea hydrogen peroxide (3 equiv). See supplementary materials for exact experimental procedures and diastereomeric ratios.

4.2.3.1 Application to *Sedum* Alkaloids

To further demonstrate the utility of this methodology, we applied it to the two-step synthesis of four *sedum* alkaloids (Scheme 77). Of these four alkaloids, sedamine **278** has shown potential to be used as a treatment for cognitive disorders, and its diastereomer allosedamine **279** has been used in the treatment of respiratory diseases.^[180] We subjected Boc-Pip-OH **274**, vinyl boronic ester **238** and iodobenzene **275** to the decarboxylative conjunctive cross-coupling reaction, followed by *in situ* oxidation using urea-H₂O₂, to give the diastereomeric 1,3-aminoalcohols **276** and **277** as two separable diastereomers in a combined yield of 70%. Subsequent treatment with LiAlH₄ resulted in the reduction of the Boc-protecting group, yielding (±)-sedamine **278** and (±)-allosedamine **279** in 84% and 71% yields, respectively. Additionally, removal of the Boc-protecting group using methanolic HCl gave (±)-norsedamine **280** and (±)-noralllosedamine **281** in 92% and 97% yields, respectively. These examples demonstrate the power of this methodology to synthesise complex molecules in a single step by

combining three different fragments. It also shows the potential to utilise this methodology in the modular synthesis of analogues of biologically relevant molecules such as sedamine.

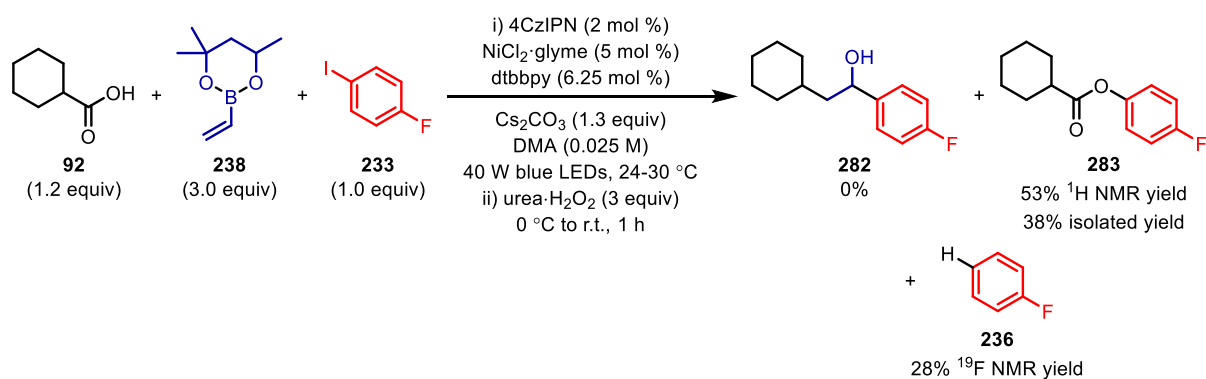


Scheme 77. Application of the decarboxylative conjunctive cross-coupling of vinyl boronic esters to *sedum* alkaloids. Yields are of isolated products.

4.2.3.2 Unsuccessful Substrates

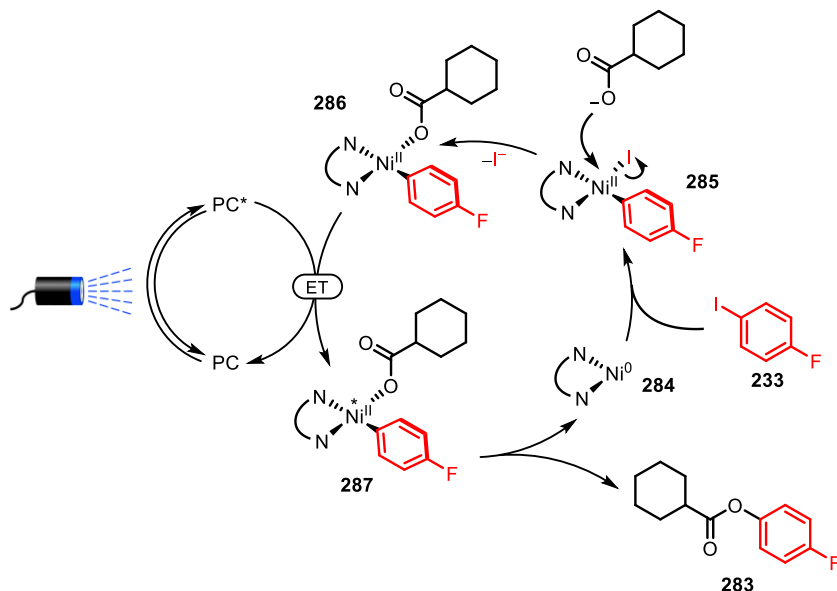
4.2.3.2.1 Alkyl Carboxylic Acids

Unfortunately, this complicated reaction system does have limitations. In general, we found that the carboxylic acid coupling partner was limited to amino acids and tertiary α -oxy acids. Upon application of an alkyl carboxylic acid, cyclohexyl carboxylic acid **91**, no conjunctive cross-coupling product **282** was observed (Scheme 78). Instead, ester formation between the carboxylate and the aryl iodide occurred in 53% NMR yield (38% isolated yield, **283**) in addition to 28% protodehalogenation product **236**; no other products were observed.



Scheme 78. Unsuccessful application of alkyl carboxylic acids in the conjunctive cross-coupling reaction.

Ester formation under metallaphotoredox catalysis has previously been reported by MacMillan and co-workers.^[123] They propose an energy transfer mechanism as depicted in Scheme 79. The active Ni(0) catalyst **284** undergoes oxidative addition to the aryl iodide **233** to yield a Ni(II) intermediate **285**. Displacement of the iodide ligand by the carboxylate yields Ni(II) species **286**. Concurrently, the photocatalyst (PC) is photoexcited (PC*). At this point, energy transfer between the excited state photocatalyst (PC*) and the Ni(II) species **286** generates an electronically excited Ni(II) species **287** and the ground state photocatalyst (PC). Reductive elimination from **287** yields the ester product **283**, regenerating the Ni(0) catalyst **284**, and thus completing the catalytic cycle.



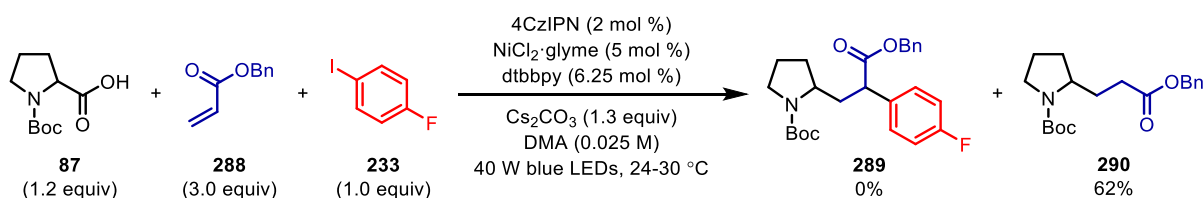
Scheme 79. Proposed mechanism for the formation of ester **283** via an energy transfer (ET) mechanism.

Mechanistic studies confirmed that it was an energy transfer mechanism and not a single electron oxidation of Ni(II) to Ni(III) from the photocatalyst. Although in the MacMillan chemistry an iridium

photocatalyst was used ($\text{Ir}(\text{ppy})_3$), they found that the minimum triplet excited energy required to generate the excited state Ni(II) species was ~ 40 kcal/mol.^[123] The triplet energy of 4CzIPN is 2.2 eV,^[181] which equates to 50.7 kcal/mol, so it is thermodynamically feasible that this mechanistic pathway could take place under our conjunctive cross-coupling conditions. However, this reactivity is surprising considering the application of alkyl carboxylic acids in metallaphotoredox-catalysed decarboxylative cross-couplings.^[121] We suspect the reason this esterification occurs is down to the slow oxidation of the carboxylate due to the lack of heteroatoms (α -amino, α -oxy) present to stabilise the resulting radical after decarboxylation, therefore competitive displacement of the iodide in **285** is favoured.

4.2.3.2.2 Acrylate Radical Acceptor

In all the concurrent reports, electron-deficient alkenes, such as acrylates, had been successfully utilised in the conjunctive cross-coupling with aryl halides and a range of radical precursors.^[169–171,174] We subjected Boc-Pro-OH (**87**), benzyl acrylate (**288**) and 4-fluoriodobenzene (**233**) to our decarboxylative conjunctive cross-coupling reaction conditions, and found that no conjunctive cross-coupling took place. Instead, we isolated the Giese hydroalkylation product **290** in 62% yield (Scheme 80). In addition, the aryl iodide starting material **233** and protodehalogenation **236** were observed in 32% and 19%, respectively by ^{19}F NMR. Other unknown peaks were also observed in the ^{19}F NMR, making up the remaining mass balance.

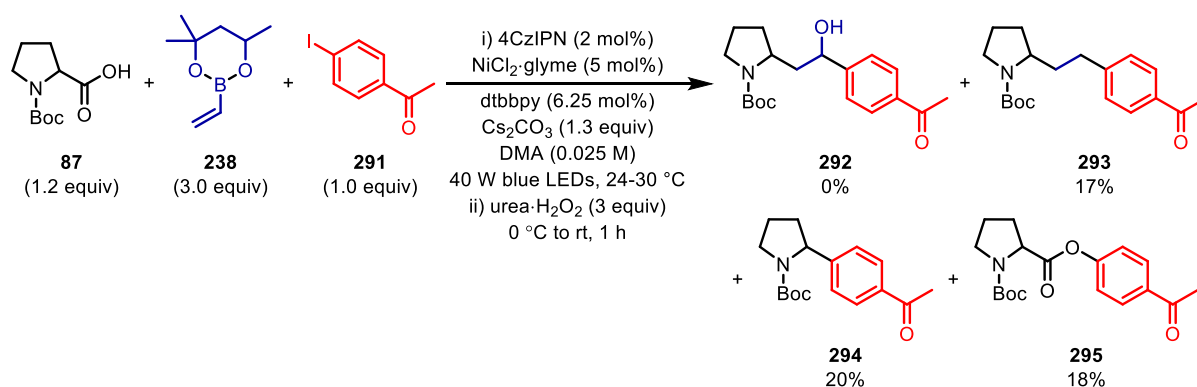


Scheme 80. Unsuccessful application of acrylate radical acceptors in the conjunctive cross-coupling reaction.

Although, we did not try any other electron-deficient alkenes, this result suggests the decarboxylative conjunctive cross-coupling is limited to vinyl boronic esters. The unique ability of vinyl boronic esters to undergo this conjunctive cross-coupling can be attributed to the slower rate of reduction of the α -boryl radical to the corresponding anion (-1.25 V)^[44] compared to the α -carboxyl radical (-0.60 V). This allows the α -boryl radical to be intercepted by the nickel complex, whereas in the case of the acrylate, the α -carboxyl radical is rapidly reduced to the corresponding anion to yield the Giese hydroalkylation product **290**.

4.2.3.2.3 Electron-deficient Aryl Iodides

When we subjected electron-deficient aryl iodides to our optimised reaction conditions, we found that they were capable coupling partners in the conjunctive cross-coupling, however the benzylic boronic ester products were unstable to protodeboronation under the reaction conditions. A similar result was seen when α -styrenyl boronic esters were used as radical acceptors in the decarboxylative radical addition reaction to vinyl boronic esters.^[44] Subjecting 4'-iodoacetophenone (**291**) to the reaction conditions, we observed none of the desired product **292**, however we isolated 17% protodeboronation product **293**, 20% direct two-component coupling **294** and 18% ester **295** (Scheme 81).

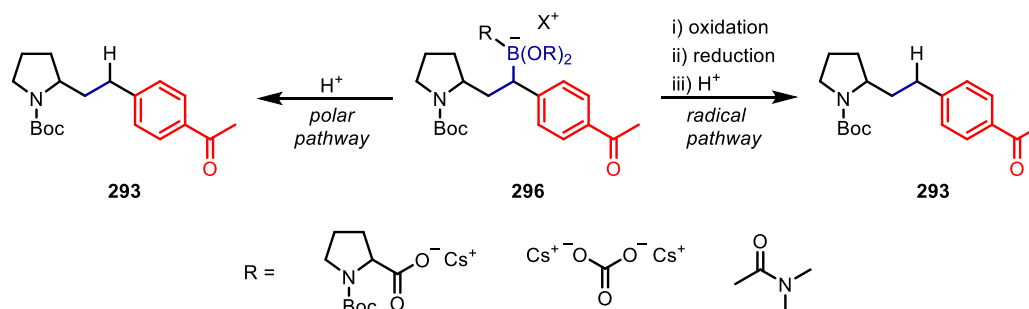


Scheme 81. Unsuccessful application of electron-deficient aryl iodides in the conjunctive cross-coupling reaction.

We suspect that protodeboronation results from the formation of transient boronate complexes (**296**) due to the increased Lewis acidity of the boronic ester from the electron-deficient aromatic group (Scheme 82). From this boronate complex, either a radical or a polar pathway will result in protodeboronation. The radical pathway involves the same mechanism previously proposed when α -styrenyl boronic esters were used as radical acceptors, whereby single-electron oxidation followed by reduction to the corresponding anion and protonation yields **293**.^[44] This route, however, may be less likely as the oxidation potential of the electron-deficient benzylic boronic ester will be more positive than the corresponding electron-neutral/rich benzylic boronic ester, which will result in less efficient single-electron oxidation. This same observation was made by Ley and co-workers in the metallaphotoredox-catalysed deboronative cross-coupling of boronic esters with aryl bromides.^[139]

An alternative pathway involves the protonation of the boronate complex. A similar reaction involving tertiary benzylic boronic esters has been reported by Aggarwal and co-workers.^[182] Boronate complexes have been shown to behave as organometallic-type nucleophiles,^[183] so it is plausible that protonation could occur from the carboxylic acid, cesium bicarbonate or upon workup. Attempts to remove proton

sources by using the cesium salt of Boc-Pro-OH (therefore not needing Cs₂CO₃) still resulted in protodeboronation.



Scheme 82. Proposed mechanisms for the protodeboronation of electron-deficient benzylic boronic esters.

In addition to the protodeboronation, the increased amounts of direct two-component coupling would be expected considering the electronics of the reaction. Oxidative addition of 4'-iodoacetophenone to Ni(0) would result in an electron-deficient Ni(II) complex, the nucleophilic α -amino radical would have a better polarity match with this electron-deficient complex than the mildly electron-deficient vinyl boronic ester. This electron-deficient Ni(II) complex may also be the source of the ester **295** as this would facilitate the displacement of the iodide by the carboxylate of Boc-Pro-OH (*vide supra*), which following photoexcitation of the resulting Ni(II) complex yields the ester **295**.

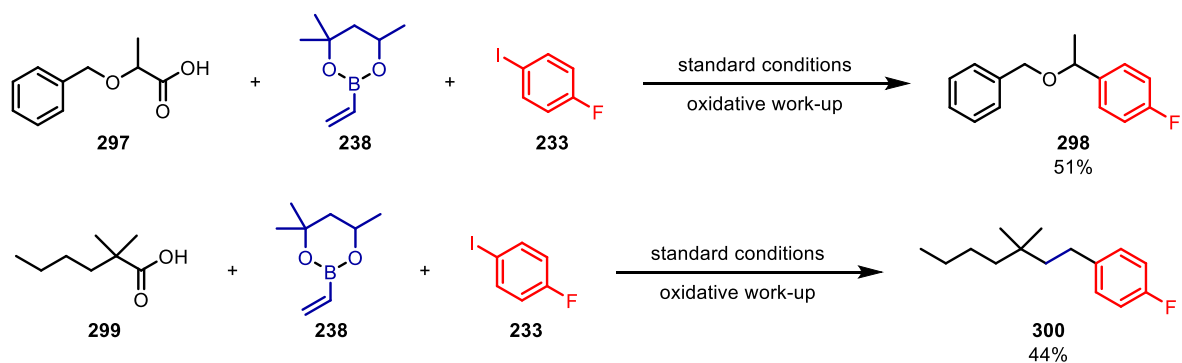
4.2.3.2.4 Other Unsuccessful Substrates

Other unsuccessful substrates, which were not further investigated, are summarised in Scheme 83. With respect to the carboxylic acids, we found that although tertiary α -oxy carboxylic acids could readily undergo the conjunctive cross-coupling in moderate to excellent yields, secondary α -oxy carboxylic acids such as 2-(benzyloxy)propanoic acid **297** failed to yield any desired product, instead exclusively giving direct two-component coupling **298**. This may be due to the lack of sterics surrounding the α -oxy radical; in the case of the secondary α -amino acids, the presence of the Boc-protecting group adds sterics around the α -amino radical. Moving to alkyl carboxylic acids, we found that tertiary alkyl carboxylic acids such as 2,2-dimethylhexanoic acid **299** were competent in the conjunctive cross-coupling, however, were susceptible to protodeboronation under the reaction conditions to give **300**. A plausible explanation could be slow single-electron oxidation of the carboxylate, resulting in greater amounts of transient boronate complex formation with the benzylic boronic ester product, which can then undergo either the radical or polar protodeboronation (*vide supra*). Due to the focus on secondary radical precursors for our transformation, we did not investigate this further.

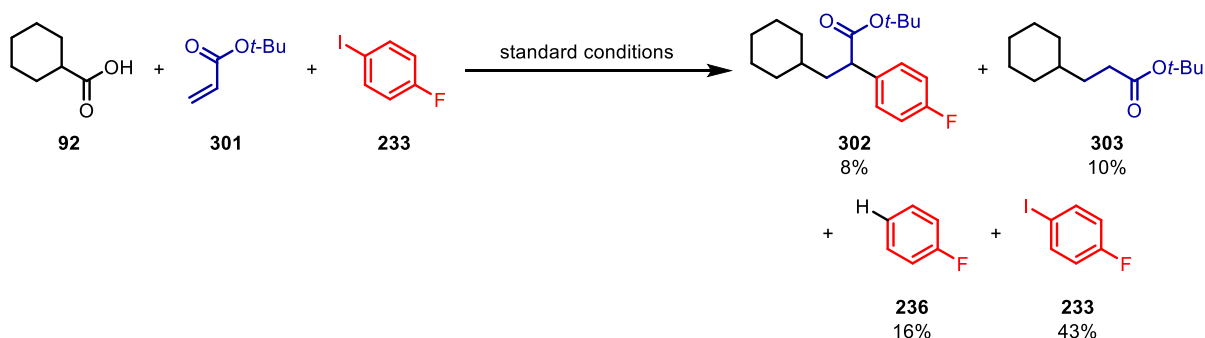
The combination of alkyl carboxylic acids **92** with acrylates **301** was also tried to determine whether increasing the electrophilicity of the radical acceptor could enable the decarboxylative conjunctive cross-coupling to proceed with less nucleophilic alkyl radicals. Although this worked to some extent (8%, **302**), the reaction also yielded 10% Giese hydroalkylation (**303**), 16% protodehalogenation (**236**) and 43% aryl iodide starting material **233**, in addition to a range of unknown side-products. We did not investigate this reaction further.

In an attempt to introduce a second functional handle into the products, 4-chloro- and 4-bromo-iodobenzene were used (**304** and **307**, respectively) as coupling partners. Despite being able to deliver the benzylic boronic ester products, the products were unstable to protodeboronation. In the case of 4-bromo-iodobenzene, both the benzylic boronic ester **308** and the protodeboronation product **309** were observed, however complete protodeboronation was observed with 4-chloro-iodobenzene.

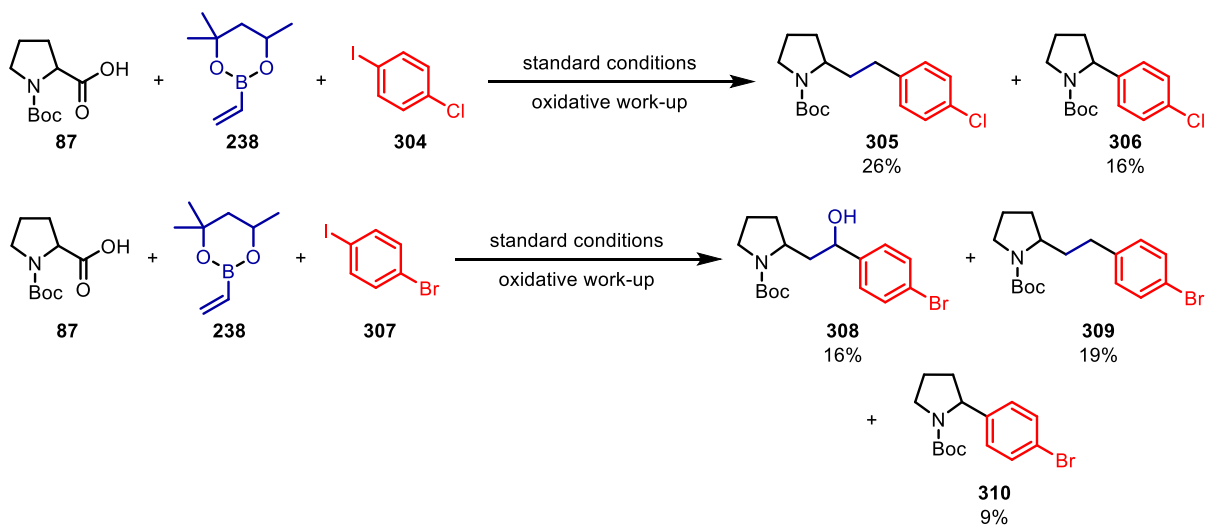
Carboxylic acids



Carboxylic acid/acceptor



Aryl iodides

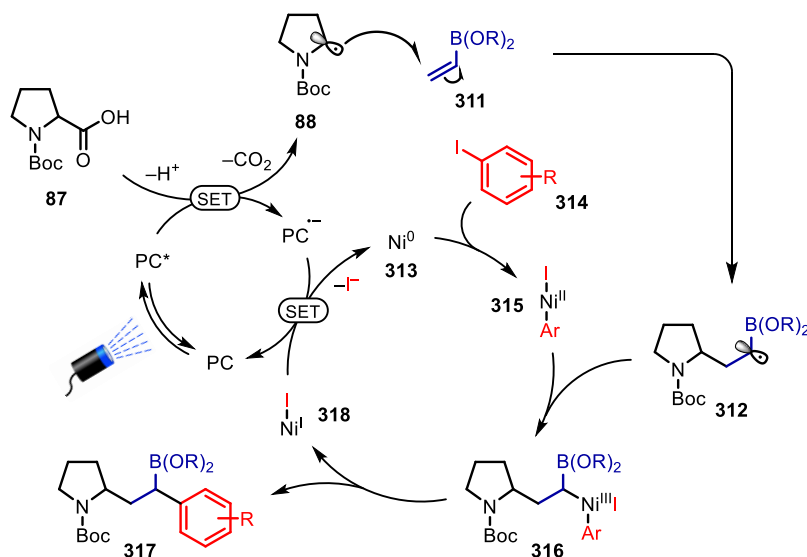


Scheme 83. Summary of unsuccessful substrates from the decarboxylative conjunctive cross-coupling reaction. Yields were determined by ^1H NMR with 1,2,4-trimethoxybenzene as an internal standard.

4.2.4 Proposed Mechanism

We propose that the mechanism of the decarboxylative conjunctive cross-coupling of vinyl boronic esters proceeds via a metallaphotoredox dual catalytic cycle depicted in Scheme 84. Under visible light

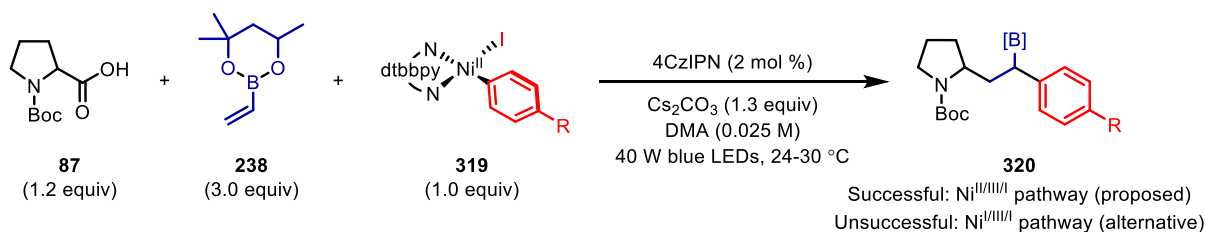
irradiation, 4CzIPN (PC) is photoexcited to a highly oxidising state (PC*). SET between this excited state photocatalyst (PC*, $E_{1/2}^{\text{red}} [^*PC/PC^{\bullet-}] = +1.35 \text{ V vs SCE in MeCN}$)^[92] and the carboxylate of Boc-Pro-OH **87** (Boc-Pro-OCs, $E_{1/2}^{\text{red}} = +0.95 \text{ V vs SCE in MeCN}$)^[95] yields a carboxyl radical, which rapidly decarboxylates to give α -amino radical **88** and the reduced state photocatalyst (PC^{•-}). The nucleophilic radical **88** then adds to the vinyl boronic ester **311** to form the stabilised α -boryl radical intermediate **312**. Meanwhile, the Ni(0) catalyst **313** undergoes oxidative addition to the aryl iodide **314** to form the Ni(II) complex **315**. This Ni(II) complex **315** then traps the α -boryl radical intermediate **312** to give the Ni(III) species **316**, which upon reductive elimination yields the conjunctive cross-coupled product **317**. Final SET transfer between the resulting Ni(I) complex **318** ($E_{1/2}^{\text{red}} [\text{Ni}^{\text{II}}/\text{Ni}^{\text{I}}] = -1.20 \text{ V vs SCE in DMF}$)^[113] and the reduced state of the photocatalyst (PC^{•-}, $E_{1/2}^{\text{red}} [PC/PC^{\bullet-}] = -1.21 \text{ V vs SCE in MeCN}$)^[92] completes the catalytic cycles. An alternative pathway, in which Ni(0) catalyst **313** engages the α -boryl radical intermediate **312** to yield a Ni(I) complex, followed by oxidative addition then reductive elimination, cannot be ruled out.



Scheme 84. Proposed mechanism for the decarboxylative conjunctive cross-coupling of vinyl boronic esters with carboxylic acids and aryl iodides.

Given that the decarboxylative direct cross-coupling of carboxylic acids with aryl halides^[113] and decarboxylative radical addition reactions to vinyl boronic esters^[44,147] using (metalla)photoredox catalysis are established, mechanistic studies were not conducted. However, in order to probe our proposed mechanism, a Ni(II) complex such as **319**, which involves a competent aryl iodide, could be synthesised (Scheme 85). Then, a stoichiometric amount of this Ni(II) complex could be subjected to the optimal reaction conditions for the decarboxylative conjunctive cross-coupling (minus the nickel catalyst and ligand). If the reaction is successful, this would suggest that the intermediate α -boryl radical **312** is trapped by the Ni(II) complex **315**, as in our proposed mechanism. If the reaction is unsuccessful

however, it may suggest the alternative Ni^{I/III} pathway, whereby the α -boryl radical **312** first interacts with the Ni(0) catalyst **313** before oxidative addition. Care must be taken in order to rule out decomposition of the Ni(II) complex during the reaction, and account for any ester formation taking place through photoexcitation of the Ni(II) complex with the aryl and carboxylate unit bound, as these could also result in the stoichiometric reaction being unsuccessful.



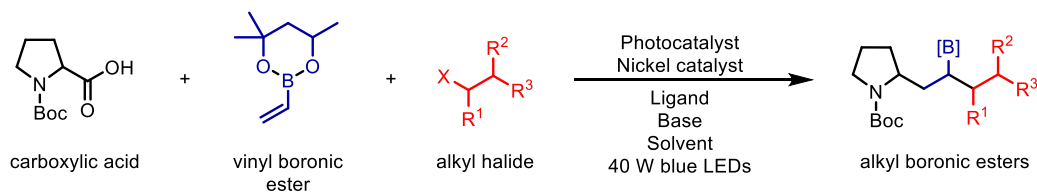
Scheme 85. Mechanistic study using a stoichiometric amount of preformed Ni(II) complex.

4.2.5 Conclusions and Outlook

In conclusion, the first decarboxylative conjunctive cross-coupling of vinyl boronic esters with carboxylic acids and aryl iodides enabled by metallaphotoredox catalysis has been developed for the synthesis of complex benzylic boronic esters from readily available feedstock starting materials. A range of α -amino acids, mainly secondary α -amino acids, as well as tertiary α -oxy acids could undergo the conjunctive cross-coupling in good yields with unexpectedly high selectivity for the conjunctive cross-coupling over the competing direct two-component coupling reaction. This makes the reaction distinct from concurrent reports in the field which rely heavily on the use of tertiary alkyl radical precursors – many of which are not commercially available – to overcome the competing direct two-component coupling.^[169–171,174] In addition to the acids, a range of electron-rich and electron-neutral aryl iodides were able to partake in the conjunctive cross-coupling with modest to excellent yields. In general, the functional group tolerance was excellent, both on the acid and aryl iodide backbone, enabling the build-up of complex benzylic boronic esters in a single step. In terms of limitations, the reaction appeared to be unique to vinyl boronic esters and carboxylic acids bearing an α -heteroatom stabilising group. Electron-deficient aryl iodides, although competent in the reaction, were susceptible to protodeboronation under the reaction conditions. To highlight the practicality and effectiveness of this methodology to rapidly access complex molecular structures in a modular fashion, four *sedum* alkaloids were synthesised in two-steps from readily available starting materials.

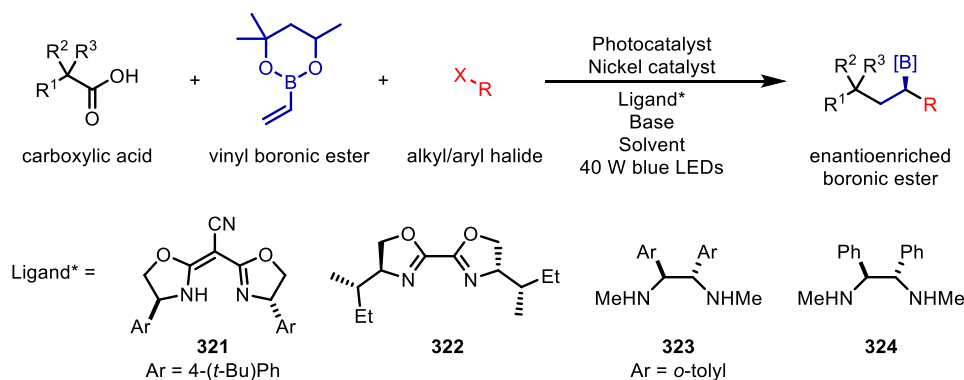
In terms of outlook, the next two logical steps will involve introducing further complexity within this reaction manifold. The first should investigate the decarboxylate conjunctive cross-coupling of vinyl boronic esters with carboxylic acids and *alkyl* halides (Scheme 86). This will allow the formation of

complex alkyl boronic esters which would otherwise be inaccessible in a single step. Decarboxylative cross-couplings of carboxylic acids and alkyl halides have already been developed by MacMillan and co-workers using metallaphotoredox catalysis,^[121] and given the success of our methodology, it should be feasible.



Scheme 86. Future work: decarboxylative conjunctive cross-coupling of vinyl boronic esters with carboxylic acids and alkyl halides.

The second development that should be investigated is introducing stereocontrol into these conjunctive cross-couplings, specifically the synthesis of enantioenriched boronic esters (Scheme 87). Control at the stereocentre formed upon decarboxylation will be very difficult and therefore the use of achiral tertiary carboxylic acids should be used. In the case of the stereocentre adjacent to the boronic ester, this is controlled through the nickel cycle and thus has the potential to be tuned by a chiral nickel catalyst. MacMillan and Fu disclosed an asymmetric decarboxylative arylation of α -amino acids using metallaphotoredox catalysis and the chiral bis(oxazoline) ligand **321**.^[120] Nevado and co-workers have also used a chiral (bis)oxazoline ligand (**322**) for the asymmetric conjunctive cross-coupling of olefins, which included vinyl boronic esters.^[50] Moreover, Fu has conducted an asymmetric arylation of α -halo boronic esters using nickel in combination with the chiral diamine ligand **323**, which features engagement of an α -boryl radical with a chiral nickel complex.^[67] Similarly, Morken used the chiral diamine ligand **324** for the asymmetric conjunctive cross-coupling of vinyl boronic esters with alkyl iodides and organozinc reagents.^[48] Utilising these precedents, an asymmetric variant of the decarboxylative conjunctive cross-coupling of vinyl boronic esters may be possible.

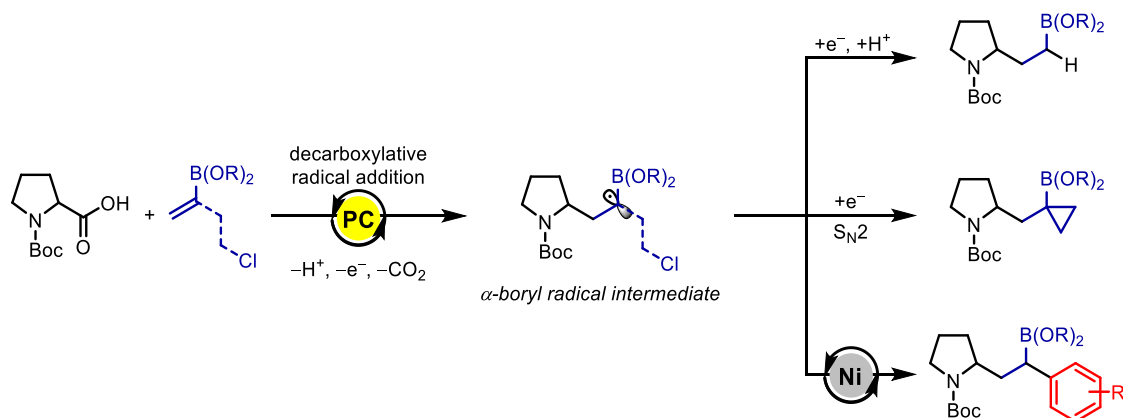


Scheme 87. Future work: asymmetric decarboxylative conjunctive cross-coupling of vinyl boronic ester with carboxylic acids and alkyl/aryl halides.

5.0 Overall Summary

Boronic esters are highly versatile synthetic intermediates in organic synthesis due to their ability to be transformed into range of functional groups. Moreover, they have recently seen more application in medicinal chemistry as the corresponding boronic acid. It is therefore unsurprising that a great deal of research has been devoted to the synthesis of boronic esters, including their incorporation into structurally complex molecules.

Radical addition reactions to vinyl boronic esters were found to be excellent methods to rapidly access boronic esters, as well as to introduce the boronic ester functional handle into complex molecules.^[33] Herein, we have developed three methodologies which feature a novel decarboxylative radical addition reaction to vinyl boronic esters, utilising abundant carboxylic acids as the alkyl radical precursors and readily available vinyl boronic esters as the radical acceptor (Scheme 88).



Scheme 88. Decarboxylative radical additions to vinyl boronic esters.

We first developed the decarboxylative radical addition to vinyl boronic esters.^[44] Under mild photoredox conditions, the reaction was amenable to a range of primary, secondary, and tertiary carboxylic acids, including α-amino, α-oxy and alkyl acids, providing the corresponding boronic ester products in good to excellent yields. Moreover, the reaction could be applied to a range of substituted vinyl boronic esters. In all, this reaction enables rapid access to alkyl boronic ester products, which are not only synthetically useful, but may also have applications as boron analogues of GABA in the case of the γ-amino boronic ester products. Mechanistic studies confirmed a radical-polar crossover mechanism involving an unprecedented single-electron reduction of an α-boryl radical to the corresponding anion. Although cyclic voltammetry was unable to determine the reduction potential of this α-boryl radical, computational studies calculated this value to be $E_{1/2}^{\text{red}} = -1.25$ V vs SCE. This methodology set the stage for the following developments in the field.

Building upon this methodology, we demonstrated that we could trap the α -boryl anion with an electrophile tethered to the vinyl boronic ester to enable the synthesis of highly functionalised, polysubstituted cyclopropyl boronic esters in generally good to excellent yields.^[147] As with our previous methodology, a host of carboxylic acids could smoothly undergo the radical addition-polar cyclisation cascade under mild organophotoredox conditions. Excellent functional group tolerance and chemoselectivity were observed, allowing us to make use of natural products and drug molecules in the chemistry. These examples highlight the potential of this method to simultaneously introduce the cyclopropyl fragment and the boronic ester functional handle in a single step during late stage functionalisation of bioactive molecules.

Finally, in order to introduce a new level of complexity in the boronic ester products, we developed a decarboxylative conjunctive cross-coupling of vinyl boronic esters with carboxylic acids and aryl iodides using metallaphotoredox catalysis.^[168] Utilising the stability of the α -boryl radical intermediate generated upon radical addition, we could trap this α -boryl radical with a nickel catalyst to enable a nickel catalysed cross-coupling. This conjunctive cross-coupling was applied to a range of amino acids and tertiary α -oxy acids. Focusing on secondary α -amino acids made this transformation distinct from concurrent reports in the field, which relied on the use of tertiary alkyl radical precursors. Electron-rich and electron-neutral aryl iodides were also successfully applied. The yields of the corresponding benzylic boronic esters ranged from modest to excellent due to the number of competing side-reactions taking place including: direct two-component coupling of the carboxylic acids with the aryl iodide, Giese hydroalkylation, protodehalogenation of the aryl iodide limiting reagent and ester formation between the carboxylic acid and the aryl iodide. To demonstrate the utility of this methodology, we applied it the two-step synthesis of four *sedum* alkaloid natural products.

Overall, these three methodologies offer mild, one step, modular approaches to highly complex boronic esters products with the potential to add further complexity through transformation of the boronic ester functional handle. They utilise readily available carboxylic acids as alkyl radical precursors, which do not require prefunctionalisation to be used under the mild (metalla)photoredox conditions. Moreover, the widespread availability of the vinyl boronic esters, aryl iodides and catalysts make these methodologies highly appealing and the go-to approaches for synthesising γ -amino boronic esters.

Going forward, these methodologies have set a foundation for future endeavours in the generation and reactivity of α -boryl radicals in organic synthesis. Future work should investigate the conjunctive cross-coupling of vinyl boronic esters with carboxylic acids and alkyl halides, and then focus on introducing stereocontrol at the centre adjacent to the boronic ester, enabling access to highly complex, enantioenriched boronic ester products.

6.0 Supplementary Materials

6.1 General Information

All reactions were carried out at room temperature (r.t.). Temperatures were recorded by placing a thermometer beside the reaction vial; heat generated from the LEDs resulted in warming of the reaction to 38 °C. If necessary, fan cooling was used to maintain a temperature range of 24-30 °C. Water was de-ionised and brine refers to a saturated aqueous solution of NaCl. DMF was reagent grade (unless otherwise stated). DMA was anhydrous. Vinylboronic acid pinacol ester **16** was purified by Kugelrohr distillation (r.t., 1 mbar, with a -78 °C collection flask) prior to use. 4CzIPN,^[92] dehydroabiatic acid^[184] and 2-methyl-2-phthalimidopropanoic^[185] were prepared according to literature procedures. All other reagents were purchased from commercial sources and used as received.

40 W blue LEDs were Kessil A160WE tuna blue LED aquarium lights (purchased from <http://charterhouse-aquatics.com>) and were used with colour dial turned fully anticlockwise and intensity turned fully clockwise.

Flash chromatography was carried out using silica gel (Aldrich, silica gel 60, 40-63 µm).

Reactions were tracked by TLC using aluminium-backed silica plates (0.25 mm, Merck, silica gel 60 F₂₅₄). Compounds were visualised under UV light, or by staining with aqueous basic potassium permanganate (KMnO₄) or an ethanolic solution of phosphomolybdic acid (PMA), followed by heating.

¹H, ¹³C, ¹³B and ¹⁹F NMR spectra were acquired at various field strengths as indicated using Bruker 400 MHz, Varian VNMR 400 MHz, Varian VNMR 500 MHz and Bruker Cryo 500 MHz spectrometers. All NMR spectra were recorded at 25 °C unless otherwise stated. Chemical shifts (δ) are given in parts per million (ppm) and coupling constants (*J*) are given in Hertz (Hz) and refer to apparent multiplicities. The ¹H NMR spectra are reported as follows: chemical shift (multiplicity, coupling constants, number of protons, assignment). Full characterization was confirmed by two-dimensional NMR spectroscopy (COSY, HSQC, HMBC).

Gas chromatography (GC) was performed on an Agilent Technologies 6890N Network GC System using an Agilent HP-5 column (15 m × 0.25 mm × 0.25 µm).

Infrared (IR) spectra were recorded on a Perkin Elmer Spectrum One FT-IR spectrometer as a thin film. Selected absorption maxima (ν_{\max}) are reported in wavenumbers (cm⁻¹).

High-resolution mass spectra (HRMS) were recorded on a Bruker micrOTOF instrument using electrospray ionisation (ESI) or Bruker UltrafleXtreme using matrix-assisted laser desorption/ionisation (MALDI).

Melting points were recorded in degrees Celsius (°C) using a Kofler hot-stage microscope or Stuart SMP30 melting point apparatus and are reported uncorrected.

Cyclic voltammetry was performed using an Autolab PGSTAT30 potentiostat. Analysis was performed using general purpose electrochemical system (GPES) software. Graphs were plotted in Microsoft Excel.

For quantum yield measurements, commercially available potassium ferrioxalate trihydrate (Alfa Aesar) was used for actinometry, and all the absorption spectra were measured using a Perkin Elmer Lambda 25 UV/Vis Spectrophotometer.

Compound names are those generated by ChemDraw 16.0 (PerkinElmer), following the IUPAC nomenclature.

6.2 Synthesis of Alkyl Boronic Esters

The data presented in this section has been partially published in:

A. Noble, R. S. Mega, D. Pflästerer, E. L. Myers, V. K. Aggarwal, *Angew. Chem. Int. Ed.* **2018**, *57*, 2155–2159.^[44]

6.2.1 General Procedures and Reaction Set-up

General Procedure 2A [for use with fully protected α -amino acids (Scheme 46, Conditions A and Scheme 47)]:

To a 7 mL vial equipped with a magnetic stir bar was added the amino acid (1.0 equiv.), Ir(dtbbpy)(ppy)₂PF₆ (1.0 mol%) and Cs₂CO₃ (1.1 equiv.). DMF (0.10 M) was then added followed by vinyl boronic ester pinacol ester **16** (1.5 equiv.). The vial was sealed with a septum and the reaction mixture degassed by sparging with nitrogen for 10 minutes. The nitrogen inlet was removed, and the vial further sealed with parafilm. The reaction mixture was stirred at 800 rpm and irradiated with 40 W blue Kessil LED lamps for between 40 and 71 h. The reaction mixture was diluted with water (20 mL) and extracted into ethyl acetate (3 × 20 mL). The organics were combined and washed with water (20 mL) and brine (20 mL), dried (Na₂SO₄), filtered, and concentrated *in vacuo*. The crude product was then purified by normal-phase flash column chromatography.

General Procedure 2B [for use with α -amino acids possessing a free NH group (Scheme 46, Conditions B) and α -oxy acids (Scheme 48)]:

To a 7 mL vial equipped with a magnetic stir bar was added the acid (1.0 equiv.), Ir[dF(CF₃)ppy]₂(dtbbpy)PF₆ (2.0 mol%) and Cs₂CO₃ (1.0 equiv.). Anhydrous DMA (0.05 M or 0.10 M) was then added followed by vinyl boronic ester pinacol ester **16** (1.5 equiv.). The vial was sealed with a septum and the reaction mixture degassed by sparging with nitrogen for 10 minutes. The nitrogen inlet was removed, and the vial further sealed with parafilm. The reaction mixture was stirred at 800 rpm and irradiated with 40 W blue Kessil LED lamps for between 40 and 62 h. The reaction mixture was diluted with water (20 mL) and extracted into ethyl acetate (3 × 20 mL). The organics were combined and washed with water (20 mL) and brine (20 mL), dried (Na₂SO₄), filtered, and concentrated *in vacuo*. The crude product was then purified by normal-phase flash column chromatography.

General Procedure 2C [for use with alkyl carboxylic acids (Scheme 48)]:

To a 7 mL vial equipped with a magnetic stir bar was added the carboxylic acid (1.0 equiv.), Ir[dF(Me)ppy]₂(dtbbpy)PF₆ (2.0 mol%) and Cs₂CO₃ (1.0 equiv.). Anhydrous DMA (0.10 M) was then added followed by vinyl boronic ester pinacol ester **16** (1.5 equiv.). The vial was sealed with a septum and the reaction mixture degassed by sparging with nitrogen for 10 minutes. The nitrogen inlet was removed, and the vial further sealed with parafilm. The reaction mixture was stirred at 800 rpm and irradiated with 40 W blue Kessil LED lamps for 64 h. The reaction mixture was diluted with water (20 mL) and extracted into ethyl acetate (3 × 20 mL). The organics were combined and washed with water (20 mL) and brine (20 mL), dried (Na₂SO₄), filtered, and concentrated *in vacuo*. The crude product was then purified by normal-phase flash column chromatography.

Reaction Set-up:

The 40 W Kessil LED lamps were positioned 5 cm from the reaction vial. When one lamp was used, a mirror was placed beneath the vial at an angle of 45° (Figure S 1A). When two lamps were used, the lamps were positioned on opposite sides of the reaction vial (Figure S 1B).

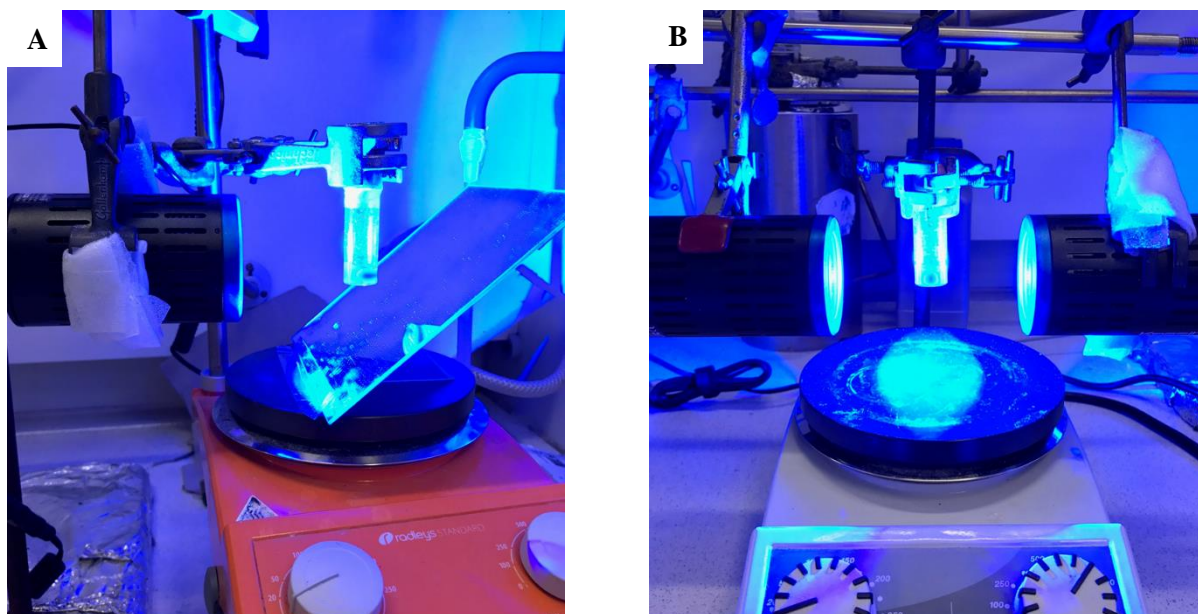
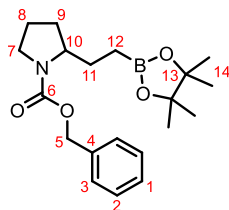


Figure S 1. Photoredox reaction set-up for the synthesis of alkyl boronic esters, using one lamp and a mirror (A) or two lamps (B).

6.2.2 Product Characterisation

Benzyl 2-(2-(4,4,5,5-tetramethyl-1,3,2-dioxaborolan-2-yl)ethyl)pyrrolidine-1-carboxylate (**117**)



Prepared following General Procedure 2A using Z-Pro-OH (75 mg, 0.30 mmol, 1.0 equiv.), Ir(dtbbpy)(ppy)₂PF₆ (2.7 mg, 0.0030 mmol, 1.0 mol%), Cs₂CO₃ (108 mg, 0.330 mmol, 1.10 equiv.), vinyl boronic acid pinacol ester **16** (76 μL, 0.45 mmol, 1.5 equiv.) and DMF (3.0 mL), which was irradiated with 1 × Kessil lamp for 40 h. Purification by flash column chromatography (20% EtOAc/pentane) gave the title compound (69 mg, 0.19 mmol, 64% yield) as a colourless oil.

TLC: R_f = 0.38 (20% EtOAc/pentane, KMnO₄ stain).

¹H NMR (400 MHz, CDCl₃): δ_H 7.42 – 7.27 (m, 5H, H¹ + H² + H³), 5.21 – 5.04 (m, 2H, H⁵), 3.87 – 3.73 (br. s, 1H, H¹⁰), 3.53 – 3.30 (m, 2H, H⁷), 1.98 – 1.64 (br. m, 5H, H⁸ + H⁹ + H¹¹), 1.51 – 1.35 (br. m, 1H, H¹¹), 1.23 (s, 12H, H¹⁴), 0.80 – 0.62 (br. m, 2H, H¹²) ppm.

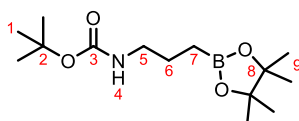
¹³C NMR (101 MHz, CDCl₃): δ_C 155.1 + 154.8 (rotameric peaks, C⁶), 137.3 (C⁴), 128.4 (2 × C²), 127.8 (C¹), 127.7 (2 × C³), 83.0 (2 × C¹³), 66.5 + 66.4 (rotameric peaks, C⁵), 59.7 + 59.0 (rotameric peaks, C¹⁰), 46.7 + 46.3 (rotameric peaks, C⁷), 29.9 + 29.1 (rotameric peaks, C⁸), 28.6 + 27.8 (rotameric peaks, C¹¹), 24.9 (2 × C¹⁴), 24.8 (2 × C¹⁴), 23.7 + 23.0 (rotameric peaks, C⁹), 7.7 (C¹²) ppm.

¹¹B NMR (128 MHz, CDCl₃): δ_B 34.4 (br. s, 1B) ppm.

IR (film) ν_{max}: 2975, 1698, 1408, 1356, 1327, 1143, 1101 cm⁻¹.

HRMS (ESI⁺): calcd. for C₂₀H₃₁BNO₄ [M+H]⁺ 360.2344, found 360.2342.

tert-Butyl (3-(4,4,5,5-tetramethyl-1,3,2-dioxaborolan-2-yl)propyl)carbamate (**129**)



Prepared following General Procedure 2B with Boc-Gly-OH (35 mg, 0.20 mmol, 1.0 equiv.), Ir[dF(CF₃)ppy]₂(dtbbpy)PF₆ (4.5 mg, 0.0040 mmol, 2.0 mol%), Cs₂CO₃ (65 mg, 0.20 mmol, 1.0 equiv.),

vinyl boronic acid pinacol ester **16** (51 μ L, 0.30 mmol, 1.5 equiv.) and DMA (4.0 mL), which was irradiated with 2 \times Kessil lamps for 62 h. Purification by flash column chromatography (10% EtOAc/pentane) gave the title compound (15 mg, 0.053 mmol, 26%) as a colourless oil.

TLC: R_f = 0.18 (10% EtOAc/pentane, KMnO₄ stain).

¹H NMR (400 MHz, CDCl₃): δ_H 4.72 + 4.35 (rotameric peaks, 2 \times br. s, 1H, H⁴), 3.12 – 3.07 (m, 2H, H⁵), 1.59 (quin, J = 7.3 Hz, 2H, H⁶), 1.43 (s, 9H, H¹), 1.24 (s, 12H, H⁹), 0.79 (t, J = 7.7 Hz, 2H, H⁷) ppm.

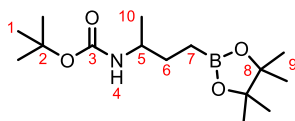
¹³C NMR (101 MHz, CDCl₃): δ_C 156.0 (C³), 83.2 (2 \times C⁸), 78.8 (C²), 42.6 (C⁵), 28.5 (3 \times C¹), 24.8 (4 \times C⁹), 24.1 (C⁶), 8.5 (br. C⁷) ppm.

¹¹B NMR (128 MHz, CDCl₃): δ_B 34.1 (br. s, 1B) ppm.

IR (film) ν_{max} : 3374, 2978 – 2874, 1705, 1517, 1380, 1366, 1320, 1247, 1168, 1145 cm⁻¹.

HRMS (ESI⁺) calcd. for C₁₄H₂₉BNO₄ [M+H]⁺ 286.2187, found 286.2195.

***tert*-Butyl (4-(4,4,5,5-tetramethyl-1,3,2-dioxaborolan-2-yl)butan-2-yl)carbamate (121)**



Prepared following General Procedure 2B using Boc-Ala-OH (57 mg, 0.30 mmol, 1.0 equiv.), Ir[dF(CF₃)ppy]₂(dtbbpy)PF₆ (6.7 mg, 0.0060 mmol, 2.0 mol%), Cs₂CO₃ (98 mg, 0.30 mmol, 1.0 equiv.), vinyl boronic acid pinacol ester **16** (76 μ L, 0.45 mmol, 1.5 equiv.) and DMA (3.0 mL), which was irradiated with 2 \times Kessil lamps for 40 h. Purification by flash column chromatography (10% EtOAc/pentane) gave the title compound (47 mg, 0.16 mmol, 52% yield) as a colourless crystalline solid.

TLC: R_f = 0.38 (10% EtOAc/pentane, KMnO₄ stain).

Mpt: 43 – 44 °C (EtOAc).

¹H NMR (400 MHz, CDCl₃): δ_H 4.53 (br. s, 1H, H⁴), 3.61 – 3.46 (br. m, 1H, H⁵), 1.59 – 1.43 (m, 2H, H⁶), 1.40 (s, 9H, H¹), 1.23 (s, 6H, H⁹), 1.22 (s, 6H, H⁹), 1.07 (d, J = 6.5 Hz, 3H, H¹⁰), 0.77 (t, J = 7.9 Hz, 2H, H⁷) ppm.

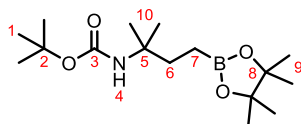
¹³C NMR (101 MHz, CDCl₃): δ_C 155.5 (C³), 83.1 (2 \times C⁸), 78.7 (C²), 48.4 (C⁵), 30.9 (C⁶), 28.4 (3 \times C¹), 24.9 (2 \times C⁹), 24.8 (2 \times C⁹), 21.2 (C¹⁰), 7.7 (br. C⁷) ppm.

¹¹B NMR (128 MHz, CDCl₃): δ_B 34.3 (br. s, 1B) ppm.

IR (film) ν_{\max} : 3361, 2977, 1670, 1511, 1366, 1167, 1145 cm^{-1} .

HRMS (ESI⁺): calcd. for $\text{C}_{15}\text{H}_{31}\text{BNO}_4$ $[\text{M}+\text{H}]^+$ 300.2343, found 300.2337.

***tert*-Butyl (2-methyl-4-(4,4,5,5-tetramethyl-1,3,2-dioxaborolan-2-yl)butan-2-yl)carbamate (133)**



Prepared following General Procedure 2B using Boc-Aib-OH (61 mg, 0.30 mmol, 1.0 equiv.), $\text{Ir}[\text{dF}(\text{CF}_3)\text{ppy}]_2(\text{dtbbpy})\text{PF}_6$ (6.7 mg, 0.0060 mmol, 2.0 mol%), Cs_2CO_3 (98 mg, 0.30 mmol, 1.0 equiv.), vinyl boronic acid pinacol ester **16** (76 μL , 0.45 mmol, 1.5 equiv.) and DMA (6.0 mL), which was irradiated with $2 \times$ Kessil lamps for 62 h. Purification by flash column chromatography (7% EtOAc/pentane) gave the title compound (54 mg, 0.17 mmol, 57% yield) as a colourless solid.

TLC: R_f = 0.54 (10% EtOAc/pentane, KMnO_4 stain).

Mpt: 58 – 60 $^\circ\text{C}$ (EtOAc).

^1H NMR (400 MHz, CDCl_3): δ_{H} 4.61 (br. s, 1H, H^4), 1.69 – 1.63 (m, 2H, H^6), 1.41 (s, 9H, H^1), 1.25 (s, 6H, H^{10}), 1.24 (s, 12H, H^9), 0.79 – 0.70 (m, 2H, H^7) ppm.

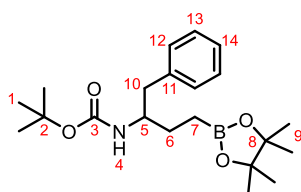
^{13}C NMR (101 MHz, CDCl_3): δ_{C} 154.6 (C^3), 83.1 ($2 \times \text{C}^8$), 78.4 (C^2), 52.8 (C^5), 35.3 (C^6), 28.5 ($3 \times \text{C}^1$), 26.4 ($2 \times \text{C}^{10}$), 24.8 ($4 \times \text{C}^9$), 5.3 (br. C^7) ppm.

^{11}B NMR (128 MHz, CDCl_3): δ_{B} 33.8 (br. s, 1B) ppm.

IR (film) ν_{\max} : 3394, 2977, 2931, 1720, 1499, 1453, 1366, 1329, 1270, 1168, 1145, 1070 cm^{-1} .

HRMS (MALDI): calcd. for $\text{C}_{16}\text{H}_{32}\text{BNO}_4\text{Na}$ $[\text{M}+\text{Na}]^+$ 336.2320, found 336.2332.

***tert*-butyl (1-phenyl-4-(4,4,5,5-tetramethyl-1,3,2-dioxaborolan-2-yl)butan-2-yl)carbamate (139)**



Prepared following General Procedure 2B using Boc-Phe-OH (80 mg, 0.30 mmol, 1.0 equiv.), $\text{Ir}[\text{dF}(\text{CF}_3)\text{ppy}]_2(\text{dtbbpy})\text{PF}_6$ (6.7 mg, 0.0060 mmol, 2.0 mol%), Cs_2CO_3 (98 mg, 0.30 mmol, 1.0 equiv.), vinyl boronic acid pinacol ester **16** (76 μL , 0.45 mmol, 1.5 equiv.) and DMA (3.0 mL), which was

0.82 (d, $J = 6.7$ Hz, 1.26H, H^{23}), 0.80 (d, $J = 6.8$ Hz, 1.74H, H^{23}), 0.67 (t, $J = 8.1$ Hz, 1.16H, H^{13}), 0.58 (ddd, $J = 9.1, 6.8, 2.2$ Hz, 0.84H, H^{13}) ppm.

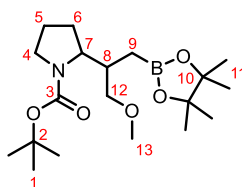
^{13}C NMR (101 MHz, CDCl_3): Mixture of diastereomers: δ_{C} 170.0 (C^9), 155.8 (C^6), 136.6 (C^{17}), 136.2 (C^4), 129.39 (minor, $2 \times \text{C}^2$), 129.36 (major, $2 \times \text{C}^2$), 128.7 ($2 \times \text{C}^{19}$), 128.53 (minor, $2 \times \text{C}^{18}$), 128.52 (major, $2 \times \text{C}^{18}$), 128.17 (minor, C^1), 128.15 (major, C^1), 128.02 (major, $2 \times \text{C}^3$), 128.00 (minor, $2 \times \text{C}^3$), 127.0 (minor, C^{20}), 126.9 (major, C^{20}), 83.12 (major, $2 \times \text{C}^{14}$), 83.06 (minor, $2 \times \text{C}^{14}$), 67.0 (C^5), 56.6 (C^8), 49.3 (major, C^{11}), 49.2 (minor, C^{11}), 44.1 (major, C^{21}), 43.9 (minor, C^{21}), 39.0 (major, C^{16}), 38.7 (minor, C^{16}), 29.5 (minor, C^{12}), 29.4 (major, C^{12}), 24.9 (C^{15}), 24.81 (major, C^{15}), 24.75 (minor, C^{15}), 24.6 (C^{15}), 23.1 (minor, C^{22}), 23.0 (major, C^{22}), 22.2 ($2 \times \text{C}^{23}$), 7.0 (br. C^{13}) ppm.

^{11}B NMR (128 MHz, CDCl_3): δ_{B} 33.7 (br. s, 1B) ppm.

IR (film) ν_{max} : 3301, 3089 – 2868, 1702, 1651, 1538, 1498, 1455, 1371, 1319, 1286, 1260, 1216, 1166, 1144, 1044, 1028 cm^{-1} .

HRMS (ESI⁺) calcd. for $\text{C}_{30}\text{H}_{43}\text{BN}_2\text{O}_5\text{Na}$ [$\text{M}+\text{Na}$]⁺ 545.3163, found 545.3166.

tert-Butyl 2-(1-methoxy-3-(4,4,5,5-tetramethyl-1,3,2-dioxaborolan-2-yl)propan-2-yl)pyrrolidine-1-carboxylate (145)



Prepared following General Procedure 2A using Boc-Pro-OH (65 mg, 0.30 mmol, 1.0 equiv.), Ir(dtbbpy)(ppy)₂PF₆ (2.7 mg, 0.0030 mmol, 1.0 mol%), Cs₂CO₃ (108 mg, 0.33 mmol, 1.1 equiv.), (*Z*)-2-(3-methoxyprop-1-en-1-yl)-4,4,5,5-tetramethyl-1,3,2-dioxaborolane (96 μL , 0.45 mmol, 1.5 equiv.) and DMF (3.0 mL), which was irradiated with 1 \times Kessil lamp for 71 h. Purification by flash column chromatography (15% EtOAc/pentane) gave the title compound as mixture of diastereomers (64 mg, 0.17 mmol, 57% yield) as a colourless oil. The diastereomeric ratio was determined to be 54:46 by high temperature NMR in DMSO-*d*₆.

TLC: $R_f = 0.22$ (15% EtOAc/pentane, KMnO₄ stain).

^1H NMR (500 MHz, DMSO-*d*₆, 100 °C): 54:46 mixture of diastereomers: δ_{H} 3.85 – 3.77 (minor, m, 1H, H^7), 3.77 – 3.71 (major, m, 1H, H^7), 3.47 – 3.37 (m, 1H, H^4), 3.34 – 3.27 (m, 1H, H^{12}), 3.27 – 3.20 (m, 3H, H^{13}), 3.20 – 3.07 (m, 2H, $H^4 + H^{12}$), 2.48 – 2.42 (minor, m, 1H, H^8), 2.31 – 2.22 (major, m, 1H, H^8), 1.86 – 1.63 (m, 4H, $H^5 + H^6$), 1.43 (major, s, 9H, H^1), 1.42 (minor, s, 9H, H^1),

1.20 (major, s, 12H, H¹¹), 1.20 (minor, s, 12H, H¹¹), 0.76 – 0.62 (m, 1H, H⁹), 0.62 – 0.55 (major, m, 1H, H⁹), 0.52 – 0.44 (minor, m, 1H, H⁹) ppm.

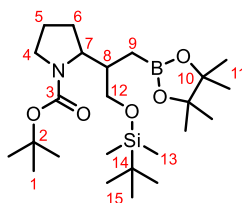
¹³C NMR (126 MHz, DMSO-*d*₆, 100 °C): Mixture of diastereomers: 154.6 (major, C³), 154.5 (minor, C³), 83.0 (minor, 2 × C¹⁰), 82.9 (major, 2 × C¹⁰), 78.57 (minor, C²), 78.55 (major, C²), 76.0 (minor, C¹²), 75.2 (major, C¹²), 60.6 (major, C⁷), 59.5 (minor, C⁷), 58.5 (major, C¹³), 58.4 (minor, C¹³), 47.3 (minor, C⁴), 47.2 (major, C⁴), 38.2 (major, C⁸), 37.3 (minor, C⁸), 28.71 (major, 3 × C¹), 28.68 (minor, 3 × C¹), 28.0 (major, C⁵), 26.6 (minor, C⁵), 25.2 (major, 2 × C¹¹), 25.1 (minor, 2 × C¹¹), 25.04 (major, 2 × C¹¹), 25.01 (minor, 2 × C¹¹), 23.9 (minor, C⁶), 23.8 (major, C⁶) ppm. The carbon directly attached to boron was not detected due to the boron quadrupole.

¹¹B NMR (128 MHz, CDCl₃): δ_B 34.2 (br. s, 1B) ppm.

IR (film) ν_{max}: 2975, 2928, 2878, 1689, 1455, 1364, 1254, 1144, 1106 cm⁻¹.

HRMS (ESI⁺): calcd. for C₁₉H₃₆BNO₅Na [M+Na]⁺ 392.2582, found 392.2591.

***tert*-Butyl 2-(1-((*tert*-butyldimethylsilyloxy)-3-(4,4,5,5-tetramethyl-1,3,2-dioxaborolan-2-yl)propan-2-yl)pyrrolidine-1-carboxylate (146)**



Prepared following General Procedure 2A using Boc-Pro-OH (65 mg, 0.30 mmol, 1.0 equiv.), Ir(dtbbpy)(ppy)₂PF₆ (2.7 mg, 0.0030 mmol, 1.0 mol%), Cs₂CO₃ (108 mg, 0.33 mmol, 1.1 equiv.), (*Z*)-*tert*-butyldimethyl((3-(4,4,5,5-tetramethyl-1,3,2-dioxaborolan-2-yl)allyloxy)silane (148 μL, 0.45 mmol, 1.5 equiv.) and DMF (3.0 mL), which was irradiated with 1 × Kessil lamp for 64 h. Purification by flash column chromatography (10% EtOAc/pentane) gave the title compound as a mixture of diastereomers (75 mg, 0.16 mmol, 53% yield) as a colourless oil. The diastereomeric ratio was determined to be 58:42 by high temperature NMR in DMSO-*d*₆.

TLC: R_f = 0.52 and 0.62 (10% EtOAc/pentane, KMnO₄ stain).

¹H NMR (500 MHz, DMSO-*d*₆, 100 °C): 58:42 mixture of diastereomers: δ_H 3.92 – 3.86 (minor, m, 1H, H⁷), 3.82 – 3.77 (major, m, 1H, H⁷), 3.59 – 3.37 and 3.25 – 3.20 (2 × m, 3H, H⁴ + H¹²), 3.19 – 3.09 (m, 1H, H⁴), 2.41 – 2.34 (minor, m, 1H, H⁸), 2.14 – 2.06 (major, m, 1H, H⁸), 1.88 – 1.64 (m, 4H, H⁵ + H⁶), 1.45 – 1.40 (m, 9H, H¹), 1.23 – 1.17 (m, 12H, H¹¹), 0.93 – 0.87 (m, 9H, H¹⁵),

0.79 (major, dd, $J = 15.8, 7.4$ Hz, 1H, H⁹), 0.67 (major, dd, $J = 15.9, 7.2$ Hz, 1H, H⁹), 0.59 (minor, dd, $J = 15.2, 5.2$ Hz, 1H, H⁹), 0.52 (minor, dd, $J = 15.4, 8.6$ Hz, 1H, H⁹) 0.08 – 0.01 (m, 6H, H¹³) ppm.

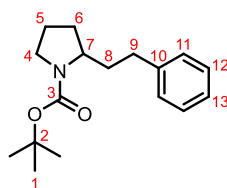
¹³C NMR (126 MHz, DMSO-*d*₆, 100 °C): Mixture of diastereomers: δ_{C} 83.1 (minor, 2 × C¹⁰), 83.0 (major, 2 × C¹⁰), 78.5 (C²), 66.2 (minor, C¹²), 65.2 (major, C¹²), 60.5 (major, C⁷), 59.3 (minor, C⁷), 47.3 (major, C⁴), 47.1 (minor, C⁴), 39.7 (C⁸), 28.7 (major, C¹), 28.7 (minor, C¹), 28.1 (minor, C⁵), 26.5 (major, C⁵), 26.3 (C¹⁵), 25.20 (major, 2 × C¹¹), 25.15 (minor, 2 × C¹¹), 25.1 (major, 2 × C¹¹), 25.0 (minor, 2 × C¹¹), 23.9 (minor, C⁶), 23.7 (major, C⁶), 18.4 (C¹⁴), –5.0 (minor, C¹³), –5.1 (major, C¹³) ppm. Carbonyl carbon was not detected. The carbon directly attached to boron was not detected due to the boron quadrupole.

¹¹B NMR (128 MHz, CDCl₃): δ_{B} 34.6 (br. s, 1B) ppm.

IR (film) ν_{max} : 2975 – 2858, 1694, 1472, 1389, 1366, 1255, 1167, 1145, 1105 cm⁻¹.

HRMS (ESI⁺): calcd. for C₂₄H₄₈BNO₅SiNa [M+Na]⁺ 492.3292, found 492.3284.

***tert*-Butyl 2-phenethylpyrrolidine-1-carboxylate (147²)**



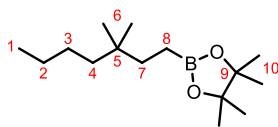
Prepared following General Procedure 2A using Boc-Pro-OH (65 mg, 0.30 mmol, 1.0 equiv.), Ir(dtbbpy)(ppy)₂PF₆ (2.7 mg, 0.0030 mmol, 1.0 mol%), Cs₂CO₃ (108 mg, 0.330 mmol, 1.10 equiv.), 4,4,5,5-tetramethyl-2-(1-phenylvinyl)-1,3,2-dioxaborolane (104 mg, 0.450 mmol, 1.50 equiv.) and DMF (6.0 mL), which was irradiated with 2 × Kessil lamps for 62 h. Purification by flash column chromatography (10% EtOAc/pentane) gave the title compound (57 mg, 0.21 mmol, 69% yield) as a colourless oil.

¹H NMR (400 MHz, CDCl₃): δ_{H} 7.30 – 7.07 (m, 5H, H¹¹ + H¹² + H¹³), 3.92 – 3.63 (br. m, 1H, H⁷), 3.44 – 3.17 (br. m, 2H, H⁴), 2.67 – 2.45 (br. m, 2H, H⁹), 2.20 – 1.48 (m, 6H, H⁵ + H⁶ + H⁸), 1.41 (s, 9H, H¹) ppm.

¹³C NMR (101 MHz, CDCl₃): δ_{C} 154.7 (C³), 142.1 (C¹⁰), 128.3 (C¹² + C¹³), 125.8 (C¹¹), 79.0 (C²), 57.3 + 57.0 (rotameric peaks, C⁷), 46.5 + 46.2 (rotameric peaks, C⁴), 36.4 + 36.0 (rotameric peaks, C⁸), 32.8 (C⁹), 30.6 + 30.1 (rotameric peaks, C⁵), 28.6 (C¹), 23.8 + 23.2 (rotameric peaks, C⁶) ppm.

Spectroscopic data matches previously reported data.^[138]

2-(3,3-dimethylheptyl)-4,4,5,5-tetramethyl-1,3,2-dioxaborolane (158)



Prepared following General Procedure 2C using 2,2-dimethylhexanoic acid (32 μ L, 0.20 mmol, 1.0 equiv.), Ir[dF(Me)ppy]₂(dtbbpy)PF₆ (4.1 mg, 0.0040 mmol, 2.0 mol%), Cs₂CO₃ (65 mg, 0.20 mmol, 1.0 equiv.), vinyl boronic acid pinacol ester **16** (51 μ L, 0.30 mmol, 1.5 equiv.) and DMA (2.0 mL), which was irradiated with 1 \times Kessil lamps for 64 h. Purification by flash column chromatography (1% EtOAc/pentane) gave the title compound (34 mg, 0.13 mmol, 67% yield) as a yellow oil.

TLC: R_f = 0.57 (100% pentane, KMnO₄ stain).

¹H NMR (400 MHz, CDCl₃): δ_{H} 1.32 – 1.10 (m, 8H, H² + H³ + H⁴ + H⁷), 1.24 (s, 6H, H¹⁰), 1.24 (s, 6H, H⁹), 0.88 (t, *J* = 7.0 Hz, 3H, H¹), 0.79 (s, 6H, H⁶), 0.71 – 0.63 (m, 2H, H⁸) ppm.

¹³C NMR (101 MHz, CDCl₃): δ_{C} 82.8 (2 \times C⁹), 41.2 (C⁴), 35.6 (C⁵), 33.0 (C⁷), 26.6 (2 \times C⁶), 26.3 (C³), 24.8 (4 \times C¹⁰), 23.7 (C²), 14.2 (C¹), 5.1 (br. C⁸) ppm.

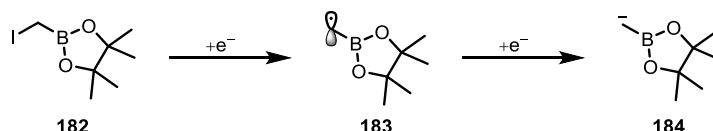
¹¹B NMR (128 MHz, CDCl₃): δ_{B} 34.8 (br. s, 1B) ppm.

IR (film) ν_{max} : 2957, 2929, 2862, 1469, 1370, 1330, 1315, 1146 cm⁻¹.

HRMS (MALDI) calcd. for C₁₅H₃₁BNaO₂ [M+Na]⁺ 277.2312, found 277.2318.

6.2.3 Cyclic Voltammetry Studies

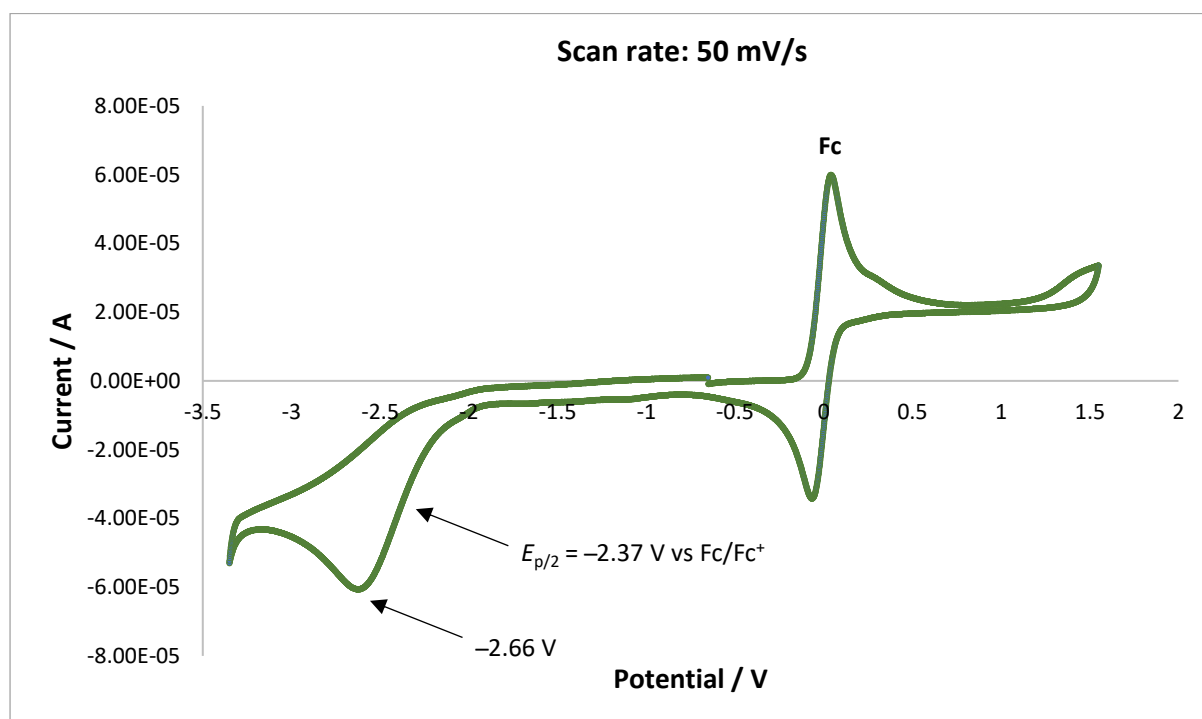
Cyclic voltammetry was carried out using iodomethylboronic acid pinacol ester **182**, which underwent two single-electron reductions to form the α -boryl anion **184** via the α -boryl radical intermediate **183** (Scheme S 1).



Scheme S 1. Reduction of iodomethylboronic acid pinacol ester **182** to α -boryl anion **184** via radical **183**.

Samples were prepared with **182** (0.025 mmol) in 4 mL of tetra-*n*-butylammonium hexafluorophosphate (5 mM) in dry, degassed (argon) MeCN. A glassy carbon working electrode, platinum wire counter electrode and a silver wire reference electrode were used. A scan rate over a range between 50 – 200 mV/s was used, and an average reduction potential was taken, referencing to Fc/Fc⁺.

An average value of $E_{p/2} = -2.38$ V vs Fc/Fc⁺ in MeCN was recorded from 50, 100 and 200 mV/s scan rates (Figure S 2). These values can be converted to SCE by adding 0.38 V.^[186] Therefore, this equates to a reduction potential of -2.00 V vs SCE.



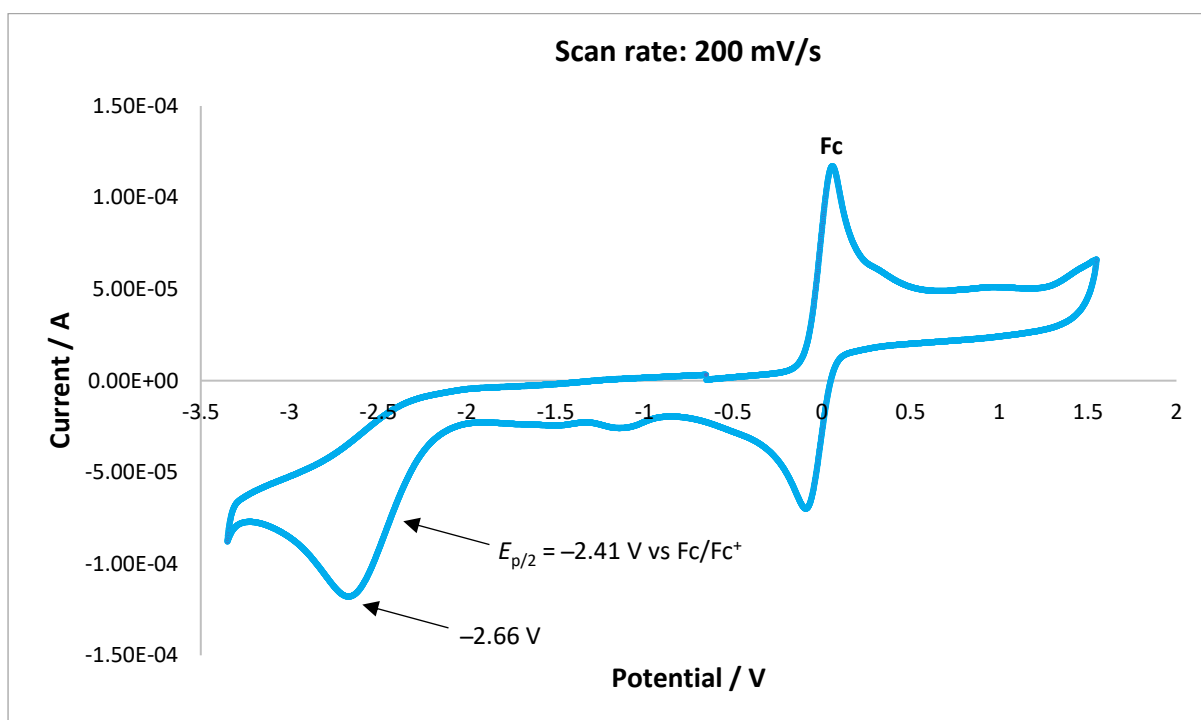
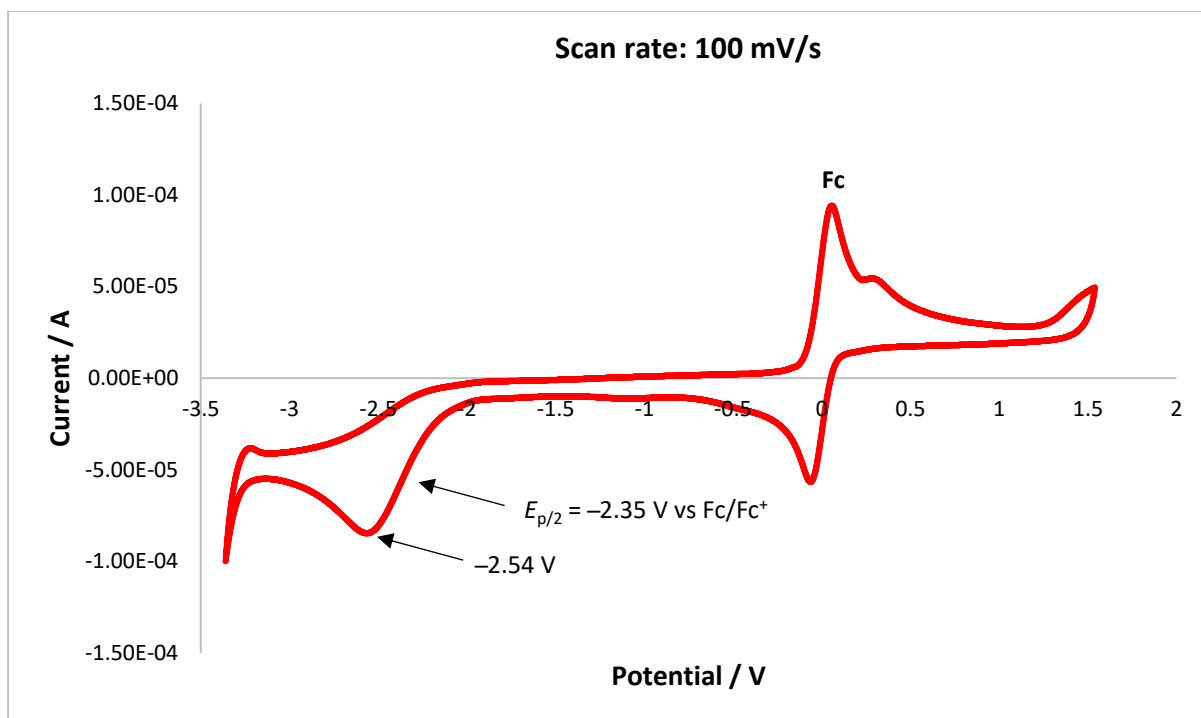
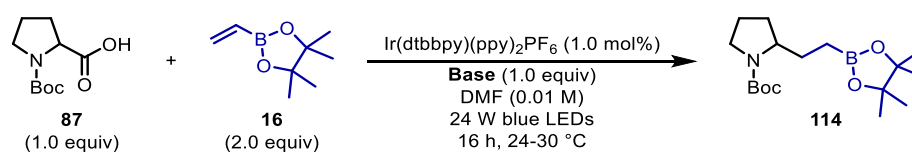


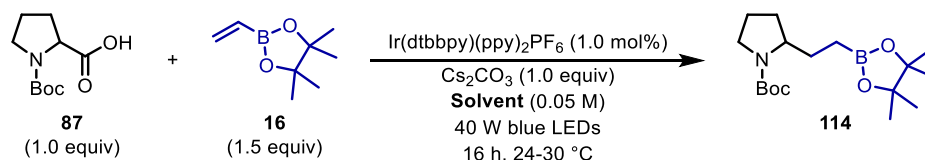
Figure S 2. Cyclic voltammograms of iodomethylboronic acid pinacol ester **182** at scan rates of 50, 100 and 200 mV/s, referencing to ferrocene (Fc).

6.2.4 Additional Optimisation Tables



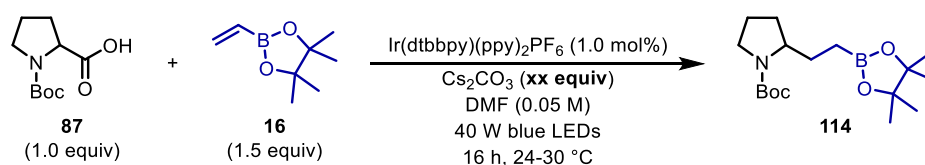
Entry	Base	GC Yield (%)	
		114	Vinyl-Bpin 16
1	None	0	114
2	Li ₂ CO ₃	1	71
3	Na ₂ CO ₃	25	41
4	K ₂ CO ₃	40	4
5	Cs ₂ CO ₃	76	36
6	NaHCO ₃	8	47
7	KHCO ₃	24	35
8	LiOH·H ₂ O	22	66
9	NaOH	6	88
10	KOH	43	41
11	NaOAc	8	57
12	KOAc	27	43
13	NaH ₂ PO ₄	0	126
14	Na ₂ HPO ₄	0	98
15	KH ₂ PO ₄	0	113
16	K ₂ HPO ₄	12	57
17	K ₃ PO ₄	34	87
18	NaF	0	99
19	Quinuclidine	4	54
20	DABCO	0	104
21	DBU	41	62
22	Pyridine	0	106
23	2,6-lutidine	0	122

Table S 1. Base screen. Yields were determined by GC with 1,2,4-trimethoxybenzene as the internal standard.



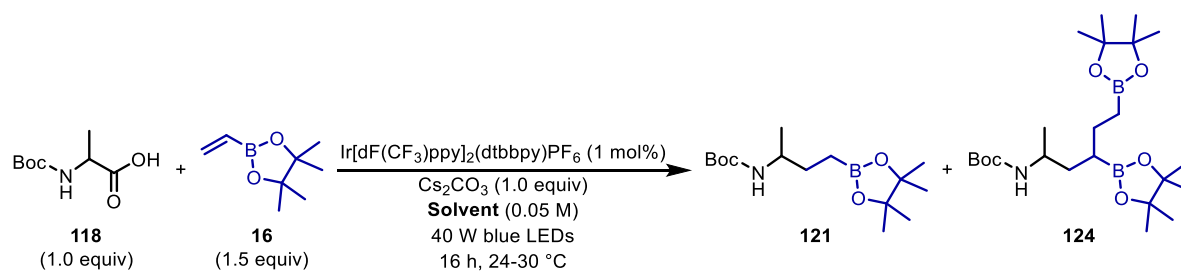
Entry	Solvent	GC Yield (%)	
		114	Vinyl-Bpin 16
1	DMF	96	0
2	DMF (anhydrous)	94	16
3	DMA (anhydrous)	82	n.d.*
4	DMPU	59	0
5	DMI (anhydrous)	83	0
6	DMSO	80	n.d.*
7	DMSO (anhydrous)	91	n.d.*
8	MeCN	6	67

Table S 2. Solvent screen. Yields were determined by GC with 1,2,4-trimethoxybenzene as the internal standard. *Not determined (n.d.) due to the overlapping solvent screen.



Entry	Equivalents of Cs ₂ CO ₃	GC Yield (%)	
		114	Vinyl-Bpin 16
1	0.75	75	31
2	1.00	72	44
3	1.10	90	21
4	1.20	76	1

Table S 3. Varying equivalents of Cs₂CO₃. Yields were determined by GC with 1,2,4-trimethoxybenzene as the internal standard.



Entry	Solvent	NMR Yield (%)	
		121	124
1	DMF (anhydrous)	29	13
2	DMI (anhydrous)	26	15
3	DMPU (anhydrous)	12	0
4	DMA (anhydrous)	58	0
5	DMSO (anhydrous)	38	0
6	CHCl ₃ (anhydrous)	0	48
7	MeCN (anhydrous)	11	0
8	Et ₂ O (anhydrous)	8	10
9	THF (anhydrous)	8	7
10	Acetone (anhydrous)	7	6
11	EtOAc (anhydrous)	4	2
12	Toluene (anhydrous)	0	33
13	CH ₂ Cl ₂ (anhydrous)	0	0
14	MeOH (anhydrous)	0	0
15	1,4-dioxane (anhydrous)	0	0

Table S 4. Complete solvent screen for monoprotected amino acid Boc-Ala-OH **118**. Yields were determined by ¹H NMR with 1,2,4-trimethoxybenzene as the internal standard.

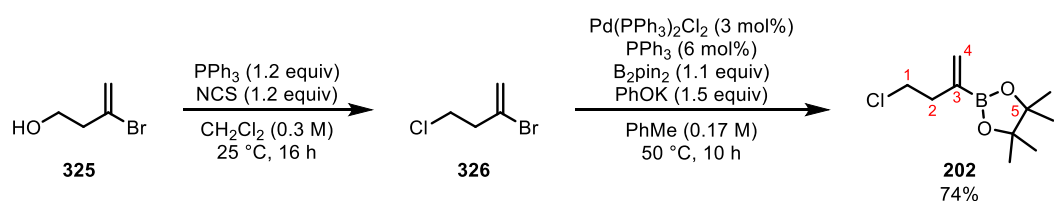
6.3 Synthesis of Cyclopropyl Boronic Esters

The data presented in this section has been partially published in:

C. Shu, R. S. Mega, B. J. Andreassen, A. Noble, V. K. Aggarwal, *Angew. Chem. Int. Ed.* **2018**, *57*, 15430–15434.^[147]

6.3.1 Synthesis of Homoallylic Chloride Vinyl Boronic Ester **202**

2-(4-Chlorobut-1-en-2-yl)-4,4,5,5-tetramethyl-1,3,2-dioxaborolane (**202**)



2-Bromo-4-chlorobut-1-ene **326** was prepared from commercially available alcohol **325** following a literature procedure.^[187]

Homoallylic chloride vinyl boronic ester **202** was prepared following a modified literature procedure.^[188] $\text{PdCl}_2(\text{PPh}_3)_2$ (126 mg, 0.180 mmol, 3.00 mol%), Ph_3P (96 mg, 0.36 mmol, 6.0 mol%), bis(pinacolato)diboron (1.67 g, 6.60 mmol, 1.10 equiv.) and PhOK (fine powder, 1.19 g, 9.00 mmol, 1.50 equiv.) were combined in a flask equipped with a magnetic stir bar, a septum inlet and a condenser. The flask was flushed with nitrogen and then charged with toluene (36 mL) and **326** (1.02 g, 6.00 mmol, 1.00 equiv.). The mixture was then stirred at 50°C for 10 h. The reaction mixture was diluted with H_2O (20 mL) at r.t., extracted into Et_2O (3×20 mL), washed with brine (20 mL), dried (MgSO_4), filtered, and concentrated *in vacuo*. The residue was purified by flash column chromatography (5% Et_2O /pentane) to give the title compound (955 mg, 4.41 mmol, 74%) as a colourless liquid.

TLC: $R_f = 0.45$ (5% Et_2O /pentane, KMnO_4 stain).

^1H NMR (400 MHz, CDCl_3): δ_{H} 5.91 (d, $J = 3.2$ Hz, 1H, H^4), 5.72 (d, $J = 3.1$ Hz, 1H, H^4), 3.62 (t, $J = 7.3$ Hz, 2H, H^1), 2.61 (t, $J = 7.3$ Hz, 1H, H^2), 1.26 (s, 12H, H^6) ppm.

^{13}C NMR (101 MHz, CDCl_3): δ_{C} 132.6 (C^4), 83.8 ($2 \times \text{C}^5$), 44.3 (C^1), 38.9 (C^2), 24.9 ($4 \times \text{C}^6$) ppm.

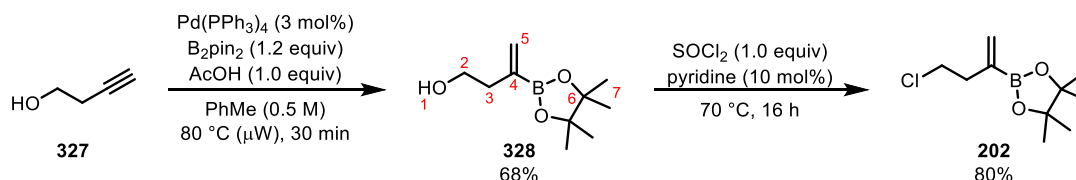
The carbon directly attached to boron was not detected due to the boron quadrupole.

^{11}B NMR (128 MHz, CDCl_3): δ_{B} 30.1 (br. s, 1B) ppm.

IR (film) ν_{max} : 2920, 2851, 1739, 1464, 1372, 1314, 1243, 1145, 1022 cm^{-1} .

HRMS (ESI⁺) calcd. for $\text{C}_{10}\text{H}_{18}\text{BClNaO}_2$ $[\text{M}+\text{Na}]^+$ 239.0982, found 239.0987.

Alternative route developed:



Homoallylic alcohol **328** is commercially available. It can also be prepared on gram scale using the following procedure:

A microwave vial containing a magnetic stir bar was charged with $\text{Pd}(\text{PPh}_3)_4$ (0.32 g, 0.28 mmol, 3.0 mol%) and bis(pinacolato)diboron (2.81 g, 11.1 mmol, 1.20 equiv.). The vial was evacuated and back-filled with nitrogen three times. Toluene (18.5 mL) was added, followed by but-3-en-1-ol **327** (758 mg, 9.23 mmol, 1.00 equiv.) and acetic acid (571 mg, 9.23 mmol, 1.00 equiv.). The reaction mixture was pre-stirred for 5 min before heating to 80 °C for 30 min in the microwave. After allowing to cool to r.t., the mixture was concentrated *in vacuo* and the residue purified directly by flash column chromatography (20% EtOAc/hexane) to give the 3-(4,4,5,5-tetramethyl-1,3,2-dioxaborolan-2-yl)but-3-en-1-ol **328** (1.25 g, 6.28 mmol, 68%) as a colourless oil.

¹H NMR (400 MHz, MeOD): δ_{H} 5.85 (br. d, $J = 3.6$ Hz, 1H, H⁵), 5.70 (br. s, 1H, H⁵), 3.62 (t, $J = 7.1$ Hz, 2H, H²), 2.40 (t, $J = 7.1$ Hz, 2H, H³), 1.30 (s, 12H, H⁷) ppm.

¹³C NMR (101 MHz, MeOD): δ_{C} 132.0 (C⁵), 84.8 (2 × C⁶), 62.8 (C²), 40.0 (C³), 25.1 (4 × C⁷) ppm. The carbon directly attached to boron was not detected due to the boron quadrupole.

Spectroscopic data matches previously reported data.^[189]

To an oven-dried flask was added 3-(4,4,5,5-tetramethyl-1,3,2-dioxaborolan-2-yl)but-3-en-1-ol **328** (1.03 mL, 5.05 mmol, 1.00 equiv.) and pyridine (40 μL , 0.50 mmol, 0.10 equiv.), and the mixture was cooled to 0 °C. Thionyl chloride (0.370 mL, 5.05 mmol, 1.00 equiv.) was added dropwise before the reaction mixture was heated to 70 °C for 16 h. After cooling to r.t., the reaction mixture was concentrated *in vacuo* and purified directly by flash column chromatography (2% EtOAc/pentane) to give **202** (877 mg, 4.05 mmol, 80%) as a colourless liquid.

6.3.2 General Procedures and Reaction Set-up

General Procedure 3A [for the synthesis of vicinally-substituted cyclopropyl boronic esters (Scheme 64, Conditions A)]:

To a 7 mL vial equipped with a magnetic stir bar was added the carboxylic acid (1.0 equiv.), 4CzIPN (5.0 mol%) and K_2CO_3 (2.0 equiv.). Anhydrous DMF (0.05 M) was then added followed by 2-chloromethyl vinyl boronic ester **198** (2.0 equiv.). The vial was sealed with a septum and the reaction mixture degassed by sparging with nitrogen for 10 min. The nitrogen inlet was removed, and the vial further sealed with parafilm. The reaction mixture was stirred at 800 rpm and irradiated with a 40 W blue Kessil LED lamp for 16 h. The reaction mixture was diluted with ethyl acetate (20 mL), washed with H_2O (3×20 mL), brine (20 mL), dried (Na_2SO_4), filtered, and concentrated *in vacuo*. The crude product was then purified by normal-phase flash column chromatography.

General Procedure 3B [for the synthesis of geminally-substituted cyclopropyl boronic esters without a free NH group (Scheme 64, Conditions B)]:

To a 7 mL vial equipped with a magnetic stir bar was added the carboxylic acid (1.0 equiv.), 4CzIPN (1.0 mol%) and Cs_2CO_3 (2.0 equiv.). Anhydrous DMF (0.05 M) was then added followed by the homoallylic chloride vinyl boronic ester **202** (1.5 equiv.). The vial was sealed with a septum and the reaction mixture degassed by sparging with nitrogen for 10 min. The nitrogen inlet was removed, and the vial further sealed with parafilm. The reaction mixture was stirred at 800 rpm and irradiated with a 40 W blue Kessil LED lamp for 20 h. The reaction mixture was diluted with ethyl acetate (20 mL), washed with H_2O (3×20 mL), brine (20 mL), dried (Na_2SO_4), filtered, and concentrated *in vacuo*. The crude product was then purified by normal-phase flash column chromatography.

General Procedure 3C [for the synthesis of geminally-substituted cyclopropyl boronic esters possessing a free NH group and use with α -oxy and alkyl carboxylic acids (Scheme 64, Conditions C)]:

To a 7 mL vial equipped with a magnetic stir bar was added the carboxylic acid (1.0 equiv.), 4CzIPN (2.0 mol%) and Cs_2CO_3 (2.0 equiv.). Anhydrous DMF (0.05 M) was then added followed by the homoallylic chloride vinyl boronic ester **202** (1.5 equiv.). The vial was sealed with a septum and the reaction mixture degassed by sparging with nitrogen for 10 min. The nitrogen inlet was removed, and the vial further sealed with parafilm. The reaction mixture was stirred at 800 rpm and irradiated with a 40 W blue Kessil LED lamp for 20–24 h. The reaction mixture was diluted with ethyl acetate (20 mL),

washed with H₂O (3 × 20 mL), brine (20 mL), dried (Na₂SO₄), filtered, and concentrated *in vacuo*. The crude product was then purified by normal-phase flash column chromatography.

Reaction Set-up:

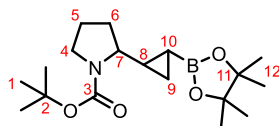
The 40 W Kessil LED lamp was positioned 5 cm from the reaction vial (Figure S 3).



Figure S 3. Photoredox reaction set-up for the synthesis of cyclopropyl boronic esters.

6.3.3 Product Characterisation

tert-Butyl 2-(2-(4,4,5,5-tetramethyl-1,3,2-dioxaborolan-2-yl)cyclopropyl)pyrrolidine-1-carboxylate (**199**)



Prepared following general procedure 3A with Boc-Pro-OH (65 mg, 0.30 mmol, 1.0 equiv.), 4CzIPN (12 mg, 0.015 mmol, 5.0 mol%), K₂CO₃ (83 mg, 0.60 mmol, 2.0 equiv.), 2-chloromethyl vinyl boronic ester **198** (118 μL, 0.600 mmol, 2.00 equiv.) and DMF (6.0 mL), which was irradiated with 1 × Kessil lamp for 16 h with fan assisted cooling. Purification by flash column chromatography (15% EtOAc/pentane) gave the title compound as a mixture of diastereomers (47 mg, 0.14 mmol, 47%) as a colourless oil. The d.r. was determined to be 56:39:5 by ¹H NMR.

TLC: R_f = 0.43 (15% EtOAc/pentane, KMnO₄ stain).

¹H NMR (400 MHz, CDCl₃): δ_H (56:39:5 ratio of diastereomers, only the major two diastereomers A and B are assigned) 3.51 – 3.14 (m, 3H, H⁴ + H⁷), 2.01 – 1.67 (m, 4H, H⁵ + H⁶), 1.49 – 1.44 (m, 9H, H¹), 1.23 – 1.15 (m, 12H, H¹² + diastereomer B, m, 0.39H, H⁸), 1.14 – 1.08 (diastereomer A, m, 0.56H, H⁸), 1.08 – 1.01 (diastereomer B, m, 0.39H, H⁹), 0.74 (diastereomer B, ddd, *J* = 7.8, 6.3, 3.6 Hz, 0.39H, H⁹), 0.56 (diastereomer A, ddd, *J* = 8.1, 6.4, 3.7 Hz, 0.56H, H⁹), 0.52 – 0.32 (diastereomers A, br. m, 0.56H, H⁹), 0.15 – –0.01 (diastereomer A, m, 0.56H, H¹⁰), –0.07 – –0.18 (diastereomer C, m, 0.05H, H¹⁰), –0.23 – –0.39 (diastereomer B, m, 0.39H, H¹⁰) ppm.

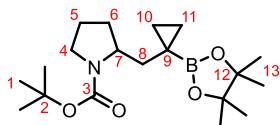
¹³C NMR (101 MHz, CDCl₃): δ_C (56:39:5 ratio of diastereomers, the minor diastereomer was not observed), 155.2 + 155.8 (diastereomeric peaks, C³), 83.00 + 82.96 (diastereomeric peaks, 2 × C¹¹), 79.3 (br., C²), 61.4 (C⁴), 46.7 (C⁷), 32.1 (br., C⁵), 28.7 + 28.6 (diastereomeric peaks, 3 × C¹), 25.0 + 24.8 + 24.7 + 24.6 (mixture of diastereomers, 4 × C¹²), 24.9 (minor, C⁸), 23.3 + 23.0 (diastereomeric peaks, C⁶), 22.6 (major, C⁸), 11.5 (br. minor, C⁹), 7.7 (major, C⁹) ppm. The carbon directly attached to boron was not detected due to the boron quadrupole.

¹¹B NMR (128 MHz, CDCl₃): δ_B 32.9 (br. s, 1B) ppm.

IR (film) ν_{max}: 2976, 1693, 1390 – 1367, 1167 – 1145 cm⁻¹.

HRMS (ESI⁺) calcd. for C₁₈H₃₃BNO₄ [M+H]⁺ 338.2500, found 338.2504.

***tert*-Butyl 2-((1-(4,4,5,5-tetramethyl-1,3,2-dioxaborolan-2-yl)cyclopropyl)methyl)pyrrolidine-1-carboxylate (203)**



Prepared following General Procedure 3B using Boc-Pro-OH (65 mg, 0.30 mmol, 1.0 equiv.), 4CzIPN (2.4 mg, 0.0030 mmol, 1.0 mol%), Cs₂CO₃ (195 mg, 0.600 mmol, 2.00 equiv.), homoallylic chloride vinyl boronic ester **202** (96 μL, 0.45 mmol, 1.5 equiv.) and DMF (6.0 mL), which was irradiated with 1 × Kessil lamp for 20 h. Purification by flash column chromatography (10% EtOAc/pentane) gave the title compound (104 mg, 0.296 mmol, 99%) as a colourless oil.

TLC: R_f = 0.45 (10% EtOAc/pentane, KMnO₄ stain).

¹H NMR (400 MHz, CDCl₃): δ_H 3.95 – 3.86 (br. m, 1H, H⁷), 3.35 – 3.29 (br. m, 2H, H⁴), 2.03 – 1.73 (m, 4H, H⁵ + H⁶), 1.63 – 1.57 (m, 1H, H⁸), 1.45 (s, 9H, H¹), 1.29 – 1.25 (m, 1H, H⁸), 1.20 (s, 6H, H¹³), 1.19 (s, 6H, H¹³), 0.75 – 0.57 (br. m, 2H, H¹⁰ + H¹¹), 0.51 – 0.31 (br. m, 2H, H¹⁰ + H¹¹) ppm.

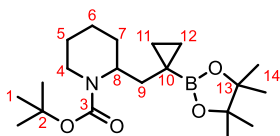
¹³C NMR (101 MHz, CDCl₃): δ_C 154.6 (C³), 83.0 (2 × C¹²), 78.8 + 78.5 (rotameric peaks, C²), 57.7 + 57.3 (rotameric peaks, C⁷), 46.2 + 45.8 (rotameric peaks, C⁴), 39.8 + 39.4 (rotameric peaks, C⁸), 29.8 (C⁵), 28.7 (3 × C¹), 24.8 (2 × C¹³), 24.6 (2 × C¹³), 23.7 + 23.0 (rotameric peaks, C⁶), 13.5 + 13.2 (rotameric peaks, C¹⁰), 10.1 (C¹¹), 1.8 (br., C⁹) ppm.

¹¹B NMR (128 MHz, CDCl₃): δ_B 33.3 (br. s, 1B) ppm.

IR (film) ν_{max}: 2975, 1691, 1389, 1139, 855 cm⁻¹.

HRMS (ESI⁺) calcd. for C₁₉H₃₅NBO₄ [M+H]⁺ 352.2657, found 352.2659.

***tert*-Butyl 2-((1-(4,4,5,5-tetramethyl-1,3,2-dioxaborolan-2-yl)cyclopropyl)methyl)piperidine-1-carboxylate (206)**



Prepared following General Procedure 3B with Boc-Pip-OH (69 mg, 0.30 mmol, 1.0 equiv.), 4CzIPN (2.4 mg, 0.0030 mmol, 1.0 mol%), Cs₂CO₃ (195 mg, 0.600 mmol, 2.00 equiv.), homoallylic chloride vinyl boronic ester **202** (96 μL, 0.45 mmol, 1.5 equiv.) and DMF (6.0 mL), which was irradiated with 1 × Kessil lamp for 20 h. Purification by flash column chromatography (5% EtOAc/pentane) gave the title compound (97 mg, 0.26 mmol, 88%) as a white solid.

TLC: $R_f = 0.48$ (5% EtOAc/pentane, KMnO_4 stain).

Mpt: 77 – 78 °C (EtOAc).

$^1\text{H NMR}$ (400 MHz, CDCl_3): δ_{H} 4.28 (br. s, 1H, H^8), 3.91 (br. d, $J = 13.2$ Hz, 1H, H^4), 2.81 (t, $J = 12.9$ Hz, 1H, H^4), 1.66 – 1.47 (m, 6H, $\text{H}^5 + \text{H}^6 + \text{H}^7$), 1.43 (s, 9H, H^1), 1.40 – 1.26 (m, 2H, H^9), 1.17 (s, 12H, H^{14}), 0.75 – 0.58 (m, 2H, $\text{H}^{11} + \text{H}^{12}$), 0.40 – 0.25 (m, 2H, $\text{H}^{11} + \text{H}^{12}$) ppm.

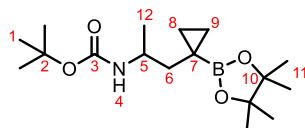
$^{13}\text{C NMR}$ (101 MHz, CDCl_3): δ_{C} 155.1 (C^3), 83.0 ($2 \times \text{C}^{13}$), 78.8 (C^2), 51.2 (br., C^8), 39.2 (br., C^4), 35.8 (C^7), 28.7 ($3 \times \text{C}^1$), 28.4 (C^5), 25.9 (C^9), 24.9 ($2 \times \text{C}^{14}$), 24.7 ($2 \times \text{C}^{14}$), 19.5 (C^6), 12.2 (C^{11}), 11.3 (br., C^{12}), 2.10 (br., C^{10}) ppm.

$^{11}\text{B NMR}$ (128 MHz, CDCl_3): δ_{B} 33.9 (br. s, 1B) ppm.

IR (film) ν_{max} : 2976 – 2930, 1686, 1414, 1364, 1140 cm^{-1} .

HRMS (ESI^+) calcd. for $\text{C}_{20}\text{H}_{36}\text{BNNaO}_4$ [$\text{M}+\text{Na}$] $^+$ 388.2633, found 388.2646.

***tert*-Butyl (1-(1-(4,4,5,5-tetramethyl-1,3,2-dioxaborolan-2-yl)cyclopropyl)propan-2-yl)carbamate (204)**



Prepared following General Procedure 3C with Boc-Ala-OH (57 mg, 0.30 mmol, 1.0 equiv.), 4CzIPN (4.7 mg, 0.0060 mmol, 2.0 mol%), Cs_2CO_3 (195 mg, 0.600 mmol, 2.00 equiv.), homoallylic chloride vinyl boronic ester **202** (96 μL , 0.45 mmol, 1.5 equiv.) and DMF (6.0 mL), which was irradiated with 1 \times Kessil lamp for 20 h. Purification by flash column chromatography (10% EtOAc/pentane) gave the title compound (85 mg, 0.26 mmol, 87%) as a colourless oil.

TLC: $R_f = 0.42$ (10% EtOAc/pentane, KMnO_4 stain).

$^1\text{H NMR}$ (400 MHz, CDCl_3): δ_{H} 5.35 (br. s, 1H, H^4), 3.65 – 3.53 (m, 1H, H^5), 1.73 (dd, $J = 14.3, 10.2$, Hz, 1H, H^6), 1.43 (s, 9H, H^1), 1.23 (s, 6H, H^{11}), 1.21 (s, 6H, H^{11}), 1.09 (d, $J = 6.4$ Hz, 3H, H^{12}), 0.93 (dd, $J = 14.3, 4.3$ Hz, 1H, H^6), 0.78 – 0.65 (m, 2H, $\text{H}^8 + \text{H}^9$), 0.41 – 0.30 (m, 2H, $\text{H}^8 + \text{H}^9$) ppm.

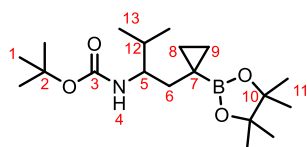
$^{13}\text{C NMR}$ (101 MHz, CDCl_3): δ_{C} 155.7 (C^3), 83.5 ($2 \times \text{C}^{10}$), 78.6 (C^2), 47.5 (C^5), 42.9 (C^6), 28.7 ($3 \times \text{C}^1$), 24.9 ($2 \times \text{C}^{11}$), 24.7 ($2 \times \text{C}^{11}$), 22.0 (C^{12}), 13.8 (C^8), 10.5 (C^9) ppm. The carbon directly attached to boron was not detected due to the boron quadrupole.

¹¹B NMR (128 MHz, CDCl₃): δ_B 33.5 (br. s, 1B) ppm.

IR (film) ν_{max}: 3406, 2977, 1714, 1416, 1167, 1140 cm⁻¹.

HRMS (ESI⁺) calcd. for C₁₇H₃₃BNO₄ [M+H]⁺ 326.2500, found 326.2505.

tert-Butyl (3-methyl-1-(1-(4,4,5,5-tetramethyl-1,3,2-dioxaborolan-2-yl)cyclopropyl)butan-2-yl)carbamate (209)



Prepared following General Procedure 3C with Boc-Val-OH (64 mg, 0.30 mmol, 1.0 equiv.), 4CzIPN (4.7 mg, 0.0060 mmol, 2.0 mol%), Cs₂CO₃ (195 mg, 0.600 mmol, 2.00 equiv.), homoallylic chloride vinyl boronic ester **202** (96 μL, 0.45 mmol, 1.5 equiv.) and DMF (6.0 mL), which was irradiated with 1 × Kessil lamp for 20 h. Purification by flash column chromatography (5% EtOAc/pentane) gave the title compound (65 mg, 0.18 mmol, 61%) as a colourless oil.

TLC: R_f = 0.34 (5% EtOAc/pentane, KMnO₄ stain).

¹H NMR (400 MHz, CDCl₃): δ_H 5.00 (d, *J* = 8.6 Hz, 1H, H⁴), 3.42 (ddt, *J* = 12.1, 8.4, 4.1 Hz, 1H, H⁵), 1.83 – 1.74 (m, 1H, H¹²), 1.67 (dd, *J* = 14.3, 11.3 Hz, 1H, H⁶), 1.42 (s, 9H, H¹), 1.22 (s, 6H, H¹¹), 1.21 (s, 6H, H¹¹), 0.88 (dd, *J* = 14.4, 4.0 Hz, 1H, H⁶), 0.83 (d, *J* = 6.8 Hz, 3H, H¹³), 0.82 (d, *J* = 6.9 Hz, 3H, H¹³), 0.75 – 0.64 (m, 2H, H⁸ + H⁹), 0.40 – 0.27 (m, 2H, H⁸ + H⁹) ppm.

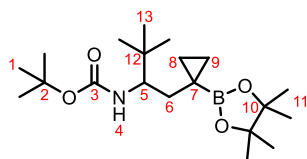
¹³C NMR (101 MHz, CDCl₃): δ_C 156.0 (C³), 83.4 (2 × C¹⁰), 78.5 (C²), 56.3 (C⁵), 36.4 (C⁶), 32.3 (C¹²), 28.6 (3 × C¹), 25.1 (2 × C¹¹), 24.7 (2 × C¹¹), 18.5 (C¹³), 18.2 (C¹³), 14.1 (C⁸), 9.9 (C⁹) ppm. The carbon directly attached to boron was not detected due to the boron quadrupole.

¹¹B NMR (128 MHz, CDCl₃): δ_B 34.3 (br. s, 1B) ppm.

IR (film) ν_{max}: 3417, 2976, 1716 – 1703, 1417, 1365, 1167, 1141 cm⁻¹.

HRMS (ESI⁺) calcd. for C₁₉H₃₇BNO₄ [M+H]⁺ 354.2814, found 354.2829.

***tert*-Butyl (3,3-dimethyl-1-(1-(4,4,5,5-tetramethyl-1,3,2-dioxaborolan-2-yl)cyclopropyl)butan-2-yl)carbamate (210)**



Prepared following General Procedure 3C with Boc-Tle-OH (69 mg, 0.30 mmol, 1.0 equiv.), 4CzIPN (4.7 mg, 0.0060 mmol, 2.0 mol%), Cs₂CO₃ (195 mg, 0.600 mmol, 2.00 equiv.), homoallylic chloride vinyl boronic ester **202** (96 μL, 0.45 mmol, 1.5 equiv.) and DMF (6.0 mL), which was irradiated with 1 × Kessil lamp for 20 h. Purification by flash column chromatography (5% EtOAc/pentane) gave the title compound (59 mg, 0.16 mmol, 53%) as a colourless oil.

TLC: R_f = 0.40 (5% EtOAc/pentane, KMnO₄ stain).

¹H NMR (400 MHz, CDCl₃): δ_H (82:18 ratio of rotamers) 4.67 (d, *J* = 10.2 Hz, 0.82H, H⁴), 4.33 (d, *J* = 10.4 Hz, 0.18H, H⁴), 3.42 (ddd, *J* = 11.8, 10.1, 3.9 Hz, 0.82H, H⁵), 3.24 (td, *J* = 11.4, 3.3 Hz, 0.18H, H⁵), 1.58 (dd, *J* = 14.1, 11.7 Hz, 1H, H⁶), 1.43 (s, 9H, H¹), 1.23 (s, 6H, H¹¹), 1.22 (s, 6H, H¹¹), 1.11 (dd, *J* = 14.1, 4.0 Hz, 1H, H⁶), 0.85 (s, 9H, H¹³), 0.75 – 0.62 (m, 2H, H⁸ + H⁹), 0.43 – 0.24 (m, 2H, H⁸ + H⁹) ppm.

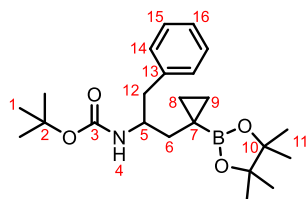
¹³C NMR (101 MHz, CDCl₃): δ_C 156.2 (C³), 83.3 (2 × C¹⁰), 78.5 (C²), 58.7 (C⁵), 35.3 (C¹²), 35.1 (C⁶), 28.7 + 28.6 (rotameric peaks, 3 × C¹), 26.6 (3 × C¹³), 25.3 + 25.1 (rotameric peaks, 2 × C¹¹), 24.8 (2 × C¹¹), 14.0 (C⁸), 9.2 (C⁹) ppm. The carbon directly attached to boron was not detected due to the boron quadrupole.

¹¹B NMR (128 MHz, CDCl₃): δ_B 33.5 (br. s, 1B) ppm.

IR (film) ν_{max}: 3426, 2973, 1720 – 1702, 1418, 1365, 1169, 1141 cm⁻¹.

HRMS (ESI⁺) calcd. for C₂₀H₃₈BNNaO₄ [M+Na]⁺ 390.2790, found 390.2805.

tert-Butyl (1-phenyl-3-(1-(4,4,5,5-tetramethyl-1,3,2-dioxaborolan-2-yl)cyclopropyl)propan-2-yl)carbamate (212)



Prepared following General Procedure 3C with Boc-Phe-OH (80 mg, 0.30 mmol, 1.0 equiv.), 4CzIPN (4.7 mg, 0.0060 mmol, 2.0 mol%), Cs₂CO₃ (195 mg, 0.600 mmol, 2.00 equiv.), homoallylic chloride vinyl boronic ester **202** (96 μL, 0.45 mmol, 1.5 equiv.) and DMF (6.0 mL), which was irradiated with 1 × Kessil lamp for 20 h. Purification by flash column chromatography (10% EtOAc/pentane) gave the title compound (109 mg, 0.27 mmol, 91%) as a colourless oil.

TLC: R_f = 0.32 (10% EtOAc/pentane, KMnO₄ stain).

¹H NMR (400 MHz, CDCl₃): δ_H 7.30 – 7.21 (m, 2H, H¹⁴), 7.21 – 7.12 (m, 3H, H¹⁵ + H¹⁶), 5.38 (br. d, *J* = 7.4 Hz, 1H, H⁴), 3.72 (dt *J* = 11.3, 7.5, 3.7 Hz, 1H, H⁵), 2.96 (dd, *J* = 13.3, 4.7 Hz, 1H, H¹²), 2.58 (dd, *J* = 13.3, 8.3 Hz, 1H, H¹²), 1.74 (dd, *J* = 14.3, 11.0 Hz, 1H, H⁶), 1.43 (s, 9H, H¹), 1.23 (s, 6H, H¹¹), 1.21 (s, 6H, H¹¹), 0.83 (dd, *J* = 14.4, 3.6 Hz, 1H, H⁶), 0.74 – 0.59 (m, 2H, H⁸ + H⁹), 0.34 – 0.15 (m, 2H, H⁸ + H⁹) ppm.

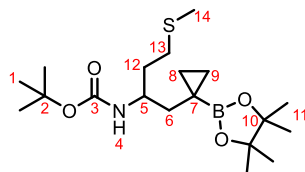
¹³C NMR (101 MHz, CDCl₃): δ_C 155.7 (C³), 139.1 (2 × C¹⁰), 129.6 (2 × C¹⁵), 128.2 (2 × C¹⁴), 126.0 (C¹⁶), 83.5 (C¹³), 78.7 (C²), 53.1 (C⁵), 42.3 (C¹²), 39.5 (C⁶), 28.6 (3 × C¹), 25.0 (2 × C¹¹), 24.6 (2 × C¹¹), 14.1 (C⁸), 10.1 (C⁹) ppm. The carbon directly attached to boron was not detected due to the boron quadrupole.

¹¹B NMR (128 MHz, CDCl₃): δ_B 34.7 (br. s, 1B) ppm.

IR (film) ν_{max}: 3407, 2977, 1712, 1505, 1417, 1365, 1167, 1139 cm⁻¹.

HRMS (ESI⁺) calcd. for C₂₃H₃₇BNO₄ [M+H]⁺ 402.2814, found 402.2815.

tert-Butyl (4-(methylthio)-1-(1-(4,4,5,5-tetramethyl-1,3,2-dioxaborolan-2-yl)cyclopropyl)butan-2-yl)carbamate (214)



Prepared following General Procedure 3C with Boc-Met-OH (75 mg, 0.30 mmol, 1.0 equiv.), 4CzIPN (4.7 mg, 0.0060 mmol, 2.0 mol%), Cs₂CO₃ (195 mg, 0.600 mmol, 2.00 equiv.), homoallylic chloride vinyl boronic ester **202** (96 μL, 0.45 mmol, 1.5 equiv.) and DMF (6.0 mL), which was irradiated with 1 × Kessil lamp for 24 h. Purification by flash column chromatography (10% EtOAc/pentane) gave the title compound (92 mg, 0.24 mmol, 79%) as a colourless oil.

TLC: R_f = 0.43 (10% EtOAc/pentane, KMnO₄ stain).

¹H NMR (400 MHz, CDCl₃): δ_H 5.19 (d, *J* = 8.1 Hz, 1H, H⁴), 3.66 – 3.54 (m, 1H, H⁵), 2.47 (t, *J* = 8.0 Hz, 2H, H¹³), 2.07 (s, 3H, H¹⁴), 1.77 – 1.64 (m, 3H, H⁶ + H¹²), 1.41 (s, 9H, H¹), 1.22 (s, 6H, H¹¹), 1.20 (s, 6H, H¹¹), 1.01 (dd, *J* = 14.5, 4.2 Hz, 1H, H⁶), 0.75 – 0.66 (m, 2H, H⁸ + H⁹), 0.40 – 0.30 (m, 2H, H⁸ + H⁹) ppm.

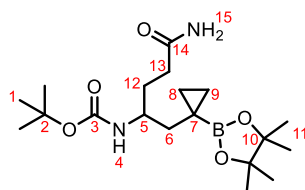
¹³C NMR (101 MHz, CDCl₃): δ_C 155.8 (C³), 83.5 (2 × C¹⁰), 78.8 (C²), 51.0 (C⁵), 40.7 (C⁶), 36.0 (C¹²), 30.8 (C¹³), 28.6 (3 × C¹), 25.0 (2 × C¹¹), 24.6 (2 × C¹¹), 15.7 (C¹⁴), 13.9 (C⁸), 10.3 (C⁹) ppm. The carbon directly attached to boron was not detected due to the boron quadrupole.

¹¹B NMR (128 MHz, CDCl₃): δ_B 34.5 (br. s, 1B) ppm.

IR (film) ν_{max}: 3405, 2977, 2918, 1713, 1417, 1365, 1167, 1139 cm⁻¹.

HRMS (ESI⁺) calcd. for C₁₉H₃₇BNO₄S [M+H]⁺ 386.2534, found 386.2536.

tert-Butyl (5-amino-5-oxo-1-(1-(4,4,5,5-tetramethyl-1,3,2-dioxaborolan-2-yl)cyclopropyl)pentan-2-yl)carbamate (216)



Prepared following General Procedure 3C with Boc-Gln-OH (74 mg, 0.30 mmol, 1.0 equiv.), 4CzIPN (4.7 mg, 0.0060 mmol, 2.0 mol%), Cs₂CO₃ (195 mg, 0.600 mmol, 2.00 equiv.), homoallylic chloride

vinyl boronic ester **202** (96 μ L, 0.45 mmol, 1.5 equiv.) and DMF (6.0 mL), which was irradiated with 1 \times Kessil lamp for 24 h. Purification by flash column chromatography (100% EtOAc) gave the title compound (94 mg, 0.25 mmol, 82%) as a white solid.

TLC: R_f = 0.20 (100% EtOAc, KMnO₄ stain).

Mpt: 165 – 166 °C (EtOAc).

¹H NMR (400 MHz, CDCl₃): δ_H 7.09 (br. s, 1H, H¹⁵), 5.45 (br. d, J = 8.2 Hz, 1H, H⁴), 5.30 (br. s, 1H, H¹⁵), 3.66 – 3.51 (m, 1H, H⁵), 2.30 (ddd, J = 14.4, 8.9, 5.5 Hz, 1H, H¹³), 2.19 (ddd, J = 14.5, 7.1, 5.3 Hz, 1H, H¹³), 1.78 – 1.62 (m, 3H, H⁶ + H¹²), 1.44 (s, 9H, H¹), 1.23 (s, 6H, H¹¹), 1.21 (s, 6H, H¹¹), 1.00 (dd, J = 14.4, 3.9 Hz, 1H, H⁶), 0.78 – 0.67 (m, 2H, H⁸ + H⁹), 0.42 – 0.29 (m, 2H, H⁸ + H⁹) ppm.

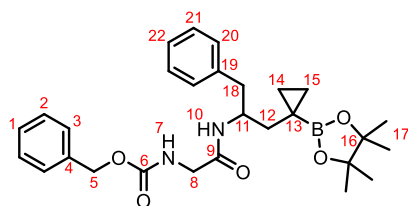
¹³C NMR (101 MHz, CDCl₃): δ_C 176.0 (C¹⁴), 157.0 (C³), 83.6 (2 \times C¹⁰), 79.3 (C²), 50.7 (C⁵), 41.0 (C⁶), 33.0 (C¹²), 32.8 (C¹³), 28.6 (3 \times C¹), 25.1 (2 \times C¹¹), 24.5 (2 \times C¹¹), 14.3 (C⁸), 10.1 (C⁹) ppm. The carbon directly attached to boron was not detected due to the boron quadrupole.

¹¹B NMR (128 MHz, CDCl₃): δ_B 33.5 (br. s, 1B) ppm.

IR (film) ν_{max} : 3345, 3174, 2977, 2922, 1681, 1417, 1168, 1141 cm⁻¹.

HRMS (ESI⁺) calcd. for C₁₉H₃₆BN₂O₅ [M+H]⁺ 383.2715, found 383.2734.

Benzyl (2-oxo-2-((1-phenyl-3-(1-(4,4,5,5-tetramethyl-1,3,2-dioxaborolan-2-yl)cyclopropyl)propan-2-yl)amino)ethyl)carbamate (**217**)



Prepared following General Procedure 3C with Z-Gly-Phe-OH (107 mg, 0.300 mmol, 1.00 equiv.), 4CzIPN (4.7 mg, 0.0060 mmol, 2.0 mol%), Cs₂CO₃ (195 mg, 0.600 mmol, 2.00 equiv.), homoallylic chloride vinyl boronic ester **202** (96 μ L, 0.45 mmol, 1.5 equiv.) and DMF (6.0 mL), which was irradiated with 1 \times Kessil lamp for 24 h. Purification by flash column chromatography (40% EtOAc/pentane) gave the title compound (56 mg, 0.11 mmol, 38%) as a colourless oil.

TLC: R_f = 0.31 (40% EtOAc/pentane, PMA stain).

¹H NMR (400 MHz, CDCl₃): δ_H 7.43 – 7.29 (m, 5H, H¹ + H² + H³), 7.27 – 7.22 (m, 2H, H²¹), 7.21 – 7.11 (m, 3H, H²⁰ + H²²), 6.39 (br. d, J = 7.7 Hz, 1H, H¹⁰), 5.45 (br. s, 1H, H⁷), 5.12 (s, 2H, H⁵),

4.26 – 4.11 (m, 1H, H¹¹), 3.80 (d, *J* = 5.1 Hz, 2H, H⁸), 2.87 (dd, *J* = 13.5, 5.7 Hz, 1H, H¹⁸), 2.71 (dd, *J* = 13.5, 7.3 Hz, 1H, H¹⁸), 1.48 (dd, *J* = 14.5, 10.0 Hz, 1H, H¹²), 1.28 – 1.25 (m, 1H, H¹²), 1.23 (s, 6H, H¹⁷), 1.19 (s, 6H, H¹⁷), 0.80 – 0.59 (m, 2H, H¹⁴), 0.34 – 0.17 (m, 2H, H¹⁵) ppm.

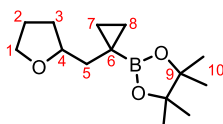
¹³C NMR (101 MHz, CDCl₃): δ_C 167.9 (C⁹), 156.4 (C⁶), 138.5 (C¹⁹), 136.5 (C⁴), 129.5 (2 × C²⁰), 128.7 (C¹), 128.4 (2 × C²), 128.3 (2 × C³), 128.2 (2 × C²¹), 126.4 (C²²), 83.6 (2 × C¹⁶), 67.1 (C⁵), 51.7 (C¹¹), 44.6 (C⁸), 41.3 (C¹⁸), 39.9 (C¹²), 25.3 (2 × C¹⁷), 24.4 (2 × C¹⁷), 14.1 (C¹⁴), 10.8 (C¹⁵) ppm. The carbon directly attached to boron was not detected due to the boron quadrupole.

¹¹B NMR (128 MHz, CDCl₃): δ_B 33.7 (br. s, 1B) ppm.

IR (film) ν_{max}: 3318, 2977, 2929, 1715, 1662, 1416, 1137 cm⁻¹.

HRMS (ESI⁺) calcd. for C₂₃H₃₇BNO₄ [M+H]⁺ 402.2814, found 402.2815.

4,4,5,5-Tetramethyl-2-(1-((tetrahydrofuran-2-yl)methyl)cyclopropyl)-1,3,2-dioxaborolane (219)



Prepared following General Procedure 3C with tetrahydro-2-furoic acid (29 μL, 0.30 mmol, 1.0 equiv.), 4CzIPN (4.7 mg, 0.0060 mmol, 2.0 mol%), Cs₂CO₃ (195 mg, 0.600 mmol, 2.00 equiv.), homoallylic chloride vinyl boronic ester **202** (96 μL, 0.45 mmol, 1.5 equiv.) and DMF (6.0 mL), which was irradiated with 1 × Kessil lamp for 24 h. Purification by flash column chromatography (7% EtOAc/pentane) gave the title compound (58 mg, 0.23 mmol, 76%) as a colourless oil.

TLC: R_f = 0.31 (7% EtOAc/pentane, KMnO₄ stain).

¹H NMR (400 MHz, CDCl₃): δ_H 3.94 (dddd, *J* = 6.3, 6.3, 6.3, 7.3 Hz, 1H, H⁴), 3.82 (ddd, *J* = 8.1, 7.2, 6.6 Hz, 1H, H¹), 3.70 (ddd, *J* = 8.0, 8.0, 5.8 Hz, 1H, H¹), 2.02 – 1.74 (m, 3H, H² + H³), 1.63 (dd, *J* = 13.6, 7.0 Hz, 1H, H⁵), 1.50 (dddd, *J* = 11.6, 8.5, 7.6, 7.6 Hz, 1H, H³), 1.29 (dd, *J* = 13.6, 7.3 Hz, 1H, H⁵), 1.20 (s, 6H, H¹⁰), 1.20 (s, 6H, H¹⁰), 0.72 – 0.61 (m, 2H, H⁷), 0.46 – 0.28 (m, 2H, H⁸) ppm.

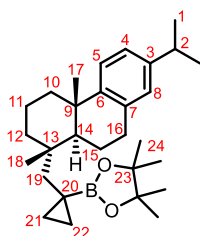
¹³C NMR (101 MHz, CDCl₃): δ_C 83.0 (2 × C⁹), 79.7 (C⁴), 67.4 (C¹), 41.9 (C⁵), 31.6 (C³), 25.9 (C²), 24.8 (C¹⁰), 24.7 (C¹⁰), 11.12 (C⁷), 11.07 (C⁸) ppm. The carbon directly attached to boron was not detected due to the boron quadrupole.

¹¹B NMR (128 MHz, CDCl₃): δ_B 33.3 (br. s, 1B) ppm.

IR (film) ν_{max}: 2976 – 2868, 1416, 1315, 1143, 1066 cm⁻¹.

HRMS (ESI⁺) calcd. for C₁₄H₂₆BO₃ [M+H]⁺ 253.1972, found 253.1978.

2-(1-(((1*S*,4*aS*,10*aS*)-7-Isopropyl-1,4*a*-dimethyl-1,2,3,4,4*a*,9,10,10*a*-octahydrophenanthren-1-yl)methyl)cyclopropyl)-4,4,5,5-tetramethyl-1,3,2-dioxaborolane (221)



Prepared following General Procedure 3C with dehydroabietic acid (94 mg, 0.30 mmol, 1.0 equiv.), 4CzIPN (4.7 mg, 0.0060 mmol, 2.0 mol%), Cs₂CO₃ (195 mg, 0.600 mmol, 2.00 equiv.), homoallylic chloride vinyl boronic ester **202** (96 μL, 0.45 mmol, 1.5 equiv.) and DMF (6.0 mL), which was irradiated with 1 × Kessil lamp for 24 h. Purification by preparative TLC (2% EtOAc/pentane) gave the title compound (95 mg, 0.22 mmol, 73%) as a colourless oil. The d.r. was determined to be >95:5 by ¹H and ¹³C NMR.

TLC: R_f = 0.46 (2% EtOAc/pentane, KMnO₄ stain).

Optical rotation: [α]_D²³ +10 (*c* 1.0, CHCl₃).

¹H NMR (400 MHz, CDCl₃): δ_H 7.16 (d, *J* = 8.2 Hz, 1H, H⁵), 6.98 (dd, *J* = 8.1, 2.0 Hz, 1H, H⁴), 6.88 (d, *J* = 2.0 Hz, 1H, H⁸), 2.96 – 2.84 (m, 1H, H¹⁶), 2.84 (h, *J* = 7.0 Hz, 1H, H²), 2.32 – 2.22 (m, 1H, H¹⁰), 1.86 (ddt, *J* = 13.1, 6.8, 2.4 Hz, 1H, H¹⁵), 1.78 – 1.56 (m, 6H, H¹¹ + H¹² + H¹⁵ + H¹⁹), 1.46 (dd, *J* = 12.4, 2.3 Hz, 1H, H⁴), 1.44 – 1.34 (m, 1H, H¹⁰), 1.23 (d, *J* = 6.9 Hz, 6H, H¹), 1.21 (s, 3H, H¹⁷), 1.22 – 1.19 (m, 1H, H¹⁹), 1.17 (s, 6H, H²⁴), 1.16 (s, 6H, H²⁴), 0.97 (s, 3H, H¹⁸), 0.69 – 0.57 (m, 2H, H²¹ + H²²), 0.39 – 0.28 (m, 2H, H²¹ + H²²) ppm.

¹³C NMR (101 MHz, CDCl₃): δ_C 148.2 (C³), 145.5 (C⁷), 135.1 (C⁶), 126.9 (C⁸), 124.1 (C⁵), 123.8 (C⁴), 82.9 (C²³), 50.8 (C¹⁹), 48.8 (C¹⁴), 39.4 (C¹²), 38.8 (C¹⁰), 38.3 (C⁹), 37.8 (C¹³), 33.6 (C²), 30.3 (C¹⁶), 25.7 (C¹⁷), 24.7 (2 × C²⁴), 24.5 (2 × C²⁴), 24.2 (C¹), 24.1 (C¹), 20.9 (C¹⁸), 19.2 (C¹⁵), 19.1 (C¹¹), 11.4 (C²¹), 11.2 (C²²) ppm. The carbon directly attached to boron was not detected due to the boron quadrupole.

¹¹B NMR (128 MHz, CDCl₃): δ_B 35.1 (br. s, 1B) ppm.

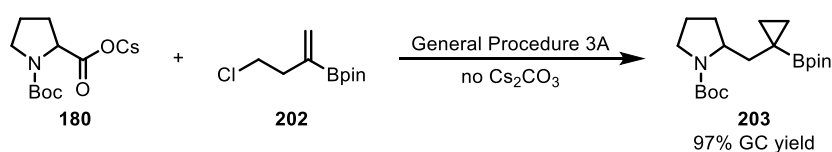
IR (film) ν_{max}: 2958 – 2866, 1413, 1302, 1142 cm⁻¹.

HRMS (ESI⁺) calcd. for C₂₉H₄₅BNaO₂ [M+Na]⁺ 459.3410, found 459.3403.

6.3.4 Quantum Yield Measurement

The quantum yield was measured for the reaction of Boc-Pro-OH **87** with homoallylic chloride vinyl boronic ester **202**. The reaction was performed in a quartz cuvette (path length (l) = 1.0 cm) positioned 5 cm away from a single 0.1 W blue LED ($\lambda_{\text{max}} = 450$ nm).

Note: under the standard reaction conditions, the reaction mixture is heterogeneous. This will have an impact on light penetration and potentially affect the accuracy of the quantum yield measurements. Therefore, to obtain a more accurate measurement, the reaction was performed using the preformed cesium carboxylate Boc-Pro-OCs **180**, which gave a homogeneous reaction mixture. The use of the preformed cesium carboxylate did not affect the efficiency of the reaction, as submitting Boc-Pro-OCs **180** (0.10 mmol) to the standard reaction conditions (General Procedure 3A, omitting Cs_2CO_3) led to the formation of geminally-substituted cyclopropyl boronic ester **203** in 97% GC yield after irradiation with a 40 W Kessil LED lamp for 12 h (Scheme S 2).



Scheme S 2. Synthesis of cyclopropyl boronic ester **203** using the preformed Boc-Pro-OCs **180**.

Determination of the Photon Flux:

The photon flux of the 0.1 W blue LED set-up was determined using standard ferrioxalate actinometry.^[190–193]

A 0.15 M ferrioxalate solution was prepared by dissolving 2.21 g of potassium ferrioxalate trihydrate in 30 mL of 0.05 M aq. H_2SO_4 . A buffered 5.5 mM phenanthroline solution was prepared by dissolving 50 mg of 1,10-phenanthroline and 11.25 g of $\text{NaOAc} \cdot 3\text{H}_2\text{O}$ in 50 mL of 0.5 M aq. H_2SO_4 . Both solutions were stored in amber bottles in the dark.

Whilst working under red light, 2.0 mL of the 0.15 M ferrioxalate solution was added to a quartz cuvette ($l = 1.0$ cm). The cuvette was placed 5 cm from a single 0.1 W blue LED and irradiated for specific time intervals of between 15 and 60 s. After irradiation, 1.0 mL of the phenanthroline solution was added to the cuvette (to give $\text{Fe}(\text{phen})_3^{2+}$). The mixture was left to stand for approximately 30 min before the absorbance at $\lambda = 510$ nm was measured by UV/Vis spectroscopy. The absorbance of a non-irradiated sample was also measured.

The number of moles of Fe²⁺ formed was calculated using the Beer-Lambert law (Table S 5), where ΔA is the difference in absorbance between the irradiated and non-irradiated ferrioxalate solutions at $\lambda = 510$ nm, ε is the molar absorptivity of the Fe(phen)₃²⁺ complex at $\lambda = 510$ nm (11100 L mol⁻¹ cm⁻¹),^[194] c is the concentration (mol L⁻¹) and l is the optical path length (1.0 cm):

$$\Delta A = \varepsilon \cdot c \cdot l$$

This can be re-written to include the number of moles of Fe²⁺ (n) and the total volume of the solution after the addition of 1,10-phenanthroline (0.0030 L) (V):

$$\Delta A = \frac{\varepsilon \cdot n \cdot l}{V}$$

Rearranging the equation gives:

$$\text{mol Fe}^{2+} = \frac{\Delta A \cdot V}{\varepsilon \cdot l}$$

Difference in Absorbance (ΔA)	Time / s	mol Fe ²⁺
0.0701	15	1.895×10 ⁻⁸
0.1217	30	3.289×10 ⁻⁸
0.1677	45	4.532×10 ⁻⁸
0.2361	60	6.381×10 ⁻⁸

Table S 5. Difference in absorbance measured at different time intervals. Moles of Fe²⁺ at different time intervals.

The moles of Fe²⁺ were plotted as a function of time (Figure S 4):

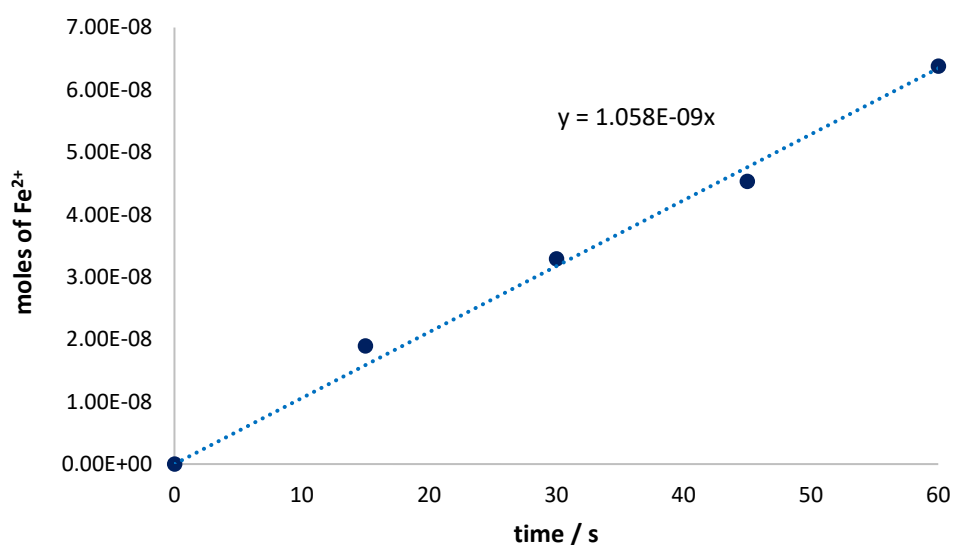


Figure S 4. Moles of Fe²⁺ vs time of irradiation for the determination of the photon flux.

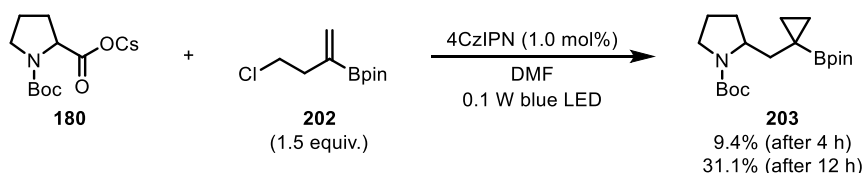
The photon flux was then calculated using:

$$\text{photon flux} = \frac{\text{mol Fe}^{2+}}{\Phi \cdot t \cdot f}$$

Where Φ is the quantum yield of the ferrioxalate actinometer (1.0 at $\lambda = 450$ nm),^[193] t is the time, and f is the fraction of absorbed light at $\lambda = 450$ nm, where $f = 1 - 10^{-A}$. The absorbance (A) of the ferrioxalate solution at $\lambda = 450$ nm was measured by UV/Vis spectroscopy to be 1.708, therefore $f = 0.9804$. Using the equation of the line at $t = 1$ s, $\text{mol Fe}^{2+} = 1.058 \times 10^{-9}$ mol.

$$\text{photon flux} = \frac{1.058 \times 10^{-9} \text{ mol}}{1.0 \cdot 1.0 \text{ s} \cdot 0.9804} = 1.08 \times 10^{-9} \text{ einstein s}^{-1}$$

Determination of the Quantum yield:



In a nitrogen-filled glovebox, a 4.5 mL quartz cuvette (path length: $l = 1.0$ cm) was charged with 4CzIPN (0.8 mg, 0.001 mmol) and Boc-Pro-OCs **180** (35 mg, 0.10 mmol, 1.0 equiv.). The cuvette was sealed with a septum, and removed from the glovebox before the addition of anhydrous DMF (2.0 mL) and homoallylic chloride vinyl boronic ester **202** (32 mg, 0.15 mmol, 1.5 equiv.). The reaction mixture was degassed by sparging with nitrogen for 10 min. The nitrogen inlet was removed, and the vial was further sealed with parafilm. The reaction was positioned 5 cm away from a single 0.1 W blue LED, stirred and irradiated for 4 h and 12 h, independently. The yield was determined by GC analysis using 1,2,4-trimethoxybenzene as an internal standard.

The quantum yield (Φ) was calculated using:

$$\Phi = \frac{\text{mol product}}{\text{photon flux} \cdot t \cdot f}$$

Where t is the time and f is the fraction of light absorbed by 4CzIPN at $\lambda = 450$ nm (for 5.0×10^{-4} M solution in DMF, this was determined by UV/Vis spectroscopy to be 0.969).

At $t = 4$ h (14400 s), the yield was 9.4% (9.40×10^{-6} mol).

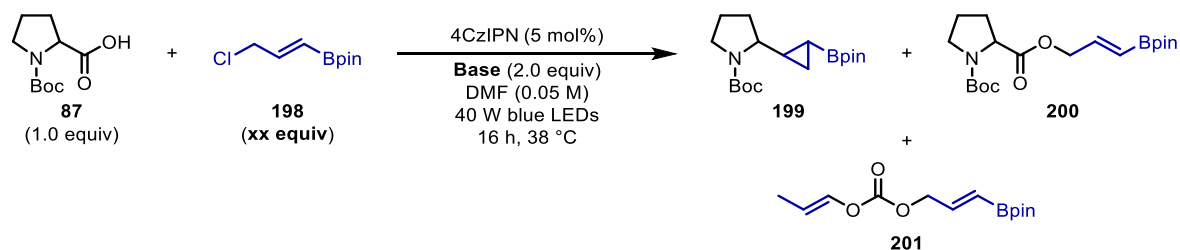
$$\Phi = \frac{9.40 \times 10^{-6} \text{ mol}}{1.08 \times 10^{-9} \text{ einstein s}^{-1} \cdot 14400 \text{ s} \cdot 0.969} = 0.624$$

At $t = 12 \text{ h}$ (43200 s), the yield was 31.1% ($3.11 \times 10^{-5} \text{ mol}$).

$$\Phi = \frac{3.11 \times 10^{-5} \text{ mol}}{1.08 \times 10^{-9} \text{ einstein s}^{-1} \cdot 43200 \text{ s} \cdot 0.969} = 0.688$$

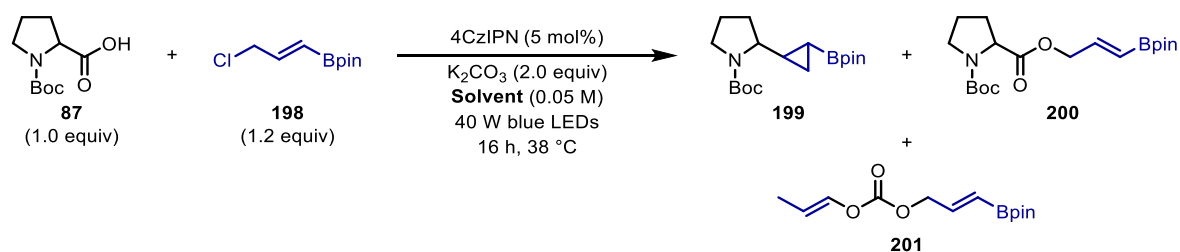
Average quantum yield (Φ) of the two experiments = 0.656

6.3.5 Additional Optimisation Tables



Entry	Base	Equivalents of 198	GC Yield (%)			
			199	200	201	198
1	Cs ₂ CO ₃	1.2	9	0	0	0
2	Cs ₂ CO ₃	1.5	34	7	2	4
3	Cs ₂ CO ₃	2.0	33	15	6	14
4	K ₂ CO ₃	1.2	36	4	2	1
5	K ₂ CO ₃	1.5	35	7	4	1
6	K ₂ CO ₃	2.0	38	10	6	2

Table S 6. Varying equivalents of 2-chloromethyl vinyl boronic ester **198** with Cs₂CO₃ and K₂CO₃. Yields were determined by GC with 1,2,4-trimethoxybenzene as the internal standard.



Entry	Solvent	GC Yield (%)			
		199	200	201	198
1	DMF (anhydrous)	32	5	1	0
2	DMA (anhydrous)	33	2	1	2
3	DCM (anhydrous)	10	0	0	22
4	DMI (anhydrous)	24	0	0	0
5	DMPU (anhydrous)	12	0	0	0
6	DMSO (anhydrous)	36	10	0	0
7	MeCN (anhydrous)	22	0	1	13

Table S 7. Solvent screen with 4CzIPN. Yields were determined by GC with 1,2,4-trimethoxybenzene as the internal standard.

6.4 Conjunctive Cross-coupling of Vinyl Boronic Esters

The data presented in this section has been partially published in:

R. S. Mega, V. K. Duong, A. Noble, V. K. Aggarwal, *Angew. Chem. Int. Ed.* **2020**, *59*, 4375–4379.^[168]

6.4.1 General Procedures and Reaction Set-up

General Procedure 4A [for the synthesis of boronic esters (Scheme 75)]:

To a 28 mL vial equipped with a magnetic stir bar was added the carboxylic acid (1.20 equiv.), 4CzIPN (2.00 mol%), dtbbpy (6.25 mol%) and, if solid, aryl iodide (1.00 equiv.). The vial was introduced into a nitrogen-filled glove box, and NiCl₂·glyme (5.00 mol%) and Cs₂CO₃ (1.30 equiv.) were added before sealing with a septum. The vial was removed from the glovebox, connected to a nitrogen inlet, and vinyl boronic ester **238** (3.00 equiv.) and, if liquid, aryl iodide (1.00 equiv.) were added via syringe. Anhydrous DMA (0.025 M) was then added and the reaction mixture was degassed by sparging with nitrogen for 10 minutes. The nitrogen inlet was removed, and the vial was further sealed with parafilm. The reaction mixture was stirred at 800 rpm and irradiated with a 40 W blue Kessil LED lamp for 16 h with fan cooling. The reaction mixture was diluted with water (20 mL) and extracted into ethyl acetate (3 × 20 mL). The organics were combined and washed with water (3 × 60 mL) and brine (60 mL), dried (Na₂SO₄), filtered, and concentrated *in vacuo*. The crude product was then purified by normal-phase flash column chromatography.

General Procedure 4B [for the one-pot synthesis of boronic esters and oxidation to the corresponding alcohol (Scheme 75, Scheme 76 and Scheme 77)]:

To a 28 mL vial equipped with a magnetic stir bar was added the carboxylic acid (1.20 equiv.), 4CzIPN (2.00 mol%), dtbbpy (6.25 mol%) and, if solid, aryl iodide (1.00 equiv.). The vial was introduced into a nitrogen-filled glove box, and NiCl₂·glyme (5.00 mol%) and Cs₂CO₃ (1.30 equiv.) were added before sealing with a septum. The vial was removed from the glovebox, connected to a nitrogen inlet, and vinyl boronic ester **238** (3.00 equiv.) and, if liquid, aryl iodide (1.00 equiv.) were added via syringe. Anhydrous DMA (0.025 M) was then added and the reaction mixture was degassed by sparging with nitrogen for 10 minutes. The nitrogen inlet was removed, and the vial was further sealed with parafilm. The reaction mixture was stirred at 800 rpm and irradiated with a 40 W blue Kessil LED lamp for 16-48 h with fan cooling. The reaction mixture was opened to air, cooled to 0 °C using an ice bath and

urea·H₂O₂ (UHP, 3.00 equiv.) was added. The reaction mixture was removed from the ice bath and stirred for 1 h. The reaction mixture was diluted with water (20 mL) and extracted into ethyl acetate (3 × 20 mL). The organics were combined and washed with water (3 × 60 mL) and brine (60 mL), dried (Na₂SO₄), filtered, and concentrated *in vacuo*. The crude product was then purified by normal-phase flash column chromatography.

Reaction Set-up:

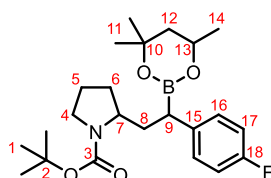
The 40 W Kessil LED lamp was positioned 7 cm from the reaction vial. Fans were positioned 15 cm from the reaction vial (Figure S 5).



Figure S 5. Photoredox reaction set-up for the conjunctive cross-coupling of vinyl boronic esters.

6.4.2 Product Characterisation

tert-Butyl 2-(2-(4-fluorophenyl)-2-(4,4,6-trimethyl-1,3,2-dioxaborinan-2-yl)ethyl)pyrrolidine-1-carboxylate (**239**-[B])



Prepared following General Procedure 4A using Boc-Pro-OH (26 mg, 0.12 mmol, 1.2 equiv.), vinyl boronic ester **238** (52 μ L, 0.30 mmol, 3.0 equiv.), 4-fluoriodobenzene (12 μ L, 0.10 mmol, 1.0 equiv.), 4CzIPN (1.6 mg, 0.0020 mmol, 2.0 mol%), NiCl₂·glyme (1.1 mg, 0.0050 mmol, 5.0 mol%), dtbbpy (1.7 mg, 0.0063 mmol, 6.3 mol%), Cs₂CO₃ (42 mg, 0.13 mmol, 1.3 equiv.) and DMA (12 mL), which was irradiated with 1 \times Kessil lamp for 16 h. Purification by flash column chromatography (15% EtOAc/hexane) gave the title compound as a mixture of diastereomers (27 mg, 0.064 mmol, 64%). The d.r. and the relative stereochemistry of the diastereomers could not be assigned.

TLC: R_f = 0.25 (15% EtOAc/hexane, KMnO₄ stain).

¹H NMR (400 MHz, CDCl₃): δ_{H} 7.21 – 7.09 (m, 2H, H¹⁶), 6.95 – 6.84 (m, 2H, H¹⁷), 4.12 (dq, $J = 12.3, 6.2, 3.0$ Hz, 1H, H¹³), 3.90 – 3.66 (m, 1H, H⁷), 3.47 – 3.12 (m, 2H, H⁴), 2.36 – 2.23 (m, 1H, H⁸), 2.21 – 2.07 (m, 1H, H⁹), 1.90 – 1.61 (m, 4H, H⁵ + H⁶), 1.53 – 1.38 (m, 12H, H¹ + H⁸ + H¹²), 1.25 – 1.15 (m, 9H, H¹¹ + H¹⁴) ppm.

¹³C NMR (126 MHz, CDCl₃): δ_{C} 160.9 (d, $J = 241.8$ Hz, C¹⁸), 154.8 (C³), 140.9 (C¹⁵), 129.6 (d, $J = 7.5$ Hz, 2 \times C¹⁶), 114.8 (d, $J = 20.8$ Hz, 2 \times C¹⁷), 79.1 (C²), 70.9 (C¹⁰), 65.0 + 64.9 (diastereotopic peaks, C¹³), 58.1 (C⁷), 46.0 (C⁴), 46.0 (C¹²), 38.0 (C⁸), 32.8 (C⁹), 31.3 (1 \times C¹¹), 31.2 (C⁶), 28.8 (3 \times C¹), 28.1 (1 \times C¹¹), 23.23 (C¹⁴), 23.19 (C⁵) ppm.

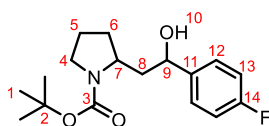
¹¹B NMR (128 MHz, CDCl₃): δ_{B} 30.0 (br. s, 1B) ppm.

¹⁹F NMR (377 MHz, CDCl₃): δ_{F} -119.5 (br. m), -119.7 (br. m) ppm.

IR (film) ν_{max} : 2972, 2930, 1691, 1506, 1392, 1157, 835, 770 cm⁻¹.

HRMS (ESI⁺): calcd. for C₂₃H₃₆BFNO₄ [M+Na]⁺ 420.2720, found 420.2708.

***tert*-Butyl 2-(2-(4-fluorophenyl)-2-hydroxyethyl)pyrrolidine-1-carboxylate (239-[OH])**



Prepared following General Procedure 4B using Boc-Pro-OH (77 mg, 0.36 mmol, 1.2 equiv.), vinyl boronic ester **238** (155 μ L, 0.90 mmol, 3.0 equiv.), 4-fluoroiodobenzene (35 μ L, 0.30 mmol, 1.0 equiv.), 4CzIPN (4.7 mg, 0.0060 mmol, 2.0 mol%), NiCl₂·glyme (3.3 mg, 0.015 mmol, 5.0 mol%), dtbbpy (5.0 mg, 0.019 mmol, 6.3 mol%), Cs₂CO₃ (127 mg, 0.39 mmol, 1.3 equiv.) and DMA (12 mL), which was irradiated with 1 \times Kessil lamp for 16 h. After oxidative work-up with UHP (84 mg, 0.90 mmol, 3.0 equiv.), purification by flash column chromatography (35% Et₂O/pentane) gave the title compound as two separable diastereomers (total yield: 71 mg, 0.23 mmol, 76%). The d.r. was determined after purification to be 48:52 (The relative stereochemistry of the two diastereomers could not be assigned).

Diastereomer A (34 mg, colourless oil):

TLC: R_f = 0.37 (35% Et₂O/pentane, KMnO₄ stain).

¹H NMR (400 MHz, CDCl₃): δ_{H} 7.39 – 7.30 (m, 2H, H¹²), 7.03 – 6.95 (m, 2H, H¹³), 5.49 (br. s, 1H, H¹⁰), 4.60 (br. d, J = 9.5 Hz, 1H, H⁹), 4.32 – 4.23 (m, 1H, H⁷), 3.37 (t, J = 6.9 Hz, 2H, H⁴), 2.05 – 1.83 (m, 3H, H⁵ + H⁸), 1.82 – 1.54 (m, 3H, H⁶ + H⁸), 1.48 (s, 9H, H¹) ppm.

¹³C NMR (101 MHz, CDCl₃): δ_{C} 161.9 (d, J = 243.9 Hz, C¹⁴), 157.0 (C³), 140.3 (C¹¹), 127.4 (d, J = 7.9 Hz, 2 \times C¹²), 115.0 (d, J = 21.3 Hz, 2 \times C¹³), 80.3 (C²), 69.5 (C⁹), 54.0 (C⁷), 46.9 (C⁴), 46.5 (C⁸), 31.3 (C⁶), 28.6 (3 \times C¹), 23.8 (C⁵) ppm.

¹⁹F NMR (377 MHz, CDCl₃): δ_{F} -115.2 (s, 1F, minor rotamer), -116.5 (tt, J = 9.3, 5.5 Hz, 1F, major rotamer) ppm.

IR (film) ν_{max} : 3398, 2974 – 2885, 1690, 1667, 1509, 1397, 1366, 1220, 1168, 1158, 1107 cm⁻¹.

HRMS (ESI⁺): calcd. for C₁₇H₂₄FNNaO₃ [M+Na]⁺ 332.1632, found 332.1643.

Diastereomer B (37 mg, colourless oil):

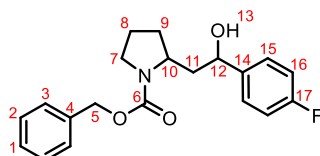
TLC: R_f = 0.19 (35% Et₂O/pentane, KMnO₄ stain).

¹H NMR (400 MHz, CDCl₃): δ_{H} 7.32 (dd, J = 8.4, 5.4 Hz, 2H, H¹²), 6.98 (t, J = 8.5 Hz, 2H, H¹³), 4.73 (br. d, J = 8.8 Hz, 1H, H⁹), 4.16 – 3.96 (br. m, 1H, H⁷), 3.44 – 3.23 (br. m, 2H, H⁴), 2.15 – 1.93 (m, 2H, H⁶ + H⁸), 1.84 (m, 2H, H⁵), 1.75 – 1.57 (m, 2H, H⁶ + H⁸), 1.44 (s, 9H, H¹) ppm.

^{13}C NMR (101 MHz, CDCl_3): 162.0 (d, $J = 245.3$ Hz, C^{14}), 155.7 (C^3), 141.1 (C^{11}), 127.3 (d, $J = 8.0$ Hz, $2 \times \text{C}^{12}$), 115.1 (d, $J = 21.1$ Hz, $2 \times \text{C}^{13}$), 80.0 (C^2), 72.1 (C^9), 55.6 (C^7), 46.6 (C^4), 46.2 (C^8), 32.4 (C^6), 28.6 ($3 \times \text{C}^1$), 23.9 (C^5) ppm.

^{19}F NMR (377 MHz, CDCl_3): δ_{F} -115.2 (s, 1F, minor rotamer), -116.3 (s, 1F, major rotamer) ppm.

Benzyl 2-(2-(4-fluorophenyl)-2-hydroxyethyl)pyrrolidine-1-carboxylate (245)



Prepared following General Procedure 4B using Z-Pro-OH (90 mg, 0.36 mmol, 1.2 equiv.), vinyl boronic ester **238** (155 μL , 0.90 mmol, 3.0 equiv.), 4-fluoroiodobenzene (35 μL , 0.30 mmol, 1.0 equiv.), 4CzIPN (4.7 mg, 0.0060 mmol, 2.0 mol%), $\text{NiCl}_2 \cdot \text{glyme}$ (3.3 mg, 0.015 mmol, 5.0 mol%), dtbbpy (5.0 mg, 0.019 mmol, 6.3 mol%), Cs_2CO_3 (127 mg, 0.39 mmol, 1.3 equiv.) and DMA (12 mL), which was irradiated with $1 \times$ Kessil lamp for 24 h. After oxidative work-up with UHP (84 mg, 0.90 mmol, 3.0 equiv.), purification by flash column chromatography (45–50% Et_2O /pentane) gave the title compound as two separable diastereomers (total yield: 63 mg, 0.18 mmol, 61%). The d.r. was determined after purification to be 48:52 (The relative stereochemistry of the two diastereomers could not be assigned).

Diastereomer A (30 mg, colourless oil):

TLC: $R_f = 0.32$ (50% Et_2O /pentane, KMnO_4 stain).

^1H NMR (400 MHz, CDCl_3): δ_{H} 7.44 – 7.28 (m, 7H, $\text{H}^1 + \text{H}^2 + \text{H}^3 + \text{H}^{15}$), 7.04 – 6.97 (m, 2H, H^{16}), 5.23 – 5.12 (m, 3H, $\text{H}^5 + \text{H}^{13}$), 4.69 – 4.54 (m, 1H, H^{12}), 4.41 – 4.28 (m, 1H, H^{10}), 3.48 (t, $J = 7.0$ Hz, 2H, H^7), 2.09 – 1.84 (m, 3H, $\text{H}^8 + \text{H}^{11}$), 1.78 – 1.59 (m, 3H, $\text{H}^9 + \text{H}^{11}$) ppm.

^{13}C NMR (126 MHz, CDCl_3): δ_{C} 162.0 (d, $J = 244.3$ Hz, C^{17}), 157.3 (C^6), 140.1 (d, $J = 3.1$ Hz, C^{14}), 136.7 (C^4), 128.7 ($2 \times \text{C}^2$), 128.3 (C^1), 128.0 ($2 \times \text{C}^3$), 127.4 (d, $J = 7.9$ Hz, $2 \times \text{C}^{15}$), 115.1 (d, $J = 21.2$ Hz, $2 \times \text{C}^{16}$), 69.6 (C^{12}), 67.5 (C^5), 54.9 (C^{10}), 46.7 (C^7), 46.2 (C^9), 31.4 (C^{11}), 23.8 (C^8).

^{19}F NMR (377 MHz, CDCl_3): δ_{F} -115.1 (s, 1F, minor rotamer), -116.2 (s, 1F, major rotamer) ppm.

IR (film) ν_{max} : 3413, 2956, 2884, 1673, 1509, 1411, 1357, 1218, 1103, 835, 698 cm^{-1} .

HRMS (ESI⁺): calcd. for $\text{C}_{20}\text{H}_{22}\text{FNO}_3$ [$\text{M}+\text{H}$]⁺ 344.1656, found 344.1655.

Diastereomer B (33 mg, colourless oil):

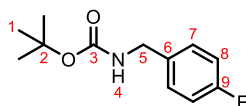
TLC: $R_f = 0.18$ (50% Et_2O /pentane, KMnO_4 stain).

¹H NMR (400 MHz, CDCl₃): δ_H 7.47 – 7.11 (m, 7H, H¹ + H² + H³ + H¹⁵), 7.03 – 6.94 (m, 2H, H¹⁶), 5.27 – 5.04 (m, 2H, H⁵), 4.86 – 4.58 (m, 1H, H¹²), 4.19 – 4.07 (m, 2H, H¹⁰ + H¹³), 3.53 – 3.32 (br. m, 2H, H⁷), 2.16 (ddd, *J* = 14.4, 9.5, 5.0 Hz, 1H, H¹¹), 2.10 – 1.97 (m, 1H, H¹¹), 1.98 – 1.81 (m, 2H, H⁸), 1.81 – 1.64 (m, 2H, H⁹) ppm.

¹³C NMR (126 MHz, CDCl₃): δ_C 162.1 (d, *J* = 244.9 Hz, C¹⁷), 155.8 + 164.9 (rotameric peaks, C⁶), 140.8 + 140.5 (rotameric peaks, C¹⁴), 137.0 + 136.8 (rotameric peaks, C⁴), 128.6 (2 × C²), 128.2 (2 × C³), 128.0 (C¹), 127.4 (d, *J* = 8.1 Hz, 2 × C¹⁵), 115.4 (d, *J* = 21.7) + 115.1 (d, *J* = 21.2 Hz) (rotameric peaks, 2 × C¹⁶), 72.0 + 71.8 (rotameric peaks, C¹²), 67.1 + 67.0 (rotameric peaks, C⁵), 56.1 + 54.7 (rotameric peaks, C¹⁰), 46.7 + 46.4 (rotameric peaks, C⁷), 45.9 + 44.2 (rotameric peaks, C¹¹), 32.4 + 31.2 (rotameric peaks, C⁹), 24.0 + 23.2 (rotameric peaks, C⁸) ppm.

¹⁹F NMR (377 MHz, CDCl₃): δ_F -115.0 (s, 1F, minor rotamer), -116.0 (s, 1F, major rotamer) ppm.

***tert*-Butyl (4-fluorobenzyl)carbamate (250')**



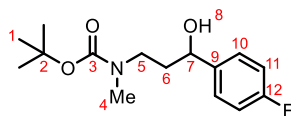
Prepared following General Procedure 4B using Boc-Gly-OH (63 mg, 0.36 mmol, 1.2 equiv.), vinyl boronic ester **238** (155 μL, 0.90 mmol, 3.0 equiv.), 4-fluoroiodobenzene (35 μL, 0.30 mmol, 1.0 equiv.), 4CzIPN (4.7 mg, 0.0060 mmol, 2.0 mol%), NiCl₂·glyme (3.3 mg, 0.015 mmol, 5.0 mol%), dtbbpy (5.0 mg, 0.019 mmol, 6.3 mol%), Cs₂CO₃ (127 mg, 0.39 mmol, 1.3 equiv.) and DMA (12 mL), which was irradiated with 1 × Kessil lamp for 24 h. After oxidative work-up with UHP (84 mg, 0.90 mmol, 3.0 equiv.), purification by flash column chromatography (40% Et₂O/pentane) gave the title compound (21 mg, 0.09 mmol, 31%) as a pale yellow oil.

¹H NMR (500 MHz, CDCl₃): δ_H 7.27 – 7.21 (m, 2H, H⁷), 7.04 – 6.96 (m, 2H, H⁸), 4.83 (br. s, 1H, H⁴), 4.28 (d, *J* = 6.0 Hz, 2H, H⁵), 1.46 (s, 9H, H¹) ppm.

¹³C NMR (126 MHz, CDCl₃): δ_C 162.3 (d, *J* = 245.3 Hz, C⁹), 156.0 (C³), 134.9 (C⁶), 129.3 (d, *J* = 8.1 Hz, 2 × C⁷), 115.6 (d, *J* = 21.4 Hz, 2 × C⁸), 79.8 (C²), 44.1 (C⁵), 28.5 (3 × C¹) ppm.

Spectroscopic data matches previously reported data.^[195]

***tert*-Butyl (3-(4-fluorophenyl)-3-hydroxypropyl)(methyl)carbamate (251)**



Prepared following General Procedure 4B using Boc-Sar-OH (68 mg, 0.36 mmol, 1.2 equiv.), vinyl boronic ester **238** (155 μ L, 0.90 mmol, 3.0 equiv.), 4-fluoroiodobenzene (35 μ L, 0.30 mmol, 1.0 equiv.), 4CzIPN (4.7 mg, 0.0060 mmol, 2.0 mol%), NiCl₂·glyme (3.3 mg, 0.015 mmol, 5.0 mol%), dtbbpy (5.0 mg, 0.019 mmol, 6.3 mol%), Cs₂CO₃ (127 mg, 0.39 mmol, 1.3 equiv.) and DMA (12 mL), which was irradiated with 1 \times Kessil lamp for 24 h. After oxidative work-up with UHP (84 mg, 0.90 mmol, 3.0 equiv.), purification by flash column chromatography (45–50% Et₂O/pentane) gave the title compound (9 mg, 0.03 mmol, 11%) as a colourless oil, and two-component coupling product **251'** (25 mg, 0.10 mmol, 35%) as a pale yellow oil.

TLC: R_f = 0.26 (50% Et₂O/pentane, KMnO₄ stain).

¹H NMR (400 MHz, CDCl₃): δ_{H} 7.37 – 7.31 (m, 2H, H¹⁰), 7.06 – 6.98 (m, 2H, H¹¹), 4.67 – 4.52 (m, 1H, H⁷), 4.36 – 3.41 (br. m, 2H, H⁵), 3.17 – 2.99 (br. m, 1H, H⁸), 2.87 (s, 3H, H⁴), 1.93 (dddd, $J = 13.7$, 9.8, 6.1, 3.6 Hz, 1H, H⁶), 1.88 – 1.68 (br. m, 1H, H⁶), 1.48 (s, 9H, H¹) ppm.

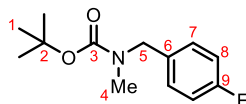
¹³C NMR (101 MHz, CDCl₃): δ_{C} 162.1 (d, $J = 243.1$ Hz, C¹²), 157.4 (C³), 140.1 (C⁹), 127.4 (d, $J = 8.0$ Hz, 2 \times C¹⁰), 115.2 (d, $J = 21.7$ Hz, 2 \times C¹¹), 80.4 (C²), 69.5 (C⁷), 45.2 (C⁵), 37.5 (C⁴), 34.5 (C⁶), 28.6 (3 \times C¹) ppm.

¹⁹F NMR (377 MHz, CDCl₃): δ_{F} -115.0 (s, 1F, minor rotamer), -116.1 (s, 1F, major rotamer) ppm.

IR (film) ν_{max} : 3418, 2974, 2929, 1669, 1509, 1222, 1169, 1056, 839 cm⁻¹.

HRMS (ESI⁺): calcd. for C₁₅H₂₃FNO₃ [M+H]⁺ 284.1656, found 284.1643.

***tert*-Butyl (4-fluorobenzyl)(methyl)carbamate (251')**

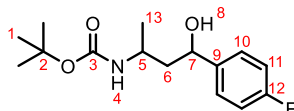


¹H NMR (500 MHz, CDCl₃): δ_{H} 7.23 – 7.13 (m, 2H, H⁷), 7.05 – 6.95 (m, 2H, H⁸), 4.38 (s, 2H, H⁵), 2.87 – 2.70 (br. m, 3H, H⁴), 1.47 (s, 9H, H¹) ppm.

¹³C NMR (126 MHz, CDCl₃): δ_{C} 162.2 (d, $J = 245.0$ Hz, C⁹), 156.2 + 155.8 (rotameric peaks, C³), 134.0 (d, $J = 3.1$ Hz, C⁶), 129.4 + 129.0 (rotameric peaks, 2 \times C⁷), 115.5 (d, $J = 21.4$ Hz, 2 \times C⁸), 79.9 (C²), 52.1 + 51.4 (rotameric peaks, C⁵), 34.0 (C⁴), 28.6 (3 \times C¹) ppm.

Spectroscopic data matches previously reported data.^[196]

***tert*-Butyl (4-(4-fluorophenyl)-4-hydroxybutan-2-yl)carbamate (252)**



Prepared following General Procedure 4B using Boc-Ala-OH (68 mg, 0.36 mmol, 1.2 equiv.), vinyl boronic ester **238** (155 μ L, 0.90 mmol, 3.0 equiv.), 4-fluoroiodobenzene (35 μ L, 0.30 mmol, 1.0 equiv.), 4CzIPN (4.7 mg, 0.0060 mmol, 2.0 mol%), NiCl₂·glyme (3.3 mg, 0.015 mmol, 5.0 mol%), dtbbpy (5.0 mg, 0.019 mmol, 6.3 mol%), Cs₂CO₃ (127 mg, 0.39 mmol, 1.3 equiv.) and DMA (12 mL), which was irradiated with 1 \times Kessil lamp for 24 h. After oxidative work-up with UHP (84 mg, 0.90 mmol, 3.0 equiv.), purification by flash column chromatography (40–50% Et₂O/pentane) gave the title compound as two separable diastereomers (total yield: 37 mg, 0.13 mmol, 44%), and the two-component coupling product **252'** (16 mg, 0.07 mmol, 22%) as a yellow oil. The d.r. of **252** was determined after purification to be 54:46 (The relative stereochemistry of the two diastereomers could not be assigned).

Diastereomer A (20 mg, pale yellow solid):

TLC: R_f = 0.48 (50% Et₂O/pentane, KMnO₄ stain).

Mpt: 100.3–101.0 °C (CHCl₃).

¹H NMR (400 MHz, CDCl₃): δ_{H} 7.38 – 7.29 (m, 2H, H¹⁰), 7.05 – 6.96 (m, 2H, H¹¹), 4.69 (br. d, J = 11.0 Hz, 1H, H⁷), 4.54 (br. d, J = 8.6 Hz, 1H, H⁴), 4.46 (s, 1H, H⁸), 4.10 – 3.95 (br. m, 1H, H⁵), 1.79 (ddd, J = 14.0, 11.0, 3.1 Hz, 1H, H⁶), 1.54 (ddd, J = 13.8, 10.9, 2.7 Hz, 1H, H⁶), 1.47 (s, 9H, H¹), 1.20 (d, J = 6.7 Hz, 3H, H¹³) ppm.

¹³C NMR (126 MHz, CDCl₃): δ_{C} 162.0 (d, J = 244.4 Hz, C¹²), 157.3 (C³), 140.1 (d, J = 3.1 Hz, C⁹), 127.3 (d, J = 7.9 Hz, 2 \times C¹⁰), 115.2 (d, J = 21.2 Hz, 2 \times C¹¹), 80.3 (C²), 69.6 (C⁷), 48.9 (C⁶), 43.7 (C⁵), 28.5 (1 \times C¹), 21.7 (C¹³) ppm.

¹⁹F NMR (377 MHz, CDCl₃): δ_{F} –116.1 (s, 1F) ppm.

IR (film) ν_{max} : 3342, 2976, 2936, 1681, 1509, 1222, 1158, 832 cm⁻¹.

HRMS (ESI⁺): calcd. for C₁₅H₂₂FNNaO₃ [M+Na]⁺ 306.1476, found 306.1477.

Diastereomer B (17 mg, colourless oil):

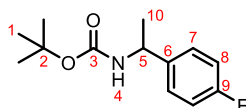
TLC: R_f = 0.23 (50% Et₂O/pentane, KMnO₄ stain).

¹H NMR (400 MHz, CDCl₃): δ_H 7.38 – 7.27 (m, 2H, H¹⁰), 7.05 – 6.94 (m, 2H, H¹¹), 4.81 – 4.71 (m, 1H, H⁷), 4.56 (br. s, 1H, H⁴), 3.76 (br. s, 1H, H⁵), 2.92 (br. s, 1H, H⁸), 1.91 (ddd, *J* = 14.2, 8.4, 7.7 Hz, 1H, H⁶), 1.79 – 1.71 (m, 1H, H⁶), 1.44 (s, 9H, H¹), 1.18 (d, *J* = 6.6 Hz, 3H, H¹³) ppm.

¹³C NMR (101 MHz, CDCl₃): δ_C 162.3 (d, *J* = 245.5 Hz, C¹²), 155.8 (C³), 140.6 (C⁹), 127.6 (d, *J* = 8.1 Hz, 2 × C¹⁰), 115.4 (d, *J* = 21.4 Hz, 2 × C¹¹), 79.7 (C²), 72.2 (C⁷), 47.2 (C⁶), 45.2 (C⁵), 28.6 (3 × C¹), 22.0 (C¹³) ppm.

¹⁹F NMR (377 MHz, CDCl₃): δ_F -115.3 (s, 1F) ppm.

***tert*-Butyl (1-(4-fluorophenyl)ethyl)carbamate (252')**



TLC: R_f = 0.51 (30% Et₂O/pentane, KMnO₄ stain).

¹H NMR (500 MHz, CDCl₃): δ_H 7.32 – 7.20 (m, 2H, H⁷), 7.04 – 6.95 (m, 2H, H⁸), 4.89 – 4.50 (br. m, 2H, H⁴ + H⁵), 1.42 (br. m, 12H, H¹ + H¹⁰) ppm.

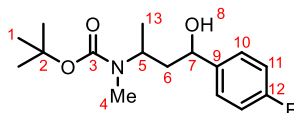
¹³C NMR (126 MHz, CDCl₃): δ_C 162.0 (d, *J* = 244.9 Hz, C⁹), 155.2 (C³), 140.0 (C⁶), 127.6 (d, *J* = 8.0 Hz, 2 × C⁷), 115.5 (d, *J* = 21.4 Hz, 2 × C⁸), 79.7 (C²), 49.7 (C⁵), 28.5 (3 × C¹), 22.8 (C¹⁰) ppm.

¹⁹F NMR (377 MHz, CDCl₃): δ_F -115.8 (s, 1F) ppm.

IR (film) ν_{max}: 3338, 2976, 2931, 1696, 1510, 1225, 1172, 1056, 835 cm⁻¹.

HRMS (ESI⁺): calcd. for C₁₃H₁₈FNNaO₂ [M+Na]⁺ 262.1214, found 262.1202.

***tert*-Butyl (4-(4-fluorophenyl)-4-hydroxybutan-2-yl)(methyl)carbamate (253)**



Prepared following General Procedure 4B using Boc-*N*-Me-Ala-OH (73 mg, 0.36 mmol, 1.2 equiv.), vinyl boronic ester **238** (155 μL, 0.90 mmol, 3.0 equiv.), 4-fluoriodobenzene (35 μL, 0.30 mmol, 1.0 equiv.), 4CzIPN (4.7 mg, 0.0060 mmol, 2.0 mol%), NiCl₂·glyme (3.3 mg, 0.015 mmol, 5.0 mol%), dtbbpy (5.0 mg, 0.019 mmol, 6.3 mol%), Cs₂CO₃ (127 mg, 0.39 mmol, 1.3 equiv.) and DMA (12 mL), which was irradiated with 1 × Kessil lamp for 24 h. After oxidative work-up with UHP (84 mg, 0.90 mmol, 3.0 equiv.), purification by flash column chromatography (40–50% Et₂O/petroleum ether) gave

the title compound as two separable diastereomers (total yield: 48 mg, 0.16 mmol, 54%). The d.r. was determined after purification to be 42:58 (The relative stereochemistry of the two diastereomers could not be assigned).

Diastereomer A (20 mg, colourless oil):

TLC: $R_f = 0.63$ (50% Et₂O/pentane, KMnO₄ stain).

¹H NMR (400 MHz, CDCl₃): δ_H 7.36 – 7.27 (m, 2H, H¹⁰), 7.04 – 6.97 (m, 2H, H¹¹), 4.72 – 4.28 (br. m, 3H, H⁵ + H⁷ + H⁸), 2.73 (s, 3H, H⁴), 1.77 – 1.57 (m, 2H, H⁶), 1.50 (s, 9H, H¹), 1.18 (d, $J = 6.9$ Hz, 3H, H¹³) ppm.

¹³C NMR (126 MHz, CDCl₃): δ_C 162.0 (d, $J = 244.5$ Hz, C¹²), 157.8 (C³), 139.8 (d, $J = 3.1$ Hz, C⁹), 127.3 (d, $J = 8.0$ Hz, 2 × C¹⁰), 115.1 (d, $J = 21.3$ Hz, 2 × C¹¹), 80.6 (C²), 69.6 (C⁷), 46.8 (C⁵), 44.4 (C⁶), 28.6 (3 × C¹), 27.5 (C⁴), 18.9 (C¹³) ppm.

¹⁹F NMR (377 MHz, CDCl₃): δ_F -115.2 (s, 1F, minor rotamer), -116.1 (s, 1F, major rotamer) ppm.

IR (film) ν_{max} : 3420, 2976, 2932, 1660, 1220, 1154, 835 cm⁻¹.

HRMS (ESI⁺): calcd. for C₁₆H₂₄FNNaO₃ [M+Na]⁺ 320.1632, found 320.1619.

Diastereomer B (28 mg, colourless oil):

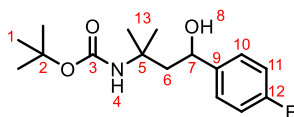
TLC: $R_f = 0.30$ (50% Et₂O/pentane, KMnO₄ stain).

¹H NMR (500 MHz, CDCl₃, 50 °C): δ_H 7.34 – 7.29 (m, 2H, H¹⁰), 7.05 – 6.98 (m, 2H, H¹¹), 4.74 – 4.62 (br. m, 1H, H⁷), 4.23 (br. s, 1H, H⁵), 2.67 (s, 3H, H⁴), 2.07 – 1.96 (m, 1H, H⁶), 1.74 (dt, $J = 14.2, 5.6$ Hz, 1H, H⁶), 1.44 (s, 9H, H¹), 1.11 (d, $J = 6.8$ Hz, 3H, H¹³) ppm.

¹³C NMR (101 MHz, CDCl₃): δ_C 162.4 (d, $J = 244.9$ Hz, C¹²), 156.2 (C³), 140.5 (C⁹), 127.6 (2 × C¹⁰), 115.4 (d, $J = 21.2$ Hz, 2 × C¹¹), 79.8 (C²), 72.1 (C⁷), 48.5 (C⁵), 43.6 (C⁶), 28.7 (3 × C¹), 28.1 (C⁴), 18.8 (C¹³) ppm.

¹⁹F NMR (377 MHz, CDCl₃): δ_F -114.8 (s, 1F, minor rotamer), -115.9 (s, 1F, major rotamer) ppm.

***tert*-Butyl (4-(4-fluorophenyl)-4-hydroxy-2-methylbutan-2-yl)carbamate (254)**



Prepared following General Procedure 4B using Boc-Aib-OH (73 mg, 0.36 mmol, 1.2 equiv.), vinyl boronic ester **238** (155 μ L, 0.90 mmol, 3.0 equiv.), 4-fluoroiodobenzene (35 μ L, 0.30 mmol, 1.0 equiv.),

4CzIPN (4.7 mg, 0.0060 mmol, 2.0 mol%), NiCl₂·glyme (3.3 mg, 0.015 mmol, 5.0 mol%), dtbbpy (5.0 mg, 0.019 mmol, 6.3 mol%), Cs₂CO₃ (127 mg, 0.39 mmol, 1.3 equiv.) and DMA (12 mL), which was irradiated with 1 × Kessil lamp for 48 h. After oxidative work-up with UHP (84 mg, 0.90 mmol, 3.0 equiv.), purification by flash column chromatography (30% Et₂O/pentane) gave the title compound (30 mg, 0.10 mmol, 34%) as a colourless oil.

TLC: R_f = 0.42 (30% Et₂O/pentane, KMnO₄ stain).

¹H NMR (400 MHz, CDCl₃): δ_H 7.34 – 7.27 (m, 2H, H¹⁰), 7.05 – 6.97 (m, 2H, H¹¹), 5.25 (s, 1H, H⁴), 4.90 (dt, *J* = 9.9, 2.6 Hz, 1H, H⁷), 2.70 – 2.56 (m, 1H, H⁸), 2.05 (dd, *J* = 14.8, 9.8, 1H, H⁶), 1.82 (dd, *J* = 14.9, 2.3 Hz, 1H, H⁶), 1.44 (s, 9H, H¹), 1.38 (s, 6H, H¹³) ppm.

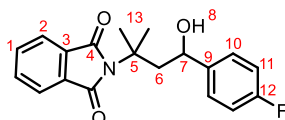
¹³C NMR (101 MHz, CDCl₃): δ_C 162.2 (d, *J* = 245.1 Hz, C¹²), 155.4 (C³), 141.5 (d, *J* = 3.2 Hz, C⁹), 127.3 (d, *J* = 8.0 Hz, 2 × C¹⁰), 115.4 (d, *J* = 21.3 Hz, 2 × C¹¹), 79.2 (C²), 71.3 (C⁷), 52.3 (C⁵), 50.4 (C⁶), 29.0 (1 × C¹³), 28.6 (3 × C¹), 27.3 (1 × C¹³) ppm.

¹⁹F NMR (377 MHz, CDCl₃): δ_F –115.4 (s, 1F) ppm.

IR (film) ν_{max}: 3361, 2975, 2932, 1692, 1508, 1169, 1076, 836 cm⁻¹.

HRMS (ESI⁺): calcd. for C₁₆H₂₄FNNaO₃ [M+Na]⁺ 320.1632, found 320.1626.

2-(4-(4-Fluorophenyl)-4-hydroxy-2-methylbutan-2-yl)isoindoline-1,3-dione (256)



Prepared following General Procedure 4B using 2-methyl-2-phthalimidopropanoic (84 mg, 0.36 mmol, 1.2 equiv.), vinyl boronic ester **238** (155 μL, 0.90 mmol, 3.0 equiv.), 4-fluoriodobenzene (35 μL, 0.30 mmol, 1.0 equiv.), 4CzIPN (4.7 mg, 0.0060 mmol, 2.0 mol%), NiCl₂·glyme (3.3 mg, 0.015 mmol, 5.0 mol%), dtbbpy (5.0 mg, 0.019 mmol, 6.3 mol%), Cs₂CO₃ (127 mg, 0.39 mmol, 1.3 equiv.) and DMA (12 mL), which was irradiated with 1 × Kessil lamp for 24 h. After oxidative work-up with UHP (84 mg, 0.90 mmol, 3.0 equiv.), purification by flash column chromatography (20% EtOAc/pentane) gave the title compound (42 mg, 0.13 mmol, 43%) as a pale yellow oil.

TLC: R_f = 0.40 (20% EtOAc/pentane, KMnO₄ stain).

¹H NMR (400 MHz, CDCl₃): δ_H 7.71 – 7.60 (m, 4H, H¹ + H²), 7.25 – 7.20 (m, 2H, H¹⁰), 6.86 – 6.78 (m, 2H, H¹¹), 4.89 (dd, *J* = 7.8, 5.1 Hz, 1H, H⁷), 2.48 (dd, *J* = 14.7, 7.8 Hz, 1H, H⁶), 2.34 (dd, *J* = 14.7, 5.1 Hz, 1H, H⁶), 1.83 (s, 3H, H¹³), 1.79 (s, 3H, H¹³) ppm.

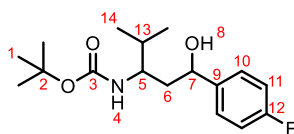
¹³C NMR (101 MHz, CDCl₃): δ_c 170.2 (2 × C⁴), 162.2 (d, *J* = 245.9 Hz, C¹²), 140.5 (d, *J* = 3.2 Hz, C⁹), 133.7 (2 × C¹), 132.1 (2 × C³), 127.8 (d, *J* = 8.2 Hz, 2 × C¹⁰), 122.6 (2 × C²), 115.3 (d, *J* = 21.5 Hz, 2 × C¹¹), 71.4 (C⁷), 59.1 (C⁵), 47.7 (C⁶), 28.64 (1 × C¹³), 28.57 (1 × C¹³) ppm.

¹⁹F NMR (377 MHz, CDCl₃): δ_F -115.0 (s, 1F) ppm.

IR (film) ν_{max}: 3466, 2930, 1699, 1370, 1317, 1220, 719 cm⁻¹.

HRMS (ESI⁺): calcd. for C₁₉H₁₈FNO₃ [M+H-H₂O]⁺ 310.1238, found 310.1241.

***tert*-Butyl (1-(4-fluorophenyl)-1-hydroxy-4-methylpentan-3-yl)carbamate (257)**



Prepared following General Procedure 4B using Boc-Val-OH (78 mg, 0.36 mmol, 1.2 equiv.), vinyl boronic ester **238** (155 μL, 0.90 mmol, 3.0 equiv.), 4-fluoroiodobenzene (35 μL, 0.30 mmol, 1.0 equiv.), 4CzIPN (4.7 mg, 0.0060 mmol, 2.0 mol%), NiCl₂·glyme (3.3 mg, 0.015 mmol, 5.0 mol%), dtbbpy (5.0 mg, 0.019 mmol, 6.3 mol%), Cs₂CO₃ (127 mg, 0.39 mmol, 1.3 equiv.) and DMA (12 mL), which was irradiated with 1 × Kessil lamp for 24 h. After oxidative work-up with UHP (84 mg, 0.90 mmol, 3.0 equiv.), purification by flash column chromatography (30–60% Et₂O/pentane) gave the title compound as two separable diastereomers (total yield: 47 mg, 0.15 mmol, 50%). The d.r. was determined after purification to be 47:53 (The relative stereochemistry of the two diastereomers could not be assigned).

Diastereomer A (22 mg, white solid):

TLC: R_f = 0.33 (30% Et₂O/pentane, KMnO₄ stain).

Mpt: 89.8–90.6 °C (CHCl₃).

¹H NMR (400 MHz, CDCl₃): δ_H 7.38 – 7.30 (m, 2H, H¹⁰), 7.05 – 6.97 (m, 2H, H¹¹), 4.67 (dt, *J* = 11.0, 3.1 Hz, 1H, H⁷), 4.52 (d, *J* = 9.6 Hz, 1H, H⁴), 4.36 (d, *J* = 3.3 Hz, 1H, H⁸), 3.76 (dddd, *J* = 14.8, 9.3, 5.4, 2.7 Hz, 1H, H⁵), 1.81 – 1.67 (m, 2H, H⁶ + H¹³), 1.58 – 1.51 (m, 1H, H⁶), 1.48 (s, 9H, H¹), 0.95 (t, *J* = 6.9 Hz, 3H, H¹⁴), 0.93 (t, *J* = 7.0 Hz, 3H, H¹⁴) ppm.

¹³C NMR (126 MHz, CDCl₃): δ_c 162.0 (d, *J* = 244.5 Hz, C¹²), 157.8 (C³), 140.3 (d, *J* = 3.1 Hz, C⁹), 127.3 (d, *J* = 8.0 Hz, 2 × C¹⁰), 115.2 (d, *J* = 21.2 Hz, 2 × C¹¹), 80.3 (C²), 69.6 (C⁷), 52.8 (C⁵), 44.1 (C⁶), 32.4 (C¹³), 28.5 (3 × C¹), 19.5 (C¹⁴), 18.4 (C¹⁴) ppm.

¹⁹F NMR (377 MHz, CDCl₃): δ_F -116.1 (s, 1F) ppm.

IR (film) ν_{max}: 3346, 2964, 1681, 1509, 1222, 1169, 834 cm⁻¹.

HRMS (ESI⁺): calcd. for C₁₇H₂₇FNO₃ [M+H]⁺ 312.1969, found 312.1975.

Diastereomer B (25 mg, colourless oil):

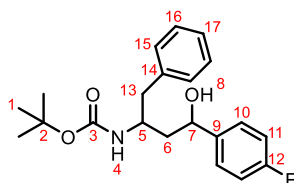
TLC: R_f = 0.30 (50% Et₂O/pentane, KMnO₄ stain).

¹H NMR (400 MHz, CDCl₃): δ_H 7.38 – 7.30 (m, 2H, H¹⁰), 7.06 – 6.97 (m, 2H, H¹¹), 4.75 (t, *J* = 6.9 Hz, 1H, H⁷), 4.54 (d, *J* = 9.4 Hz, 1H, H⁴), 3.51 – 3.40 (br. m, 1H, H⁵), 3.04 (br. s, 1H, H⁸), 1.89 – 1.63 (m, 3H, H⁶ + H¹³), 1.45 (s, 9H, H¹), 0.87 (d, *J* = 6.8 Hz, 3H, H¹⁴), 0.84 (d, *J* = 6.9 Hz, 3H, H¹⁴) ppm.

¹³C NMR (126 MHz, CDCl₃): δ_C 162.3 (d, *J* = 245.1 Hz, C¹²), 156.4 (C³), 140.5 (C⁹), 127.7 (d, *J* = 8.1 Hz, 2 × C¹⁰), 115.4 (d, *J* = 21.3 Hz, 2 × C¹¹), 79.7 (C²), 72.8 (C⁷), 53.8 (C⁵), 43.0 (C⁶), 32.7 (C¹³), 28.5 (3 × C¹), 18.9 (C¹⁴), 17.7 (C¹⁴) ppm.

¹⁹F NMR (377 MHz, CDCl₃): δ_F –115.3 (s, 1F) ppm.

***tert*-Butyl (4-(4-fluorophenyl)-4-hydroxy-1-phenylbutan-2-yl)carbamate (258)**



Prepared following General Procedure 4B using Boc-Phe-OH (96 mg, 0.36 mmol, 1.2 equiv.), vinyl boronic ester **238** (155 μL, 0.90 mmol, 3.0 equiv.), 4-fluoroiodobenzene (35 μL, 0.30 mmol, 1.0 equiv.), 4CzIPN (4.7 mg, 0.0060 mmol, 2.0 mol%), NiCl₂-glyme (3.3 mg, 0.015 mmol, 5.0 mol%), dtbbpy (5.0 mg, 0.019 mmol, 6.3 mol%), Cs₂CO₃ (127 mg, 0.39 mmol, 1.3 equiv.) and DMA (12 mL), which was irradiated with 1 × Kessil lamp for 24 h. After oxidative work-up with UHP (84 mg, 0.90 mmol, 3.0 equiv.), purification by flash column chromatography (10–15% Et₂O/CH₂Cl₂) gave the title compound as two separable diastereomers (total yield: 36 mg, 0.10 mmol, 33%). The d.r. was determined after purification to be 47:53 (The relative stereochemistry of the two diastereomers could not be assigned).

Diastereomer A (17 mg, colourless oil):

TLC: R_f = 0.66 (15% Et₂O/CH₂Cl₂, KMnO₄ stain).

¹H NMR (500 MHz, CDCl₃): δ_H 7.30 (m, 4H, H¹⁰ + H¹⁶), 7.25 – 7.21 (m, 1H, H¹⁷), 7.20 – 7.16 (m, 2H, H¹⁵), 7.05 – 6.93 (m, 2H, H¹¹), 4.70 (br. d, *J* = 10.9 Hz, 1H, H⁷), 4.59 (br. d, *J* = 9.1 Hz, 1H, H⁴), 4.31 – 4.16 (m, 2H, H⁵ + H⁸), 2.89 – 2.74 (m, 2H, H¹³), 1.82 (ddd, *J* = 14.0, 10.9, 2.8 Hz, 1H, H⁶), 1.58 (ddd, *J* = 13.9, 11.1, 2.6 Hz, 1H, H⁶), 1.43 (s, 9H, H¹) ppm.

¹³C NMR (126 MHz, CDCl₃): δ_C 162.0 (d, *J* = 244.6 Hz, C¹²), 157.3 (C³), 140.0 (d, *J* = 3.1 Hz, C⁹), 137.5 (C¹⁴), 129.4 (2 × C¹⁵), 128.7 (2 × C¹⁶), 127.3 (d, *J* = 7.9 Hz, 2 × C¹⁰), 126.8 (C¹⁷), 115.2 (d, *J* = 21.1 Hz, 2 × C¹¹), 80.4 (C²), 69.6 (C⁷), 48.5 (C⁵), 45.9 (C⁶), 41.6 (C¹³), 28.5 (3 × C¹) ppm.

¹⁹F NMR (377 MHz, CDCl₃): δ_F -115.9 (s, 1F) ppm.

IR (film) ν_{max}: 3347, 2978, 2928, 1683, 1509, 1222, 1167 cm⁻¹.

HRMS (ESI⁺): calcd. for C₂₁H₂₆FNNaO₃ [M+Na]⁺ 382.1789, found 382.1778.

Diastereomer B (19 mg, colourless oil):

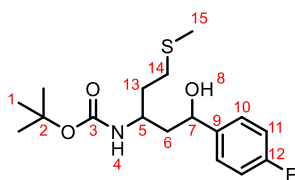
TLC: R_f = 0.20 (15% Et₂O/CH₂Cl₂, KMnO₄ stain).

¹H NMR (500 MHz, CDCl₃): δ_H 7.32 – 7.19 (m, 5H, H¹⁰ + H¹⁶ + H¹⁷), 7.17 – 7.09 (m, 2H, H¹⁵), 7.03 – 6.96 (m, 2H, H¹¹), 4.75 – 4.67 (br. m, 1H, H⁷), 4.67 – 4.51 (br. m, 1H, H⁴), 3.88 (br. s, 1H, H⁵), 2.90 – 2.62 (m, 3H, H⁸ + H¹³), 1.92 – 1.78 (m, 2H, H⁶), 1.41 (s, 9H, H¹) ppm.

¹³C NMR (126 MHz, CDCl₃): δ_C 162.3 (d, *J* = 245.3 Hz, C¹²), 155.9 (C³), 140.2 (C⁹), 137.7 (C¹⁴), 129.6 (2 × C¹⁵), 128.6 (2 × C¹⁶), 127.6 (d, *J* = 8.1 Hz, 2 × C¹⁰), 126.7 (C¹⁷), 115.4 (d, *J* = 21.3 Hz, 2 × C¹¹), 79.8 (C²), 72.4 (C⁷), 50.2 (C⁵), 44.2 (C⁶), 42.0 (C¹³), 28.5 (3 × C¹) ppm.

¹⁹F NMR (377 MHz, CDCl₃): δ_F -115.2 (s, 1F) ppm.

***tert*-Butyl (1-(4-fluorophenyl)-1-hydroxy-5-(methylthio)pentan-3-yl)carbamate (259)**



Prepared following General Procedure 4B using Boc-Met-OH (90 mg, 0.36 mmol, 1.2 equiv.), vinyl boronic ester **238** (155 μL, 0.90 mmol, 3.0 equiv.), 4-fluoroiodobenzene (35 μL, 0.30 mmol, 1.0 equiv.), 4CzIPN (4.7 mg, 0.0060 mmol, 2.0 mol%), NiCl₂·glyme (3.3 mg, 0.015 mmol, 5.0 mol%), dtbbpy (5.0 mg, 0.019 mmol, 6.3 mol%), Cs₂CO₃ (127 mg, 0.39 mmol, 1.3 equiv.) and DMA (12 mL), which was irradiated with 1 × Kessil lamp for 24 h. After oxidative work-up with UHP (84 mg, 0.90 mmol, 3.0 equiv.), purification by flash column chromatography (30–35% EtOAc/pentane) gave the title compound as two separable diastereomers (total yield: 33 mg, 0.10 mmol, 32%). The d.r. was determined after purification to be 48:52 (The relative stereochemistry of the two diastereomers could not be assigned).

Diastereomer A (16 mg, pale yellow oil):

TLC: $R_f = 0.67$ (35% EtOAc/pentane, KMnO_4 stain).

^1H NMR (400 MHz, CDCl_3): δ_{H} 7.38 – 7.29 (m, 2H, H^{10}), 7.07 – 6.94 (m, 2H, H^{11}), 4.70 (br. d, $J = 11.1$ Hz, 1H, H^7), 4.64 (br. d, $J = 9.3$ Hz, 1H, H^4), 4.28 (br. d, $J = 3.7$ Hz, 1H, H^8), 4.09 – 3.94 (m, 1H, H^5), 2.66 – 2.47 (m, 2H, H^{14}), 2.11 (s, 3H, H^{15}), 1.88 – 1.75 (m, 2H, H^{13}), 1.75 – 1.65 (m, 1H, H^6), 1.61 – 1.58 (m, 1H, H^6), 1.47 (s, 9H, H^1) ppm.

^{13}C NMR (126 MHz, CDCl_3): δ_{C} 162.1 (d, $J = 244.9$ Hz, C^{12}), 157.4 (C^3), 139.8 (C^9), 127.3 (d, $J = 8.0$ Hz, $2 \times \text{C}^{10}$), 115.4 (d, $J = 21.3$ Hz, $1 \times \text{C}^{11}$) + 115.3 (d, $J = 21.4$ Hz, $1 \times \text{C}^{11}$), 80.5 (C^2), 69.7 + 69.6 (rotameric peaks, C^7), 51.5 + 50.8 (rotameric peaks, C^{14}), 47.7 + 47.5 (rotameric peaks, C^5), 46.6 + 46.5 (rotameric peaks, C^6), 38.9 + 38.6 (rotameric peaks, C^{15}), 28.5 ($3 \times \text{C}^1$), 27.8 (C^{13}) ppm.

^{19}F NMR (377 MHz, CDCl_3): δ_{F} -115.5 and -115.6 (s, 1F, rotameric peaks) ppm.

IR (film) ν_{max} : 3318, 2978, 2926, 1694, 1509, 1222, 1168, 1022, 837 cm^{-1} .

HRMS (ESI⁺): calcd. for $\text{C}_{17}\text{H}_{26}\text{FNNaO}_3\text{S}$ [$\text{M}+\text{Na}$]⁺ 366.1510, found 366.1505.

Diastereomer B (17 mg, pale yellow oil):

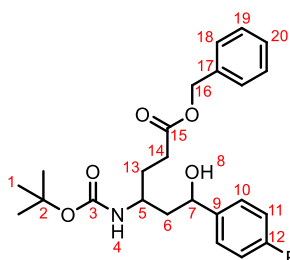
TLC: $R_f = 0.33$ (35% EtOAc/pentane, KMnO_4 stain).

^1H NMR (500 MHz, CDCl_3): δ_{H} 7.37 – 7.30 (m, 2H, H^{10}), 7.07 – 7.00 (m, 2H, H^{11}), 4.83 – 4.76 (m, 1H, H^7), 4.64 – 4.51 (br. m, 1H, H^4), 3.79 – 3.67 (br. m, 1H, H^5), 2.67 (br. s, 1H, H^8), 2.57 – 2.42 (m, 2H, H^{14}), 2.08 (s, 3H, H^{15}), 1.97 – 1.77 (m, 3H, $\text{H}^6 + \text{H}^{13}$), 1.76 – 1.65 (m, 1H, H^6), 1.45 (s, 9H, H^1) ppm.

^{13}C NMR (126 MHz, CDCl_3): δ_{C} 162.4 (d, $J = 244.0$ Hz, C^{12}), 156.0 (C^3), 140.3 (C^9), 127.7 (d, $J = 8.0$ Hz, $2 \times \text{C}^{10}$), 115.5 (d, $J = 21.3$ Hz, $2 \times \text{C}^{11}$), 79.8 (C^2), 72.2 (C^7), 48.7 (C^5), 45.3 (C^{13}), 35.7 (C^6), 30.7 (C^{14}), 28.5 ($3 \times \text{C}^1$), 15.8 (C^{15}) ppm.

^{19}F NMR (377 MHz, CDCl_3): δ_{F} -115.0 (s, 1F) ppm.

Benzyl 4-((*tert*-butoxycarbonyl)amino)-6-(4-fluorophenyl)-6-hydroxyhexanoate (260)



Prepared following General Procedure 4B using Boc-Glu(OBzl)-OH (121 mg, 0.36 mmol, 1.2 equiv.), vinyl boronic ester **238** (155 μ L, 0.90 mmol, 3.0 equiv.), 4-fluoriodobenzene (35 μ L, 0.30 mmol, 1.0 equiv.), 4CzIPN (4.7 mg, 0.0060 mmol, 2.0 mol%), NiCl₂-glyme (3.3 mg, 0.015 mmol, 5.0 mol%), dtbbpy (5.0 mg, 0.019 mmol, 6.3 mol%), Cs₂CO₃ (127 mg, 0.39 mmol, 1.3 equiv.) and DMA (12 mL), which was irradiated with 1 \times Kessil lamp for 40 h. After oxidative work-up with UHP (84 mg, 0.90 mmol, 3.0 equiv.), purification by flash column chromatography (10–20% Et₂O/CH₂Cl₂) gave the title compound as two separable diastereomers (total yield: 30 mg, 0.07 mmol, 23%). The d.r. was determined after purification to be 57:43 (The relative stereochemistry of the two diastereomers could not be assigned).

Diastereomer A (17 mg, pale orange oil):

TLC: R_f = 0.60 (20% Et₂O/CH₂Cl₂, KMnO₄ stain).

¹H NMR (500 MHz, CDCl₃): δ_{H} 7.39 – 7.30 (m, 7H, H¹⁰ + H¹⁸ + H¹⁹ + H²⁰), 7.04 – 6.96 (m, 2H, H¹¹), 5.13 (s, 2H, H¹⁶), 4.72 – 4.62 (m, 2H, H⁴ + H⁷), 4.28 (d, J = 3.7 Hz, 1H, H⁸), 3.96 – 3.84 (m, 1H, H⁵), 2.48 (t, J = 7.4 Hz, 2H, H¹⁴), 1.91 – 1.83 (m, 1H, H⁶), 1.83 – 1.73 (m, 2H, H¹³), 1.57 (ddd, J = 13.8, 11.0, 2.6 Hz, 1H, H⁶), 1.46 (s, 9H, H¹) ppm.

¹³C NMR (126 MHz, CDCl₃): δ_{C} 173.4 (C¹⁵), 162.1 (d, J = 244.6 Hz, C¹²), 157.5 (C³), 139.9 (d, J = 3.1 Hz, C⁹), 135.9 (C¹⁷), 128.8 (2 \times C¹⁹), 128.5 (C²⁰), 128.4 (2 \times C¹⁸), 127.3 (d, J = 8.0 Hz, 2 \times C¹⁰), 115.2 (d, J = 21.4 Hz, 2 \times C¹¹), 80.4 (C²), 69.4 (C⁷), 66.7 (C¹⁶), 48.1 (C⁵), 47.1 (C⁶), 31.5 (C¹⁴), 30.4 (C¹³), 28.5 (3 \times C¹) ppm.

¹⁹F NMR (377 MHz, CDCl₃): δ_{F} –115.9 (s, 1F) ppm.

IR (film) ν_{max} : 3374, 2974, 29934, 1731, 1685, 1509, 1161, 1051, 835 cm⁻¹.

HRMS (ESI⁺): calcd. for C₂₄H₃₁FNO₅ [M+H]⁺ 432.2181, found 432.2197.

Diastereomer B (13 mg, pale orange oil):

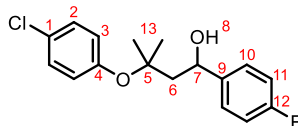
TLC: R_f = 0.22 (20% Et₂O/CH₂Cl₂, KMnO₄ stain).

¹H NMR (500 MHz, CDCl₃): δ_H 7.40 – 7.28 (m, 7H, H¹⁰ + H¹⁸ + H¹⁹ + H²⁰), 7.08 – 6.94 (m, 2H, H¹¹), 5.10 (s, 2H, H¹⁶), 4.81 – 4.73 (m, 1H, H⁷), 4.60 – 4.46 (br. m, 1H, H⁴), 3.74 – 3.57 (br. s, 1H, H⁵), 2.68 (br. s, 1H, H⁸), 2.42 (t, *J* = 7.5 Hz, 2H, H¹⁴), 1.95 – 1.85 (m, 2H, H⁶ + H¹³), 1.85 – 1.77 (m, 1H, H⁶), 1.77 – 1.67 (m, 1H, H¹³), 1.43 (s, 9H, H¹) ppm.

¹³C NMR (126 MHz, CDCl₃): δ_C 173.4 (C¹⁵), 162.4 (d, *J* = 245.6 Hz, C¹²), 156.0 (C³), 140.3 (C⁹), 136.0 (C¹⁷), 128.7 (2 × C¹⁹), 128.4 (C²⁰), 128.4 (2 × C¹⁸), 127.6 (d, *J* = 8.2 Hz, 2 × C¹⁰), 115.5 (d, *J* = 21.3 Hz, 2 × C¹¹), 79.8 (C²), 72.0 (C⁷), 66.6 (C¹⁶), 48.9 (C⁵), 45.7 (C⁶), 31.1 (C¹⁴), 30.9 (C¹³), 28.5 (3 × C¹) ppm.

¹⁹F NMR (377 MHz, CDCl₃): δ_F -115.1 (s, 1F) ppm.

3-(4-Chlorophenoxy)-1-(4-fluorophenyl)-3-methylbutan-1-ol (263)



Prepared following General Procedure 4B using clofibric acid (77 mg, 0.36 mmol, 1.2 equiv.), vinyl boronic ester **238** (155 μL, 0.90 mmol, 3.0 equiv.), 4-fluoroiodobenzene (35 μL, 0.30 mmol, 1.0 equiv.), 4CzIPN (4.7 mg, 0.0060 mmol, 2.0 mol%), NiCl₂·glyme (3.3 mg, 0.015 mmol, 5.0 mol%), dtbbpy (5.0 mg, 0.019 mmol, 6.3 mol%), Cs₂CO₃ (127 mg, 0.39 mmol, 1.3 equiv.) and DMA (12 mL), which was irradiated with 1 × Kessil lamp for 40 h. After oxidative work-up with UHP (84 mg, 0.90 mmol, 3.0 equiv.), purification by flash column chromatography (20% Et₂O/pentane) gave the title compound (21 mg, 0.07 mmol, 23%) as a colourless oil.

TLC: R_f = 0.23 (20% Et₂O/pentane, KMnO₄ stain).

¹H NMR (400 MHz, CDCl₃): δ_H 7.42 – 7.36 (m, 2H, H¹⁰), 7.30 – 7.24 (m, 2H, H²), 7.08 – 7.02 (m, 2H, H¹¹), 7.02 – 6.97 (m, 2H, H³), 5.18 (dd, *J* = 10.6, 2.0 Hz, 1H, H⁷), 4.13 (s, 1H, H⁸), 2.25 (dd, *J* = 14.8, 10.5 Hz, 1H, H⁶), 1.81 (dd, *J* = 14.9, 2.0 Hz, 1H, H⁶), 1.47 (s, 3H, H¹³), 1.29 (s, 3H, H¹³) ppm.

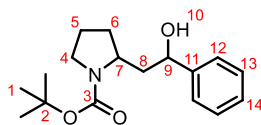
¹³C NMR (101 MHz, CDCl₃): δ_C 162.2 (d, *J* = 244.9 Hz, C¹²), 152.5 (C⁴), 140.7 (d, *J* = 3.0 Hz, C⁹), 129.9 (C¹), 129.3 (2 × C²), 127.5 (d, *J* = 8.1 Hz, 2 × C¹⁰), 125.8 (2 × C³), 115.3 (d, *J* = 21.4 Hz, 2 × C¹¹), 82.6 (C⁵), 71.0 (C⁷), 51.7 (C⁶), 28.1 (C¹³), 25.2 (C¹³) ppm.

¹⁹F NMR (377 MHz, CDCl₃): δ_F -115.6 (s, 1F) ppm.

IR (film) ν_{max}: 3497, 2977, 2925, 1509, 1487, 1216, 1129, 842 cm⁻¹.

HRMS (ESI⁺): calcd. for C₁₇H₁₈ClFNaO₂ [M+Na]⁺ 331.0872, found 331.0874.

***tert*-Butyl 2-(2-hydroxy-2-phenylethyl)pyrrolidine-1-carboxylate (264)**



Prepared following General Procedure 4B using Boc-Pro-OH (77 mg, 0.36 mmol, 1.2 equiv.), vinyl boronic ester **238** (155 μ L, 0.90 mmol, 3.0 equiv.), iodobenzene (34 μ L, 0.30 mmol, 1.0 equiv.), 4CzIPN (4.7 mg, 0.0060 mmol, 2.0 mol%), NiCl₂·glyme (3.3 mg, 0.015 mmol, 5.0 mol%), dtbbpy (5.0 mg, 0.019 mmol, 6.3 mol%), Cs₂CO₃ (127 mg, 0.39 mmol, 1.3 equiv.) and DMA (12 mL), which was irradiated with 1 \times Kessil lamp for 24 h. After oxidative work-up with UHP (84 mg, 0.90 mmol, 3.0 equiv.), purification by flash column chromatography (35–40% Et₂O/pentane) gave the title compound as two separable diastereomers (total yield: 50 mg, 0.17 mmol, 57%). The d.r. was determined after purification to be 44:56 (The relative stereochemistry of the two diastereomers could not be assigned).

Diastereomer A (22 mg, pale yellow oil):

TLC: R_f = 0.59 (50% Et₂O/pentane, KMnO₄ stain).

¹H NMR (400 MHz, CDCl₃): δ_{H} 7.42 – 7.36 (m, 2H, H¹²), 7.35 – 7.29 (m, 2H, H¹³), 7.26 – 7.18 (m, 1H, H¹⁴), 5.47 – 5.34 (m, 1H, H¹⁰), 4.77 – 4.57 (br. m, 1H, H⁹), 4.37 – 4.21 (br. m, 1H, H⁷), 3.44 – 3.32 (br. m, 2H, H⁴), 2.06 – 1.84 (m, 3H, H⁵ + H⁸), 1.78 – 1.55 (m, 3H, H⁶ + H⁸), 1.49 (s, 9H, H¹) ppm.

¹³C NMR (101 MHz, CDCl₃): δ_{C} 157.0 (C³), 144.6 (C¹¹), 128.3 (2 \times C¹³), 126.9 (C¹⁴), 125.8 (2 \times C¹²), 80.2 (C²), 70.1 (C⁹), 54.1 (C⁷), 46.8 (C⁴), 46.5 (C⁶), 31.4 (C⁸), 28.6 (3 \times C¹), 23.8 (C⁵) ppm.

IR (film) ν_{max} : 3405, 2972, 1666, 1393, 1365, 1166, 1104, 700 cm⁻¹.

HRMS (ESI⁺): calcd. for C₁₇H₂₅NNaO₃ [M+Na]⁺ 314.1727, found 314.1720.

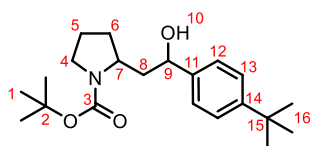
Diastereomer B (28 mg, pale orange oil):

TLC: R_f = 0.34 (50% Et₂O/pentane, KMnO₄ stain).

¹H NMR (500 MHz, CDCl₃): δ_{H} 7.40 – 7.34 (m, 2H, H¹²), 7.34 – 7.28 (m, 2H, H¹³), 7.26 – 7.20 (m, 1H, H¹⁴), 4.82 – 4.70 (m, 1H, H⁹), 4.10 (br. s, 1H, H⁷), 3.43 – 3.25 (m, 2H, H⁴), 2.21 – 2.10 (m, 1H, H⁸), 2.09 – 1.92 (m, 1H, H⁸), 1.91 – 1.78 (m, 2H, H⁵), 1.78 – 1.63 (m, 2H, H⁶), 1.47 (s, 9H, H¹) ppm.

¹³C NMR (126 MHz, CDCl₃): δ_{C} 155.7 (C³), 145.3 (C¹¹), 128.4 (2 \times C¹³), 127.1 (C¹⁴), 125.7 (2 \times C¹²), 79.9 (C²), 72.8 (C⁹), 55.8 (C⁷), 46.6 (C⁴), 46.3 (C⁸), 32.5 (C⁶), 28.7 (3 \times C¹), 23.9 (C⁵) ppm.

***tert*-Butyl 2-(2-(4-(*tert*-butyl)phenyl)-2-hydroxyethyl)pyrrolidine-1-carboxylate (265)**



Prepared following General Procedure 4B using Boc-Pro-OH (77 mg, 0.36 mmol, 1.2 equiv.), vinyl boronic ester **238** (155 μ L, 0.90 mmol, 3.0 equiv.), 4-*tert*-butyliodobenzene (53 μ L, 0.30 mmol, 1.0 equiv.), 4CzIPN (4.7 mg, 0.0060 mmol, 2.0 mol%), NiCl₂·glyme (3.3 mg, 0.015 mmol, 5.0 mol%), dtbbpy (5.0 mg, 0.019 mmol, 6.3 mol%), Cs₂CO₃ (127 mg, 0.39 mmol, 1.3 equiv.) and DMA (12 mL), which was irradiated with 1 \times Kessil lamp for 24 h. After oxidative work-up with UHP (84 mg, 0.90 mmol, 3.0 equiv.), purification by flash column chromatography (8–15% EtOAc/pentane) gave the title compound as two separable diastereomers (total yield: 59 mg, 0.17 mmol, 57%). The d.r. was determined after purification to be 42:58 (The relative stereochemistry of the two diastereomers could not be assigned).

Diastereomer A (25 mg, colourless oil):

TLC: R_f = 0.33 (15% EtOAc/pentane, KMnO₄ stain).

¹H NMR (400 MHz, CDCl₃): δ_{H} 7.39 – 7.27 (m, 4H, H¹² + H¹³), 5.39 – 5.23 (m, 1H, H¹⁰), 4.75 – 4.53 (br. m, 1H, H⁹), 4.39 – 4.23 (br. m, 1H, H⁷), 3.51 – 3.30 (m, 2H, H⁴), 2.06 – 1.92 (m, 1H, H⁸), 1.92 – 1.84 (m, 2H, H⁵), 1.78 – 1.66 (m, 2H, H⁶), 1.66 – 1.55 (m, 1H, H⁸), 1.49 (s, 9H, H¹), 1.31 (s, 9H, H¹⁶) ppm.

¹³C NMR (101 MHz, CDCl₃): δ_{C} 156.9 (C³), 149.8 (C¹⁴), 141.6 (C¹¹), 125.5 (2 \times C¹²), 125.2 (2 \times C¹³), 80.2 (C²), 70.0 (C⁹), 54.2 (C⁷), 46.8 (C⁴), 46.3 (C⁶), 34.6 (C¹⁵), 31.5 (3 \times C¹⁶), 31.3 (C⁸), 28.6 (3 \times C¹), 23.8 (C⁵) ppm.

IR (film) ν_{max} : 3414, 2964, 1668, 1393, 1365, 1167, 1108 cm⁻¹.

HRMS (ESI⁺): calcd. for C₂₁H₃₃NNaO₃ [M+Na]⁺ 370.2353, found 370.2347.

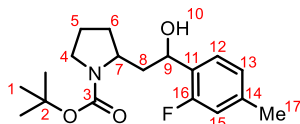
Diastereomer B (34 mg, colourless oil):

TLC: R_f = 0.17 (15% EtOAc/pentane, KMnO₄ stain).

¹H NMR (400 MHz, CDCl₃): δ_{H} 7.41 – 7.26 (m, 4H, H¹² + H¹³), 4.81 – 4.62 (br. m, 1H, H⁹), 4.27 – 3.97 (br. m, 2H, H⁷ + H¹⁰), 3.46 – 3.21 (br. m, 2H, H⁴), 2.24 – 2.08 (m, 1H, H⁸), 2.08 – 1.92 (m, 1H, H⁸), 1.88 – 1.79 (m, 2H, H⁵), 1.78 – 1.60 (m, 2H, H⁶), 1.46 (s, 9H, H¹), 1.31 (s, 9H, H¹⁶) ppm.

^{13}C NMR (126 MHz, CDCl_3): δ_{C} 155.6 (C^3), 150.0 (C^{14}), 142.3 (C^{11}), 125.5 ($2 \times \text{C}^{12}$), 125.3 ($2 \times \text{C}^{13}$), 79.8 (C^2), 72.5 (C^9), 55.8 (C^7), 46.5 (C^4), 46.0 (C^8), 34.6 (C^{15}), 32.5 (C^6), 31.5 ($3 \times \text{C}^{16}$), 28.7 ($3 \times \text{C}^1$), 23.9 (C^5) ppm.

***tert*-Butyl 2-(2-(2-fluoro-4-methylphenyl)-2-hydroxyethyl)pyrrolidine-1-carboxylate (266)**



Prepared following General Procedure 4B using Boc-Pro-OH (77 mg, 0.36 mmol, 1.2 equiv.), vinyl boronic ester **238** (155 μL , 0.90 mmol, 3.0 equiv.), 2-fluoro-4-iodotoluene (40 μL , 0.30 mmol, 1.0 equiv.), 4CzIPN (4.7 mg, 0.0060 mmol, 2.0 mol%), $\text{NiCl}_2 \cdot \text{glyme}$ (3.3 mg, 0.015 mmol, 5.0 mol%), dtbbpy (5.0 mg, 0.019 mmol, 6.3 mol%), Cs_2CO_3 (127 mg, 0.39 mmol, 1.3 equiv.) and DMA (12 mL), which was irradiated with 1 \times Kessil lamp for 30 h. After oxidative work-up with UHP (84 mg, 0.90 mmol, 3.0 equiv.), purification by flash column chromatography (30–35% Et_2O /pentane) gave the title compound as two separable diastereomers (total yield: 41 mg, 0.13 mmol, 42%). The d.r. was determined after purification to be 49:51 (The relative stereochemistry of the two diastereomers could not be assigned).

Diastereomer A (20 mg, colourless oil):

TLC: R_f = 0.50 (35% Et_2O /pentane, KMnO_4 stain).

^1H NMR (500 MHz, CDCl_3): δ_{H} 7.46 (t, J = 7.8 Hz, 1H, H^{12}), 6.95 (d, J = 7.5 Hz, 1H, H^{13}), 6.80 (d, J = 11.4 Hz, 1H, H^{15}), 5.53 (d, J = 4.1 Hz, 1H, H^{10}), 4.90 (d, J = 10.8 Hz, 1H, H^9), 4.34 – 4.21 (m, 1H, H^7), 3.46 – 3.31 (m, 2H, H^4), 2.31 (s, 3H, H^{17}), 2.05– 1.81 (m, 3H, $\text{H}^5 + \text{H}^6$), 1.82 – 1.69 (m, 1H, H^8), 1.67 – 1.54 (m, 2H, $\text{H}^6 + \text{H}^8$), 1.49 (s, 9H, H^1) ppm.

^{13}C NMR (126 MHz, CDCl_3): δ_{C} 159.2 (d, J = 243.9 Hz, C^{16}), 157.0 (C^3), 138.6 (d, J = 7.68 Hz, C^{14}), 128.5 (d, J = 13.8 Hz, C^{11}), 127.1 (d, J = 5.2 Hz, C^{12}), 125.1 (d, J = 2.18 Hz, C^{13}), 115.5 (d, J = 21.6 Hz, C^{15}), 80.3 (C^2), 64.2 (C^9), 54.0 (C^7), 46.7 (C^4), 44.9 (C^8), 31.3 (C^6), 28.6 ($3 \times \text{C}^1$), 23.7 (C^5), 21.1 (C^{17}) ppm.

^{19}F NMR (377 MHz, CDCl_3): δ_{F} –120.9 (s, 1F) ppm.

IR (film) ν_{max} : 3404, 2974, 1668, 1400, 1367, 1169, 1115 cm^{-1} .

HRMS (ESI $^+$): calcd. for $\text{C}_{18}\text{H}_{27}\text{FNO}_3$ [$\text{M}+\text{H}$] $^+$ 324.1969, found 324.1962.

Diastereomer B (21 mg, colourless oil):

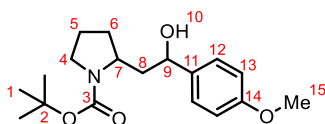
TLC: $R_f = 0.19$ (35% Et₂O/pentane, KMnO₄ stain).

¹H NMR (500 MHz, CDCl₃): δ_H 7.48 – 7.27 (m, 1H, H¹²), 6.93 (br. d, $J = 7.9$ Hz, 1H, H¹³), 6.80 (br. d, $J = 11.6$ Hz, 1H, H¹⁵), 5.11 – 4.88 (m, 1H, H⁹), 4.48 (br. s, 1H, H¹⁰), 4.17 – 3.98 (m, 1H, H⁷), 3.44 – 3.24 (m, 2H, H⁴), 2.32 (s, 3H, H¹⁷), 2.09 – 1.92 (m, 2H, H⁶ + H⁸), 1.92 – 1.80 (m, 2H, H⁵), 1.79 – 1.71 (m, 2H, H⁶ + H⁸), 1.47 (s, 9H, H¹) ppm.

¹³C NMR (126 MHz, CDCl₃): δ_C 159.4 (d, $J = 249.6$ Hz, C¹⁶), 155.8 (C³), 138.8 (C¹⁴), 129.3 (d, $J = 15.9$ Hz, C¹¹), 126.9 (d, $J = 5.2$ Hz, C¹²), 125.0 (C¹³), 115.6 (d, $J = 21.2$ Hz, C¹⁵), 80.0 (C²), 67.0 (d, $J = 2.2$ Hz, C⁹), 56.1 (C⁷), 46.6 (C⁴), 45.8 (C⁸), 32.7 (C⁶), 28.7 (3 × C¹), 24.0 (C⁵), 21.1 (C¹⁷) ppm.

¹⁹F NMR (377 MHz, CDCl₃): δ_F -121.0 (s, 1F) ppm.

***tert*-Butyl 2-(2-hydroxy-2-(4-methoxyphenyl)ethyl)pyrrolidine-1-carboxylate (267)**



Prepared following General Procedure 4B using Boc-Pro-OH (77 mg, 0.36 mmol, 1.2 equiv.), vinyl boronic ester **238** (155 μ L, 0.90 mmol, 3.0 equiv.), 4-iodoanisole (70 mg, 0.30 mmol, 1.0 equiv.), 4CzIPN (4.7 mg, 0.0060 mmol, 2.0 mol%), NiCl₂·glyme (3.3 mg, 0.015 mmol, 5.0 mol%), dtbbpy (5.0 mg, 0.019 mmol, 6.3 mol%), Cs₂CO₃ (127 mg, 0.39 mmol, 1.3 equiv.) and DMA (12 mL), which was irradiated with 1 × Kessil lamp for 24 h. After oxidative work-up with UHP (84 mg, 0.90 mmol, 3.0 equiv.), purification by flash column chromatography (25% EtOAc/pentane) gave the title compound as two separable diastereomers (total yield: 68 mg, 0.21 mmol, 71%). The d.r. was determined after purification to be 40:60 (The relative stereochemistry of the two diastereomers could not be assigned).

Diastereomer A (27 mg, pale yellow oil):

TLC: $R_f = 0.36$ (25% EtOAc/pentane, KMnO₄ stain).

¹H NMR (400 MHz, CDCl₃): δ_H 7.30 (d, $J = 8.2$ Hz, 2H, H¹²), 6.86 (d, $J = 8.5$ Hz, 2H, H¹³), 5.41 – 5.27 (m, 1H, H¹⁰), 4.69 – 4.53 (br. m, 1H, H⁹), 4.34 – 4.22 (br. m, 1H, H⁷), 3.79 (s, 3H, H¹⁵), 3.37 (t, $J = 7.0$ Hz, 2H, H⁴), 2.05 – 1.82 (m, 3H, H⁵ + H⁸), 1.73 – 1.55 (m, 3H, H⁶ + H⁸), 1.49 (s, 9H, H¹) ppm.

¹³C NMR (126 MHz, CDCl₃): δ_C 158.7 (C¹⁴), 157.0 (C³), 136.8 (C¹¹), 127.0 (2 × C¹²), 113.7 (2 × C¹³), 80.2 (C²), 69.7 (C⁹), 55.4 (C¹⁵), 54.1 (C⁷), 46.8 (C⁴), 46.4 (C⁶), 31.3 (C⁸), 28.6 (3 × C¹), 23.8 (C⁵) ppm.

IR (film) ν_{\max} : 3406, 2973, 1668, 1395, 1246, 1170, 832 cm⁻¹.

HRMS (ESI⁺): calcd. for C₁₈H₂₇NNaO₄ [M+Na]⁺ 344.1832, found 344.1825.

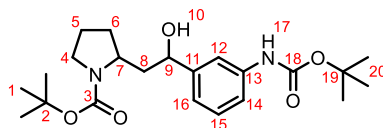
Diastereomer B (41 mg, colourless oil):

TLC: R_f = 0.20 (25% EtOAc/pentane, KMnO₄ stain).

¹H NMR (500 MHz, CDCl₃, 50 °C): δ_H 7.28 (d, *J* = 8.4 Hz, 2H, H¹²), 6.89 – 6.83 (m, 2H, H¹³), 4.78 – 4.64 (br. m, 1H, H⁹), 4.16 – 3.99 (br. m, 1H, H⁷), 3.79 (s, 3H, H¹⁵), 3.44 – 3.24 (m, 2H, H⁴), 2.22 – 2.09 (m, 1H, H⁸), 2.05 – 1.92 (m, 1H, H⁸), 1.93 – 1.75 (m, 2H, H⁵), 1.75 – 1.61 (m, 2H, H⁶), 1.47 (s, 9H, H¹) ppm.

¹³C NMR (126 MHz, CDCl₃): δ_C 158.8 (C¹⁴), 155.6 (C³), 137.5 (C¹¹), 127.0 (2 × C¹²), 113.8 (2 × C¹³), 79.9 (C²), 72.4 (C⁹), 55.8 (C⁷), 55.4 (C¹⁵), 46.6 (C⁴), 46.2 (C⁸), 32.5 (C⁶), 28.7 (3 × C¹), 23.9 (C⁵) ppm.

***tert*-Butyl 2-(2-(3-((*tert*-butoxycarbonyl)amino)phenyl)-2-hydroxyethyl)pyrrolidine-1-carboxylate (269)**



Prepared following General Procedure 4B using Boc-Pro-OH (77 mg, 0.36 mmol, 1.2 equiv.), vinyl boronic ester **238** (155 μL, 0.90 mmol, 3.0 equiv.), *N*-Boc-3-iodoaniline (96 mg, 0.30 mmol, 1.0 equiv.), 4CzIPN (4.7 mg, 0.0060 mmol, 2.0 mol%), NiCl₂·glyme (3.3 mg, 0.015 mmol, 5.0 mol%), dtbbpy (5.0 mg, 0.019 mmol, 6.3 mol%), Cs₂CO₃ (127 mg, 0.39 mmol, 1.3 equiv.) and DMA (12 mL), which was irradiated with 1 × Kessil lamp for 24 h. After oxidative work-up with UHP (84 mg, 0.90 mmol, 3.0 equiv.), purification by flash column chromatography (20–30% EtOAc/pentane) gave the title compound as two separable diastereomers (total yield: 62 mg, 0.15 mmol, 51%). The d.r. was determined after purification to be 44:56 (The relative stereochemistry of the two diastereomers could not be assigned).

Diastereomer A (27 mg, colourless oil):

TLC: R_f = 0.43 (30% EtOAc/pentane, KMnO₄ stain).

¹H NMR (400 MHz, CDCl₃): δ_H 7.41 – 7.36 (m, 1H, H¹²), 7.26 – 7.18 (m, 2H, H¹⁴ + H¹⁵), 7.07 (d, *J* = 6.8 Hz, 1H, H¹⁶), 6.49 (s, 1H, H¹⁷), 5.46 (br. s, 1H, H¹⁰), 4.67 – 4.55 (m, 1H, H⁹), 4.32 – 4.22 (m, 1H, H⁷), 3.44 – 3.29 (m, 2H, H⁴), 2.05 – 1.81 (m, 3H, H⁵ + H⁸), 1.76 – 1.54 (m, 3H, H⁶ + H⁸), 1.51 (s, 9H, H²⁰), 1.48 (s, 9H, H¹) ppm.

¹³C NMR (101 MHz, CDCl₃): δ_C 157.0 (C³), 152.9 (C¹⁸), 145.8 (C¹³), 138.3 (C¹¹), 129.0 (C¹⁵), 120.5 (C¹⁶), 117.1 (C¹⁴), 116.0 (C¹²), 80.5 (C²), 80.3 (C¹⁹), 70.0 (C⁹), 54.1 (C⁷), 46.9 (C⁴), 46.5 (C⁶), 31.4 (C⁸), 28.6 (3 × C¹), 28.5 (3 × C²⁰), 23.8 (C⁵) ppm.

IR (film) ν_{max}: 3319, 2975, 1669, 1402, 1239, 1161, 732 cm⁻¹.

HRMS (ESI⁺): calcd. for C₂₂H₃₅N₂O₅ [M+H]⁺ 407.2540, found 407.2522.

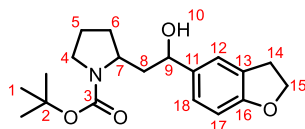
Diastereomer B (35 mg, colourless oil):

TLC: R_f = 0.28 (30% EtOAc/pentane, KMnO₄ stain).

¹H NMR (500 MHz, CDCl₃, 50 °C): δ_H 7.35 (s, 1H, H¹²), 7.30 – 7.20 (m, 2H, H¹⁴ + H¹⁵), 7.03 (d, *J* = 7.2 Hz, 1H, H¹⁶), 6.48 (s, 1H, H¹⁷), 4.79 – 4.67 (m, 1H, H⁹), 4.15 – 4.00 (m, 1H, H⁷), 3.45 – 3.24 (m, 2H, H⁴), 2.20 – 2.06 (m, 1H, H⁸), 2.05 – 1.93 (m, 1H, H⁸), 1.92 – 1.77 (m, 2H, H⁵), 1.77 – 1.65 (m, 2H, H⁶), 1.52 (s, 9H, H²⁰), 1.47 (s, 9H, H¹) ppm.

¹³C NMR (126 MHz, CDCl₃, 50 °C): δ_C 152.9 (C¹⁸), 146.4 (C¹³), 138.7 (C¹¹), 129.1 (C¹⁵), 120.5 (C¹⁶), 117.6 (C¹⁴), 116.2 (C¹²), 80.6 (C²), 79.8 (C¹⁹), 72.7 (C⁹), 55.7 (C⁷), 46.5 (2 × C by HSQC, C⁴ + C⁸), 32.5 (C⁶), 28.7 (3 × C¹), 28.5 (3 × C²⁰), 23.9 (C⁵) ppm. One of the carbonyl carbons was not observed.

***tert*-Butyl 2-(2-(2,3-dihydrobenzofuran-5-yl)-2-hydroxyethyl)pyrrolidine-1-carboxylate (273)**



Prepared following General Procedure 4B using Boc-Pro-OH (77 mg, 0.36 mmol, 1.2 equiv.), vinyl boronic ester **238** (155 μL, 0.90 mmol, 3.0 equiv.), 5-iodo-2,3-dihydrobenzofuran (74 mg, 0.30 mmol, 1.0 equiv.), 4CzIPN (4.7 mg, 0.0060 mmol, 2.0 mol%), NiCl₂·glyme (3.3 mg, 0.015 mmol, 5.0 mol%), dtbbpy (5.0 mg, 0.019 mmol, 6.3 mol%), Cs₂CO₃ (127 mg, 0.39 mmol, 1.3 equiv.) and DMA (12 mL), which was irradiated with 1 × Kessil lamp for 24 h. After oxidative work-up with UHP (84 mg, 0.90 mmol, 3.0 equiv.), purification by flash column chromatography (10–15% Et₂O/CH₂Cl₂) gave the title compound as two separable diastereomers (total yield: 51 mg, 0.15 mmol, 51%). The d.r. was determined after purification to be 63:37 (The relative stereochemistry of the two diastereomers could not be assigned).

Diastereomer A (32 mg, colourless oil):

TLC: R_f = 0.44 (15% Et₂O/CH₂Cl₂, KMnO₄ stain).

¹H NMR (500 MHz, CDCl₃): δ_H 7.30 – 7.26 (m, 1H, H¹²), 7.11 – 7.05 (m, 1H, H¹⁸), 6.72 (d, *J* = 8.2 Hz, 1H, H¹⁷), 5.31 (d, *J* = 3.9 Hz, 1H, H¹⁰), 4.65 – 4.47 (m, 1H, H⁹), 4.54 (t, *J* = 8.6 Hz, 2H, H¹⁵), 4.35 – 4.18 (m, 1H, H⁷), 3.37 (t, *J* = 7.0 Hz, 2H, H⁴), 3.18 (t, *J* = 8.6 Hz, 2H, H¹⁴), 2.05 – 1.93 (m, 1H, H⁸), 1.94 – 1.82 (m, 2H, H⁵), 1.75 – 1.59 (m, 3H, H⁶ + H⁸), 1.49 (s, 9H, H¹) ppm.

¹³C NMR (126 MHz, CDCl₃): δ_C 159.2 (C¹⁶), 157.0 (C³), 136.8 (C¹¹), 127.1 (C¹³), 125.7 (C¹⁸), 122.6 (C¹²), 108.9 (C¹⁷), 80.2 (C²), 71.4 (C¹⁵), 70.0 (C⁹), 54.1 (C⁷), 46.8 (C⁴), 46.6 (C⁶), 31.3 (C⁸), 29.9 (C¹⁴), 28.6 (3 × C¹), 23.8 (C⁵) ppm.

IR (film) ν_{max}: 3411, 2973, 1668, 1398, 1168, 1105 cm⁻¹.

HRMS (ESI⁺): calcd. for C₁₉H₂₇NNaO₄ [M+Na]⁺ 356.1832, found 356.1844.

Diastereomer B (19 mg, colourless oil):

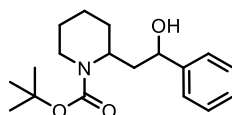
TLC: R_f = 0.28 (15% Et₂O/CH₂Cl₂, KMnO₄ stain).

¹H NMR (500 MHz, CDCl₃): δ_H 7.25 – 7.15 (m, 1H, H¹²), 7.07 (dd, *J* = 8.2, 1.9 Hz, 1H, H¹⁸), 6.71 (d, *J* = 8.1 Hz, 1H, H¹⁷), 4.75 – 4.59 (br. m, 1H, H⁹), 4.54 (t, *J* = 8.7 Hz, 2H, H¹⁵), 4.20 (br. s, 1H, H¹⁰), 4.14 – 3.94 (br. m, 1H, H⁷), 3.45 – 3.28 (m, 2H, H⁴), 3.18 (t, *J* = 8.7 Hz, 2H, H¹⁴), 2.22 – 2.07 (m, 1H, H⁸), 2.05 – 1.91 (m, 1H, H⁸), 1.89 – 1.78 (m, 2H, H⁵), 1.75 – 1.57 (m, 2H, H⁶), 1.46 (s, 9H, H¹) ppm.

¹³C NMR (126 MHz, CDCl₃): δ_C 159.3 (C¹⁶), 155.7 (C³), 137.6 (C¹¹), 127.1 (C¹³), 125.7 (C¹⁸), 122.5 (C¹²), 108.9 (C¹⁷), 79.9 (C²), 72.8 (C⁹), 71.4 (C¹⁵), 55.9 (C⁷), 46.6 (2 × C by HSQC, C⁴ + C⁸), 32.6 (C⁶), 29.9 (C¹⁴), 28.7 (3 × C¹), 24.0 (C⁵) ppm.

6.4.2.1 Application to *Sedum* Alkaloids

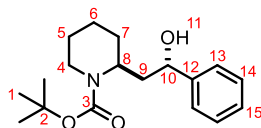
tert-Butyl 2-(2-hydroxy-2-phenylethyl)piperidine-1-carboxylate (276 + 277)



Prepared following General Procedure 4B using Boc-Pip-OH (83 mg, 0.36 mmol, 1.2 equiv.), vinyl boronic ester **238** (155 μL, 0.90 mmol, 3.0 equiv.), iodobenzene (34 μL, 0.30 mmol, 1.0 equiv.), 4CzIPN (4.7 mg, 0.0060 mmol, 2.0 mol%), NiCl₂·glyme (3.3 mg, 0.015 mmol, 5.0 mol%), dtbbpy (5.0 mg, 0.019 mmol, 6.3 mol%), Cs₂CO₃ (127 mg, 0.39 mmol, 1.3 equiv.) and DMA (12 mL), which was irradiated with 1 × Kessil lamp for 24 h. After oxidative work-up with UHP (84 mg, 0.90 mmol, 3.0 equiv.), purification by flash column chromatography (10–15% EtOAc/pentane) gave the title compound as two separable diastereomers (total yield: 64 mg, 0.21 mmol, 70%). The d.r. was

determined after purification to be 44:56 (The relative stereochemistry of the two diastereomers was assigned by comparison to previously reported spectroscopic data).^[197]

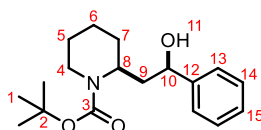
276 (36 mg, pale yellow oil):



¹H NMR (400 MHz, CDCl₃): δ_H 7.40 – 7.29 (m, 4H, H¹³ + H¹⁴), 7.27 – 7.21 (m, 1H, H¹⁵), 4.74 (br. s, 1H, H¹⁰), 4.40 (br. s, 1H, H⁸), 3.90 (br. s, 1H, H⁴), 2.77 (td, *J* = 13.3, 2.6 Hz, 1H, H⁴), 2.09 (dt, *J* = 15.3, 7.9 Hz, 1H, H⁹), 1.87 (ddd, *J* = 14.3, 5.8, 4.5 Hz, 1H, H⁹), 1.68 – 1.48 (m, 6H, H⁵ + H⁶ + H⁷), 1.45 (s, 9H, H¹) ppm.

¹³C NMR (101 MHz, CDCl₃): δ_C 155.8 (C³), 144.9 (C¹²), 128.5 (2 × C¹⁴), 127.4 (C¹⁵), 125.9 (2 × C¹³), 79.9 (C²), 72.8 (C¹⁰), 48.7 (C⁸), 40.9 (C⁹), 39.7 (C⁴), 29.4 (C⁵), 28.6 (3 × C¹), 25.6 (C⁶), 19.2 (C⁷) ppm.

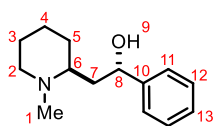
277 (28 mg, pale yellow solid):



¹H NMR (400 MHz, CDCl₃): δ_H 7.41 – 7.30 (m, 4H, H¹³ + H¹⁴), 7.27 – 7.21 (m, 1H, H¹⁵), 4.72 (br. s, 1H, H¹¹), 4.60 (br. s, 1H, H¹⁰), 4.42 (br. s, 1H, H⁸), 4.17 – 3.90 (br. m, 1H, H⁴), 2.80 (t, *J* = 13.2 Hz, 1H, H⁴), 2.21 (ddd, *J* = 14.5, 12.3, 2.4 Hz, 1H, H⁵), 1.82 – 1.70 (m, 1H, H⁹), 1.67 – 1.50 (m, 6H, H⁵ + H⁶ + H⁷ + H⁹), 1.50 (s, 9H, H¹) ppm.

¹³C NMR (101 MHz, CDCl₃): δ_C 144.3 (C¹²), 128.4 (2 × C¹⁴), 127.2 (C¹⁵), 125.7 (2 × C¹³), 80.5 (C²), 70.0 (C¹⁰), 46.8 (C⁸), 40.5 (C⁹), 39.7 (C⁴), 29.4 (C⁵), 28.6 (3 × C¹), 25.7 (C⁶), 19.3 (C⁷) ppm. The carbonyl carbon was not observed.

(±)-Sedamine (278)



(±)-Sedamine **278** was prepared following a modified literature procedure.^[180] To a solution of **276** (36 mg, 0.12 mmol, 1.0 equiv.) in anhydrous THF (1.8 mL) at 0 °C was added LiAlH₄ (23 mg, 0.61 mmol,

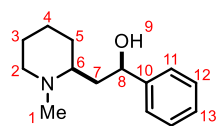
5.0 equiv.). The reaction mixture was heated to 60 °C for 14 h. The reaction mixture was then cooled to 0 °C and 1 M HCl was added slowly to pH 2. The mixture was diluted with water and washed with CH₂Cl₂ (2 × 5 mL). The aqueous phase was basified with 2 M NaOH and extracted into CH₂Cl₂ (5 × 5 mL). The combined organics were dried (Na₂SO₄), filtered and the solvent was removed in vacuo to give a colourless oil which solidified upon standing to a white solid (22 mg, 0.10 mmol, 84%).

¹H NMR (400 MHz, CDCl₃): δ_H 7.42 – 7.29 (m, 4H, H¹¹ + H¹²), 7.27 – 7.21 (m, 1H, H¹³), 4.90 (dd, *J* = 10.6, 2.8 Hz, 1H, H⁸), 3.08 (ddd, *J* = 13.3, 8.0, 3.3 Hz, 1H, H²), 2.92 – 2.81 (m, 1H, H⁶), 2.56 (ddd, *J* = 13.4, 7.2, 3.4 Hz, 1H, H²), 2.50 (s, 3H, H¹), 2.12 (ddd, *J* = 14.5, 10.6, 9.6 Hz, 1H, H⁷), 1.80 – 1.70 (m, 1H, H⁵), 1.70 – 1.40 (m, 5H, H³ + H⁴ + H⁷), 1.38 – 1.29 (m, 1H, H⁵) ppm.

¹³C NMR (101 MHz, CDCl₃): δ_C 145.8 (C¹⁰), 128.4 (2 × C¹²), 127.1 (C¹³), 125.7 (2 × C¹¹), 74.9 (C⁸), 61.0 (C⁶), 51.3 (C²), 40.1 (C¹), 39.9 (C⁷), 25.9 (C⁵), 22.5 (C³), 20.6 (C⁴) ppm.

Spectroscopic data matches previously reported data.^[197]

(±)-Allosedamine (279)



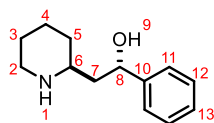
(±)-Allosedamine **279** was prepared following a modified literature procedure.^[180] To a solution of **277** (28 mg, 0.09 mmol, 1.0 equiv.) in anhydrous THF (1.8 mL) at 0 °C was added LiAlH₄ (17 mg, 0.45 mmol, 5.0 equiv.). The reaction mixture was heated to 60 °C for 14 h. The reaction mixture was then cooled to 0 °C and 1 M HCl was added slowly to pH 2. The mixture was diluted with water and washed with CH₂Cl₂ (2 × 5 mL). The aqueous layer was basified with 2 M NaOH and extracted into CH₂Cl₂ (5 × 5 mL). The combined organics were dried (Na₂SO₄), filtered and the solvent was removed in vacuo to give a colourless oil which solidified upon standing to a white solid (14 mg, 0.06 mmol, 71%).

¹H NMR (400 MHz, CDCl₃): δ_H 7.43 – 7.29 (m, 4H, H¹¹ + H¹²), 7.26 – 7.21 (m, 1H, H¹³), 5.13 (dd, *J* = 10.7, 3.5 Hz, 1H, H⁸), 2.97 (dtd, *J* = 11.7, 3.6, 1.5 Hz, 1H, H²), 2.42 (s, 3H, H¹), 2.28 (dq, *J* = 10.8, 3.5 Hz, 1H, H⁶), 2.17 (ddd, *J* = 14.6, 10.7, 3.7 Hz, 1H, H⁷), 2.04 (td, *J* = 11.5, 3.5 Hz, 1H, H²), 1.94 – 1.77 (m, 2H, H⁴ + H⁵), 1.74 – 1.51 (m, 4H, H³ + H⁵ + H⁷), 1.38 – 1.27 (m, 1H, H⁴) ppm.

¹³C NMR (101 MHz, CDCl₃): δ_C 145.7 (C¹⁰), 128.4 (2 × C¹²), 127.0 (C¹³), 125.7 (2 × C¹¹), 72.0 (C⁸), 62.8 (C⁶), 57.1 (C²), 44.0 (C¹), 39.6 (C⁷), 29.4 (C⁵), 25.6 (C³), 24.4 (C⁴) ppm.

Spectroscopic data matches previously reported data.^[197]

(±)-Norsedamine (280)



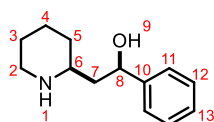
(±)-Norsedamine **280** was prepared following a modified literature procedure.^[180] To a solution of **276** (29 mg, 0.09 mmol) in MeOH (1 mL) was added 3 M HCl (0.30 mL). The reaction mixture was heated to 50 °C for 3 h. The reaction mixture was cooled to r.t. and the solvent removed in vacuo. The residue was dissolved in 1 M HCl (2 mL) and washed with CH₂Cl₂ (2 × 3 mL). The aqueous phase was basified with 2 M NaOH and extracted into CH₂Cl₂ (5 × 3 mL). The combined organics were dried (Na₂SO₄), filtered and the solvent was removed in vacuo to give a white solid (17 mg, 0.08 mmol, 92%).

¹H NMR (400 MHz, CDCl₃): δ_H 7.39 – 7.29 (m, 4H, H¹¹ + H¹²), 7.26 – 7.20 (m, 1H, H¹³), 4.94 (dd, *J* = 10.7, 2.6 Hz, 1H, H⁸), 3.08 (ddt, *J* = 13.8, 4.5, 2.3 Hz, 1H, H²), 2.90 (tt, *J* = 10.7, 2.5 Hz, 1H, H⁶), 2.66 (ddd, *J* = 13.7, 11.9, 3.0 Hz, 1H, H²), 1.88 – 1.78 (m, 1H, H⁴), 1.74 – 1.49 (m, 5H, H³ + H⁴ + H⁵ + H⁷), 1.39 – 1.28 (m, 1H, H³), 1.18 – 1.04 (m, 1H, H⁵) ppm.

¹³C NMR (101 MHz, CDCl₃): δ_C 145.4 (C¹⁰), 128.4 (2 × C¹²), 127.1 (C¹³), 125.7 (2 × C¹¹), 75.7 (C⁸), 58.5 (C⁶), 46.2 (C²), 45.3 (C⁷), 34.5 (C⁵), 27.6 (C³), 24.6 (C⁴) ppm.

Spectroscopic data matches previously reported data.^[198]

(±)-Norallostedamine (281)



(±)-Norallostedamine **281** was prepared following a modified literature procedure.^[180] To a solution of **277** (24 mg, 0.08 mmol) in MeOH (1 mL) was added 3 M HCl (0.25 mL). The reaction mixture was heated to 50 °C for 3 h. The reaction mixture was cooled to r.t. and the solvent removed in vacuo. The residue was dissolved in 1 M HCl (2 mL) and washed with CH₂Cl₂ (2 × 3 mL). The aqueous phase was basified with 2 M NaOH and extracted into CH₂Cl₂ (5 × 3 mL). The combined organics were dried (Na₂SO₄), filtered and the solvent was removed in vacuo to give a white solid (16 mg, 0.08 mmol, 97%).

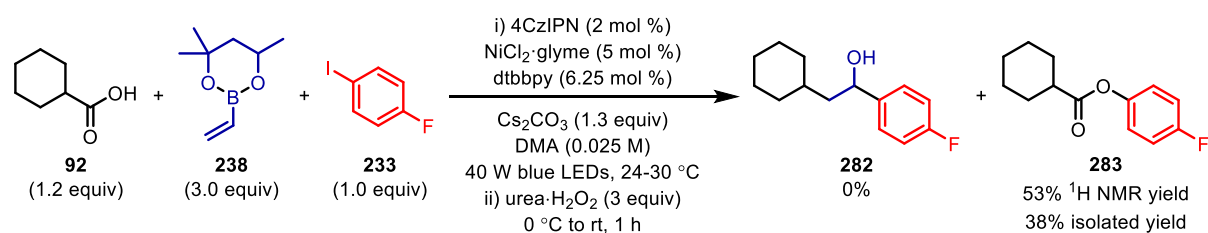
¹H NMR (400 MHz, CDCl₃): δ_H 7.39 – 7.30 (m, 4H, H¹¹ + H¹²), 7.26 – 7.21 (m, 1H, H¹³), 5.04 (dd, *J* = 7.4, 3.8 Hz, 1H, H⁸), 3.12 – 3.02 (m, 1H, H²), 2.83 – 2.73 (m, 1H, H⁶), 2.61 – 2.51 (m, 1H, H²), 1.87 (ddd, *J* = 14.5, 7.6, 3.8 Hz, 1H, H⁷), 1.83 – 1.76 (m, 1H, H⁴), 1.72 (ddd, *J* = 14.5, 7.4, 2.9 Hz, 1H, H⁷), 1.62 – 1.52 (m, 2H, H³ + H⁵), 1.45 – 1.33 (m, 3H, H³ + H⁴ + H⁵) ppm.

^{13}C NMR (101 MHz, CDCl_3): δ_{C} 145.6 (C^{10}), 128.3 ($2 \times \text{C}^{12}$), 126.9 (C^{13}), 125.8 ($2 \times \text{C}^{11}$), 72.2 (C^8), 54.7 (C^6), 46.8 (C^2), 44.1 (C^7), 32.1 (C^5), 26.6 (C^3), 24.7 (C^4) ppm.

Spectroscopic data matches previously reported data.^[199]

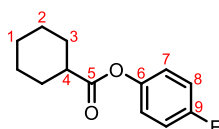
6.4.2.2 Unsuccessful Substrates

Alkyl Carboxylic Acids:



Prepared following General Procedure 4B using cyclohexanecarboxylic acid **92** (45 μL , 0.36 mmol, 1.2 equiv.), vinyl boronic ester **238** (155 μL , 0.90 mmol, 3.0 equiv.), 4-fluoroiodobenzene **233** (35 μL , 0.30 mmol, 1.0 equiv.), 4CzIPN (4.7 mg, 0.0060 mmol, 2.0 mol%), $\text{NiCl}_2 \cdot \text{glyme}$ (3.3 mg, 0.015 mmol, 5.0 mol%), dtbbpy (5.0 mg, 0.019 mmol, 6.3 mol%), Cs_2CO_3 (127 mg, 0.39 mmol, 1.3 equiv.) and DMA (12 mL), which was irradiated with 1 \times Kessil lamp for 24 h. After oxidative work-up with UHP (84 mg, 0.90 mmol, 3.0 equiv.), purification by flash column chromatography (5% Et_2O /pentane) gave 4-fluorophenyl cyclohexanecarboxylate **283** (25 mg, 0.11 mmol, 38%) as a pale yellow oil.

4-Fluorophenyl cyclohexanecarboxylate (**283**)

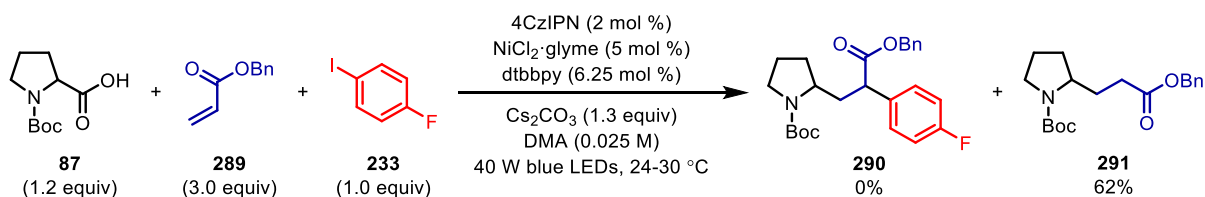


^1H NMR (400 MHz, CDCl_3): δ_{H} 7.09 – 6.99 (m, 4H, $\text{H}^7 + \text{H}^8$), 2.55 (tt, $J = 11.2, 3.7$ Hz, 1H, H^4), 2.10 – 2.01 (m, 2H, H^3), 1.87 – 1.78 (m, 2H, H^2), 1.74 – 1.65 (m, 1H, H^1), 1.65 – 1.51 (m, 2H, H^3), 1.46 – 1.26 (m, 3H, $\text{H}^1 + \text{H}^2$) ppm.

^{13}C NMR (101 MHz, CDCl_3): δ_{C} 174.7 (C^5), 160.3 (d, $J = 243.8$ Hz, C^9), 146.9 (d, $J = 2.9$ Hz, C^6), 123.1 (d, $J = 8.6$ Hz, $2 \times \text{C}^7$), 116.1 (d, $J = 23.5$ Hz, $2 \times \text{C}^8$), 43.3 (C^4), 29.1 ($2 \times \text{C}^3$), 25.8 (C^1), 25.5 ($2 \times \text{C}^2$) ppm.

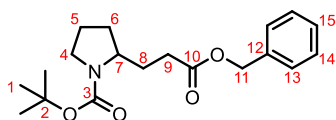
Spectroscopic data matches previously reported data.^[200]

Acrylate Radical Acceptor:



Prepared following General Procedure 4B using Boc-Pro-OH **87** (77 mg, 0.36 mmol, 1.2 equiv.) benzyl acrylate **289** (138 μ L, 0.90 mmol, 3.0 equiv.), 4-fluoriodobenzene **233** (35 μ L, 0.30 mmol, 1.0 equiv.), 4CzIPN (4.7 mg, 0.0060 mmol, 2.0 mol%), NiCl₂·glyme (3.3 mg, 0.015 mmol, 5.0 mol%), dtbbpy (5.0 mg, 0.019 mmol, 6.3 mol%), Cs₂CO₃ (127 mg, 0.39 mmol, 1.3 equiv.) and DMA (12 mL), which was irradiated with 1 \times Kessil lamp for 24 h. After oxidative work-up with UHP (84 mg, 0.90 mmol, 3.0 equiv.), purification by flash column chromatography (8% acetone/pentane) gave *tert*-butyl 2-(3-(benzyloxy)-3-oxopropyl)pyrrolidine-1-carboxylate **291** (62 mg, 0.19 mmol, 62%) as a pale yellow oil.

tert-Butyl 2-(3-(benzyloxy)-3-oxopropyl)pyrrolidine-1-carboxylate (**291**)

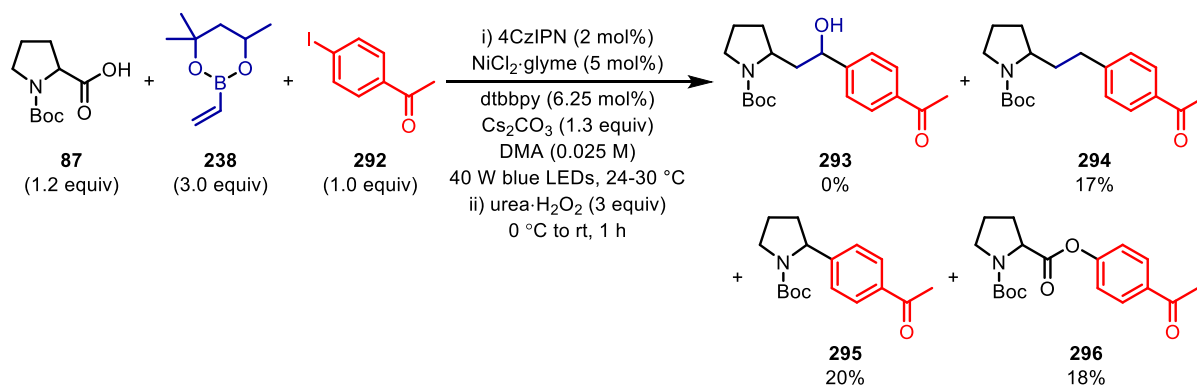


¹H NMR (500 MHz, CDCl₃): δ_{H} 7.41 – 7.27 (m, 5H, H¹³ + H¹⁴ + H¹⁵), 5.11 (s, 2H, H¹¹), 3.93 – 3.70 (br. m, 1H, H⁷), 3.47 – 3.19 (br. m, 2H, H⁴), 2.47 – 2.24 (m, 2H, H⁹), 2.11 – 1.54 (m, 6H, H⁵ + H⁶ + H⁸), 1.45 (s, 9H, H¹) ppm.

¹³C NMR (126 MHz, CDCl₃): δ_{C} 173.3 (C¹⁰), 154.9 (C³), 136.1 (C¹²), 128.7 (2 \times C¹³), 128.3 (2 \times C¹⁴), 128.1 (C¹⁵), 79.5 + 79.2 (rotameric peaks, C²), 66.4 (C¹¹), 56.7 (C⁷), 46.6 + 46.3 (rotameric peaks, C⁴), 31.5 + 31.4 (rotameric peaks, C⁹), 30.9 (C⁸), 30.1 + 29.7 (rotameric peaks, C⁶), 28.6 (3 \times C¹), 23.9 + 23.2 (rotameric peaks, C⁵) ppm.

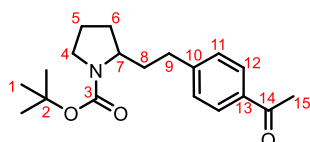
Spectroscopic data matches previously reported data.^[201]

Electron-deficient Aryl Iodides:



Prepared following General Procedure 4B using Boc-Pro-OH **87** (77 mg, 0.36 mmol, 1.2 equiv.), vinyl boronic ester **238** (155 μ L, 0.90 mmol, 3.0 equiv.), 4'-iodoacetophenone **292** (74 mg, 0.30 mmol, 1.0 equiv.), 4CzIPN (4.7 mg, 0.0060 mmol, 2.0 mol%), NiCl₂·glyme (3.3 mg, 0.015 mmol, 5.0 mol%), dtbbpy (5.0 mg, 0.019 mmol, 6.3 mol%), Cs₂CO₃ (127 mg, 0.39 mmol, 1.3 equiv.) and DMA (12 mL), which was irradiated with 1 \times Kessil lamp for 16 h. After oxidative work-up with UHP (84 mg, 0.90 mmol, 3.0 equiv.), purification by flash column chromatography (20–60% Et₂O/pentane) gave *tert*-butyl 2-(4-acetylphenethyl)pyrrolidine-1-carboxylate **294** (17 mg, 0.05 mmol, 17%) as a pale yellow oil, *tert*-butyl 2-(4-acetylphenyl)pyrrolidine-1-carboxylate **295** (17 mg, 0.06 mmol, 20%) as a colourless oil and 2-(4-acetylphenyl) 1-(*tert*-butyl) pyrrolidine-1,2-dicarboxylate **296** (18 mg, 0.05 mmol, 18%) as a pale yellow oil.

tert-Butyl 2-(4-acetylphenethyl)pyrrolidine-1-carboxylate (**294**)



TLC: R_f = 0.46 (25% EtOAc/pentane, KMnO₄ stain).

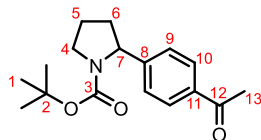
¹H NMR (500 MHz, CDCl₃): δ_{H} 7.87 (d, J = 7.8 Hz, 2H, H¹¹), 7.33 – 7.26 (m, 2H, H¹²), 3.94 – 3.68 (br. m, 1H, H⁷), 3.51 – 3.24 (br. m, 2H, H⁴), 2.76 – 2.60 (br. m, 2H, H⁹), 2.58 (s, 3H, H¹⁵), 2.21 – 1.91 (br. m, 2H, H⁶), 1.91 – 1.77 (m, 2H, H⁵), 1.77 – 1.62 (m, 2H, H⁸), 1.45 (s, 9H, H¹) ppm.

¹³C NMR (126 MHz, CDCl₃): δ_{C} 198.0 (C¹⁴), 154.8 (C³), 148.3 + 148.0 (rotameric peaks, C¹⁰), 135.2 (C¹³), 128.7 (2 \times C¹¹ + 2 \times C¹²), 79.3 + 79.2 (rotameric peaks, C²), 57.2 + 56.9 (rotameric peaks, C⁷), 46.7 + 46.3 (rotameric peaks, C⁴), 36.2 + 35.7 (rotameric peaks, C⁶), 33.0 (C⁹), 30.8 + 30.2 (rotameric peaks, C⁸), 28.7 (3 \times C¹), 26.7 (C¹⁵), 24.0 + 23.3 (rotameric peaks, C⁵) ppm.

IR (film) ν_{max} : 2971, 1685, 1394, 1268, 1170 cm⁻¹.

HRMS (ESI⁺): calcd. for C₁₉H₂₈NO₃ [M+H]⁺ 318.2064, found 318.2062.

***tert*-Butyl 2-(4-acetylphenyl)pyrrolidine-1-carboxylate (295)**

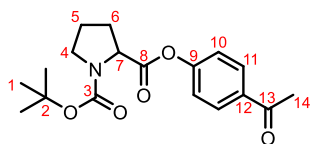


¹H NMR (500 MHz, CDCl₃): δ_H 7.92 – 7.87 (m, 2H, H⁹), 7.29 – 7.22 (m, 2H, H¹⁰), 5.05 – 4.75 (br. m, 1H, H⁷), 3.72 – 3.50 (m, 2H, H⁴), 2.59 (s, 3H, H¹³), 2.43 – 2.26 (m, 1H, H⁶), 1.95 – 1.74 (m, 3H, H⁵ + H⁶), 1.49 – 1.40 (m, 4H, H¹), 1.17 (s, 5H, H¹) ppm.

¹³C NMR (126 MHz, CDCl₃): δ_C 198.0 (C¹²), 154.6 (C³), 151.0 (C⁸), 135.9 (C¹¹), 128.8 + 128.6 (rotameric peaks, 2 × C¹⁰), 125.8 (2 × C⁹), 79.7 (C²), 61.3 + 60.8 (rotameric peaks, C⁷), 47.6 + 47.3 (rotameric peaks, C⁴), 36.1 + 35.0 (rotameric peaks, C⁶), 28.6 + 28.3 (rotameric peaks, 3 × C¹), 26.8 (C¹³), 23.8 + 23.4 (rotameric peaks, C⁵) ppm.

Spectroscopic data matches previously reported data.^[113]

2-(4-Acetylphenyl) 1-(*tert*-butyl) pyrrolidine-1,2-dicarboxylate (296)

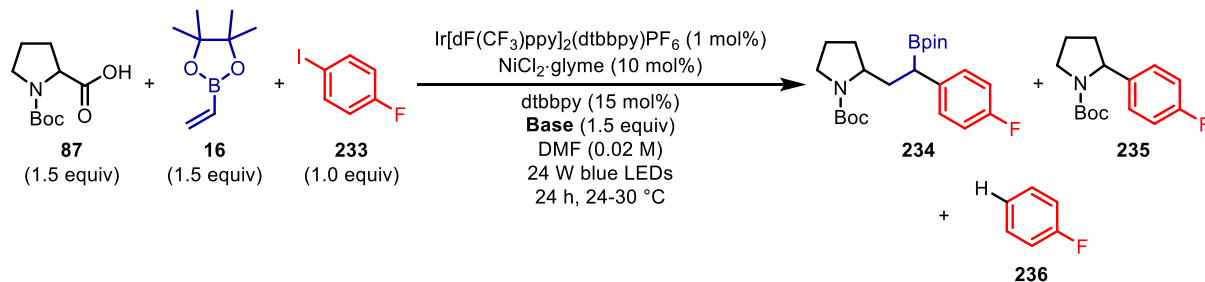


¹H NMR (500 MHz, CDCl₃): 56:44 rotameric mixture: δ_H 8.06 – 7.93 (m, 2H, H¹¹), 7.24 – 7.17 (m, 2H, H¹⁰), 4.53 (dd, *J* = 8.6, 4.4 Hz, 0.44H, H⁷), 4.46 (dd, *J* = 8.7, 4.4 Hz, 0.56H, H⁷), 3.68 – 3.40 (m, 2H, H⁴), 2.60 + 2.59 (2 × s, rotameric peaks, 3H, H¹⁴), 2.47 – 2.28 (m, 1H, H⁶), 2.23 – 2.11 (m, 1H, H⁶), 2.11 – 1.90 (m, 2H, H⁵), 1.48 + 1.45 (2 × s, rotameric peaks, 9H, H¹) ppm.

¹³C NMR (126 MHz, CDCl₃): δ_C 197.1 + 196.9 (rotameric peaks, C¹³), 171.3 + 171.3 (rotameric peaks, C⁸), 154.7 + 154.6 (rotameric peaks, C⁹), 154.4 + 153.8 (rotameric peaks, C³), 135.0 + 134.9 (rotameric peaks, C¹²), 130.2 + 130.0 (rotameric peaks, 2 × C¹¹), 121.8 + 121.5 (rotameric peaks, 2 × C¹⁰), 80.5 + 80.3 (rotameric peaks, C²), 59.3 + 59.2 (rotameric peaks, C⁷), 46.8 + 46.6 (rotameric peaks, C⁴), 31.2 + 30.1 (rotameric peaks, C⁶), 28.6 (3 × C¹), 26.7 (C¹⁴), 24.7 + 23.9 (rotameric peaks, C⁵) ppm.

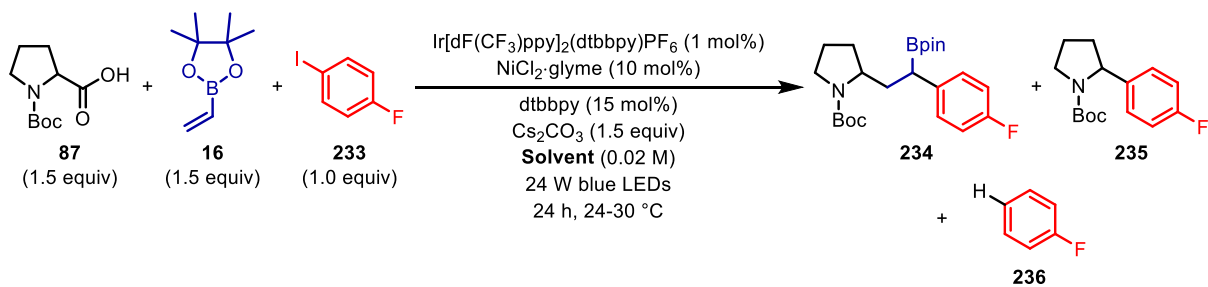
Spectroscopic data matches previously reported data.^[202]

6.4.3 Additional Optimisation Tables



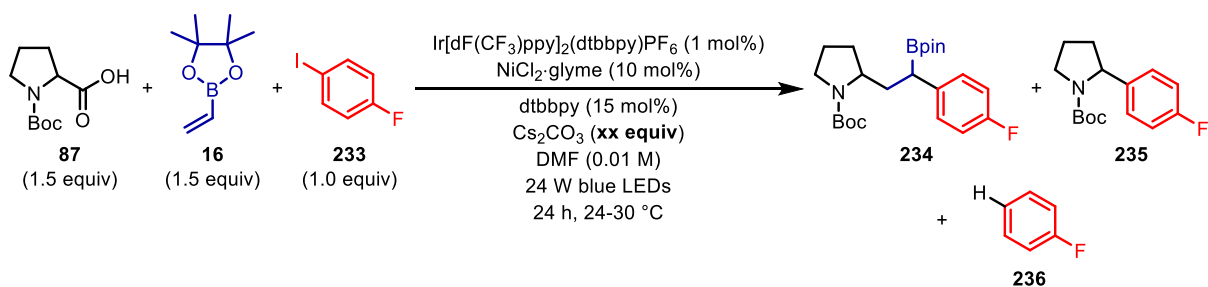
Entry	Base	¹⁹ F NMR Yield (%)			
		234	235	236	233
1	Cs ₂ CO ₃	33	14	27	11
2	K ₂ CO ₃	24	6	24	22
3	Na ₂ CO ₃	10	6	21	28
4	KHCO ₃	23	7	32	37
5	NaHCO ₃	7	4	33	51
6	CsOH·H ₂ O	10	4	29	29
7	KOH	13	2	24	43
8	NaOH	24	3	25	27
9	LiOH·H ₂ O	10	0	22	50
10 [†]	K ₂ HPO ₄	1	0	28	64
11 [†]	Na ₂ HPO ₄	0	0	4	93
12 [†]	KH ₂ PO ₄	0	0	1	90
13 [†]	NaH ₂ PO ₄	0	0	0	91
14 [†]	NaOAc	2	0	36	52
15 [†]	NaF	0	0	2	90
16 [†]	DBU	19	4	25	35
17 [†]	DBN	15	2	25	42
18	Pyridine	0	0	0	100
19	2,6-lutidine	0	0	0	93
20 [†]	DABCO	0	0	16	83
21 [†]	Quinuclidine	1	1	20	68

Table S 8. Base screen. Yields were determined by ¹⁹F NMR with hexafluorobenzene as the internal standard.



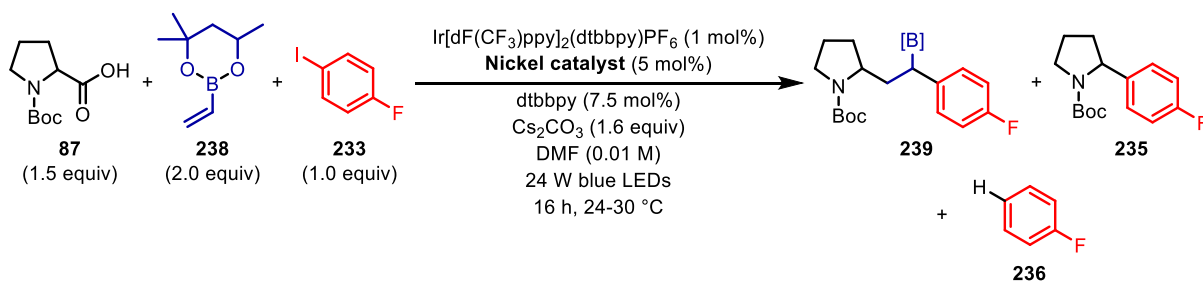
Entry	Solvent	^{19}F NMR Yield (%)			
		234	235	236	233
1 [‡]	DMF (anhydrous)	40	10	18	13
2 [‡]	DMA (anhydrous)	38	7	15	21
3 [‡]	DMI (anhydrous)	18	8	26	17
4	NMP (anhydrous)	8	4	15	36
5 [‡]	DMPU (anhydrous)	7	13	16	35
6	TMU (anhydrous)	0	0	24	52
7	2-pyrrolidinone (anhydrous)	0	0	0	100

Table S 9. Solvent screen. Yields were determined by ^{19}F NMR with hexafluorobenzene as the internal standard.



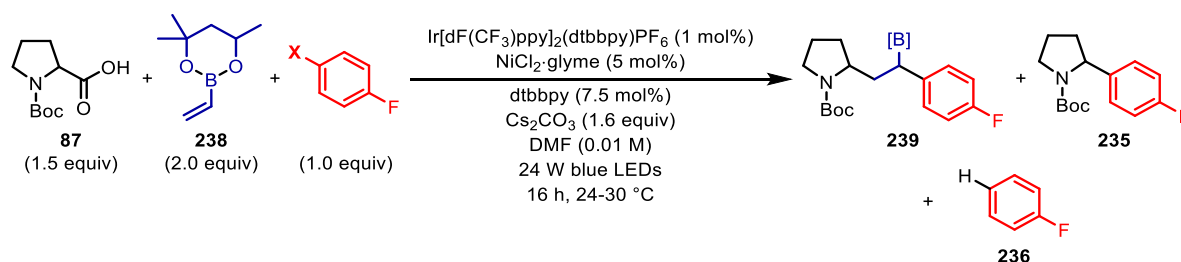
Entry	Equivalents of Cs_2CO_3	^{19}F NMR Yield (%)			
		234	235	236	233
1	1.5	41	18	24	0
2	2.0	46	19	22	0
3	2.5	35	20	23	0
4	3.0	16	16	28	0

Table S 10. Equivalents of Cs_2CO_3 screen. Yields were determined by ^{19}F NMR with hexafluorobenzene as the internal standard.



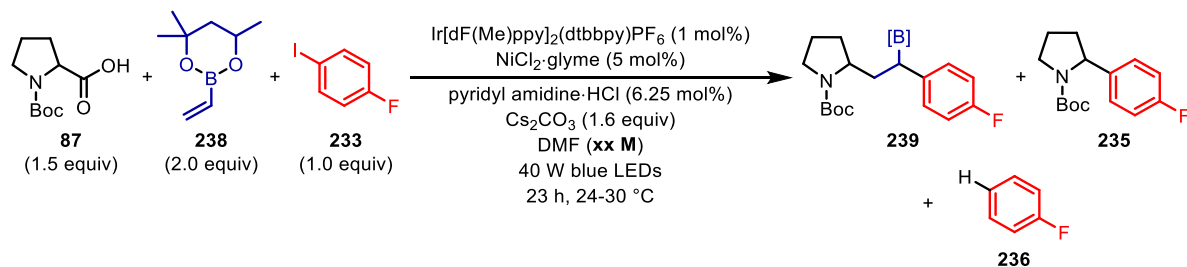
Entry	Nickel catalyst	¹⁹ F NMR Yield (%)			
		239	235	236	233
1	NiCl ₂ ^[a]	43	10	20	2
2	NiBr ₂ ^[a]	44	12	19	5
3	NiCl ₂ ·glyme	43	11	17	3
4	NiBr ₂ ·diglyme	42	10	18	3
5	Ni(OTf) ₂	11	2	17	36

Table S 11. Nickel catalyst screen. [a] Catalyst pre-complexed with dtbbpy in DMF prior to adding to reaction mixture due to insolubility. Yields were determined by ¹⁹F NMR with hexafluorobenzene as the internal standard.



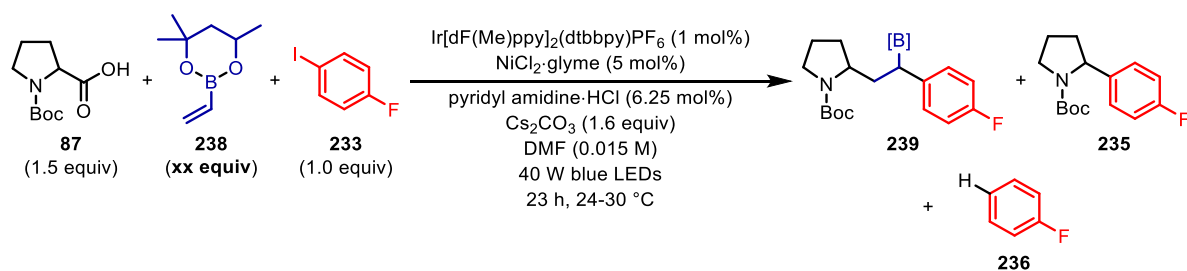
Entry	X	¹⁹ F NMR Yield (%)			
		239	235	236	238
1 [‡]	I	63	12	17	0
2 [‡]	Br	2	5	18	67
3 [‡]	OTf	19	27	34	4

Table S 12. Aryl (pseudo)halide coupling partner. Yields were determined by ¹⁹F NMR with hexafluorobenzene as the internal standard.



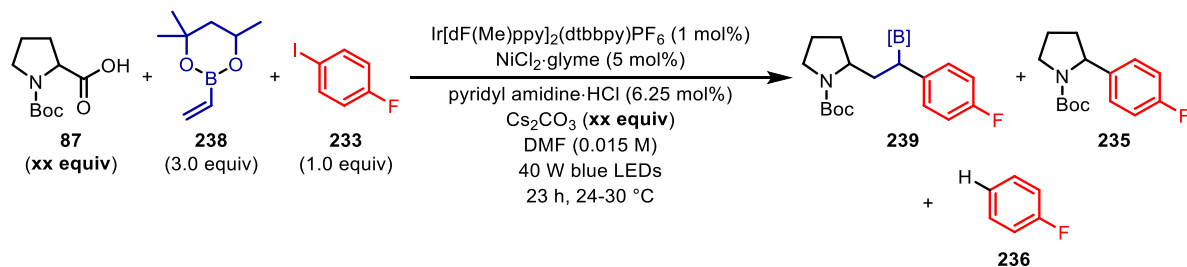
Entry	Concentration / M	¹⁹ F NMR Yield (%)			
		239	235	236	233
1 [‡]	0.015 M	67	18	6	0
2 [‡]	0.020 M	65	16	7	2
3 [‡]	0.025 M	65	14	8	6

Table S 13. Concentration screen. Yields were determined by ¹⁹F NMR with hexafluorobenzene as the internal standard.



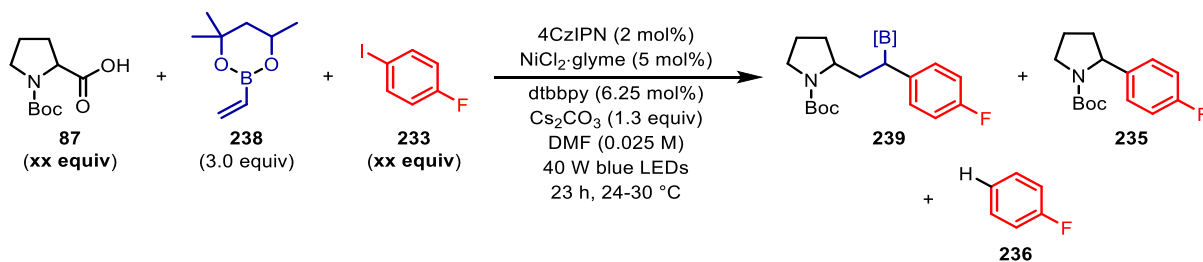
Entry	Equivalents of vinyl boronic ester 238	¹⁹ F NMR Yield (%)			
		239	235	236	233
1 [‡]	1.5	61	22	7	0
2 [‡]	2.0	67	21	7	0
3 [‡]	2.5	64	19	7	0
4 [‡]	3.0	69	14	7	0

Table S 14. Equivalents of vinyl boronic ester **238** screen. Yields were determined by ¹⁹F NMR with hexafluorobenzene as the internal standard.



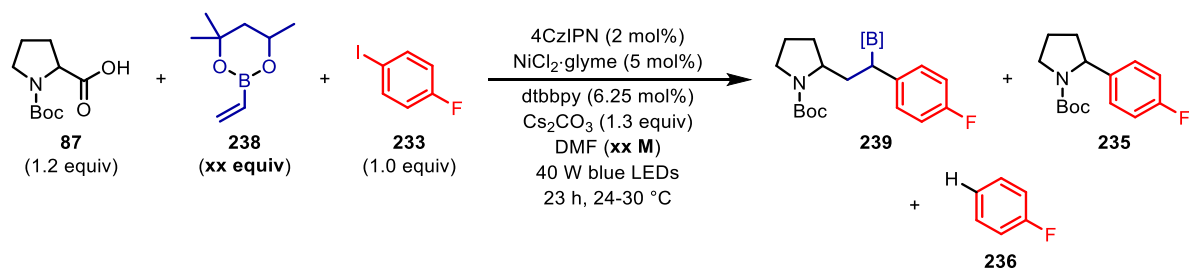
Entry	Equivalents of Boc-Pro-OH 87	Equivalents of Cs ₂ CO ₃	¹⁹ F NMR Yield (%)			
			239	235	236	233
1 [‡]	1.25	1.35	70	15	9	0
2 [‡]	1.50	1.60	68	16	7	0
3 [‡]	1.75	1.85	68	14	8	0
4 [‡]	2.0	2.10	66	15	9	0

Table S 15. Boc-Pro-OH equivalents, maintaining the excess of Cs₂CO₃. Yields were determined by ¹⁹F NMR with hexafluorobenzene as the internal standard.



Entry	Equivalents of Boc-Pro-OH 87	Equivalents of aryl iodide 233	¹⁹ F NMR Yield (%)			
			239	235	236	233
1	1.2	1.0	63	11	19	0
2	1.0	1.5	51	10	18	13

Table S 16. Ratio of 87:233. Yields were determined by ¹⁹F NMR with hexafluorobenzene as the internal standard.



Entry	Equivalents of vinyl boronic ester 238	Concentration / M	¹⁹ F NMR Yield (%)			
			239	235	236	233
1	2.5	0.025	60	11	17	1
2	3.0	0.025	68	11	16	0
3	2.5	0.050	60	8	20	5
4	3.0	0.050	61	7	22	6

Table S 17. Screening of equivalents of vinyl boronic ester **238** against concentration using 4CzIPN as photocatalyst. Yields were determined by ¹⁹F NMR with hexafluorobenzene as the internal standard.

7.0 References

- [1] D. G. Hall, Ed., *Boronic Acids: Preparation and Applications in Organic Synthesis, Medicine and Materials, Vols. 1 and 2*, Wiley-VCH Verlag GmbH & Co. KGaA, Weinheim, Germany, **2011**.
- [2] D. G. Hall, *Chem. Soc. Rev.* **2019**, *48*, 3475–3496.
- [3] A. J. J. Lennox, G. C. Lloyd-Jones, *Chem. Soc. Rev.* **2014**, *43*, 412–443.
- [4] C. Sandford, V. K. Aggarwal, *Chem. Commun.* **2017**, *53*, 5481–5494.
- [5] E. Fernandez, Ed., *Science of Synthesis: Advances in Organoboron Chemistry towards Organic Synthesis*, Georg Thieme Verlag KG, Stuttgart, Germany, **2019**.
- [6] H. C. Brown, G. Zweifel, *J. Am. Chem. Soc.* **1961**, *83*, 2544–2551.
- [7] H. Wang, C. Jing, A. Noble, V. K. Aggarwal, *Angew. Chem. Int. Ed.* **2020**, DOI: 10.1002/anie.202008096.
- [8] M. Kischkewitz, F. W. Friese, A. Studer, *Adv. Synth. Catal.* **2020**, *362*, 2077–2087.
- [9] F. Yang, M. Zhu, J. Zhang, H. Zhou, *MedChemComm* **2018**, *9*, 201–211.
- [10] J. P. M. António, R. Russo, C. P. Carvalho, P. M. S. D. Cal, P. M. P. Gois, *Chem. Soc. Rev.* **2019**, *48*, 3513–3536.
- [11] S. J. Baker, J. W. Tomsho, S. J. Benkovic, *Chem. Soc. Rev.* **2011**, *40*, 4279.
- [12] P. C. Trippier, C. McGuigan, *MedChemComm* **2010**, *1*, 183.
- [13] K. A. Koehler, G. E. Lienhard, *Biochemistry* **1971**, *10*, 2477–2483.
- [14] R. Smoum, A. Rubinstein, V. M. Dembitsky, M. Srebnik, *Chem. Rev.* **2012**, *112*, 4156–4220.
- [15] K. Knott, J. Fishovitz, S. B. Thorpe, I. Lee, W. L. Santos, *Org. Biomol. Chem.* **2010**, *8*, 3451.
- [16] M. P. Curran, K. McKeage, *Drugs* **2009**, *69*, 859–888.
- [17] K. G. Ramirez, PharmD, BCPS, *J. Adv. Pract. Oncol.* **2017**, *8*, 401–405.
- [18] G. F. S. Fernandes, W. A. Denny, J. L. Dos Santos, *Eur. J. Med. Chem.* **2019**, *179*, 791–804.
- [19] R. Wiczorek, K. Adamala, T. Gasperi, F. Polticelli, P. Stano, *Life* **2017**, *7*, 19.
- [20] C. M. Crudden, D. Edwards, *Eur. J. Org. Chem.* **2003**, 4695–4712.
- [21] I. A. I. Mkhaliid, J. H. Barnard, T. B. Marder, J. M. Murphy, J. F. Hartwig, *Chem. Rev.* **2010**, *110*, 890–931.
- [22] D. Leonori, V. K. Aggarwal, *Acc. Chem. Res.* **2014**, *47*, 3174–3183.
- [23] F. W. Friese, A. Studer, *Chem. Sci.* **2019**, *10*, 8503–8518.
- [24] B. S. L. Collins, C. M. Wilson, E. L. Myers, V. K. Aggarwal, *Angew. Chem. Int. Ed.* **2017**, *56*, 11700–11733.
- [25] N. Kumar, R. R. Reddy, N. Eghbarieh, A. Masarwa, *Chem. Commun.* **2020**, *56*, 13–25.
- [26] D. S. Matteson, *J. Am. Chem. Soc.* **1959**, *81*, 5004–5005.
- [27] D. S. Matteson, *J. Am. Chem. Soc.* **1960**, *82*, 4228–4233.

- [28] J. C. Walton, A. J. McCarroll, Q. Chen, B. Carboni, R. Nziengui, *J. Am. Chem. Soc.* **2000**, *122*, 5455–5463.
- [29] M. L. Coote, C. Y. Lin, A. A. Zavitsas, *Phys. Chem. Chem. Phys.* **2014**, *16*, 8686–8696.
- [30] D. J. Pasto, R. Krasnansky, C. Zercher, *J. Org. Chem.* **1987**, *52*, 3062–3072.
- [31] A. S. Menon, D. J. Henry, T. Bally, L. Radom, *Org. Biomol. Chem.* **2011**, *9*, 3636.
- [32] G. S. C. Srikanth, S. L. Castle, *Tetrahedron* **2005**, *61*, 10377–10441.
- [33] G. J. Lovinger, J. P. Morken, *Eur. J. Org. Chem.* **2020**, 2362–2368.
- [34] D. S. Matteson, K. Peacock, *J. Am. Chem. Soc.* **1960**, *82*, 5759–5760.
- [35] D. S. Matteson, J. D. Liedtke, *J. Org. Chem.* **1963**, *28*, 1924–1926.
- [36] D. S. Matteson, G. D. Schaumberg, *J. Org. Chem.* **1966**, *31*, 726–731.
- [37] N. Guennouni, F. Lhermitte, S. Cochard, B. Carboni, *Tetrahedron* **1995**, *51*, 6999–7018.
- [38] E. Lee, K. Zong, H. Y. Kang, J. Lim, J. Y. Kim, *Bull. Korean Chem. Soc.* **2000**, *21*, 765.
- [39] B. Giese, J. A. González-Gómez, T. Witzel, *Angew. Chem. Int. Ed.* **1984**, *23*, 69–70.
- [40] D. J. Pasto, J. Chow, S. K. Arora, *Tetrahedron* **1969**, *25*, 1557–1569.
- [41] H. Lopez-Ruiz, S. Z. Zard, *Chem. Commun.* **2001**, 2618–2619.
- [42] M. R. Heinrich, L. A. Sharp, S. Z. Zard, *Chem. Commun.* **2005**, 3077–3079.
- [43] X. Shu, R. Xu, Q. Ma, S. Liao, *Org. Chem. Front.* **2020**, *7*, 2003–2007.
- [44] A. Noble, R. S. Mega, D. Pflästerer, E. L. Myers, V. K. Aggarwal, *Angew. Chem. Int. Ed.* **2018**, *57*, 2155–2159.
- [45] R. H. Fish, *J. Organomet. Chem.* **1972**, *42*, 345–351.
- [46] N. Guennouni, C. Rasset-Deloge, B. Carboni, M. Vaultier, *Synlett* **1992**, *1992*, 581–584.
- [47] H. Cao, H. Jiang, H. Feng, J. M. C. Kwan, X. Liu, J. Wu, *J. Am. Chem. Soc.* **2018**, *140*, 16360–16367.
- [48] M. Chierchia, P. Xu, G. J. Lovinger, J. P. Morken, *Angew. Chem. Int. Ed.* **2019**, *58*, 14245–14249.
- [49] O. Gutierrez, J. C. Tellis, D. N. Primer, G. A. Molander, M. C. Kozlowski, *J. Am. Chem. Soc.* **2015**, *137*, 4896–4899.
- [50] X. Wei, W. Shu, A. García-Domínguez, E. Merino, C. Nevado, *J. Am. Chem. Soc.* **2020**, *142*, 13515–13522.
- [51] A. García-Domínguez, Z. Li, C. Nevado, *J. Am. Chem. Soc.* **2017**, *139*, 6835–6838.
- [52] W. Shu, A. García-Domínguez, M. T. Quirós, R. Mondal, D. J. Cárdenas, C. Nevado, *J. Am. Chem. Soc.* **2019**, *141*, 13812–13821.
- [53] B. Quiclet-Sire, S. Z. Zard, *J. Am. Chem. Soc.* **2015**, *137*, 6762–6765.
- [54] M. Kublicki, M. Dąbrowski, K. Durka, T. Kliś, J. Serwatowski, K. Woźniak, *Tetrahedron Lett.* **2017**, *58*, 2162–2165.
- [55] M. Kublicki, K. Durka, T. Kliś, *Tetrahedron Lett.* **2018**, *59*, 2700–2703.
- [56] M. Ueda, Y. Kato, N. Taniguchi, T. Morisaki, *Org. Lett.* **2020**, DOI:

10.1021/acs.orglett.0c01807.

- [57] M. Kischkewitz, K. Okamoto, C. Mück-Lichtenfeld, A. Studer, *Science* **2017**, *355*, 936–938.
- [58] N. D. C. Tappin, M. Gnägi-Lux, P. Renaud, *Chem. Eur. J.* **2018**, *24*, 11498–11502.
- [59] M. Silvi, C. Sandford, V. K. Aggarwal, *J. Am. Chem. Soc.* **2017**, *139*, 5736–5739.
- [60] B. Zhao, Z. Li, Y. Wu, Y. Wang, J. Qian, Y. Yuan, Z. Shi, *Angew. Chem. Int. Ed.* **2019**, *58*, 9448–9452.
- [61] C. Gerleve, M. Kischkewitz, A. Studer, *Angew. Chem. Int. Ed.* **2018**, *57*, 2441–2444.
- [62] G. J. Lovinger, J. P. Morken, *J. Am. Chem. Soc.* **2017**, *139*, 17293–17296.
- [63] R. A. Batey, B. Pedram, K. Yong, G. Baquer, *Tetrahedron Lett.* **1996**, *37*, 6847–6850.
- [64] R. A. Batey, D. V. Smil, *Tetrahedron Lett.* **1999**, *40*, 9183–9187.
- [65] D. Kurandina, M. Parasram, V. Gevorgyan, *Angew. Chem. Int. Ed.* **2017**, *56*, 14212–14216.
- [66] D. Kurandina, M. Rivas, M. Radzhabov, V. Gevorgyan, *Org. Lett.* **2018**, *20*, 357–360.
- [67] J. Schmidt, J. Choi, A. T. Liu, M. Slusarczyk, G. C. Fu, *Science* **2016**, *354*, 1265–1269.
- [68] A. S. Dudnik, G. C. Fu, *J. Am. Chem. Soc.* **2012**, *134*, 10693–10697.
- [69] S.-Z. Sun, R. Martin, *Angew. Chem. Int. Ed.* **2018**, *57*, 3622–3625.
- [70] S. Biswas, D. J. Weix, *J. Am. Chem. Soc.* **2013**, *135*, 16192–16197.
- [71] J. C. Lo, J. Gui, Y. Yabe, C. M. Pan, P. S. Baran, *Nature* **2014**, *516*, 343–348.
- [72] J. C. Lo, D. Kim, C. M. Pan, J. T. Edwards, Y. Yabe, J. Gui, T. Qin, S. Gutiérrez, J. Giacoboni, M. W. Smith, P. L. Holland, P. S. Baran, *J. Am. Chem. Soc.* **2017**, *139*, 2484–2503.
- [73] S. A. Green, J. L. M. Matos, A. Yagi, R. A. Shenvi, *J. Am. Chem. Soc.* **2016**, *138*, 12779–12782.
- [74] S. A. Green, S. Vásquez-Céspedes, R. A. Shenvi, *J. Am. Chem. Soc.* **2018**, *140*, 11317–11324.
- [75] S. A. Green, T. R. Huffman, R. O. McCourt, V. Van Der Puyl, R. A. Shenvi, *J. Am. Chem. Soc.* **2019**, *141*, 7709–7714.
- [76] D. Wang, C. Mück-Lichtenfeld, A. Studer, *J. Am. Chem. Soc.* **2019**, *141*, 14126–14130.
- [77] D. S. Matteson, R. W. H. Mah, *J. Am. Chem. Soc.* **1963**, *85*, 2599–2603.
- [78] C. Shu, A. Noble, V. K. Aggarwal, *Angew. Chem. Int. Ed.* **2019**, *58*, 3870–3874.
- [79] D. Wang, C. Mück-Lichtenfeld, A. Studer, *J. Am. Chem. Soc.* **2020**, *142*, 9119–9123.
- [80] M. A. Ischay, M. E. Anzovino, J. Du, T. P. Yoon, *J. Am. Chem. Soc.* **2008**, *130*, 12886–12887.
- [81] D. A. Nicewicz, D. W. C. MacMillan, *Science* **2008**, *322*, 77–80.
- [82] J. M. R. Narayanam, J. W. Tucker, C. R. J. Stephenson, *J. Am. Chem. Soc.* **2009**, *131*, 8756–8757.
- [83] T. J. Meyer, *Acc. Chem. Res.* **1989**, *22*, 163–170.
- [84] K. Kalyanasundaram, *Coord. Chem. Rev.* **1982**, *46*, 159–244.
- [85] C. Ulbricht, B. Beyer, C. Friebe, A. Winter, U. S. Schubert, *Adv. Mater.* **2009**, *21*, 4418–4441.
- [86] M. H. Shaw, J. Twilton, D. W. C. MacMillan, *J. Org. Chem.* **2016**, *81*, 6898–6926.

- [87] J. W. Tucker, C. R. J. Stephenson, *J. Org. Chem.* **2012**, *77*, 1617–1622.
- [88] R. A. Angnes, Z. Li, C. R. D. Correia, G. B. Hammond, *Org. Biomol. Chem.* **2015**, *13*, 9152–9167.
- [89] H. Roth, N. Romero, D. Nicewicz, *Synlett* **2015**, *27*, 714–723.
- [90] K. Teegardin, J. I. Day, J. Chan, J. Weaver, *Org. Process Res. Dev.* **2016**, *20*, 1156–1163.
- [91] C. K. Prier, D. A. Rankic, D. W. C. MacMillan, *Chem. Rev.* **2013**, *113*, 5322–5363.
- [92] J. Luo, J. Zhang, *ACS Catal.* **2016**, *6*, 873–877.
- [93] J. Xuan, Z.-G. Zhang, W.-J. Xiao, *Angew. Chem. Int. Ed.* **2015**, *54*, 15632–15641.
- [94] T. Patra, D. Maiti, *Chem. Eur. J.* **2017**, *23*, 7382–7401.
- [95] Z. Zuo, D. W. C. MacMillan, *J. Am. Chem. Soc.* **2014**, *136*, 5257–5260.
- [96] L. Chu, C. Ohta, Z. Zuo, D. W. C. MacMillan, *J. Am. Chem. Soc.* **2014**, *136*, 10886–10889.
- [97] A. Noble, D. W. C. MacMillan, *J. Am. Chem. Soc.* **2014**, *136*, 11602–11605.
- [98] F. Le Vaillant, T. Courant, J. Waser, *Angew. Chem. Int. Ed.* **2015**, *54*, 11200–11204.
- [99] C. Cassani, G. Bergonzini, C.-J. Wallentin, *Org. Lett.* **2014**, *16*, 4228–4231.
- [100] J. D. Griffin, M. A. Zeller, D. A. Nicewicz, *J. Am. Chem. Soc.* **2015**, *137*, 11340–11348.
- [101] M. Rueda-Becerril, O. Mahé, M. Drouin, M. B. Majewski, J. G. West, M. O. Wolf, G. M. Sammis, J.-F. Paquin, *J. Am. Chem. Soc.* **2014**, *136*, 2637–2641.
- [102] S. Ventre, F. R. Petronijevic, D. W. C. MacMillan, *J. Am. Chem. Soc.* **2015**, *137*, 5654–5657.
- [103] X. Wu, C. Meng, X. Yuan, X. Jia, X. Qian, J. Ye, *Chem. Commun.* **2015**, *51*, 11864–11867.
- [104] P. Perlmutter, *Conjugate Addition Reactions in Organic Synthesis*, Pergamon, Oxford, **1992**.
- [105] M. P. Sibi, S. Manyem, *Tetrahedron* **2000**, *56*, 8033–8061.
- [106] S. Bloom, C. Liu, D. K. Kölmel, J. X. Qiao, Y. Zhang, M. A. Poss, W. R. Ewing, D. W. C. MacMillan, *Nat. Chem.* **2018**, *10*, 205–211.
- [107] R. J. Wiles, G. A. Molander, *Isr. J. Chem.* **2020**, *60*, 281–293.
- [108] D. Kalyani, K. B. McMurtrey, S. R. Neufeldt, M. S. Sanford, *J. Am. Chem. Soc.* **2011**, *133*, 18566–18569.
- [109] J. Twilton, C. Le, P. Zhang, M. H. Shaw, R. W. Evans, D. W. C. MacMillan, *Nat. Rev. Chem.* **2017**, *1*, 0052.
- [110] J. A. Milligan, J. P. Phelan, S. O. Badir, G. A. Molander, *Angew. Chem. Int. Ed.* **2019**, *58*, 6152–6163.
- [111] S. Z. Tasker, E. A. Standley, T. F. Jamison, *Nature* **2014**, *509*, 299–309.
- [112] V. P. Ananikov, *ACS Catal.* **2015**, *5*, 1964–1971.
- [113] Z. Zuo, D. T. Ahneman, L. Chu, J. A. Terrett, A. G. Doyle, D. W. C. MacMillan, *Science* **2014**, *345*, 437–440.
- [114] X. Zhang, D. W. C. MacMillan, *J. Am. Chem. Soc.* **2016**, *138*, 13862–13865.
- [115] C. L. Joe, A. G. Doyle, *Angew. Chem. Int. Ed.* **2016**, *55*, 4040–4043.

- [116] J. C. Tellis, D. N. Primer, G. A. Molander, *Science* **2014**, *345*, 433–436.
- [117] V. Corcé, L.-M. Chamoreau, E. Derat, J.-P. Goddard, C. Ollivier, L. Fensterbank, *Angew. Chem. Int. Ed.* **2015**, *54*, 11414–11418.
- [118] K. Nakajima, S. Nojima, Y. Nishibayashi, *Angew. Chem. Int. Ed.* **2016**, *55*, 14106–14110.
- [119] H. Huang, K. Jia, Y. Chen, *ACS Catal.* **2016**, *6*, 4983–4988.
- [120] Z. Zuo, H. Cong, W. Li, J. Choi, G. C. Fu, D. W. C. MacMillan, *J. Am. Chem. Soc.* **2016**, *138*, 1832–1835.
- [121] C. P. Johnston, R. T. Smith, S. Allmendinger, D. W. C. MacMillan, *Nature* **2016**, *536*, 322–325.
- [122] A. Noble, S. J. McCarver, D. W. C. MacMillan, *J. Am. Chem. Soc.* **2015**, *137*, 624–627.
- [123] E. R. Welin, C. Le, D. M. Arias-Rotondo, J. K. McCusker, D. W. C. MacMillan, *Science* **2017**, *355*, 380–385.
- [124] W. L. A. Brooks, B. S. Sumerlin, *Chem. Rev.* **2016**, *116*, 1375–1397.
- [125] S. D. Bull, M. G. Davidson, J. M. H. van den Elsen, J. S. Fossey, A. T. A. Jenkins, Y.-B. Jiang, Y. Kubo, F. Marken, K. Sakurai, J. Zhao, T. D. James, *Acc. Chem. Res.* **2013**, *46*, 312–326.
- [126] K. A. Margrey, D. A. Nicewicz, *Acc. Chem. Res.* **2016**, *49*, 1997–2006.
- [127] K. Hong, X. Liu, J. P. Morken, *J. Am. Chem. Soc.* **2014**, *136*, 10581–10584.
- [128] C. S. Hampe, H. Mitoma, M. Manto, *GABA and Glutamate: Their Transmitter Role in the CNS and Pancreatic Islets*, InTechOpen, **2018**.
- [129] K. Gajcy, S. Lochynski, T. Librowski, *Curr. Med. Chem.* **2010**, *17*, 2338–2347.
- [130] T. Nishikawa, M. Ouchi, *Angew. Chem. Int. Ed.* **2019**, *58*, 12435–12439.
- [131] D. M. Arias-Rotondo, J. K. McCusker, *Chem. Soc. Rev.* **2016**, *45*, 5803–5820.
- [132] G. Dijkstra, W. H. Kruizinga, R. M. Kellogg, *J. Org. Chem.* **1987**, *52*, 4230–4234.
- [133] L. Chu, C. Ohta, Z. Zuo, D. W. C. MacMillan, *J. Am. Chem. Soc.* **2014**, *136*, 10886–10889.
- [134] R. J. Stoodley, N. R. Whitehouse, *J. Chem. Soc. Perkin Trans. 1* **1973**, 32.
- [135] B. A. Sim, D. Griller, D. D. M. Wayner, *J. Am. Chem. Soc.* **1989**, *111*, 754–755.
- [136] H. Yokoi, T. Nakano, W. Fujita, K. Ishiguro, Y. Sawaki, *J. Am. Chem. Soc.* **1998**, *120*, 12453–12458.
- [137] K. Donabauer, M. Maity, A. L. Berger, G. S. Huff, S. Crespi, B. König, *Chem. Sci.* **2019**, *10*, 5162–5166.
- [138] G. H. Lovett, B. A. Sparling, *Org. Lett.* **2016**, *18*, 3494–3497.
- [139] F. Lima, M. A. Kabeshov, D. N. Tran, C. Battilocchio, J. Sedelmeier, G. Sedelmeier, B. Schenkel, S. V. Ley, *Angew. Chem. Int. Ed.* **2016**, *55*, 14085–14089.
- [140] F. Lima, U. K. Sharma, L. Grunenberg, D. Saha, S. Johannsen, J. Sedelmeier, E. V. Van der Eycken, S. V. Ley, *Angew. Chem. Int. Ed.* **2017**, *56*, 15136–15140.
- [141] F. Lima, L. Grunenberg, H. B. A. Rahman, R. Labes, J. Sedelmeier, S. V. Ley, *Chem. Commun.* **2018**, *54*, 5606–5609.
- [142] C. Dai, F. Meschini, J. M. R. Narayanam, C. R. J. Stephenson, *J. Org. Chem.* **2012**, *77*, 4425–4431.

- [143] N. Elgrishi, K. J. Rountree, B. D. McCarthy, E. S. Rountree, T. T. Eisenhart, J. L. Dempsey, *J. Chem. Educ.* **2018**, *95*, 197–206.
- [144] C. Sandford, M. A. Edwards, K. J. Klunder, D. P. Hickey, M. Li, K. Barman, M. S. Sigman, H. S. White, S. D. Minter, *Chem. Sci.* **2019**, *10*, 6404–6422.
- [145] Y. Fu, L. Liu, H.-Z. Yu, Y.-M. Wang, Q.-X. Guo, *J. Am. Chem. Soc.* **2005**, *127*, 7227–7234.
- [146] A. A. Isse, A. Gennaro, *J. Phys. Chem. B* **2010**, *114*, 7894–7899.
- [147] C. Shu, R. S. Mega, B. J. Andreassen, A. Noble, V. K. Aggarwal, *Angew. Chem. Int. Ed.* **2018**, *57*, 15430–15434.
- [148] A. M. del Hoyo, A. G. Herraiz, M. G. Suero, *Angew. Chem. Int. Ed.* **2017**, *56*, 1610–1613.
- [149] A. M. del Hoyo, M. García Suero, *Eur. J. Org. Chem.* **2017**, 2122–2125.
- [150] M. Sayes, G. Benoit, A. B. Charette, *Angew. Chem. Int. Ed.* **2018**, *57*, 13514–13518.
- [151] T. T. Talele, *J. Med. Chem.* **2016**, *59*, 8712–8756.
- [152] D. Y.-K. Chen, R. H. Pouwer, J.-A. Richard, *Chem. Soc. Rev.* **2012**, *41*, 4631.
- [153] I. A. Novakov, A. S. Babushkin, A. S. Yablokov, M. B. Nawrozkij, O. V. Vostrikova, D. S. Shejkin, A. S. Mkrtchyan, K. V. Balakin, *Russ. Chem. Bull.* **2018**, *67*, 395–418.
- [154] L. Dian, I. Marek, *Chem. Rev.* **2018**, *118*, 8415–8434.
- [155] W. Wu, Z. Lin, H. Jiang, *Org. Biomol. Chem.* **2018**, *16*, 7315–7329.
- [156] C. Ebner, E. M. Carreira, *Chem. Rev.* **2017**, *117*, 11651–11679.
- [157] J. P. Phelan, S. B. Lang, J. S. Compton, C. B. Kelly, R. Dykstra, O. Gutierrez, G. A. Molander, *J. Am. Chem. Soc.* **2018**, *140*, 8037–8047.
- [158] A. G. Herraiz, M. G. Suero, *Synthesis* **2019**, *51*, 2821–2828.
- [159] J. A. Milligan, J. P. Phelan, V. C. Polites, C. B. Kelly, G. A. Molander, *Org. Lett.* **2018**, *20*, 6840–6844.
- [160] W. Luo, Y. Yang, Y. Fang, X. Zhang, X. Jin, G. Zhao, L. Zhang, Y. Li, W. Zhou, T. Xia, B. Chen, *Adv. Synth. Catal.* **2019**, *361*, 4215–4221.
- [161] J. A. Milligan, K. L. Burns, A. V. Le, V. C. Polites, Z. Wang, G. A. Molander, C. B. Kelly, *Adv. Synth. Catal.* **2020**, *362*, 242–247.
- [162] T. Guo, L. Zhang, X. Liu, Y. Fang, X. Jin, Y. Yang, Y. Li, B. Chen, M. Ouyang, *Adv. Synth. Catal.* **2018**, *360*, 4459–4463.
- [163] Y. Liu, W. Luo, J. Wu, Y. Fang, Y. Li, X. Jin, L. Zhang, Z. Zhang, F. Xu, C. Du, *Org. Chem. Front.* **2020**, *7*, 1588–1592.
- [164] W. Luo, Y. Fang, L. Zhang, T. Xu, Y. Liu, Y. Li, X. Jin, J. Bao, X. Wu, Z. Zhang, *Eur. J. Org. Chem.* **2020**, 1778–1781.
- [165] C. García-Ruiz, J. L.-Y. Chen, C. Sandford, K. Feeney, P. Lorenzo, G. Berionni, H. Mayr, V. K. Aggarwal, *J. Am. Chem. Soc.* **2017**, *139*, 15324–15327.
- [166] C. “Chip” Le, M. K. Wismer, Z.-C. Shi, R. Zhang, D. V. Conway, G. Li, P. Vachal, I. W. Davies, D. W. C. MacMillan, *ACS Cent. Sci.* **2017**, *3*, 647–653.
- [167] Y.-W. Wu, M.-C. Tseng, C.-Y. Lu, H.-H. Chou, Y.-F. Tseng, H.-J. Hsieh, *J. Chinese Chem. Soc.* **1999**, *46*, 861–863.

- [168] R. S. Mega, V. K. Duong, A. Noble, V. K. Aggarwal, *Angew. Chem. Int. Ed.* **2020**, *59*, 4375–4379.
- [169] L. Guo, H.-Y. Tu, S. Zhu, L. Chu, *Org. Lett.* **2019**, *21*, 4771–4776.
- [170] A. García-Domínguez, R. Mondal, C. Nevado, *Angew. Chem. Int. Ed.* **2019**, *58*, 12286–12290.
- [171] M. W. Campbell, J. S. Compton, C. B. Kelly, G. A. Molander, *J. Am. Chem. Soc.* **2019**, *141*, 20069–20078.
- [172] D. N. Primer, I. Karakaya, J. C. Tellis, G. A. Molander, *J. Am. Chem. Soc.* **2015**, *137*, 2195–2198.
- [173] G. R. Dick, E. M. Woerly, M. D. Burke, *Angew. Chem. Int. Ed.* **2012**, *51*, 2667–2672.
- [174] S. Sun, Y. Duan, R. S. Mega, R. J. Somerville, R. Martin, *Angew. Chem. Int. Ed.* **2020**, *59*, 4370–4374.
- [175] D. E. Yerien, R. Conde, S. Barata-Vallejo, B. Camps, B. Lantaño, A. Postigo, *RSC Adv.* **2017**, *7*, 266–274.
- [176] T. Constantin, M. Zanini, A. Regni, N. S. Sheikh, F. Juliá, D. Leonori, *Science* **2020**, *367*, 1021–1026.
- [177] J. D. Nguyen, E. M. D’Amato, J. M. R. Narayanam, C. R. J. Stephenson, *Nat. Chem.* **2012**, *4*, 854–859.
- [178] G. Desimoni, G. Faita, K. A. Jørgensen, *Chem. Rev.* **2011**, *111*, PR284–PR437.
- [179] H. Yin, G. C. Fu, *J. Am. Chem. Soc.* **2019**, *141*, 15433–15440.
- [180] S. G. Davies, A. M. Fletcher, P. M. Roberts, A. D. Smith, *Tetrahedron* **2009**, *65*, 10192–10213.
- [181] P. Lundberg, Y. Tsuchiya, E. M. Lindh, S. Tang, C. Adachi, L. Edman, *Nat. Commun.* **2019**, *10*, 5307.
- [182] S. Nave, R. P. Sonawane, T. G. Elford, V. K. Aggarwal, *J. Am. Chem. Soc.* **2010**, *132*, 17096–17098.
- [183] R. Larouche-Gauthier, T. G. Elford, V. K. Aggarwal, *J. Am. Chem. Soc.* **2011**, *133*, 16794–16797.
- [184] C. Thommen, C. K. Jana, M. Neuburger, K. Gademann, *Org. Lett.* **2013**, *15*, 1390–1393.
- [185] M. A. DeNardo, M. R. Mills, A. D. Ryabov, T. J. Collins, *J. Am. Chem. Soc.* **2016**, *138*, 2933–2936.
- [186] V. V Pavlishchuk, A. W. Addison, *Inorganica Chim. Acta* **2000**, *298*, 97–102.
- [187] L. Bunch, B. Nielsen, A. A. Jensen, H. Bräuner-Osborne, *J. Med. Chem.* **2006**, *49*, 172–178.
- [188] J. Takagi, K. Takahashi, T. Ishiyama, N. Miyaura, *J. Am. Chem. Soc.* **2002**, *124*, 8001–8006.
- [189] F. Gao, A. H. Hoveyda, *J. Am. Chem. Soc.* **2010**, *132*, 10961–10963.
- [190] M. A. Cismesia, T. P. Yoon, *Chem. Sci.* **2015**, *6*, 5426–5434.
- [191] S. P. Pitre, C. D. McTiernan, W. Vine, R. DiPucchio, M. Grenier, J. C. Scaiano, *Sci. Rep.* **2015**, *5*, 16397.
- [192] A. Roibu, S. Fransen, M. E. Leblebici, G. Meir, T. Van Gerven, S. Kuhn, *Sci. Rep.* **2018**, *8*, 5421.
- [193] M. Montalti, A. Credi, L. Prodi, M. T. Gandolfi, *Handbook of Photochemistry*, CRC Press, Boca

- Raton, FL, **2006**.
- [194] B. Oktavia, L. W. Lim, T. Takeuchi, *Anal. Sci.* **2008**, *24*, 1487–1492.
- [195] G. A. Molander, I. Shin, *Org. Lett.* **2013**, *15*, 2534–2537.
- [196] A. Millet, D. Dailler, P. Larini, O. Baudoin, *Angew. Chem. Int. Ed.* **2014**, *53*, 2678–2682.
- [197] R. A. Pilli, L. C. Dias, *Synth. Commun.* **1991**, *21*, 2213–2229.
- [198] P.-J. Tirel, M. Vaultier, R. Carrié, *Tetrahedron Lett.* **1989**, *30*, 1947–1950.
- [199] B. V. Subba Reddy, S. Ghanty, N. S. S. Reddy, Y. J. Reddy, J. S. Yadav, *Synth. Commun.* **2014**, *44*, 1658–1663.
- [200] R. S. Reddy, J. N. Rosa, L. F. Veiros, S. Caddick, P. M. P. Gois, *Org. Biomol. Chem.* **2011**, *9*, 3126.
- [201] S. Munnuri, A. M. Adebessin, M. P. Paudyal, M. Yousufuddin, A. Dalipe, J. R. Falck, *J. Am. Chem. Soc.* **2017**, *139*, 18288–18294.
- [202] B. Pieber, J. A. Malik, C. Cavedon, S. Gisbertz, A. Savateev, D. Cruz, T. Heil, G. Zhang, P. H. Seeberger, *Angew. Chem. Int. Ed.* **2019**, *58*, 9575–9580.